THE UNIVERSITY OF CHICAGO

THE DEVELOPMENT OF A SYNBIOTIC BUTYRATE-PRODUCING BACTERIAL THERAPEUTIC FOR FOOD ALLERGY

A DISSERTATION SUBMITTED TO
THE FACULTY OF THE PRITZKER SCHOOL OF MOLECULAR ENGINEERING
IN CANDIDACY FOR THE DEGREE OF
DOCTOR OF PHILOSOPHY

BY
LAUREN ANDERS HESSER

CHICAGO, ILLINOIS
JUNE 2023

I would like to dedicate this thesis to my family, who have shaped me into who I am today and who are incredible examples of the type of person I strive to be.

TABLE OF CONTENTS

LIST OF ABBREVIATIONS

Ahr: arylhydrocarbon receptor

AMP: antimicrobial peptide

APC: antigen presenting cell

BLG: β-lactoglobulin

CAZyme: carbohydrate accessible enzyme

CMA: cow's milk allergic, cow's milk allergy

CSR: class switch recombination

CT: Cholera toxin

DC: dendritic cell

DMEM: Dulbecco's modified eagle medium

DSS: dextran sodium sulfate

ELISA: enzyme-linked immunosorbent assay

ELISpot: enzyme-linked immunoSpot assay

FCS: fetal calf serum

FDA: Food and Drug Association

FMT: fecal microbiota transplant

GALT: gut associated lymphoid tissue

GC: germinal center

GF: germ free

GI: gastrointestinal

GPCR: G protein coupled receptor

GRAF: Gnotobiotic Research Animal Facility

HMO: human milk oligosaccharide

IEC: intestinal epithelial cell

i.g.: intragastric

Ig: immunoglobulin

IL: interleukin

ILC: innate lymphoid cell

i.p.: intraperitoneal

LP: lamina propria

LPS: lipopolysaccharide

mLN: mesenteric lymph node

Ova: ovalbumin

PBS: phosphate-buffered saline

PC: plasma cell

PCA: principal coordinate analysis

PCR: polymerase chain reaction

RA: retinoic acid

RT: room temperature

RT-qPCR: reverse transcription quantitative PCR

SAA: serum amyloid A

SCFA: short chain fatty acid

SPF: specific pathogen free

Tfh: T follicular helper

Tfr: T follicular regulatory

Th: T helper

TLR: Toll-like receptor

Treg: regulatory T cell

qPCR: quantitative PCR

TSLP: thymic stromal lymphopoietin

LIST OF FIGURES

LIST OF TABLES

ACKNOWLEDGMENTS

Over the last several years, I have had the pleasure of working with some of the most brilliant, kind, hardworking, and generous people I have ever known. I would like to take the opportunity to thank some of them here. To my primary research advisor, Dr. Cathy Nagler, I would like to thank you for your continuous support and guidance through this process. By working with you I have developed a sense of scientific rigor, endurance, joy in discovery, and confidence that I expect will continue to influence me throughout my career. Thank you for giving me these opportunities to grow as a scientist and as a person.

I would like to thank my co-advisor, Dr. Jeffrey Hubbell, for your additional support and mentorship. I have benefited immensely from your insights and that of your lab members. I would also like to thank my committee members, Dr. Mark Mimee and Dr. Sam Light. You have both been involved in my project from very early on, providing insights that truly made this project possible.

I would like to thank Rebecca Ortiz, Dr. Betty Theriault, and Kristin Kolar of the Gnotobiotic Research Animal Facility for their expertise and dedication which make our gnotobiotic experiments possible. I worked closely with Rebecca for several years, and she was truly essential to the success of many of the experiments presented here. Becky, thank you for your advice, your hard work, and your general thoughtfulness.

I am also so incredibly grateful for the amazing lab mates I have been able to work with during this time. Dr. Rob Patry, Dr. Andrea Kemter, Dr. Mohamed Bashir, Dr. Lisa Maccio-Marreto, Dr. Evelyn Campbell, and Dr. Shijie Cao have acted as influential mentors, and were responsible for teaching me the long list of techniques and experimental protocols which made this project possible. Thank you all for your patience, kindness, and expertise. Our lab members all also helped with numerous experiments, brightened the long workdays, and contributed ideas. Thank you to Jack Arnold, Edward Ionescu, Armando Puente, Yanlin Su, Matthew Bauer, and Peter Zwarycz for your help and camaraderie. I also had the pleasure to mentor three undergraduate students working

in our laboratory. Teaching, learning from, and growing with these students has truly been one of the great pleasures of my PhD. Thank you, Anjali Mirmira, Nidhi Talasani, and Tracy Chen, for your enthusiasm, kindness, and energy.

It truly takes a village, and I am so grateful for the village I have found here.

ABSTRACT

Commensal microbiota regulate human health and homeostasis through a variety of mechanisms. Modern lifestyle factors deplete populations of beneficial microbes, and this dysbiosis has been correlated with the rising incidence of numerous noncommunicable chronic diseases. Re-introduction of rationally selected, protective bacteria (or their products) will likely be an effective strategy to prevent or treat these diseases by targeting the underlying cause of immune dysregulation. Our group has previously characterized the bacterial communities in the feces of food allergic patient cohorts and demonstrated a marked lack of Clostridial taxa compared to healthy counterparts. Commensal Clostridia regulate host immunity through many mechanisms, one of which is the production of butyrate. Further work from our laboratory demonstrated that healthy infant microbiotas, a single Clostridial species (*Anaerostipes caccae*), or butyrate can protect against the allergic response to food in murine models. We now seek to expand on this knowledge by optimizing delivery of *A. caccae* as a biotherapeutic to mice with dysbiotic microbiota. We outline the isolation of a novel strain, *A. caccae* LAHUC, from the feces of a healthy infant and the characterization of this strain *in vitro*. We then discuss various mechanisms by which commensal microbiota or their products (e.g., butyrate) can modulate the host, focusing on intestinal barrier integrity. Finally, we establish that a synbiotic composed of *A. caccae* LAHUC and lactulose increases luminal butyrate in mice with a dysbiotic microbiota (gnotobiotic mice colonized with feces derived from an allergic infant or antibiotic treated mice). This synbiotic formulation both prevents and treats allergic responses to food in various models and microbial contexts, and we demonstrate innate and adaptive immune mechanisms for this effect. Together this thesis describes the pathway towards development of an *A. caccae* synbiotic, a novel therapeutic strategy for food allergy.

CHAPTER 1

INTRODUCTION

1.1 The commensal microbiome in health and disease

1.1.1 Symbiosis between host and commensal bacteria

The human body, and that of all multicellular organisms, exists in constant mutualism with a wide diversity of microorganisms. All external and mucosal surfaces of the body including the skin, respiratory tract, gastrointestinal (GI) tract, and reproductive tract are exposed to trillions of bacterial, viral, fungal, and other microorganisms. These collections of microorganisms which inhabit a shared ecosystem are referred to as microbiomes. The term microbiome includes microorganisms, their genes and gene products, and in some cases, the environment which they inhabit (in this report, the human body) (*1*). Humans have closely evolved with our microbiomes over thousands of years, such that our physiology and homeostasis rely on bacteria and other organisms, just as those organisms rely on the host (*2*, *3*). Some have suggested that this interdependence could in some ways be considered a ‘chimera’, a cooperative system comprising all commensal microorganisms and the host organs with the common goal of growth, nourishment, and elimination of pathogens (*4*). The rise of genetic sequencing and improved bacterial culture methods have begun to illuminate just how vast and unique human microbiomes can be (*5*–*7*). In fact, it is suggested that the number of bacterial cells that colonize the human body slightly outnumbers human cells (*8*). Beyond this, the number of unique genes produced by these bacteria is more than one hundred times greater than the human genome, demonstrating the vast diversity of bacteria and their capabilities (*8*).

The GI tract is one of the body sites with the most diverse and abundant bacterial microbiomes, due to a constant influx of nutrients from the host diet and vast surface area for colonization along the intestinal epithelium. The composition of the fecal microbiota

changes drastically over the lifetime and is also affected by diet, lifestyle, disease, and many other factors. As much of the intestinal tract is devoid of oxygen, many of the common fecal or intestinal microbes are facultative or strict anaerobes. Bacteria in the class Firmicutes are particularly dominant, and specifically those within the Lachnospiraceae family are characterized to be highly abundant, diverse, and play many functional roles to impact host health (*9*).

However, this tightly controlled balance between host and microbiota can be easily perturbed. Alterations in the steady state, 'healthy' microbiota are collectively termed dysbiosis, although this is still ill-defined. Dysbiosis may refer to a lack of specific bacterial taxa or functions that have specific roles in maintaining host health, increased abundance of opportunistic pathogens, and may cause (or be caused by) immune or inflammatory reactions (*10*). The correlations between microbiota composition and health are well documented, however determining causal relationships has been more difficult (*11*). New advances in culturing systems, computational models, and work with gnotobiotic animals have begun to address this gap (*11*, *12*). This progress is pivotal in moving our understanding of commensal microbiota towards the effective production of microbial therapeutics.

1.1.2 Links between dysbiosis, lifestyle factors, and noncommunicable disease outcomes

While dysbiosis itself is difficult to define, many dysbiotic microbial populations have been characterized in various cohorts, along with links to specific lifestyle factors (**Fig. 1.1**). Because it is thought that humans have co-evolved with colonizing microbiota over long timescales, some researchers have turned to traditional farming and hunter/gatherer populations to understand what healthy microbiomes may have looked like historically (*13*, *14*). Traditional farming and hunter/gatherer populations live in non-industrialized communities, consume diets containing high fiber and low processed foods, and live in

close proximity with animals (*13*). The fecal microbiota of these cohorts is often strikingly different than that of modern, Westernized populations, exhibiting higher diversity and abundance of many bacterial taxa (*13*, *14*). The Sonnenburg group has defined particular bacterial taxa that are vulnerable to industrial life which they have termed VANISH (volatile and/or associated negatively with industrialized societies of humans) taxa (*15*).

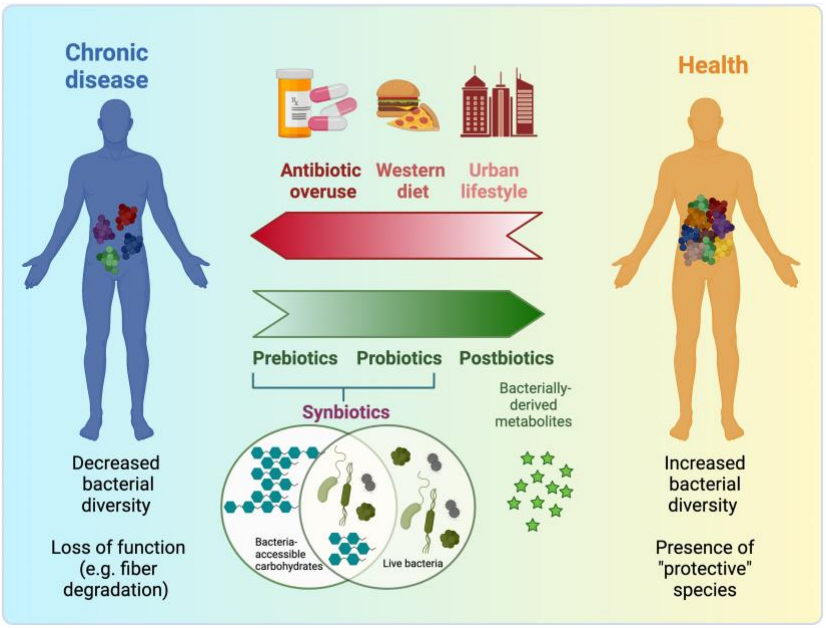

Figure 1.1: Modern lifestyle factors induce bacterial dysbiosis and correlate to noncommunicable disease outcomes | Historically, humans have existed in a state of symbiosis with commensal microbiota, which conferred a state of health. Modern lifestyle factors have negatively impacted the commensal microbiota, including decreasing bacterial diversity and depleting taxa with necessary functional roles. This depletion is correlated to the rise in noncommunicable chronic diseases. Microbial therapeutics aim to re-introduce these missing bacterial taxa or functions to return to a state of health and homeostasis.

These VANISH taxa are consistently present across many traditional populations, but strikingly absent in industrialized cohorts. The loss of beneficial microbes can occur rapidly, within a single individual's lifetime. Vangay et al. reported that cohorts of individuals emigrating from Southeast Asia to the United States suffered a loss of bacterial diversity and taxa abundance within months of this transition (*16*). These changes became even more pronounced in second-generation immigrants and correlated with

increased body mass index (*16*). There are likely many lifestyle factors at play in this difference between modern and traditional communities, and much study has been done to define impacts of specific practices. However, it should be noted that these studies predominantly examine correlative links between lifestyle and the microbiota, and additional work understanding causal relationships is required.

One of the most obvious lifestyle factors to impact the gut microbiota is diet. Unlike historical and traditional communities, the modern Western diet is commonly devoid of bacterial-accessible nutrients like complex fibers and fermented foods. Dietary fiber is not directly broken down by host digestive enzymes; only commensal bacteria are able to perform initial stages of fiber digestion, releasing smaller carbohydrates which are available to the host and microbiota for consumption. Low-fiber diets predictably reduce the abundance of fiber-consuming bacteria in humans and mouse models (*17*). This reduction in fiber-consuming bacteria compounds over generations, such that re-introduction of dietary fiber to offspring is not sufficient to expand these populations (*17*). The Western diet is also characterized by high dietary fat, and high-fat diets deplete bacterial diversity, reduce populations of 'beneficial' taxa, and increase abundance of 'non-protective' species reproducibly in mice and humans (*18*).

Beyond diet, other lifestyle factors, particularly early in life, can negatively affect the commensal microbiota. Modernized populations rely heavily on antibiotic use, and while these therapies are extremely effective and, in many cases, necessary, their overuse depletes nonpathogenic resident microbiota (*19*). Antibiotic exposure even in short term can induce bacterial dysbiosis, and repeated dosing can permanently deplete some taxa and prevent complete recovery of the steady-state microbiota (*20*).

In the late 1980s, an idea called the 'hygiene hypothesis', gained much recognition. This hypothesis stemmed from the observation that the incidence of hay fever was negatively correlated with family size (*21*). At the time, this hypothesis had little or nothing to do with the microbiome (*22*), although it has frequently been misused in this context

and its definition has been modified many times (*23*). However, this initial observation led to further study of other early-life 'infectious stressors', and over the past three decades a large body of work has shown that various modern lifestyle factors which reduce the diversity of the commensal microbiota are strongly correlated with a rising incidence of allergy and other diseases (*24*). All of these lifestyle factors are particularly detrimental in early life, a critical developmental window for both the microbiota and the immune system (*25*).

1.1.3 Early life microbiome and immune regulation

Birth mode (vaginal or Cesarean), formula feeding, and neonatal antibiotic exposure substantially impact the microbiota in early life (*26*, *27*). Some groups have posited that there is a placental microbiome which influences host physiology *in utero* (*28*). However, these studies are limited by low bacterial biomass and potential for contaminating DNA in sample preparation being over-represented (*29*). It is currently more widely accepted that initial bacterial colonization occurs at birth, and first exposure originates from either the bacteria lining the vaginal tract or from skin microbiota in the case of Cesarean birth (*30*–*32*). These distinct birth modes substantially impact the microbiota in early life, and Cesarean birth has been correlated with increased susceptibility to infection and allergy (*33*, *34*).

Infant microbiomes at birth are relatively homogenous across body sites, but specialize and mature into distinct, functional populations within six weeks (*35*, *36*). Maternally-derived microbiota can originate from the vaginal tract, breast milk, skin, feces, or other body sites (*36*). These microbiomes continue to undergo major shifts over time and are particularly affected by factors such as the cessation of breastfeeding and introduction of solid foods, adopting a generally "adult-like" composition and stability by two years of age (*27*, *37*). It is during this critical window that factors which impact the microbiota can also have out-sized effects on long-term health.

At weaning, the relative and absolute abundance of Clostridia greatly increases, while

‘milk-consuming’ species including *Lactobacillus* and *Bifidobacterium* wane (*38*). Mice undergo a specific immune reaction at weaning (*39*). This ‘weaning reaction’ is dependent on microbiota, occurs during the transition to solid food, and is required to prevent multiple pathologies in adulthood including colitis, colon carcinoma, and allergy (*39*). During the first 4 weeks of life in mice, and the first 6 months in humans, the mucosal immune system undergoes rapid maturation (*40*). Immunoglobulin A (IgA) from maternal breastmilk constitutes much of the neonatal adaptive immune response pre-weaning, and only after weaning do IgA-producing plasma cells (PCs), as well as peripheral regulatory T cells (Tregs) mature. During this window the murine intestinal epithelium also rapidly matures, beginning to develop specialized cell types, while the human epithelium is fully developed at birth (*40*). Microbiota/immune interactions in early life must be carefully controlled, and any disruptions during this phase can have lasting impacts on health in mice and humans (*41*, *42*). However, this also reveals a ‘window of opportunity’ for intervention (*40*), and bacterial therapeutics may be particularly efficacious when introduced within the first few years of life to prevent long-term negative health outcomes.

Early-life antibiotic use and other measures of bacterial dysbiosis have been correlated with various disease outcomes in children, including atopic diseases of dermatitis, food allergy, and asthma (*43–45*). Additional factors including formula feeding, maternal diet, and early introduction of dietary antigens may impact both microbial and immune system development in infancy (*27*, *46*, *47*). Of the many microbiome-correlated health outcomes, atopic dermatitis and food allergy are of particular interest, because these two diseases typically present early in life and comprise the initial steps of the ‘atopic march’ (*48*). Children who develop atopic dermatitis or eczema in infancy are at higher risk for developing food allergy in early childhood, followed by similarly increased risks for asthma and allergic rhinitis. All of these atopic diseases follow similar etiology, and they may result from the same underlying microbiological dysregulation early in life (*48*, *49*). In the following sections we will discuss known mechanisms of bacteria/immune interactions in

the gut, the complex series of interactions which occur at the initiation of allergic disease, and potential strategies to prevent or treat food allergy with microbiota-focused intervention.

1.2 Immune regulation by commensal Clostridia

1.2.1 Immune regulation by bacterial consortia and defined isolates

As discussed above, beginning at weaning and into adulthood the gut microbiota is dominated by Gram positive, strictly anaerobic bacteria in the Clostridia class (*9*, *50*). While it is likely that the pre-weaning community dominated by *Bifidobacterium* and *Lactobacillus* species also modulate host immunity, we will focus on known interactions of Clostridia and their products.

Some of the first evidence that specific bacterial taxa can regulate host immunity came from monocolonizing mice with segmented filamentous bacteria (SFB), a host-associated organism that strongly induces type 17 CD4 helper T cells (Th17) (*51*). At the time of this publication, SFB had not yet been isolated or cultured; monocolonized mice were produced by repeat exposure to antibiotics over several generations to completely deplete all other resident microbes. Since this initial discovery, much work has been done to further characterize the roles of SFB as well as other Clostridial isolates which induce a Treg rather than Th17 phenotype (*52*).

Many groups, including our own, initially studied interactions of Clostridia by isolating fecal bacteria via antibiotic depletion or spores by chloroform extraction (*53–56*). Atarshi et al. were some of the first to isolate fractions of chloroform-resistant, spore-forming fractions and demonstrate that that colonization of germ free (GF) mice with these spores increased Treg populations in the colonic lamina propria (LP) (*54*). They further narrowed this fraction down to 17 Clostridial strains by *in vitro* culture and demonstrated that colonization with this strain mixture increased Tregs in the colon LP *in vivo* and prevented

ovalbumin (OVA)-induced diarrhea in a murine model of food allergy (*54*). Further exploration of the metabolic capabilities of these strains demonstrated that the mix contained some strains which produce butyrate, degrade mucins, and convert dietary tryptophan to indole metabolites (*55*).

Others have explored the role of commensal bacteria, particularly Clostridia, in prevention of colitis. It has been shown that Clostridia and bacteria in the Lachnospiraceae family, specifically, are associated with less severe colitis in murine models (*56*). Repetitive culturing of human feces with antibiotics increased the relative abundance of Lachnospiraceae, and treating mice with this Lachnospiraceae-enriched consortium, or a single isolate *Clostridium immunis*, improved survival in a model of intestinal injury mediated by dextran sodium sulfate (DSS) (*56*).

Antibiotic depletion of fecal communities has also been used to identify bacteria which can confer protection against vancomycin-resistant *Enterococcus faecium* (VRE), a common source of nosocomial infections. Members of the Pamer group isolated ampicillin-resistant microbiota (predominantly *Blautia*, Bacteroides, and *Oscillospiraceae*) and demonstrated that transfer of these microbes to mice prevented initial colonization of VRE and cleared established VRE infection (*57*). They further narrowed this ampicillin-resistant microbiota down to a four-member consortium consisting of 2 bacteria within *Clostridium* Cluster XIVa and 2 *Bacteroidetes* and demonstrated that this smaller consortium prevents VRE colonization via secretion of a lantibiotic (*57*, *58*).

Our group demonstrated that spore-forming Clostridia from murine feces induced IL-22 production in colonized mice and protected against sensitization to peanut (*53*). Our consortium is predominantly contains Lachnospiraceae strains (*53*). While colonization with our Clostridia consortium also induced Treg populations in the colonic LP, we additionally demonstrated that colonization increased fecal IgA and regulated the epithelial barrier via IL-22 production and expression of down-stream antimicrobial peptides (AMPs) Reg3β and Reg3γ in the ileal epithelial cell (IEC) compartment.

Conversely, some consortia can also have immune-activating roles, expanding Th1 cells and activating cytotoxic CD8 T cells (*59*). Various combinations of 4 to 20 strains of bacteria from a healthy human differentially induced expression of IFNγ- producing CD8 T cells in the colon of gnotobiotic mice. Mice colonized with a particular mix of strains demonstrated increased IFNγ$^+$ CD8 T cell populations, effectively cleared pathogenic *Listeria monocytogenes*, and exhibited anti-tumor immunity which was amplified by treatment with checkpoint immunotherapy (*59*). The role of commensal microbiota in the pathogenesis and treatment of colorectal cancer has been well studied, and the direct cellular interactions between microbes and cytolytic T cells will contribute to further advancement in this field (*52*, *60*).

These studies of bacterial consortia have been critical in moving from correlation to causation in understanding bacterial regulation of immunity. However, complex consortia do not allow for direct understanding of the role(s) of specific taxa or functions in modulating host immunity. Advances in gnotobiotic colonization with carefully defined communities and administration of individual bacterial metabolites have begun to illuminate the potential mechanisms of Clostridia/immune interactions.

1.2.2 Identification of individual taxa or metabolites that impact host physiology

Defined communities and combinatorial analyses in gnotobiotic models have been highly beneficial in determining the roles of specific bacterial taxa in mediating host phenotype. Colonizing mice with a complex microbiota, identifying a particular phenotype, then selectively depleting individual organisms to observe presence/absence of that phenotype is a work-intensive, but effective method to define these relationships (*61*). Computer models can perform similar manipulations at a much faster timescale, in many cases effectively predicting inter-species interactions or metabolic outputs (*62*, *63*).

Together, these methods, along with metagenomic sequencing and *in vitro* bacterial characterization have allowed for greater understanding of the specific mechanisms by which commensal bacteria interact with the host.

Many of the known immuno-reactive bacterial metabolites are products from the digestion of compounds found in the human diet. Many dietary compounds including fiber, tryptophan, and vitamin A, as well as host-derived metabolites like primary bile acids are consumed and converted by commensal bacteria into secondary metabolites (**Fig. 1.2**) (*64*). Additionally, bacterial cell wall compounds (such as peptidoglycans or lipopolysaccharides (LPS)), nucleic acids, or proteins (e.g., flagellins) are recognized by host pattern recognition receptors and can have strong adjuvant activity. We are beginning to understand, however, that bacterial components from disparate taxa are not equal – the structures of LPS and flagellins differ between some commensal and pathogenic strains, and these structural alterations greatly impact their recognition by the host (*65*, *66*).

Dietary tryptophan is broken down by commensal microbiota into small indole-containing metabolites, which signal through the arylhydrocarbon receptor (Ahr) expressed highly on type 3 innate lymphoid cells (ILC3) and other immune cells in the intestinal LP. We, and others, have shown that various Clostridia produce indole metabolites, and signaling of indoles through the Ahr induces IL-22 production and epithelial homeostasis (*53*, *67*, *68*). Other work from our lab showed that a cell-specific knockout of the Ahr in Rorγt^{+} cells (namely ILC3s) reduced baseline production of IL-22 in the LP, and these mice (*Rorγt^{Cre} Ahr$^{fl/fl}$*) developed stronger allergic responses to food than their Ahr-sufficient littermates (*69*). The digestion of tryptophan results in production of many indole-containing compounds which may impact host physiology (*70*), but indole metabolites are not all produced to similar levels in the gut and have different signaling capacity through the Ahr. More studies are necessary to determine the pathways of production and immune effects of individual metabolites. Indole signaling through the Ahr

also synergizes with retinoic acid (RA) signaling to induce IL-22 from ILC3s, tolerize local antigen presenting cells (APCs), and induce TGF*β* production in the intestinal LP (*67*, *70*). Colonizing GF mice with a spore-forming Clostridial fraction (predominantly *Ruminococcaceae*) regulated expression of RA-conversion genes in the intestinal epithelium and increased local concentrations of retinol and retinyl ester (*71*). Additionally, oral administration of RA increased IL-22 production and reduced pathogen colonization in mice deficient in a RA-conversion enzyme , effectively attributing the effect of a bacterial consortium to a single metabolite.

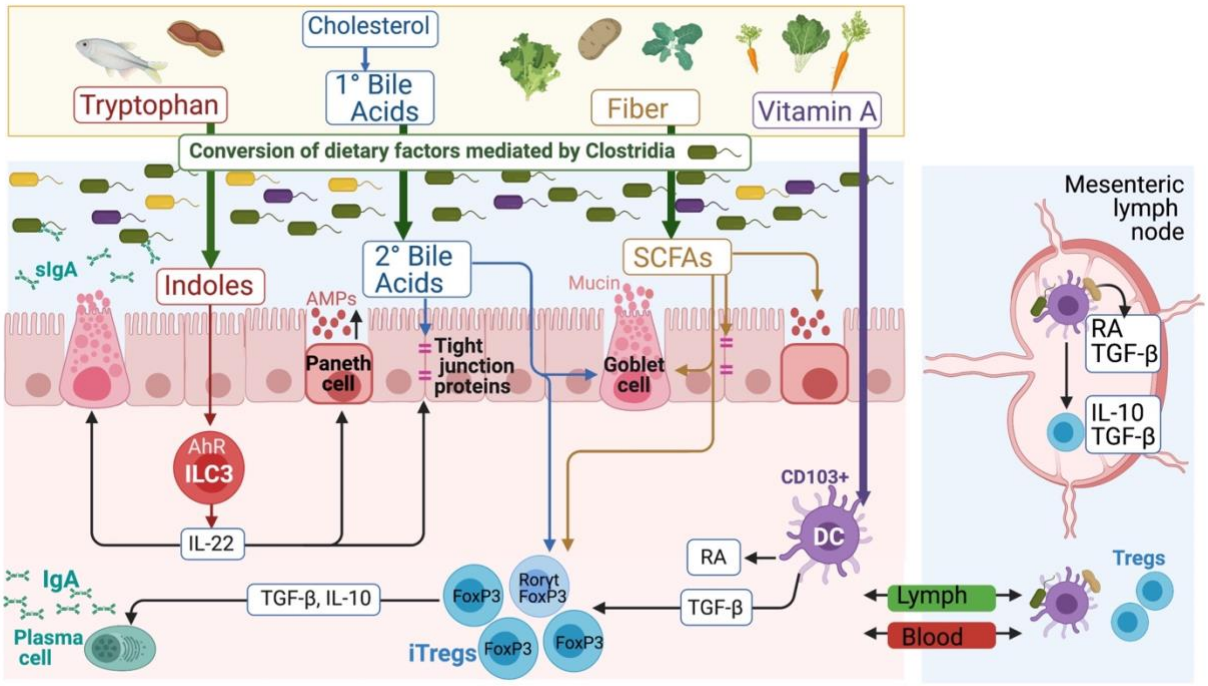

Figure 1.2: Dietary compounds are converted by commensal Clostridia into bioactive metabolites | Various dietary factors are consumed or converted by commensal Clostridia into downstream products which mediate host immunity. These pathways include breakdown of tryptophan into indoles which stimulate the aryl hydrocarbon receptor, digestion of dietary fiber into short chain fatty acids (SCFAs), and conversion of liver-derived bile acids into secondary bile acids. Additionally, dietary vitamin A is converted by host cells into retinoic acid, and this conversion is dependent on commensal microbes.

Other members of our group have characterized the metabolic and cellular characteristics of members of the IL-22-inducing, allergy protective Clostridia consortium previously described (*53*, *69*). Metagenomic sequencing and *in vitro* culture tests revealed that various members of the consortium produce butyrate, indoles, and flagella. Cellular lysates from the consortium or isolated Clostridial flagella induced IL-22 production from intestinal explants. Additionally, Clostridial flagella, but not isolated flagellin from pathogenic *Salmonella typhimurium*, reduced epithelial barrier permeability to FITC-dextran administered via intragastric (i.g.) gavage. This finding was supported by other recent work which showed that flagellins from some commensal Lachnospiraceae only weakly signal through TLR5, a potential mechanism of how flagellated commensals avoid immune activation and targeted clearance (*66*). One- or two-member strain isolates from our consortium have been isolated and examined for their production of each of these three immune-regulating components, and further work will determine how these individual strains (and strain products) may mediate host physiology (*69*).

Primary bile acids are produced by the liver in response to fat consumption. While most bile acids are rapidly reabsorbed into circulation in the upper small intestine, about 10% progress down through the GI tract, where they can be converted into bioactive secondary bile acids by commensal bacteria. The metabolic and immune-regulating properties of secondary bile acids are diverse; secondary bile acids regulate intestinal Foxp3^{+}Rorγt^{+} Treg populations and decrease Th17 differentiation (*72–74*). Conversely, other secondary bile acids may in fact potentiate allergic sensitization by increasing activation of mucosal dendritic cells (DCs) by binding the retinoic acid receptor alpha (RARα) (*75*). Further study into the roles of individual secondary bile acids, and the bacteria that produce them, will contribute to our understanding of these pathways.

The degradation of dietary fiber by commensal bacteria into short chain fatty acids (SCFAs) is by far the most well studied pathway of host-microbe interaction in the gut. We will focus on butyrate in the next section, but other SCFAs including acetate, propionate, and lactate also have established roles in maintaining gut homeostasis. Acetate and

lactate can not only act as carbon sources for other bacteria, but additionally signal through G-protein coupled receptors (GPCRs) expressed on IECs to modulate epithelial function and adaptive immune functions such as IgA production (*76*, *77*). Acetate is the most abundant SCFA in the colon, and lower colonic pH (mostly mediated by acetate) is generally associated with health and reduced risk for colitis or carcinoma (*78*). Propionate signals through several GPCRs and regulates host immunity through a variety of mechanisms *(79*).

1.2.3 Butyrate is a critical metabolite for mucosal homeostasis

Low concentrations of SCFAs in the gut luminal contents have been correlated with many disease outcomes, although it is still not entirely clear the exact combination or concentrations of each required to maintain homeostasis (*79*, *80*). The production, signaling capabilities, and effects of SCFAS on epithelial barrier function, antimicrobial activities, anti-inflammatory and anti-tumorigenic properties, and metabolic functions have been extensively characterized elsewhere (*78*, *79*). Here we will focus on specific mechanisms of butyrate in the lower gut that may be critical to the prevention of food allergy pathology.

Butyrate is predominantly produced in the colon, where it is rapidly consumed by colonocytes which utilize butyrate as one of their main carbon sources (*81*). Consumption of butyrate induces colonocytes to undergo aerobic glycolysis, consuming local oxygen and producing hypoxia-inducible factor (HIF). Thus, butyrate consumption creates an oxygen-depleted local niche for anaerobes to thrive, simultaneously preventing expansion of aerobic pathogens (*82*, *83*). Colonic and ileal IECs also produce GPR41 and 43, which bind butyrate as well as other SCFAs to mediate epithelial homeostasis, produce AMPs, and regulate inflammation (*84*, *85*).

Beyond the epithelium, butyrate also influences various cell populations in the intestinal LP and at distant sites. It is well known that butyrate induces colonic Treg populations, either directly through inhibition of histone deacetylation (HDAC) on T cells to increase expression of Foxp3 or indirectly via binding GPR109a (*84*, *86–89*). GPR109a is predominantly expressed on APCs including macrophages and DCs. Butyrate can reduce APC activation *in vitro* and *in vivo*, and these APCs will then provide less activating co-stimulation to T cells, resulting in greater inhibitory co-stimulation and further Treg induction (*90–92*). Butyrate binding GPR43 (also known as FFAR2) on colonic ILC3s induces IL-22 production and downstream protection from intestinal injury by DSS (*93*). Butyrate can additionally elicit IL-22 production by CD4 T cells through similar mechanisms (*94*).

Interestingly, butyrate promotes expression of the Ahr on T cells, ILCs, and B cells, potentially allowing opportunity for synergistic signaling between SCFAs and Ahr ligands (*94*, *95*). Butyrate induced populations of IL-10-producing B cells *in vitro* (*96*), and increased populations of these regulatory B cells *in vivo*, reducing severity of arthritis (*95*). This high-dose oral administration of sodium butyrate also altered the availability of Ahr ligands via modulation of the resident microbiota (*95*). Additionally, feeding butyrylated starches induced populations of T follicular regulatory cells (Tfr) in a model of rheumatoid arthritis (*97*). While it was once considered that Tfr cells were only thymically derived, peripheral Tfr's induced by butyrate may be critical regulators of B cell tolerance. The regulation of B/T cell dynamics, both locally and in the periphery, may have key roles in preventing allergy as well.

Fiber-derived butyrate also regulates food allergies in mice (*98*). Much of this prior work utilized high fiber diets, sodium butyrate, or butyrylated starch, and showed that butyrate specifically could reduce anaphylaxis to peanut via induction of $CD103^+$ DC populations and vitamin A metabolism, which was dependent on GPR43 or GPR109a signaling (*98*). This led the group to conclude that butyrate is likely a key regulator of

allergic responses, but further work was required to elucidate the role(s) of butyrate in the mucosal environment, specifically.

More recently, we have shown that targeted delivery of butyrate to the distal gut via polymer micelles (ButM) effectively treats murine models of food allergy and colitis (*92*). Previous studies have relied upon administration of sodium butyrate in water or butyrylated starches, which require continuous, *ad libitum* exposure at high doses (typically 150-300mM sodium butyrate in drinking water) (*87*, *97*, *98*). A single gavage of our micelles (at 60mM butyrate) released butyrate in the ileum and cecum, increasing the local concentration by approximately 3-fold over the duration of several hours. This controlled, slow release of butyrate to the lower GI tract greatly increased its therapeutic potential, and we show that ButM, but not sodium butyrate, prevented anaphylactic responses to peanut in previously sensitized mice (*92*). Treatment with these micelles decreased APC activation, improved epithelial barrier integrity, and reduced serum concentrations of peanut-specific IgE and IgG1. In this model of peanut allergy, mice were treated with vancomycin neonatally and throughout the sensitization window to induce dysbiosis. After cessation of vancomycin, treatment with ButM increased the relative abundance of bacteria in *Clostridium* Cluster XIVa, a group which contained many butyrate-producing species (*9*), and this expansion of butyrate-producing species may elicit more long-term effects (*92*).

Butyrate has also been shown to directly decrease activation of mast cells *in vitro* and reduce their expression of FcεR1 (*99*). Antigen cross-linking of surface-bound IgE on mast cells and downstream degranulation is the immediate mediator of an anaphylactic response; reducing FcεR1 expression on mast cells may be the most direct mechanism by which butyrate can exert an allergy-protective effect. However, further work is required to determine if butyrate or other microbial metabolites can affect the activation or accumulation of intestinal mast cells *in vivo*.

There is evidence that a reduced ability of the fecal microbiota to produce butyrate may be a biomarker of allergic disease risk. In infant cohorts, reduced abundance of some butyrate-producing and carbohydrate-active enzyme (CAZyme)-producing species correlates with the development of atopy in early childhood (*45*, *49*, *100*). Additionally, formula-fed infants have lower concentrations of fecal butyrate and lactate compared to breastfed infants, and these changes in fecal SCFA concentrations correlate to increased rates of eczema later in infancy (*101*). In food-allergic children whose allergies resolve naturally, representation of Firmicutes and Clostridia is increased compared to children whose allergies persist (*102*). Cow's milk allergic infants have distinct fecal microbiota from healthy infants, and the allergic infants have decreased abundance of several Clostridial taxa (*103*, *104*). Another large prospective cohort study demonstrated reduced concentrations of butyrate in feces of children with food allergy and/or respiratory allergy compared to healthy controls (*105*). This lack of butyrate, and butyrate producing species, demonstrates the potential of butyrate therapeutics for food allergy. Utilizing butyrate, an abundant metabolite in the healthy gut with many well described immuno-regulatory properties, has the potential to be safe and prevent/treat a wide variety of indications in the clinic, particularly those with demonstrated links to bacterial dysbiosis.

1.3 Current understanding of food allergy pathology

1.3.1 Food allergy epidemiology

Food allergy is a rapidly growing problem across the United States and globally (*106*, *107*). This rising incidence is particularly evident in children, such that now approximately 1 in every 13 children in the US has been diagnosed with food allergy (*108*). Food allergies typically present in early childhood; cow's milk allergy presents at the earliest age, commonly in infancy (*109*). Food allergies may resolve without any intervention or may be sustained throughout the lifetime (*110*). The precise factors involved in the initial

sensitization to food allergen(s), and the development of natural tolerance versus sustained responsiveness are not yet known. Many have correlated this rise in food allergy incidence with dysbiosis of the bacterial microbiota (*24*). Several groups have characterized striking differences in the fecal microbiota of healthy and food allergic cohorts of infants and children (*103*, *104*, *111*) and adults (*112*). In this section we will discuss current understanding of the biological basis of food sensitization and allergic responses, as well as potential mechanisms of regulation by the commensal microbiota.

1.3.2 Innate immunity in regulation and pathogenesis of food allergy

Food allergies are mediated by type 2 immune responses, governed by highly specialized lymphocytes. Upstream of this specialized, adaptive response, type 2 immunity is initiated by stress signals, typically alarmins produced by epithelial cells (*24*). These alarmins, including TSLP, IL-25, and IL-33, can be produced in the intestinal epithelium in response to chemical stress or physical damage and signal to ILC2s to produce type 2 cytokines including IL-4, IL-13, and IL-5, which initiate the adaptive response (*113*). Alarmins can also be produced at distal sites, namely the skin epithelium, and travel systemically to the gut to initiate an allergic response to food antigens (*114*). Skin barrier regulation of allergy has been demonstrated in both mouse models and human cohorts, and it is now suggested that initial exposure to a food antigen via a disrupted skin barrier may be a major instigator of food allergies (*115*). However, methods of clinical treatment or prevention of epicutaneous sensitization are not yet clear. Treatment with a neutralizing antibody against IL-33 increased the likelihood of passing an oral food challenge and significantly decreased various immune markers of allergy in a short-term phase 2 clinical trial (*116*). This demonstrates that targeting upstream alarmins, which circulate in high concentrations in allergic individuals may be a potential avenue to reduce immediate allergic responses to food.

Our group has demonstrated the necessity for a bacteria-induced, barrier-protective program in the intestinal epithelium to prevent allergic responses to food in murine models (*53*, *117*). The healthy epithelium maintains its barrier function via mucus production by goblet cells (GCs), production of AMPs by specialized cells such as Paneth cells, expression of tight junction proteins which form intercellular bonds, and carefully controlled, constant epithelial cell turnover (*117*, *118*). This barrier function is broadly mediated by ILC3-derived IL-22 but can also be controlled by other signals such as GC-derived mucus (*53*, *118*). Disruption of any of these pathways can allow translocation of food and microbial antigens from the gut lumen into the underlying LP, where they could directly stimulate local immune cell populations (*53*).

1.3.3 Cellular and humoral immune components of food allergy

Antigens are sampled in the intestinal LP by local APCs including DCs and $CX3CR1^+$ macrophages, which may reach across the epithelium to sample luminal antigens (*119*). These APCs then migrate to the draining lymph node and present antigen to naïve T cells expressing the cognate antigen receptor (*109*). These antigen-experienced T cells then multiply and adopt a specific phenotype in the presence of specific cytokines (in the case of allergy, T cells become Th2 in the presence of IL-4 and IL-13) (*109*). Mature Th2 cells then migrate back to the tissue to exert their effect via production of type 2 cytokines (*109*). These type 2 cytokines induce nearby B cells to undergo class-switch recombination (CSR), reconfiguring their B cell receptor (BCR) into IgG1 or IgE immunoglobulins (*120*).

CSR occurs within specialized in specialized compartments of lymphoid organs called germinal centers (GC). In the GC, B cells undergo CSR and somatic hypermutation, a series of rapid mutations which result in production of some high-affinity BCRs. Somatic hypermutation and rapid proliferation of B cell clones within a GC causes them to compete for antigen presented by follicular DCs and help from $CD4^+$ follicular helper T cells (Tfh),

eventually leading to the maturation of only B cell clones with the highest affinity BCR, which then leave the GC and further differentiate into memory B cells or antibody-secreting PCs.

Food allergy is canonically mediated by IgE antibodies, although IgG1 antibodies may play some role (*121*, *122*). Food antigen-specific IgE antibodies bind FcεR1 on mast cells, basophils, and eosinophils (*123*); IgG1 binds various Fcγ receptors on these same cells (*124*). Upon antigen re-exposure, receptor-bound antibodies are cross-linked by binding the allergen, causing rapid downstream intracellular signaling, degranulation, and release of anaphylactic mediators including histamine, eicosanoids, and others (*123*).

Recent studies have elucidated the dynamics specifically eliciting IgE responses in mice. Zhang et al. demonstrated that a specific population of IL13-producing Tfh cells (Tfh-13) are required for the production of high-affinity food-specific IgE and IgG1 (*125*). However, the role of Tfh-13 interactions directly with IgE^+ B cells is unclear, as it is generally understood that IgE^+ B cells do not persist in GCs (*126*, *127*). In order to produce high affinity IgE, it is thought that cells must undergo an 'alternative affinity maturation pathway' in which they enter a GC and undergo SHM with an IgG1 BCR, then later perform CSR to produce IgE outside of the GC (*128*). However, a recent study demonstrates that preventing $IgG1^+$ B cells from persisting in the GC (i.e., preventing the alternative pathway) does not substantially reduce the affinity of food-specific IgE or severity of allergic responses in mice (*129*). This seemingly contradictory evidence contributes to the many unanswered questions surrounding the origins of high affinity IgE.

Unlike IgE and IgG1, food-specific IgA does not depend on the presence of Tfh cells (*125*). Small intestinal Peyer's patches are inductive sites for IgA, and the development of Peyer's patches in early life depends on the presence of food antigens. This is supported by work which showed that GF mice fed antigen-free diets had smaller Peyer's patches, less total IgA, and fewer Tfh and IgA-producing cells in the small intestine than mice fed a standard diet (*130*). The dynamics of production and biological role of food-

specific IgA is not yet clear; these antibodies may have allergy-protective or allergy-potentiating functions (*125*, *131*, *132*).

Peyer's patches are unique in that their GCs are continuously present, unlike other immune organs (e.g., spleen and lymph nodes) where GCs form in response to immunization or infection (*133*). This is thought to be due to the constant availability of microbial (and food) antigens present in the intestine (*133*). There is some evidence to suggest that in the absence of a homeostatic IgA response (e.g., in GF mice), CSR to IgE can occur within Peyer's patches and mesenteric lymph nodes (mLN) (*134*). Most IgE-secreting PCs reside in lymphoid tissues or the bone marrow, and some may circulate in the blood (*135*, *136*). However, populations of peanut-specific IgE^+ B cells have also been characterized in duodenal biopsies of patients with food allergies (*137*). BCRs from duodenal and stomach biopsies had more clonal similarity to each other than to those from the blood, suggesting a role for local clonal divergence in the intestinal tract of food allergic humans (*137*, *138*).

Finally, the mechanisms of life-long allergy and immunological memory to food antigens is not entirely clear, as it is generally considered that IgE^+ B cells cannot become memory B cells (*127*, *139*). Instead, it is thought that 'IgE memory' is instead sustained through IgG1-expressing memory B cells, which can then later class switch to IgE and become PCs upon subsequent activation (*139*, *140*). Understanding the conditions which stimulate IgE production, where this occurs, and how these responses are maintained long term will be critical to developing better therapeutic strategies for food allergy.

1.3.4 Oral tolerance and the role(s) of regulatory T cells in mucosal immunity

As discussed above, the onset of food allergy results from a break in tolerance to a food antigen, initiated by epithelial barrier dysfunction (either in the gut or skin), then

amplified by a type 2 antigen-specific response mediated by T and B cells. However, the gut is constantly exposed to food antigens, and overall sensitization to these antigens is quite rare. The gut associated-lymphoid tissue (GALT) is, under normal circumstances, poised to be generally tolerogenic. This concept of 'oral tolerance', while still somewhat undefined, refers to the broad immune nonresponsiveness to orally ingested antigens, mediated by Treg populations in the GALT (*141*).

Oral antigens can be sampled by various APC populations in the GALT and intestinal LP. These antigens can reach these cells via GC associated passages (GAPs), can be translocated across the epithelium by M cells, or sampled by CXC3R1$^+$ macrophages (*24*). In the presence of RA and TGF-*β*, CD103$^+$ DCs in the LP migrate to the mLN and present antigen to naïve T cells in a context which primes them to become peripherally-derived Tregs (pTregs). Antigen presentation by both CX3CR1$^+$ macrophages and CD103$^+$ migratory DCs has been shown to be critical for pTreg-mediated oral tolerance (*142–144*).

While the collective mLN were once considered to be phenotypically similar, more recent work has demonstrated LNs draining from each distinct gut segment (duodenal, jejunal, ileal, and cecal-colonic) house distinct APC and T cell phenotypes with differing potential to mount tolerogenic or inflammatory responses (*145*). More proximal mLNs are responsible for greater nutrient uptake, RA dehydrogenase activity, and tolerogenic DC phenotypes, resulting in larger populations of 'classical' Foxp3$^+$Rorγt$^-$ Tregs. Conversely, there is greater inflammatory potential in the cecal-colonic LN, characterized by Th17 induction and a unique population of Foxp3$^+$Rorγt$^+$ co-expressing Tregs (*145*).

This population of Foxp3$^+$Rorγt$^+$ Tregs is induced by commensal microbiota, is most prevalent in the colon LP, and was first described by Eberl and colleagues to specifically prevent type 2 responses to helminths in the gut (*146*). It was later shown that specific bacteria or metabolites such as SCFAs or bile acids could induce these cells (*73*, *111*, *147*). Further, blocking MyD88 signaling in Foxp3$^+$ cells (*Foxp3^{Cre}Myd88$^{fl/fl}$*) reduced the proportion of Rorγt expressing cells within the Foxp3$^+$ Treg population and exacerbated

allergic responses to food (*111*). Recent work from 3 independent groups suggested that Foxp3$^+$Rorγt$^+$ Tregs may not be dependent on antigen presentation by classical DC populations, and instead that ILC3s and ILC3-like cells which express Rorγt and MHCII in the mLNs are necessary for induction of these Tregs (*148–150*).

Some intestinal Tregs also express Gata3, the canonical transcription factor for Th2 cells. Foxp3$^+$ Gata3$^+$ Tregs exist at higher proportions in the intestinal LP than in the LNs or spleen (*151*). However, the role(s) of Foxp3$^+$ Gata3$^+$ Tregs are not entirely clear, as some groups show that these cells are more Th2-like than Treg-like, producing IL-4 but little IL-10 (*146*). Others suggest that there are two differing functions of Foxp3$^+$ pTregs in the gut: Rorγt$^+$ Tregs mediate tolerance to dietary antigens and commensal microbiota, while Gata3$^+$ Tregs mediate tissue repair and response to injury (*152*). Overall, whether Foxp3$^+$Gata3$^+$ Tregs play a role in allergy is not yet clear.

The fates of food-antigen specific T cells classically falls within one of these tolerogenic states: functionally inactivated or anergic T cells, IL-10$^+$ or TGF-*β* producing Tregs, or generalized Foxp3$^+$ Treg cells (*141*). However, many of the studies that determined these cell fates utilized T cell receptor (TCR) transgenic mice, which are useful for the study of antigen-specific T cell responses but are known to respond abnormally to inflammatory stimuli compared to animals with a normal T cell repertoire. This has led to a transition towards characterizing populations of resident, food antigen-specific populations in conventional mice. Hong et al. recently demonstrated that SPF C57BL/6 mice harbor CD4 T cells with gliadin-specific TCRs in the GALT (*153*). Gliadin is the major protein component of dietary gluten, and mice fed a gliadin-free diet expressed less than 10% as many gliadin-specific CD4 T cells as gliadin-fed mice. The group went on to show that many of the gliadin-specific T cells in fed mice lacked canonical Treg or Th17 markers, and instead characterized them as ‘Th-lineage-negative cells’ which expressed markers of anergy including FR4 and CD73 (*153*). This suggests that oral tolerance may depend

on both Tregs and anergic 'Th-lineage-negative' cells, but further characterization of these cells and their functional capacity in the context of allergic inflammation is necessary.

1.3.5 Food allergy and the gut microbiome

Members of the Nagler laboratory were the first to demonstrate bacterial regulation of allergic responses to food by showing that neonatal administration of antibiotics increased antigen specific IgE in mice that received five weekly sensitizations to peanut (PN), starting at weaning (*154*). Additionally, higher concentrations of PN-specific IgE were detected in the serum of TLR4 deficient mice compared to TLR4 sufficient controls (*154*). Depletion of commensal bacteria in early life via antibiotics is detrimental to the development of nonresponsiveness to food antigens. We later demonstrated that the reduction in intestinal bacterial diversity induced by neonatal antibiotic treatment impaired epithelial barrier function, resulting in enhanced access of food allergens to the systemic circulation (53). Colonization of GF mice with a consortium of Clostridia elicited a barrier protective response and prevented against an allergic sensitization to PN (*53*).

Additional support for the role of the microbiome in regulating allergic responses to food came from the observation that GF mice produced high concentrations of IgE, large populations of type 2-skewed Tfh cells, and had more circulating basophils than standard SPF mice in the absence of sensitization (*134*, *155*). This aberrant IgE response in GF mice was mounted in response to food antigens; feeding mice antigen free diets reduced circulating IgE and type 2-skewed Tfh responses (*155*). Microbial colonization was also sufficient to reduce this elevated IgE, but only when introduced in a specific time window around weaning (*134*). Other groups have used defined bacterial communities to determine which microbial components or taxa were necessary to reduce this spontaneous IgE response in GF mice. Wyss et al. used several defined communities and demonstrated that more complex microbiotas reduced circulating IgE more efficiently than

one- or two-member consortia, but none of the tested groups fully reduced the IgE levels to that of SPF mice (*156*).

There is also some evidence to suggest that type 2 immune signaling may negatively affect bacterial composition in the gut, creating a feed-forward loop of microbial/immune dysregulation. It is well known that intestinal IgA regulates the composition and function of the gut microbiota (*131*), but the same is not clear for other immune pathways. Mice with canonically active IL4 receptor signaling due to a gain-of-function mutation in the IL4 receptor (*IL4Ra*^{F709}) have distinct microbiota from WT mice, and these differences are exacerbated with allergic sensitization (*157*). However, the conclusions from this study were limited due to a lack of littermate controls. Overall, the bi-directional nature of interactions between the intestinal epithelium (and underlying immune compartment) with the microbiota are complex, and teasing apart cause and effect is complicated by continual networks of signaling (*158*).

More recently, translational work from our group characterized the fecal microbiota of a cohort of healthy and cow's milk allergic (CMA) infants and described how these communities impacted the development of allergic responses to milk in gnotobiotic mice (*104*). This study utilized fecal samples from 4 healthy and 4 CMA demographically matched infants from Naples, Italy. Fecal samples from these infant donors were introduced into GF mice to analyze their effect on the host phenotype. 16S rRNA sequencing revealed many differentially abundant bacterial taxa between the two cohorts, and these differences were strikingly similar between both the infant donor feces and the feces of colonized mice (*104*). RNA sequencing of the ileal IEC compartment of colonized mice revealed that the different microbial populations elicited unique transcriptional programs, with many differentially regulated genes. These two datasets were then bioinformatically overlayed to correlate the relative abundance of bacterial taxa with changes in epithelial gene expression. This matrix identified a single species,

Anaerostipes caccae, which was more abundant in healthy infants and strongly associated with changes in epithelial gene expression (*104*).

Beyond the changes in gene expression induced simply by colonization with these infant-derived feces, the gnotobiotic mice mirrored the allergic phenotype of their infant donors when sensitized with the cow's milk allergen *β*-lactoglobulin (BLG). Mice colonized with the CMA microbiotas exhibited strong allergic responses to BLG following sensitization and intragastric challenge, while those colonized with the healthy infant microbiotas were protected (*104*). This led to the hypothesis that certain bacterial taxa, or bacterial products, may be present in the healthy microbiota but lacking in the CMA microbiota such that a homeostatic, allergy-protective response was not initiated. Strikingly, mice monocolonized with *A. caccae* were also protected, demonstrating that this single species could mimic the effect of the replete healthy microbiota (*104*). Others have replicated this finding, showing that the fecal bacteria of healthy and allergic infants are distinct and do not equally protect against allergen sensitization in gnotobiotic mice (*111*). Additionally, a consortium of Clostridiales, but not Proteobacteria, protected GF *IL4Ra*^{F709} mice from developing allergic responses to ovalbumin, which was attributed to increased populations of Foxp3^{+}Rorγt^{+} Tregs and decreased mast cell accumulation in the intestinal LP. Interestingly, both the Clostridiales and Proteobacteria consortia induced Foxp3^{+} Tregs, but only the Clostridiales consortium increased the Foxp3^{+}Rorγt Treg population (*111*).

Further study of our healthy and CMA infant communities focused on the fecal microbiota of a single CMA infant (donor 5) who displayed severe allergic symptoms and whose microbiota elicited a unique transcriptional profile in colonized mice (*159*). This transcriptional program was dominated by Th17-like genes, specifically very high expression of serum amyloid A-1 (SAA-1). SAA-1 is an inflammatory molecule produced by IECs in response to the microbiota and is associated with the initiation of pathogenic Th17 responses (*160*, *161*). This increased expression of SAA-1 in CMA5-colonized mice

was ablated when TLR4 (which binds LPS) was knocked out globally or in $CD11c^+$ cells. The CMA microbiotas, particularly that of donor 5, have higher abundance of Bacteroides and Proteobacteria than the healthy infant microbiotas. The CMA5 microbiome has increased prevalence of LPS genes, suggesting that there may be a relationship between LPS sensing, type-17 responses to bacteria, and heightened susceptibility to food allergy (*159*).

The overall associations between the microbiome and allergy in both animal models and human cohorts have been extensively reviewed (*24*, *162*). Gnotobiotic models which utilize human-derived microbiota are driving the field towards understanding *causal* host/microbe interactions in the context of food allergy, and these studies are likely to be more translationally relevant than those in mice with standard laboratory microbiota. Identifying specific bacteria in the human microbiota which demonstrably impact health and homeostasis is the first step in developing microbiome-modulating therapeutics.

1.4 Strategies for microbiome therapeutics

1.4.1 Bacterial therapeutics: from historical tactics to recent advances

Over the last few decades, there has been great effort in harnessing new understanding of host/microbe interactions and translating this into microbial therapeutics. While humans have been consuming microbiota-accessible foods (e.g., fiber-rich carbohydrates), microbiota-containing foods (e.g., yogurt), and fermented foods (e.g., kimchi, sauerkraut) for centuries, the development of novel therapeutic strategies is complex and has been relatively slow so far. These well-known microbiome-associated foods and treatments have been plentifully studied but have little evidence of therapeutic efficacy overall (*163*). However, metagenomic and metabolomic analyses of fecal samples now provide the opportunity to uncover specific diet related changes in the microbiome or metabolome that may have previously gone unnoticed (*164*, *165*).

As explained in the previous section, advances in preclinical research have identified many bacteria which play causal roles in regulating human health. This has opened the door for more intentional design of microbiome therapeutics, but there are many hurdles yet to overcome (*166–168*). The next generation of bacterial therapeutics will have to overcome the same limitations of current options, which largely stem from the fact that these therapeutics must associate with and attempt to modulate a complex bacterial ecosystem. Engraftment of therapeutically delivered bacteria is likely key to their efficacy but is difficult to achieve. The production of new bacterial therapeutics is additionally complicated by the fact that most strains of interest are strict anaerobes; maintaining high cell yield during production and administration of these products may be difficult (*169*, *170*). Further, questions of dose, administration regimen, and disease indications remain largely unanswered to date. Even with all of these hurdles, many new therapeutics are currently in the clinical pipeline, ranging from prebiotic diets to engineered bacteria, and it is likely that many bacterial candidates could potentially reach patients within the next 10 years.

1.4.2 Understanding pre-, pro-, syn- and post-biotics

Microbiome-modulating therapeutics fall within several broad categories. These strategies can target to deliver products upstream of bacterial utilization (prebiotics), deliver bacteria themselves (probiotics / live biotherapeutic products), or downstream bacterial products (postbiotics) (*171*).

Prebiotics, also termed microbiota-accessible carbohydrates (*172*), typically refer to food products which are not readily digested by host enzymes and instead are consumed by commensal bacteria. Dietary fibers are the most commonly used prebiotics, but other sources including oligosaccharides and sugar alcohols are becoming more common (*173*, *174*). Probiotics are living bacteria, and historically probiotics have consisted of aerobic

strains such as *Lactobacillus* which exist naturally in food products like yogurt. However, as there is little evidence for efficacy of these probiotics (*175*, *176*), many groups are transitioning to production of next generation probiotics. These next generation probiotics consist of bacterial strains with known roles in modulating host health, typically strict anaerobes derived from human fecal samples (*177*). These are also referred to as live biotherapeutic products (LBPs), and within the last 5 years the clinical development of LBPs has increased dramatically. Pre- and pro-biotics can also be intentionally paired and delivered together, a strategy which is termed a synbiotic. Synbiotics have an advantage in that the prebiotic is delivered with the bacterium which benefits from it, improving the chances that (i) the prebiotic will be fully digested into whichever metabolites have host-beneficial effects and (ii) the probiotic has access to a nutrient source which improves its potential for engraftment or metabolic output.

Finally, as these upstream strategies (pre- and pro-biotics) may have several disparate outcomes, there is also interest in developing more streamlined, downstream approaches of microbiome therapeutics. Therapeutics which consist of bacteria-derived molecules or components are termed post-biotics, and these may be effective for targeting a single or few pathways. However, the successful development of postbiotics will depend on in-depth study of the biological mechanisms imparted by individual molecules and may require additional manipulations for drug delivery.

These strategies for microbiome-modulating therapeutics, their potential and pitfalls, as well as current clinical stages will be discussed in the following sections.

1.4.3 Prebiotics and microbiota-accessible diets

Correlative and causative links between the diet and commensal microbiota are clear, so it is no surprise that dietary interventions are commonly used (*178*, *179*). Prebiotic intervention is more logistically straightforward than microbial formulations, but

compliance and consistency may still be a problem, making overarching conclusions across studies difficult (*180*).

Dietary fibers, both soluble and nonsoluble, have been widely studied in pre-clinical and clinical settings in the context of a wide variety of immune and metabolic disorders (*178*). As discussed above, dietary fibers are directly utilized by commensal bacteria, which can impact the host through expansion of these populations, production of SCFAs, or other mechanisms (*178*). However, very high concentrations of fiber (>50g/ day, nearly twice the daily recommended value) may be necessary for therapeutic effect (*181*, *182*). It is difficult to consume this much fiber in current diets with standard eating habits, making long-term adoption of this practice unlikely (*178*). Additionally, not all individuals are similarly capable of digesting dietary fiber, and this may result in undesired gastrointestinal symptoms particularly in individuals with dysbiotic microbiota (*183*, *184*). The inability to digest fiber in some individuals may be due to a lack of so called 'keystone' bacterial species which perform much of the initial degradation. *Ruminococcus bromii* has been described as one of these keystone species for the digestion of nonsoluble potato starch (*185*, *186*). Addition of nonsoluble, resistant potato starch to a standard diet increased the relative abundance of *R. bromii* in adult men, and this correlated to increased butyrate in the feces (*187*, *188*). However, subjects who did not have any detectable *R. bromii* prior to intervention showed no change over the course of the study and received seemingly little benefit of the prebiotic (*187*). Another study in healthy volunteers demonstrated that of 3 dietary fibers, only resistant potato starch increased the concentration of butyrate in the feces over the study window, and this increased butyrate correlated strongly with the relative abundance of *R. bromii* (*189*). The influences of these microbiota-effects on disease outcomes are still unknown, although several clinical studies are in progress.

One such study recently compared short-term addition of high-fiber foods or fermented foods into the diet and examined changes in both the fecal microbiome and serum

immune markers (*190*). This study allowed participants to choose the foods which they consumed, which resulted in high compliance but made it difficult to determine the effects of individual food products. Wastyk et al. demonstrated that consuming high fiber foods increased microbiome functionality, including increased expression of CAZymes and SCFA-related genes, but these individuals demonstrated little to no change in immune status before and after treatment (*190*). In contrast, consumption of a diet high in fermented foods decreased several markers of inflammation in the blood of study participants including cytokine and chemokine profiles as well as immune signaling in various cell subsets (*190*). This suggests that not all microbiome-modulating prebiotics will similarly influence the host phenotype, at least with regards to these serum readouts of inflammation. Further work from this group is working to 'reverse translate' these findings, investigating the impacts of individual dietary and microbial components in mouse models to understand mechanistic roles which may be responsible for clinical outcomes (*191*).

Prebiotics may be particularly important (and efficacious) in early life, as both the microbiota and immune system are sensitive to perturbations during this stage (*25*). Because the diet and lifestyle of infants is less varied, evidence of prebiotic efficacy in infants is much more compelling than in adults (*179*). One of the most important natural sources of prebiotics in early life is breastmilk, particularly human milk oligosaccharides (HMOs) which are readily degraded by commensal *Bifidobacterium* species. HMOs are structurally diverse and are highly abundant in human milk (*192*). Exclusively formula fed infants develop atopy and other inflammatory conditions at higher rates than breastfed infants; HMOs may play a role in this effect. HMOs have many direct and indirect effects on infant immunity including eliciting production of AMPs, modulating the intestinal epithelium, and regulating T cell differentiation and neuronal development (*192*). There has been substantial interest in prebiotic supplementation with HMOs, such that several HMO-supplemented infant formulas are now commercially available (Mead Johnson

Nutrition). Randomized controlled clinical studies supplementing infant formula with HMOs demonstrate varying degrees of efficacy. Overall results suggest that infants consuming HMO-supplemented formula have more similar fecal bacterial composition to breastfed infants (expansion of *Bifidobacterium*), fewer reported infections which necessitated antibiotics, and demonstrated an altered fecal metabolome (reviewed in (*193*, *194*)).

1.4.4 Classical probiotics, fecal microbiota transplant, and live biotherapeutic products

A probiotic is a live microorganism that, when administered in sufficient quantities, confers a health benefit on the recipient (*176*). This concept is in no way new but has been in use in several societies for centuries. However, the barrier to truly prove a 'health benefit on the recipient' has been very difficult to overcome. While probiotics have entered the market as nutritional supplements at rapid scale, the Food and Drug Association (FDA) has not approved any classical probiotics as therapeutics (*175*).

Traditionally, probiotics have consisted of readily culturable organisms within the *Lactobacillus*, *Lactococcus*, and *Bifidobacterium* genera (*175*). However, the species-level or strain-level mechanisms by which these isolates may affect host health are not clear (*175*). While some groups have shown efficacy with these probiotics in certain indications, the overwhelming evidence is that these classical probiotics, as currently administered, have minimal therapeutic impact (*163*).

As such, a necessary transition towards the development of more robust probiotics, composed of diverse bacterial taxa with established links to human health has begun. These strategies all seek to harness the diversity and multifaceted roles of gut bacteria and include delivery of whole fecal communities (fecal microbiota transplant, FMT), complex bacterial consortia, or individual species. In 2016, the FDA defined a new category of therapeutics, live biotherapeutic products (LBPs), with the strict guideline that

these compositions must include bacteria that are ‘applicable to the prevention, treatment, or cure of a disease or condition of human beings’ (*177*). FMT and LBPs are similar, but distinct, strategies to approach probiotic drug development with greater diversity, functionality, and potential efficacy by utilization of new and different microorganisms.

FMT was first posited as a treatment for enterocolitis in the 1950’s, and since then has been explored in a variety of disease indications (*195*). The idea of supplementing the fecal microbiome of a dysbiotic individual with that of a healthy, homeostatic fecal community is appealing; however, concerns over safety and efficacy remain (*196*). Administration of a replete microbiota comes with the risk of accidental introduction of pathogens to patients who are already highly susceptible to virulent organisms and has resulted in serious consequences in some patients (*197*, *198*). However, in many cases FMT has proved highly efficacious and safe, particularly for treatment of recurrent *Clostridioides difficile* infection (*196*, *199*). Efficacy of FMT has been correlated to engraftment success of donor strains, including Clostridial butyrate-producers such as *Faecalibacterium prauznitzii* (*200– 202*). Reboyta, a product of Ferring Pharmaceuticals, is now the first FMT drug to gain approval for treatment of recurrent *C. difficile* infection as of November 2022 (*203–205*). This first-to-clinic advancement will be an example to others attempting to follow this same path and opens the door for potential FMT and LBP formulations in development.

Since LBPs were officially defined in 2016, dozens of drug candidates have advanced into the clinical pipeline (*177*). These candidates are composed of varied bacterial strains including, but not limited to *Bacteroides* sp., *Clostridium* sp., and *Akkermansia*. They also target diverse disease indications including cancer, inflammatory bowel diseases and colitis, cardiovascular and metabolic diseases, asthma, and allergy (*177*, *206*).

Many of the initial LBPs moving into clinical trials consist of complex consortia, containing tens to hundreds of strains. These strain mixtures have shown some promise in early trials of safety and microbiome modulation, but engraftment remains a problem,

even with extensive antibiotic pre-treatment (*207*). A consortium product from Seres Therapeutics, SER109, demonstrated some promising results in a phase III clinical trial for recurrent *C. difficile* infection, but even these results were not sufficient, and the product failed to advance (NCT03183128) (*208*). Rational design of consortia, based on deep understanding of strains' functional capacity will likely be a more successful approach. For example, a 17-member consortium was designed to specifically include taxa capable of producing SCFAs, tryptophan metabolites, secondary bile acids, and antimicrobials (*209*). Gavage of this consortium to *Il10*$^{-/-}$ mice modulated the microbiome, altered metabolomic profiles in the feces, and reduced the severity of pathobiont-induced colitis in both preventative and therapeutic models (*209*). While this particular consortium has not yet advanced beyond pre-clinical study, this work demonstrates the potential efficacy of more controlled, functionally designed LBPs. A transition to rationally designed, small consortia or single-strain LBPs may improve quality control, replicability across studies, and overall efficacy of these products.

1.4.5 Genetically engineered LBPs

Delivery of commensal bacteria may be improved or expanded upon by engineering those species to exhibit certain functionalities. These functionalities may include digestion of unique carbohydrates to improve selective colonization, production of host-modulating compounds, degradation of drugs and environmental toxins, or sensing and response to environmental factors (*210*). Genetic engineering technologies have opened the door for precise manipulation of singular pathways in commensal bacteria, although to date these technologies have generally only been broadly applied to model organisms, such as *Escherichia coli* Nissle 1917. Expanding these tools into *Bacteroides* sp (*211*) and Clostridia (*212*) has been challenging, though broad application of these technologies will doubtless be highly impactful.

Engineering commensal bacteria to consume specialized carbohydrates is an efficient strategy to increase strain engraftment in a complex microenvironment. This successfully overcomes competition for nutrients, creating a 'personalized' metabolic niche. Members of the Sonnenburg group demonstrated this concept by introducing a gene locus into a *Bacteroides* strain which allowed consumption of porphyran, a carbohydrate found in seaweed which is rarely present in Western diets (*213*). This engineered *Bacteroides* strain was then administered to gnotobiotic mice colonized with the fecal microbiota of healthy human donors. Co-administration of porphyran dramatically increased engraftment of the engineered *Bacteroides*, such that it was able to out-compete isogenic *Bacteroides* strains and colonize colonic crypts (*213*). Others have developed similar tools to manipulate the genome of *B. thetaiotaomicron*, such that engineered strains could sense and consume specialized carbohydrates (e.g., arabinogalactan or rhamnose) *in vivo*, which stimulated production of luciferase as a signal readout (*211*). These precise, tunable LBPs may be suitable for further manipulation which could take advantage of this consistent presence in the gut to diagnose changes in the diet or metabolome and potentially even correct metabolic imbalances.

Other engineered LBPs are designed to consume toxic or harmful substances which accumulate in the gut. The most commonly targeted pathways are transformation of phenylalanine via specialized enzymes to treat phenylketonuria and nitrogen conversion in the case of hyperammonemia and urea cycle disorders (*210*). These engineered LBPs (typically *E. coli* Nissile 1917 variants) may be preferable to current treatment strategies, as continuous metabolic activity by engineered LBPs could overcome the need for repeat dosing and continuous disease monitoring. In fact, one such engineered LBP which expresses a phenylalanine lyase showed significant promise in murine and primate models (*214*) and has now advanced to early-stage clinical trials (NCT03516487).

Further examples have manipulated probiotic bacteria to produce immunological or inflammatory factors, to act as a continuous source of these proteins in the gut lumen.

Many studies of this strategy involve bacterial production of cytokines. Some early studies focused on IL-10, since this cytokine has clear immunoregulatory roles in the gut and has shown potential as a biologic for treatment of colitis (*215*). These studies utilized an engineered strain of *Lactococcus lactis*, and intragastric gavage of this bacterial strain to mice previously exposed to DSS or to *Il10*$^{-/-}$ mice resulted in reduced severity of colitis (*215*). Furthermore, in a model of cow's milk allergy, gavage with this *L. lactis*-mIL10 strain reduced sensitization to the allergen BLG as measured by reduced concentrations of BLG-specific IgE and IgG1 in the serum (*216*). More recently, a strain of *Lactobacillus reuteri* was engineered to produce IL-22, and oral administration of this bacterium induced expression of AMPs to restore intestinal epithelial barrier function and reduced severity of ethanol-induced liver injury (*217*). Phase I clinical trials are in progress for two engineered LBPs designed to deliver an IL-12 plasmid or IL-10 for cancer or type 1 diabetes, respectively (NCT04025307, NCT03751007). While continual production of cytokines in the gut lumen is an exciting prospect for immune regulation, much work in determining the dose, administration regime, and pharmacokinetics of these products is still required to monitor their safety and efficacy.

1.4.6 Synbiotics

As an alternative to genetic engineering and antibiotic pre-treatment, co-administration of a prebiotic with LBPs may similarly increase engraftment and therapeutic efficacy. This synergistic delivery of a probiotic and prebiotic is hence termed a synbiotic (*218*). According to the International Scientific Association for Probiotics and Prebiotics (ISAPP), synbiotics fall within two categories: complementary or synergistic. Complementary synbiotics are comprised of a probiotic which alone demonstrates health benefits in the host that is co-administered with a prebiotic which is specifically utilized by this probiotic and enhances its effect. Conversely, the components of synergistic synbiotics may

individually not qualify as true prebiotics or probiotics, but together confer a health benefit (*218*).

Many preclinical and clinical trials of synbiotics have been pursued (*218*, *219*). These studies have typically utilized *Bifidobacterium* or *Lactobacillus* sp. in combination with galacto-oligosaccharides (GOS), fructo-oligosaccharides (FOS), or nonsoluble fibers, and they aimed to treat varied metabolic and inflammatory conditions (*218*). While these formulations showed some promise, many suggest that greater mechanistic understanding is necessary to demonstrate selective utilization of the prebiotic and true 'synergistic' cooperation between the pre- and pro-biotics (*219*).

One such study recently demonstrated that synbiotic administration of *Bifidobacterium infantis* with HMOs resulted in selective engraftment and metabolic alteration in healthy adults (*174*). *B. infantis* produces unique and plentiful enzymes for digestion of HMOs, making this species one of the most abundant and diet-responsive taxa in the infant gut. However, *B. infantis* is essentially undetectable in adults, and typically shows little to no engraftment as a probiotic. Button et al. demonstrated that synbiotic administration allowed persistent engraftment of *B. infantis* without any antibiotic pre-treatment, but administration of this probiotic alone had no effect. In gnotobiotic mice, synbiotic treatment increased luminal butyrate, which the authors suggest results from cross-feeding between *B. infantis* and butyrate-producing Clostridia (e.g., *A. caccae*, *Eubacterium rectale*, or *Clostridium innocuum*) which utilize lactate and downstream products from the digestion of HMOs (*174*). Overall, this work and other studies of next-generation synbiotics may aid in our understanding of bacterial relationships *in vivo* and drastically increase the efficacy of current probiotics and LBPs.

1.4.7 Postbiotics

Postbiotics represent the most recently described class of microbiome therapeutics, however these therapies may have some of the greatest impact. Postbiotics are defined

as a class of therapeutics which contain ‘preparations of inanimate microorganisms and/or their components that confer a health benefit on the host’ (*220*). To date, some studied postbiotics include SCFAs, bacterial lysates, culture supernatants, exopolysaccharides, enzymes, and other vitamins and metabolites (*221*). Many of the postbiotics which have progressed into clinical trials are heat heat-killed bacterial strains or lysates (NCT05339243, NCT04151823). Some studies have demonstrated positive readouts in respiratory health, although outcomes in large cohorts remain to be seen (*222*, *223*).

We have investigated the utility of butyrate as a postbiotic and have demonstrated that targeted delivery of butyrate to the lower gastrointestinal tract (via polymer micelles) prevented and treated food allergy and colitis in mice (*92*). However, it should be noted that the recent consensus definition of postbiotics does not include synthetically produced metabolites, and these should instead be classified simply by their chemical composition (*220*).

Administration of bacterial components, rather than living cells, overcomes the need for engraftment, association with the microenvironment, and other limitations of LBPs. This strategy additionally allows for targeted delivery of isolated bacterial components, which may stimulate known pathways of host modulation without unwanted side effects otherwise elicited by living cells. However, unlike LBPs, postbiotics will likely require frequent dosing to achieve efficacy.

1.4.8 Strategies of microbiome-modulation for food allergy

To date, only one therapeutic for food allergy has advanced to the clinic: peanut oral immunotherapy (OIT) (*224*). OIT consists of continuous oral dosing with the allergen, slowly increasing the dose over a period of up to two years (*225*). This treatment is sufficient to prevent a severe allergic response upon accidental exposure, however true tolerance is not achieved, and efficacy is greatly reduced once treatment is stopped (*226*). As such, there is substantial interest in developing additional, microbiome-modulating

therapies for food allergy. These may be used alone or in combination with OIT. As described above, while OIT alone can be efficacious in achieving short-term desensitization, as many as 70% of patients exhibit some negative side effects (*227*). Most of these side-effects involve gastrointestinal issues (*224*). Many individuals with food allergies have dysbiotic microbiota (*103*, *104*) and may have disrupted epithelial barrier function, which may contribute to these symptoms of OIT. This hypothesis has led our group, and others, to pursue adjunctive or novel microbiome-therapies to target this underlying cause of food allergy (*228*).

As food allergy often presents in early childhood, and there are links between the early life microbiome and the development of atopic diseases, many microbial therapeutics target this stage. These include many prebiotics supplemented in infant formula, typically various oligosaccharides. Some studies suggest prebiotic-supplemented formula alters the fecal microbiome and metabolome to be more like that of exclusively breast-fed infants, by increasing relative abundance of *Bifidobacterium* and the acids which these species produce (e.g., lactate) (*101*, *229*). Prebiotic supplementation did not reduce the incidence of eczema at one year of age. Those infants that do develop eczema, however, have reduced abundance of butyrate-producing *Anaerostipes* and *Eubacterium* species in the feces (*101*). Overall, the World Allergy Organization suggests that the evidence does not yet support a role for prebiotics in the prevention of food allergy (*230*).

Several probiotics have been examined in the context of food allergy, both in pre-clinical and clinical settings. In mice, various bacterial consortia have shown efficacy in models of food allergy. These consortia consist of *Clostridiales* (*111*, *231*, *232*), *Lactobacillus* (*233*, *234*), *Bifidobacterium* (*234*), and *Bacteroides* (*111*). The broad diversity of bacteria studied in pre-clinical models represents many potential metabolic pathways that could be targeted by treatment with these species, but additional evidence of specific mechanisms or functional readouts is required. Most clinical studies of probiotics for food allergy to date have utilized *Lactobacillus rhamnosus GG* (LGG), which

was supplemented in extensively hydrolyzed casein formula administered to infants with CMA (*103*, *235*). While this strain did not engraft itself, LGG treatment increased the relative abundance of several Clostridial taxa, suggesting potential cross-feeding stimulated by the probiotic (*103*). Cow's milk tolerant infants also demonstrated increased concentrations of fecal butyrate which correlated with the abundance of these Clostridial taxa (*103*), and there was an observed decrease in gastrointestinal disorders in infants fed LGG (*235*). There is currently an ongoing clinical trial in Australia which will assess whether LGG improves tolerance to peanut in oral food challenges or affects levels of peanut-specific antibodies IgE and IgG4 measured in serum of children undergoing OIT (ACTRN12608000594325). Initial studies showed positive results comparing LGG plus OIT treatment to untreated controls (*236*), but this new trial will reveal whether LGG truly has an additive effect to OIT.

A defined bacterial consortium (VE416) is now also entering phase I clinical trials for treatment of peanut allergy in combination with peanut OIT (NCT03936998). This consortium, produced by Vedanta Biosciences, will be administered with or prior to OIT, and some groups will additionally receive vancomycin (theoretically to improve engraftment of the strains). FMT is also being pursued for treatment of food allergy, although there were initial safety concerns over accidental exposure to allergens via the feces (NCT02960074). The results of this study will be the first to show whether FMT is safe or effective in reducing the severity of response to an oral food challenge as much as one year after the FMT administration.

Synbiotics are also being pursued for food allergy, a method which may be simpler to administer (and potentially more effective) than complex consortia. In particular, *Bifidobacterium breve* M-16V has been explored in combination with prebiotic oligosaccharides and inulin in several reports of managing CMA in infants (*237*). Overall, this synbiotic formulation shifted the fecal microbiota of infants to increase the prevalence of *Bifidobacterium* and decrease *Eubacterium* and *Clostridium* species (similar to

breastfed infants) as described for other prebiotic/probiotic infant interventions (*101*). The synbiotic formulation did not significantly reduce incidence of allergic symptoms compared to standard formula in infants with IgE-mediated (*238*) or non-IgE mediated cow's milk allergy (*239*). However, use of this synbiotic was significantly correlated with reduced hospitalizations, infections, and antibiotic use, suggesting that microbiome-modulation by this synbiotic may have other beneficial effects on host health (*237*). We predict that transitioning into probiotic and synbiotic administration of other taxa (e.g., Clostridia), will improve the efficacy of these strategies for food allergy indications.

We have demonstrated a role for Clostridia-derived butyrate, specifically, in the prevention and treatment of food allergy in murine models (*92*). Others have studied the effects of butyrylated starch diets in a variety of disease contexts including type 1 diabetes, cancer, and rheumatoid arthritis, with mixed results (*95*, *97*, *240*, *241*). Sodium butyrate has shown promising results in clinical studies of other indications, particularly colitis, however these studies often must use intrarectal delivery to target delivery to the colon (*242–244*).

It is more difficult to deliver butyrate to the small intestine, where food allergens are absorbed and allergic responses are initiated. In our studies, we have conjugated butyrate to a polymer which self assembles into micellar structures, protecting butyrate during initial transit through the upper GI tract and allowing slow, enzymatic release throughout the lower gut, including the ileum, cecum, and colon (*92*). We showed that sodium butyrate administered by i.g. gavage did not transit past the stomach, but our micelles (containing 60mM butyrate) released butyrate in the ileum and cecum slowly over several hours, increasing the concentration of butyrate by greater than 3-fold in SPF mice (*92*).

Other literature which showed a similar increase in luminal butyrate relied on long term, *ad libitum* administration of sodium butyrate or butyrylated starches (*86, 245*). In our study, a single i.g. gavage of sodium butyrate did not transit past the stomach (*92*), but some other publications have shown that long term *ad libitum* administration can affect the lower

GI tract, although this is not a clinically relevant route of administration. For example, feeding sodium butyrate at a dose of 36mM in the drinking water *ad libitum* for at least one week to antibiotic-treated mice also increased the concentration of cecal butyrate by approximately 3-fold (*86*). Administration of butyrylated starches to rats over a period of four weeks doubled the concentration of luminal butyrate in the cecum and colon (*245*). The butyrate micelles achieved similar increases in luminal butyrate after only a single i.g. gavage, while additionally releasing in the ileum (*92*). This controlled drug delivery system is likely to be a better candidate for clinical applications of butyrate in food allergy than these other strategies.

An ongoing clinical trial is testing whether administration of butyrylated starch to peanut allergic adults improves efficacy and reduces side effects of OIT (ACTRN12617000914369). As standard, nonsoluble potato starch has also been shown to increase fecal butyrate (*189*), an interventional study at the University of Chicago is administering potato starch to children undergoing peanut OIT and assessing similar outcomes (NCT05138757).

While microbiome-modulating therapeutics for food allergy represent a relatively young field, interest and progress in this area are quickly growing. Correlative and causative links between the commensal microbiota and food allergy are strong; targeting the microbiome may address the underlying cause of food allergy. Additionally, these therapeutics are antigen agnostic – many individuals have allergies to several different foods, and this issue is not addressed by OIT. Our group is developing microbiome-modulating therapeutics for food allergy based on our deep understanding of Clostridial regulation of epithelial barrier function and mucosal immunity. The following section will describe the proposed therapeutic strategy used in this thesis project.

1.4.9 Proposed strategy: Anaerostipes caccae as a single-species LBP administered as a synbiotic with lactulose

The fecal microbiome of healthy infants is distinct from that of infants with CMA, including increased representation of Clostridial species and decreased Gram-negative taxa (*103*, *104*, *159*). Previous work from our lab identified a single species, *Anaerostipes caccae*, which was more abundant in healthy infants and prevented the allergic response to the cow's milk allergen BLG in monocolonized mice (*104*). We now suggest that *A. caccae* may be used as therapeutic LBP to prevent or treat food allergy in mice with dysbiotic microbiota. We isolated a novel strain of *A. caccae*, termed *A. caccae* LAHUC, from the feces of a healthy infant in a manner which is suitable for clinical translation. With a candidate LBP strain in-hand, we characterized this species to optimize its efficacy.

A. caccae is a butyrate producing species in the family Lachnospiraceae (*246*). In fact, it produces the highest concentration of butyrate compared to other species in an *in vitro* model (*63*). *A. caccae* often forms cross-feeding relationships with other bacteria which perform initial degradation of large polysaccharides to produce small metabolites including lactate and acetate which *A. caccae* can convert to butyrate (*247*, *248*). *A. caccae* is specifically dependent on lactate, and in the presence of this metabolite may produce butyrate more efficiently than in culture with sugars alone (*63*). These cross-feeding relationships have been described in detail between *A. caccae* and several primary-degrader species including *Bifidobacterium*, *Akkermansia*, or other lactate- or acetate- producing species (*249–251*). We propose that butyrate production is critical to *A. caccae*'s therapeutic effect *in vivo*, and that this may depend on the formation of cross-feeding relationships with other resident bacterial species.

It was not known whether *A. caccae* would be able to survive or produce butyrate when introduced into a replete microenvironment *in vivo*, we predicted that it would not. We thus approached a synbiotic method: administering *A. caccae* with prebiotics designed to improve its growth and metabolic opportunity. There was some known precedent for this strategy. In a previous study, administration of *A. caccae* plus GOS (a Bifidogenic

prebiotic acquired from Yakult) increased the concentration of SCFAs including butyrate in the colon of SPF rats (*252*).

Due to *A. caccae*'s dependence on lactate and beneficial relationships with *Bifidobacteria*, we chose to focus on lactulose as our primary prebiotic of interest. Lactulose is a noncaloric, semi-synthetic disaccharide with a similar chemical structure to lactose. However, unlike lactose, lactulose is not broken down by host enzymes and is accessible for bacterial digestion (*253*). Lactulose was initially produced for medicinal use; at high doses it is effective for management of constipation and hepatic encephalopathy (*253*). In the colon, lactulose is broken down by commensal microbiota, namely *Bifidobacterium* and *Lactobacillus* sp., which produce high concentrations of acids, degrade urea, and regulate colonic motility (*253*).

In more recent years, low-dose lactulose has been explored as a prebiotic, as its 'Bifidogenic effect' is well recognized (*253*). The enhanced abundance of *Bifidobacterium* and its production of lactate may in turn increase butyrate production. *In vitro* culture systems which mimic colonic microbiota demonstrated that addition of lactulose increased the relative abundance of *Anaerostipes* and modestly increased butyrate accumulation in a dose-dependent manner (*254*). Another such system demonstrated that lactulose introduction into a 'dysbiotic' fecal community reduced the growth of *C. difficile* (*255*). Low-dose lactulose has also been studied for its prebiotic properties in pre-clinical and clinical settings. These studies have confirmed the increases in abundance of *Bifidobacteria* and corresponding decreases in abundance of *Bacteroidaceae* (*256*). However, low-dose lactulose only modestly increased butyrate in SPF mice (*257*) and there is not yet conclusive evidence to suggest any change in fecal butyrate in healthy adults (*256*).

We predict that synbiotic administration of lactulose with *A. caccae* will overcome the limitations of these studies, completely fermenting lactulose into butyrate via a multi-step, multi-species process. Lactulose will first be digested by resident commensal bacteria (*Bifidobacteria*) into lactate, which *A. caccae* will readily convert into butyrate. This

synbiotic has the potential to modulate host immune responses through a variety of mechanisms, including expansion of *Bifidobacteria*, introduction of an allergy-protective Clostridial species, and production of immuno-regulatory butyrate. In the following chapters, we will describe our isolation of *A. caccae* LAHUC and characterization of this strain *in vitro*. We will further describe mechanisms by which this species, or other bacterial communities or metabolites, can modulate epithelial barrier integrity in mice. Finally, we will describe our progress towards developing this synbiotic. Our synbiotic effectively prevents cow's milk allergy in gnotobiotic mice which are colonized with the fecal microbiota of a dysbiotic, CMA infant. Additionally, the synbiotic treats established peanut allergy in antibiotic-exposed SPF mice that were previously sensitized to PN. This synbiotic strategy has potential to address many underlying microbial deficiencies which have been correlated to immune dysregulation, and our formulation may be a clinically relevant new therapy for food allergy.

CHAPTER 2

METHODS

2.1 Bacterial *in vitro* fermentation

Bacteria were cultured within a plastic film anaerobic chamber (Coy Labs) within a 37°C incubator. Gas mix within the isolator was maintained with 2.5% hydrogen and <50ppm oxygen. Bacteria were cultured in various anaerobically reduced media (see descriptions and source in **Table 2.1**). Isolated strains were stored as frozen stocks in 25% glycerol. Infant feces were stored in the form of a homogenous slurry preserved in 25% glycerol and frozen at -80°C (*104*). For all culture experiments, cells from frozen stocks were inoculated into primary cultures, grown to peak growth (24-48h), and passaged into secondary, experimental cultures. To achieve approximately equal cell numbers passaged into secondary cultures, inoculation volume was tailored such that 10μl of primary culture at OD_{600}=1.0 would be transferred (e.g., 20μl of a culture with OD_{600}=0.5). For co-cultures, the inoculation volume was halved; the equivalent of 5μl of primary culture at OD_{600}=1.0 was transferred from each primary culture. Following secondary cultures, cell fractions or supernatants were maintained for further analysis. For bacterial enumeration, frozen stocks or primary cultures were serially diluted from 10^{-1} to 10^{-8} and plated on anaerobic BHI agar plates. Colonies were counted after 2-4 days of growth within the anaerobic incubator. For testing motility and indole production, primary cultures of bacteria (*A. caccae* LAHUC or a consortium of murine-derived Clostridia) were dipped into anaerobically reduced PYG medium containing 0.175% agar and incubated for 48h at 37°C under anaerobic conditions. 1mL of Kovac's reagent (Sigma-Aldrich) was added to the top of cultures for analysis of indole production.

Table 2.1: Bacterial culture media

Medium	Form	Additive	Vendor
Chopped meat glucose (CMG)	Broth	N/A	Anaerobe Systems
Peptone yeast (PY)	Broth	N/A	Anaerobe Systems
Peptone yeast (PY)	Broth	Glucose (10mg/mL)	Anaerobe Systems
Peptone yeast (PY)	Broth	Sucrose (10mg/mL)	Anaerobe Systems
Peptone yeast (PY)	Broth	Lactose (10mg/mL)	Anaerobe Systems
Peptone yeast (PY)	Broth	Cellobiose (10mg/mL)	Anaerobe Systems
Peptone yeast (PY)	Broth	Potato Starch (10mg/mL)	Anaerobe Systems
Peptone yeast (PY)	Broth	Myo-inositol (10mg/mL)	Anaerobe Systems (PY), Sigma (MI)
Peptone yeast (PY)	Broth	Lactulose (10mg/mL)	Anaerobe Systems (PY), Sigma (LU)
Brain heart infusion (BHI)	Agar	N/A	Anaerobe Systems
Trypticase soy broth (TSB)	Broth	N/A	Corning

2.2 Isolation of *A. caccae* from infant feces

Fecal slurry from healthy infant donor 2 (*104*) was plated (100μl) on BHI agar plates supplemented with ciprofloxacin (16μg/ml) or a combination of four antibiotics (16μg/ml ciprofloxacin, 6μg/ml gentamycin, 5μg/ml aztreonam, and 10μg/ml colistin) as previously described (*56*, *258*) and grown for 72h at 37°C anaerobically to develop a full lawn. *A. caccae* (DSM 147662) was grown from a glycerol stock as a positive control. Total bacterial growth was scraped and suspended in 1mL of 25% glycerol in PBS solution and is referred to as the primary culture. An aliquot of this mixture was spun at 800xg for 10 minutes to pellet cells, isolate DNA, and perform PCR/qPCR. The remaining volume was stored at -80°C. For any samples that demonstrated high concentration of *A. caccae* by

qPCR, the frozen primary culture was thawed and plated on BHI agar with dilutions from 10^{-1} to 10^{-8}. Dilution plates were incubated anaerobically for 72h at 37°C, then individual colonies were picked, inoculated in CMG broth, and grown for 48h anaerobically at 37°C. After incubation of individual colonies, 1mL of culture broth was aliquoted and diluted to 25% glycerol and separated as above for DNA isolation and storage at -80°C. Any colony(s) which appeared to be *A. caccae* by PCR were passaged sequentially two more times and final stocks of *A. caccae* LAHUC were stored at -80°C in CMG with 25% glycerol. The 16S sequence of *A. caccae* was analyzed by PCR and qPCR with species-specific primers and by Sanger sequencing (**Table 2.2**).

2.3 Isolation of bacterial DNA from cultured cells or feces

Bacterial DNA was isolated from *in vitro* cultures and fecal samples for PCR and qPCR analysis using the PowerSoil Pro kit (Quiagen) according to the manufacturer's protocol. Cells from 1mL of culture were pelleted by spinning at 800xg for 5 minutes, supernatant was removed, and cell pellet was transferred to a PowerSoil tube. For mouse fecal pellets, 1-2 pellets were used per reaction after recording fecal weight.

2.4 Antibiotic plate culturing

To examine antibiotic resistance, antibiotic coated disks were placed on BHI agar plates, on which *A. caccae* LAHUC had been spread. Antibiotics consisted of streptomycin (10μg, Fisher Scientific), kanamycin (30μg, Fisher Scientific), tetracycline (30μg, BD), and ampicillin (10μg, Fisher Scientific). Distance of growth inhibition from the center of each disk was measured after 4 days of growth in the anaerobic incubator.

2.5 PCR and qPCR of bacterial abundance

The abundance of bacteria was assessed by total copies 16S using qPCR with universal primers (**Table 2.2**). Primers specific for the 16S sequence of individual taxa were identified from the literature (**Table 2.2**). DNA amplification and visualization with qPCR utilized PowerUp SYBR green master mix (Applied Biosystems) on a QuantStudio 3 qPCR machine (Thermo Fisher Scientific) according to manufacturer's instructions. The abundance of individual bacterial taxa was calculated by 2^{-CT}, multiplied by a constant (10^{16}) to bring all values above 1, and normalized per gram of raw fecal content.

Table 2.2: Primer sequences for PCR and qPCR of bacterial taxa.

Target	Type	Sequence	Ref.
A. caccae, F	Bacterial 16S	GTTTTCGGATGGATTTCCTATAT	(*259*)
A. caccae, R	Bacterial 16S	GTTTTCGGATGGATTTCCTATAT	(*259*)
Bifido., F	Bacterial 16S	CTCCTGGAAACGGGTGG	(*260*)
Bifido., R	Bacterial 16S	GGTGTTCTTCCCGATATCTACA	(*260*)
8F	Bacterial 16S	AGAGTTTGATCCTGGCTCAG	(*261*)
338R	Bacterial 16S	TGCTGCCTCCCGTAGGAGT	(*262*)

2.6 Whole genome shotgun sequencing

DNA isolation and sequencing was performed by CosmosID™. DNA from cell pellets was isolated using the QIAGEN dNeasy PowerSoil Pro Kit according to the manufacturer's protocol. Extracted DNA samples were quantified using Qubit 4 fluorometer and Qubit™ dsDNA HS Assay Kit (Thermofisher Scientific). DNA libraries were prepared using the Thermo

Fisher IonXpress Plus Fragment Library Kit, according to the manufacturer's protocol. DNA libraries were quantified using Qubit 4 fluorometer and Qubit™ dsDNA HS Assay Kit. Libraries were then sequenced on a Thermo Ion S5 XL sequencer. Single nucleotide polymorphisms (SNPs) were identified within a core genome defined by orthologous sequences conserved in aligned genomes.

2.7 Quantification of short chain fatty acids

Butyrate, acetate, and propionate concentrations from culture supernatants and cecal samples were measured by reverse phase high precision liquid chromatography (HPLC) UV-Vis on an Agilent 1290 UHPLC as previously described (*92*, *263*). Lactate concentration was measured using a Lactate Assay Kit (Sigma-Aldrich) according to manufacturer's instructions. Samples for HPLC UV-Vis were derivatized with 0.25M 1-ethyl-3-(3-dimethylaminopropyl)carbodiimide (EDC) and 0.2M 3-nitrophenylhydrazine (NPH), in 1:1 water: acetonitrile (AcN, v/v). Cecal contents were stored at -80°C, thawed and diluted to 0.1g/mL in 1:1 AcN:H_2O, vortexed for 10 minutes to mix well, then spun at 10,000xg for 10 minutes and the supernatant was used for analysis. For *in vitro* cultures, cells were pelleted by centrifuging at 10,000xg for 5 minutes and culture supernatants were aliquoted and stored at -80°C. Samples were diluted in 1:1 AcN:H_2O and mixed with EDC and NPH stock solutions at a 1:1:1 volumetric ratio and heated for 30 minutes to perform the reaction. 2'ethyl-butyric acid was used as an internal standard. Glacial butyric acid, acetic acid, and propionic acid (Sigma) were used for quantitative standards. 5μl of sample was injected via autosampler and flowed through a Thermo Fisher C18 column (4.6x50mm) at room temperature (RT). Mobile phases were H_2O with 0.1% formic acid (A) and AcN with 0.1% formic acid (B). The mobile phase gradient ran from 15% mobile phase B at 0 min, 100% mobile phase B at 3.5 min, 100% mobile phase B at 6 min, 15%

mobile phase B at 6.5 min with a 0.5ml/min flow rate. Peaks were quantified on a UV-Vis detector at 400nm.

2.8 Bacterial lyophilization

The process for lyophilization of bacterial cultures is shown in **Fig. 3.19**. *A. caccae* LAHUC was cultured for 24h in CMG medium at 37°C under anaerobic conditions. Cultures were spun at 10,000xg for 10 minutes to pellet cells, supernatant was discarded, and cells were resuspended in cryopreservant (10% sucrose or Reagent 18 (ATCC Bacteriology Culture Guide)). This solution was transferred into sterilized flute-neck glass ampules, which were topped with glass wool and frozen at -80°C. Ampules were then lyophilized overnight on dry ice into smooth powders. Ampules were heat sealed and stored at RT.

2.9 Mice

Gnotobiotic mice were bred and housed within the University of Chicago Gnotobiotic Research Animal Facility (GRAF). Germ free C3H/HeN mice were bred and housed in Trexler-style flexible film isolators (Class Biologically Clean) within Ancare polycarbonate mouse cages (N10HT). Gnotobiotic mice were weaned at 21 days of age and were fed an autoclaved, plant-based mouse chow. Specific pathogen free (SPF) C3H/HeN mice were transferred from our gnotobiotic colony and bred in house in an SPF colony free of murine norovirus (MNV), *Pasteurella*, *Helicobacter* spp, and SFB. SPF mice were weaned at 21 days of age and were fed an autoclaved, plant-based mouse chow (Purina Lab Diet 5K67) and autoclaved sterile water. All mice were housed in cages containing autoclaved Teklad Pine Shavings (cat# 7088) with a 12 hour light/dark cycle at a standard RT of 20-24°C. All mice are euthanized by CO_2 asphyxiation followed by cardiac exsanguination as a secondary measure. All experiments were littermate controlled and performed in

accordance with 'The Guide for the Care and Use of Laboratory Animals (8th edn)'. All experiments were approved by the Institutional Animal Care and Use Committee of the University of Chicago.

2.10 Colonic mucus isolation

Mucus of SPF mice was collected as described in (*264*). Colonic tissue was excised, opened longitudinally, and mucus was scraped into HEPES-Hank's buffer. Epithelial cells were removed by centrifugation at 12,000xg for 10 minutes, then 20,000xg for 15 minutes at 4°C. Mucus from 4 mice of each genotype was pooled and stored at -80°C.

2.11 Colonization of germ free mice with human fecal bacteria or *A. caccae* LAHUC

Human donor microbiota (healthy or CMA, (*104*)) were maintained by serial passage in C3H/HeN mice which served as live repositories. Repository mice were initially colonized by i.g. gavage with a fecal slurry from the infant donor at weaning. These initial colonizations occurred in 2017 (healthy donor 2) or 2019 (CMA donor 6). Subsequent recipients were colonized at weaning by an i.g. gavage with a fecal slurry from a live repository mouse. Feces were collected just prior to use, and a single pellet was suspended in 1mL sterile PBS. The pellet was crushed, pieces were allowed to settle, and 250μl was gavaged to each recipient mouse. The fecal composition of repository mice and all experimental mice was confirmed by 16S rRNA sequencing for success of colonization and long-term maintenance of the donor phenotype. To best maintain the engraftment of human infant feces in mice (*104*), all mice were fed infant extensively hydrolyzed casein infant formula (EHCF, Nutramigen Hypoallergenic Infant Formula) *ad libitum*. Formula is diluted 1:10 in sterile cell grade water and provided in cage water bottles. For monocolonization with *A. caccae* LAHUC, GF C3H/HeN mice were i.g.

gavaged once at weaning with 10^6 CFU of *A. caccae* in 250μl from frozen culture stocks in 25% glycerol stored at -80°C. Control mice received a single gavage of sterile CMG medium. Experimental mice for monocolonization experiments were housed in positive-pressure cages in a gnotobiotic rack system.

2.12 Cell preparations from intestinal tissue, mesenteric lymph nodes, and spleen

Single cell suspensions were prepared from ileum lamina propria, mesenteric lymph nodes (mLN), or spleens. Spleens were harvested, crushed through a 70μm filter (Thermo Fisher), and rinsed with RPMI containing 4% fetal calf serum (FCS). Cell suspensions were treated with Red Blood Cell Lysis Buffer Hybri-Max (Sigma-Aldrich) for 10 minutes on ice, and finally resuspended in RPMI+4% FCS for cell counting (Countess). The cecal-colon-draining and ileum-draining lymph nodes (iLN, cLN) were anatomically identified following the literature (*145*). mLNs were digested for 30 minutes with 40μg/mL Liberase^{TM} (Roche) and 40μg/mL DNAse1 (Sigma-Aldrich) in RPMI+4% FCS, then rinsed through a 70μm filter (Thermo Fisher) and resuspended for further use. To isolate lamina propria lymphocytes from the ileum (defined as the terminal 10cm of the small intestine), Peyer's patches were excised from the tissue during dissection. Epithelial cells (IECs) were first removed by incubating for 20 minutes on ice in PBS containing 30mM EDTA and 1.5mM DTT. Tissues were then incubated for 10 minutes in PBS-EDTA at 37°C, then shaken by hand to separate IECs from underlying tissue. Remaining LP tissue was digested in RPMI media containing 4% FCS, Liberase^{TM} and DNAse1 for 40 minutes at 37°C with shaking. Cells were rinsed through a 70μm filter and lymphocytes were eluted using an 80/40 Percoll gradient. Single cells were enumerated and used for following protocols.

2.13 RNA isolation and RT-qPCR

For RNA analysis, IECs were harvested as described above and stored in Trizol at -80°C. Intestinal lamina propria samples were fixed in RNAlater at 4°C overnight before long term storage at -80°C. For RNA-extraction, whole tissue samples were transferred into Trizol and physically disrupted by shaking at 30bps for 2min in SafeLock tubes containing a 5mm stainless steel bead. Single cell IEC suspensions were pipetted to lyse cells. RNA was extracted using the PureLink RNA Mini Kit (Ambion/Invitrogen) according to manufacturer's recommendations.

Table 2.3: Primer sequences for RT-qPCR of murine gene expression.

Target	Sequence	Ref.
HPRT, F	TGAAGAGCTACTGTAATGATCAGTCAAC	(*265*)
HPRT, R	AGCAAGCTTGCAACCTTAAGCA	(*265*)
IL10, F	CAGGGCCCTTTGCTATGG	GenScript
IL10, R	GATCTCCCTGGTTTCTCTTCC	GenScript
IL22, F	TTGAGGTGTCCAACTTCCAGCA	(*266*)
IL22, R	AGCCGGACGTCTGTGTTGTTA	(*266*)
IL25, F	GAGTTGGACAGGGACTTGAA	GenScript
IL25, R	AGGTGGTGAGCATGACTAAG	GenScript
IL33, F	TCCTTGCTTGGCAGTATCCA	*(267)*
IL33, R	TGCTCAATGTGTCAACAGACG	*(267)*
Reg3b, F	ATGGCTCCTACTGCTATGCC	*(265)*
Reg3b, R	GTGTCCTCCAGGCCTCTTT	*(265)*
Reg3g, F	ATGGCTCCTATTGCTATGCC	*(265)*
Reg3g, R	GATGTCCTGAGGGCCTCTT	*(265)*
Muc2, F	ATGCCCACCTCCTCAAAGAC	*(268)*
Muc2, R	GTAGTTTCCGTTGGAACAGTGAA	*(268)*
TSLP, F	GTAGTTTCCGTTGGAACAGTGAA	*(269)*
TSLP, R	GCAGTGGTCATTGAGGGCTTC	*(269)*

RNA expression in tissue samples was quantified by reverse transcription quantitative polymerase chain reaction (RT-qPCR) as previously described (*53*). RNA was reverse transcribed into cDNA using the iScript cDNA Synthesis Kit (BioRad). cDNA amplification performed with Quantinova SYBR green PCR Kit (Quantinova) on a QuantStudio 3 qPCR machine (Thermo Fisher Scientific) according to the manufacturer's instructions. Primer sequences are listed in **Table 2.3**. Gene expression was calculated by 2^{-CT} relative to a housekeeping gene, HPRT, and normalized to the average expression of the control group within each experiment.

2.14 Colonic mucus and goblet cell histology

Tissue sections of the distal colon were harvested and preserved in Carnoy's fixative for histological analysis as previously described (*53*). Fixed tissues were paraffin embedded, cut in transverse cross-sections, and stained with periodic acid Schiff (PAS) by the UChicago Histology Tissue Resource Center. Slides were imaged with a Cri Pannoramic SCAN 40x Whole Slide Scanner. Goblet cells and mucus thickness were quantified using ImageJ.

2.15 Synbiotic treatment

Gnotobiotic mice were treated with 10^6 CFUs of *A. caccae* LAHUC in 200μl by daily i.g. gavage following the timelines outlined within each figure. *A. caccae* LAHUC stocks were grown in anaerobic CMG for 24 hours and stored in 25% glycerol at -80°C. A new vial of this *A. caccae* LAHUC glycerol stock was thawed for each treatment. All control groups received gavages of 200μl sterile CMG with 25% glycerol. Lactulose was administered to gnotobiotic mice *ad libitum* at a final concentration of 5g/L in the 1:10 EHCF : water supplied in mouse water bottles. For studies utilizing lyophilized *A. caccae* LAHUC, 500μl of bacterial culture was lyophilized and resuspended in 2.5mL sterile,

anaerobically reduced PBS in an anaerobic chamber just prior to gavage. Mice were gavaged with 10^7 CFUs of *A. caccae* LAHUC resuspended in sterile PBS or with 200μl of sterile PBS. Lactulose was administered to SPF mice *ad libitum* at a final concentration of 5g/L in sterile water.

2.16 16S rRNA sequencing and analysis

16S rRNA sequencing and analysis was performed by the University of Chicago Duchossois Family Institute Microbiome Metagenomics Facility as previously described (*92*). Bacterial DNA was isolated using the QIAamp PowerFecal Pro DNA kit (Qiagen) according to manufacturer's protocol. 16S rRNA V4-V5 hypervariable regions were amplified using the following primers: 563F (5'-nnnnnnnn-NNNNNNNNNNNN-AYTGGGYDTAAA-GNG3') and 926R (5'-nnnnnnnn-NNNNNNNNNNNN-CCGTCAATTYHT- TTRAGT-3'), where 'N' represents the barcodes and 'n' represents additional nucleotides added to offset primer sequencing. Dual index adapters were ligated onto amplified pools which were compatible with Illumina sequencing (QIAsep 1-step amplicon library kit, Qiagen). Prepared libraries underwent quality control with Qubit and Tapestation, then were sequenced on an Illumina MiSeq machine. Forward and reverse reads (250 bp) were analyzed for amplicon sequence variants (ASVs) using the divisive amplicon de-noising algorithm (DADA2 v1.14) and taxonomy was assigned according to the Ribosomal Database Project (RDP). Assigned ASVs, taxonomy, and metadata were compiled into a phyloseq data package and further analyzed with R studio version 4.2.1. Principle component analysis was performed and analyzed in Orange3 software. Linear discriminant analysis effect size (LEfSe) was analyzed in R Studio to determine differences in relative abundance of individual taxa. The microbiomeMarker package and run_Lefse functions were used for LEfSe analysis, effect size was computed as LDA score (*270*, *271*). ASVs were compared at the genus level, using a significance

level of 0.05 for Kruskall-Wallis and Wilxicon tests and a linear discriminant analysis cut-off of 1.0.

2.17 FITC-dextran assay for epithelial permeability

Mice were fasted for 3 hours before receiving a single i.g. gavage with 4kDa FITC-dextran dosed at 500mg/kg bodyweight (*92*). Blood was collected by cardiac puncture at either 2h post-gavage for gnotobiotic mice or 1.5h post-gavage for SPF mice. Differing times are due to different intestinal motility across microbiota backgrounds; times were chosen such that FITC-dextran would transit entirely through the small intestine but not yet reach the colon (as examined visually during dissection). Blood was allowed to clot in SST Microtainer Serum tubes (BD) at RT in the dark for 30min, then spun at 12,000xg for 7 minutes to separate the serum. Serum was diluted 1:3 in PBS and plated in duplicate on black flat bottom polystyrene 96 well plates (Corning). Stock FITC-dextran was added to 1:3 normal mouse serum (NMS, Jackson ImmunoResearch) to PBS and serially diluted 1:2 for a standard curve. 1:3 NMS:PBS was used as a blank. Fluorescent excitement (485nm) / emission (528nm) spectra were measured using a SpectraMax M3 reader (Molecular Devices).

2.18 Intestinal explants

To measure cytokine expression in intestinal tissues *ex vivo*, ileal (distal 10cm of small intestine), jejunal (5cm just proximal to ileum), or colonic tissues were harvested, flushed with PBS, cut open longitudinally, and stored in HBSS (Corning Cellgro) supplemented with 50μM 2-mercaptoethanol, 100U/mL penicillin/streptomycin, 0.25μg/mL Fungizone and 10μg/mL gentamicin. Tissues were cultured at 50mg/mL (colon) or 100mg/mL (small intestine) in DMEM (HyClone) containing 10% FCS, 10mM HEPES, 50μM 2-mercaptoethanol, 100U/mL penicillin/streptomycin, 0.25μg/mL Fungizone, 2mM L-

glutamine, 0.1mM nonessential amino acids and 1mM sodium pyruvate for 24h at 37°C. Duodenal tissues were stimulated with 10ng/mL recombinant murine IL-23 (Invitrogen). IL-22 concentration in culture supernatants was measured by ELISA (Biolegend) according to the manufacturer's instructions.

2.19 Splenocyte restimulation and cytokine quantification

To quantify cytokine production, splenocytes from mice collected 24h post-challenge were plated at $2x10^6$ cells/mL in complete DMEM containing 10% FCS, 10mM HEPES, 50μM 2-mercaptoethanol, 100U/mL penicillin/streptomycin, and 2mM L-glutamine. Samples were additionally stimulated with either 10mg/mL BLG or 1μg/mL anti-CD3 (Invitrogen) plus 1μg/mL anti-CD28 (Invitrogen) antibodies for 72h. Cells were then pelleted by centrifugation at 800xg for 5 minutes and supernatants were collected for analysis. Cytokine concentrations including IL-13 (Invitrogen), IL-5 (BioLegend), and IL-9 (Thermo Scientific) were measured by ELISA according to manufacturer's instructions.

2.20 ELISpot assay for quantification of IgG1- and IgE- secreting cells

ELISpots for total IgE and BLG-specific IgG1 were performed from single cell suspensions prepared as described in section 2.12. For BLG-specific IgG1, PVDF membrane plates were coated with 10μg/ml BLG overnight, blocked with PBS with 5% FCS for 2h at 37°C, then cells were plated in dilutions (500,000; 250,000; 125,000) in triplicate and incubated for 16h at 37°C. Cells were then washed off with 5 washes of PBS + 4% FCS, and detection antibody (anti-IgG1-HRP, Southern Biotech) was added for 2hrs at RT. Plates were then washed and developed with tetramethylbenzidine (TMB) for membranes (Sigma-Aldrich). Total IgE ELISpots were detected using an ELISpot Flex: Mouse IgE (HRP) ELISpot kit (Mabtech) according to manufacturer's instructions. Single

cell suspensions were incubated for 5 days at 37°C in complete DMEM. Cells were either unstimulated or cultured in IgE stimulating conditions (0.5μg/mL anti-CD40 and 10ng/mL IL-4) plus 1mg/mL BLG.

2.21 Flow cytometry

For flow cytometric analysis of CD4 T cell populations (Treg, Tfh, Tfr), single cell suspensions from mLN were prepared as described in section 2.12. Single cells were plated in 96 well round bottom assay plates and stained with Live/Dead Fixable Aqua (ThermoFisher) cell viability dye. Cells were then stained with antibodies targeting cell surface markers in PBS + 4% FCS at RT for 20 minutes. Antibodies for cell surface markers included anti-mouse CD3, CD4, CD25, PD1, and CXCR5 (**Table 2.4, 2.5**). Cells were fixed overnight at 4°C using the eBioscience Foxp3/Transcription Factor Staining Buffer set and permeabilized prior to intracellular staining (Invitrogen). Cells were stained with antibodies for nuclear transcription factors (Foxp3, Rorγt, Gata3, Bcl6) in permeabilization buffer at RT for 40 minutes. Cells were analyzed on an Attune Nxt Flow Cytometer (Thermo Fisher) or Aurora Spectral flow cytometer (CytekBio). Antibody clones and panels are shown in **Tables 2.4** and **2.5**.

Table 2.4: Antibodies for flow cytometric analysis of Tregs

Marker	Fluorophore	Vendor	Cat	Isotype
Viability Dye	Live Dead Aqua	Fisher	L34966	-
Rorγt	BV421	BD Horizon	Q31-378	Mouse IgG2a, k
CD4	BUV605	BioLegend	RM4-5	Rat IgG2a, k
Foxp3	AF488	eBioscience	FJK-16S	Rat IgG2b, k
CD3	PerCP/Cy5.5	BioLegend	145-2C11	Armenian hamster IgG
CD25	PE/Cy7	eBioscience	PC61.5	Rat IgG2a, k
Gata3	AF647	BD	L50-823	Mouse IgG1, k

Table 2.5: Antibodies for flow cytometric analysis of Tfh/Tfr cells

Marker	Fluorophore	Vendor	Cat	Isotype
Viability Dye	Live Dead Aqua	Fisher	L34966	-
Rorγt	BV421	BD Horizon	Q31-378	Mouse IgG2a, k
PD1 (CD279)	BUV605	Biolegend	29F.1A12	Rat IgG2a, k
CD25	BV650	Biolegend	PC61	Rat IGg1, l
Gata3	AF488	Invitrogen;	twai	Mouse IgG1, k
CD3	PerCP/Cy5.5	BioLegend	145-2C11	Armenian hamster IgG
Bcl6	PE	BD	K112-91	Mouse IgG1, k
Foxp3	PE/Cy7	Invitrogen	FKJ-16S	Rat IgG2b, k
CXCR5 (CD185)	APC	Biolegend	L138D7	Rat IgG2a, k
CD4	AF700	Invitrogen	RM4-5	Rat IgG2a, k

2.22 BLG sensitization and challenge

Mice were sensitized weekly with 20mg BLG + 10μg CT by i.g. gavage for 5 weeks beginning one-week post-weaning as previously described (*104*). For each sensitization, mice were fasted for 3 hours in the morning, then received a gavage with 0.2M sodium bicarbonate; 20mg BLG + 10μg CT was gavaged 30min later. One week after the last sensitization, mice were challenged i.g. with 200mg BLG. Again, mice were fasted for 3 hours, gavaged with 0.2M sodium bicarbonate, then received 2 doses of 100mg BLG i.g. 30min apart. Core body temperature was measured immediately following the first BLG gavage and every 10 minutes thereafter with a rectal temperature probe (PhysiTemp) and serum was collected 90min later for measurement of mMCPT-1. Serum mMCPT-1 was measured by ELISA (Invitrogen) according to manufacturer's instructions. Mice were

euthanized 24h later. For ELISpot experiments, mice were sensitized 4 times with 20mg BLG + 10μg CT as described above. In these experiments, the first sensitization occurred 4 days post-weaning; sensitizations were 5 days apart. Following the last sensitization, mice were challenged with 75mg BLG i.g. in a single dose. Mice were euthanized 7 days later.

2.23 Peanut sensitization and challenge

Mice were sensitized to PN as previously described (*92*). All mice were age-matched and littermate controlled. Beginning one week prior to weaning (day 14 of life), mice were i.g. gavaged daily with 0.45mg vancomycin until weaning. On the day of weaning, and weekly for 4 weeks, mice were sensitized i.g. with 6mg PN extract + 10μg CT, except during the first week during which mice only received 5μg CT. PN extract was prepared in house from unsalted roasted peanuts (Hampton Farms) as previously described (*53*). For sensitizations, mice were fasted for 4-5h in the morning, then gavaged with 0.2M sodium bicarbonate 30min before the PN+CT gavage. Mice received 200mg/L vancomycin in the drinking water throughout the sensitization period. One week after the last sensitization, mice were randomly assigned treatment groups and transferred to a BSL2 animal housing facility. One group of mice was challenged at this point to confirm uniform sensitization. For challenge, mice were i.p. injected with 1mg PN extract, and core body temperature was measured with a rectal temperature probe (PhysiTemp). Following 2 weeks of treatment as described in the text, mice were challenged with 1mg PN i.p. and core body temperature was measured. Blood was collected 70min post-challenge for measurement of mMCPT-1 in serum by ELISA (Invitrogen). Mice were euthanized one week later.

2.24 Measurement of antigen-specific antibodies by ELISA

BLG-specific IgG1 and IgE (*104*), and PN-specific IgG1 and IgE (*53*, *92*) were measured in serum by ELISA as previously described. Plates were coated overnight with antigen (100μg/mL BLG or 40μg/mL in 100 mM carbonate-bicarbonate buffer) at 4°C. Plates were blocked with PBS + 4% BSA at RT for 2 hours. Serum was diluted in PBS + 1% BSA, added to plates, and incubated overnight at 4°C. Antigen specific IgE and IgG1 standards were purified using a CNBr-Sepharose affinity column conjugated to either antigen (BLG or PN). Standard antibodies were isolated from SPF C3H/HeN mice sensitized with BLG + alum or PN + CT. Antigen-specific IgE and IgG1 was detected using the antibodies listed below and developed using TMB or p-nitrophenyl phosphate (SeraCare Life Sciences) as described in **Table 2.6**.

Total IgA was quantified in feces by ELISA as previously described (*53*). A protocol for measurement of fecal BLG-specific IgA was modified from (*125*). ELISA plates were coated with 100μg/mL BLG mL in 100 mM carbonate-bicarbonate buffer overnight at 4°C. Fecal pellets were homogenized at 100 mg/mL PBS and large debris was pelleted by spinning at 12,000xg for 10min. Supernatant was collected, diluted in PBS + 1% BSA, and added to ELISA plates after 2h of blocking with PBS + 3% BSA at RT. Samples were incubated overnight at 4°C. Antigen-specific IgA was detected using a goat anti-mouse IgA antibody conjugated to alkaline phosphatase AP (**Table 2.6**) and developed using p-nitrophenyl phosphate (SeraCare Life Sciences). BLG-specific IgA was quantified as arbitrary units (AU) against a standard curve isolated from the feces of BLG-sensitized C3H/HeN mice. BLG-specific IgA is presented as the ratio to total fecal IgA. ELISAs were analyzed with a SpectraMax M3 reader (Molecular Devices), measuring optical density at 405nm (IgE) or 450nm (IgG1).

Table 2.6: Antibodies for ELISA detection of IgE, IgG1, and IgA

Antigen	Antibody Target	Vendor
IgE	Goat-anti–mouse IgE-UNLB	Southern Biotech
IgE	Rabbit-anti-goat AP	Invitrogen
IgG1	Goat-anti-mouse IgG1-HRP	Southern Biotech
IgA	Goat-anti-mouse IgA-AP	Southern Biotech

CHAPTER 3

BACTERIAL ISOLATION, CELLULAR CHARACTERIZATION, AND PRODUCTION OF SHORT CHAIN FATTY ACIDS IN MONOCULTURES AND INTER-SPECIES INTERACTIONS

3.1 Introduction

Bacterial isolation and culture have been standards of microbiological sciences for over a century. However, until quite recently, our understanding of the vast diversity of the bacteria colonizing the human gut has been limited by culture techniques optimized for aerobic, readily culturable bacteria. With the rise of genetic sequencing, the breadth of unique bacteria colonizing the human body is now much better understood (*6*). The 16S ribosomal subunit RNA is well conserved across all bacterial taxa, and variations in this gene can be readily tracked to identify bacterial taxonomy and inter-species relationships. Along with 16S rRNA sequencing, novel methods and materials for anaerobic bacterial culture have provided new possibilities for the identification and isolation of specific bacteria (*7*). In this chapter, I will discuss various *in vitro* culture methods used for whole fecal bacteria, individual isolates, and two-species culture systems. We were able to isolate a strain of *A. caccae* from human feces and culture this bacterium in a variety of contexts to understand its growth, characteristics, and metabolic requirements. This laid the groundwork for utilizing this isolate most efficiently as an LBP.

3.2 Isolation of a novel strain of *A. caccae* from the feces of a healthy infant

A. caccae was previously identified by our laboratory as a beneficial member of the healthy infant microbiota which protected against the development of allergic response to

food in monocolonized mice (*104*). This work utilized the type strain *A. caccae* DSM 14662. To explore the therapeutic potential of this species as an LBP, we next isolated a novel strain of this species from the feces of a healthy infant, as strain level differences can be highly impactful. Additionally, the FDA has strict requirements for donor health and history of any strains utilized for clinical development (*177*).

While *A. caccae* was shown to be more abundant in healthy infants than CMA infants, it still was only prevalent at approximately 0.1% abundance in the healthy community (*104*). So, strategies to isolate this species first relied upon increasing the relative abundance of this bacterium. Antibiotics were used to deplete more abundant, fast-growing bacteria from the feces in plated culture and to increase opportunity for *A. caccae*, a relatively slow growing bacterium, to survive. Previous literature demonstrated that ciprofloxacin increased the relative abundance of *Clostridium* Cluster XIVa, the cluster to which *A. caccae* has been ascribed, in cultures of human feces (*258*). Other authors utilized a combination of gentamycin, aztreonam, and colistin to increase the relative abundance of Cluster XIVa (*56*). Here we tested both ciprofloxacin alone or the combination of ciprofloxacin, gentamycin, aztreonam, and colistin (4-mix). The antibiotic depletion and bacterial isolation strategy is shown in **Fig. 3.1**.

The fecal slurry of healthy donor 2 was chosen for isolation, as this infant had the highest relative abundance of *A. caccae* of the 4 healthy donors (*104*). The fecal slurry, or a pure culture of *A. caccae* DSM 14662, was spread on BHI agar plates containing no antibiotics or the antibiotics listed above. All bacterial cultures took place at 37°C within an anaerobic chamber. After 48h of growth, all plates had lawn growth, which was scraped, resuspended in sterile PBS, and aliquoted into stocks containing 25% glycerol and stored at -80°C. One stock was used for PCR and qPCR analysis of *A. caccae* abundance. PCR with primers specific for the 16S rRNA sequence of *A. caccae* demonstrated that two of the plates containing ciprofloxacin had substantial *A. caccae* present to produce a visible band comparable to the pure culture control (**Fig. 3.2a**). qPCR

validated these results and demonstrated that the two plates that produced PCR bands contained 100-1000 times more *A. caccae* than the growth on control plates containing no antibiotics (**Fig. 3.2b**).

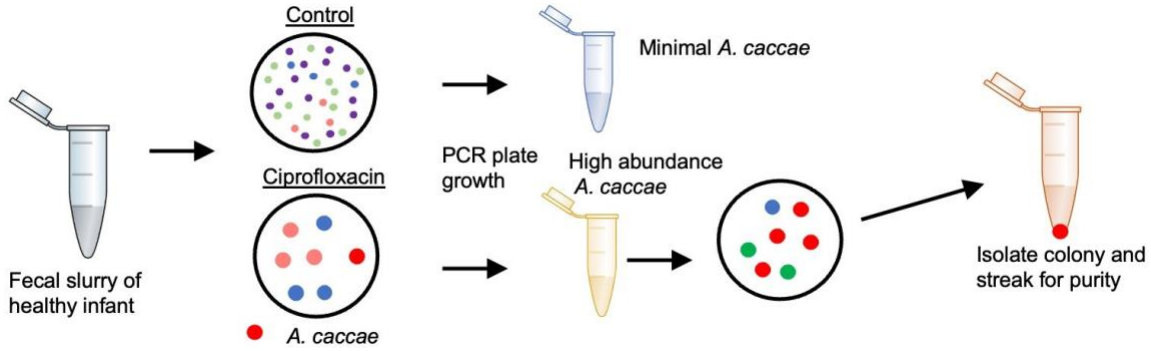

Figure 3.1: Strategy used to isolate *A. caccae* from feces of a healthy infant | Fecal slurries were spread on agar plates, some of which contained ciprofloxacin to deplete the growth of competitive species. Full plate growth was then collected and PCR analyzed for the presence/absence of *A. caccae*. Plate(s) which contained measurable *A. caccae* were passaged again and individual colonies were isolated and analyzed.

It was expected that the combination of 4 antibiotics would be more effective than ciprofloxacin alone, however no *A. caccae* was measured on any of the "4 mix" plates. This may be due to the overall greater depletion of total bacterial growth on the "4 mix plates", and this combination of antibiotics may have been too toxic for growth to overcome (**Fig. 3.2c**). The bacterial stocks from the plate culture of ciprofloxacin_D were then spread on BHI plates containing no antibiotics in dilutions from 10^{-1} to 10^{-8} to obtain pure colonies, which were isolated and inoculated into CMG broth. Individual colonies were passaged twice in CMG, stocks of the second passage were aliquoted and stored in 25% glycerol at -80°C, as well as spread on BHI plates to confirm pure cultures.

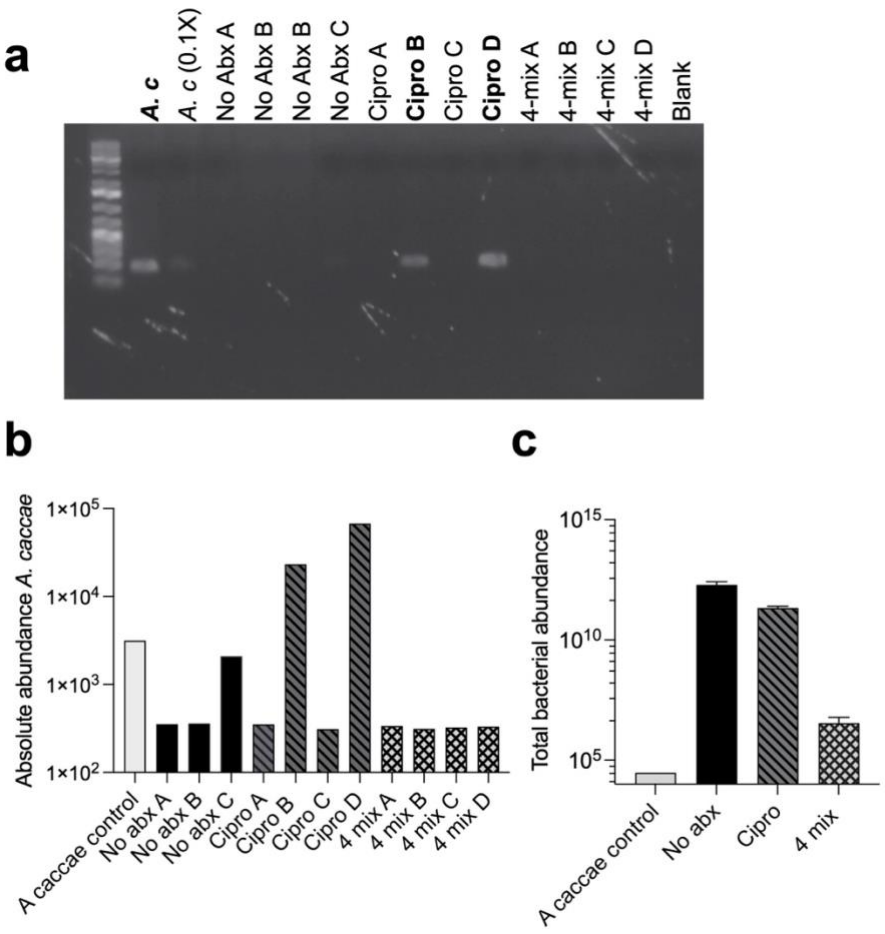

Figure 3.2: Abundance of *A. caccae* from growth of feces on antibiotic supplemented media | **a**, PCR amplification of the 16S sequence specific to *A. caccae* from plate growth of human fecal slurry on brain heart infusion (BHI) agar supplemented with ciprofloxacin (cipro) or a combination of four antibiotics (4 mix). Each row represents the total growth obtained from a single culture plate. **b**, qPCR analysis of *A. caccae* abundance from the same samples shown in **a. c**, Total bacterial abundance (copies 16S) from plate culture growth measured by qPCR. *A. c*: *A. caccae* DSM 14662 positive control.

PCR with *A. caccae*-specific primers confirmed that isolate 66 (a and b represent 2 colonies picked from the final passage to confirm purity of the isolate) were identified as *A. caccae* (**Fig. 3.3a**). Stocks of the colony 66a were submitted for whole genome shotgun sequencing by CosmosID™, which confirmed that the isolate (66a Rep 1) had greater than 98.5% sequence identity to other *A. caccae* type strains, meeting the cutoff to be considered an isolate within this species (**Fig. 3.3b**).

a

b

Legend: Above species cutoff (>95%) | Below cutoff (<95%) | Suspicious alignment

	66a Rep 1	Anaerostipes caccae DSM 14662	Anaerostipes sp. AF04-45	Anaerostipes caccae 3256FAA	Anaerostipes sp. BG01	Anaerostipes rhamnosivorans 1y2	Anaerostipes hadrus BPB5	Anaerostipes sp. 494a	Anaerostipes hadrus 2789STDY560886	Anaerostipes hadrus DSM 2219
66a Rep 1	*	98.7	98.78	98.68	92.77	84.7	84.04	84.47	84.45	84.5
Anaerostipes caccae DSM 14662	98.7	*	98.64	98.58	92.76	85.05	84.27	85.73	85.37	84.58
Anaerostipes sp. AF04-45	98.77	98.65	*	99.55	92.66	84.97	84.15	84.74	84.1	84.21
Anaerostipes caccae 3256FAA	98.67	98.56	99.55	*	92.65	84.85	86.19	84.57	86.09	84.18
Anaerostipes sp. BG01	92.77	92.77	92.67	92.65	*	86.48	84.41	84.83	84.52	84.87
Anaerostipes rhamnosivorans 1y2	84.71	85.05	84.96	84.85	86.48	*	84.66	86.35	85.58	84.25
Anaerostipes hadrus BPB5	83.98	84.27	84.16	86.19	84.41	84.66	*	84.8	98.69	98.61
Anaerostipes sp. 494a	84.45	85.73	84.75	84.58	84.84	86.35	84.85	*	84.98	84.49
Anaerostipes hadrus 2789STDY5608868	84.44	85.36	84.1	86.09	84.6	85.58	98.69	84.92	*	98.8
Anaerostipes hadrus DSM 2219	84.49	84.57	84.2	84.18	84.87	84.31	98.61	84.43	98.8	*

Figure 3.3: Identification of colony isolate 66 as a novel strain of *A. caccae* | a, PCR amplification of the 16S sequence specific to *A. caccae* from isolated colonies. **b**, Sequence identity between whole genome of isolate 66a compared to closest related species. Cutoff (95%) refers to genetic similarity required to consider two isolates unique strains of the same species. Whole genome shotgun sequencing of the 66a isolate was performed by CosmosID.

Our isolate contains approximately 20 single nucleotide polymorphisms (SNPs) unique from the other two characterized type strains within a ‘core genome’ of conserved sequences between related organisms (**Fig. 3.4**). A SNP tree generated from this core genome associated our isolate with other strains of *A. caccae* (**Fig. 3.5**). Together this

evidence led us to conclude that we had isolated a pure, novel strain of *A. caccae*, herein referred to as *A. caccae* LAHUC. In the time since this initial short-read shotgun sequencing was performed, long-read sequencing has become more available and allows for the analysis of a closed genome of bacterial isolates. Future work will sequence *A. caccae* LAHUC with this new technique to analyze differences between this strain and other type strains in specific genes across the entire genome. Unless otherwise noted, all further experiments utilize this strain. With a healthy-infant derived strain in-hand, it was necessary to further characterize this isolate. Understanding the metabolic requirements, optimal growth conditions, and cellular properties of our isolate was critical for optimizing its production and administration for further clinical development.

	66a Rep 1	Anaerostipes caccae 3256FAA	Anaerostipes caccae DSM 14662	Anaerostipes hadrus 2789STDY560883	Anaerostipes hadrus 2789STDY560886	Anaerostipes hadrus 2789STDY583486	Anaerostipes hadrus 2789STDY583490	Anaerostipes hadrus 2789STDY583495	Anaerostipes hadrus DSM 3319	Anaerostipes hadrus PEL 85	Anaerostipes rhamnosivorans 1y2	Anaerostipes sp. 494a	Anaerostipes sp. 992a	Anaerostipes sp. AF04-45	Anaerostipes sp. BG01	Anaerostipes hadrus BPB5
66a Rep 1	0	25	22	333	214	215	231	242	214	224	148	392	304	27	100	155
Anaerostipes caccae 3256FAA	25	0	28	328	213	212	228	237	209	221	145	388	301	6	91	152
Anaerostipes caccae DSM 14662	22	28	0	332	213	214	230	241	213	223	153	390	303	30	105	154
Anaerostipes hadrus 2789STDY5608830	333	328	332	0	222	188	196	206	186	189	334	422	335	326	331	190
Anaerostipes hadrus 2789STDY5608868	214	213	213	222	0	77	99	104	80	88	211	310	232	211	212	67
Anaerostipes hadrus 2789STDY5834860	215	212	214	188	77	0	54	67	49	47	218	313	223	210	211	62
Anaerostipes hadrus 2789STDY5834908	231	228	230	196	99	54	0	87	57	63	236	329	237	226	227	80
Anaerostipes hadrus 2789STDY5834959	242	237	241	206	104	67	87	0	66	78	247	342	254	235	240	91
Anaerostipes hadrus DSM 3319	214	209	213	186	80	49	57	66	0	58	219	318	222	207	210	63
Anaerostipes hadrus PEL 85	224	221	223	189	88	47	63	78	58	0	231	324	234	219	224	75
Anaerostipes rhamnosivorans 1y2	148	145	153	344	211	218	236	247	219	231	0	390	303	147	155	158
Anaerostipes sp. 494a	392	388	390	422	310	313	329	342	318	324	390	0	399	388	401	273
Anaerostipes sp. 992a	204	301	303	335	232	223	237	254	222	234	303	399	0	299	301	167
Anaerostipes sp. AF04-45	27	6	30	326	211	210	226	235	207	219	147	388	299	0	91	152
Anaerostipes sp. BG01	100	91	105	331	212	211	227	240	210	224	155	401	301	91	0	153
Anaerostipes hadrus BPB5	155	152	154	190	67	62	80	91	63	75	158	273	167	152	153	0

Figure 3.4: Single nucleotide polymorphisms between *A. caccae* LAHUC and closely related organisms | Number of single nucleotide polymorphisms (SNPs) identified between isolate *A. caccae* LAHUC and close relatives from whole genome shotgun sequencing from CosmosID. SNPs were counted within a 'core genome' of aligned sequences conserved across shown strains.

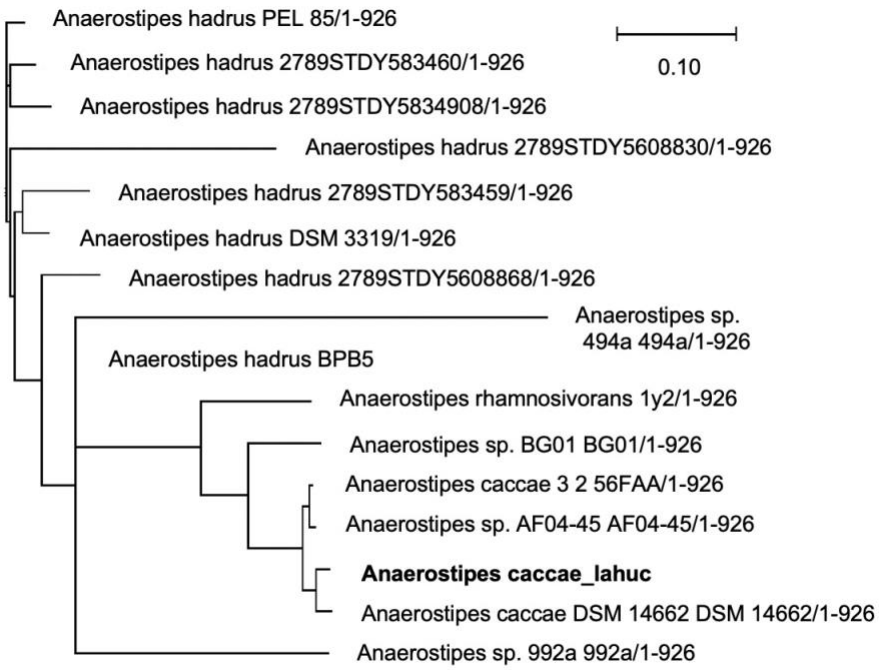

Figure 3.5: Genetic relatedness tree of *A. caccae* LAHUC and closely related organisms | SNP distance was used to generate a relationship tree of *A. caccae* and other organisms. Work was performed by CosmosID.

3.3 Cellular Characterization of *A. caccae* LAHUC

Once our healthy infant-derived strain of *A. caccae* was isolated, we began characterizing its growth and phenotype by various assays to optimize later experiments. *A. caccae* is a strictly anaerobic Clostridia in the family *Lachnospiraceae* and has also been assigned to the *Clostridium* Cluster XIVa (*246*, *247*). Most initial cultures of *A. caccae* were grown in CMG, a rich medium developed for Clostridia (Anaerobe Systems). However, *A. caccae* demonstrates relatively fast growth in CMG, peaking in optical density (OD600) and live cell counts (colony forming units, CFUs) within 8 hours of culture (**Fig. 3.6a**). Stocks of secondary cultures of *A. caccae* LAHUC grown in CMG for 16 hours were frozen at -80°C with 25% glycerol for long term storage. This freezing process resulted in approximately a 2-log decrease in viable cell count after thawing (**Fig. 3.6b**). Flash-freezing bacterial cultures in liquid nitrogen can improve cell viability of frozen

stocks (*272*). However, this flash-freeze did not improve cell recovery of *A. caccae* LAHUC after thawing (**Fig. 3.6c**). Some stocks of the flash-frozen bacteria were thawed within an anaerobic chamber, and others were thawed while exposed to oxygen. This short-term oxygen exposure (30min) did not further reduce the cell recovery (**Fig. 3.6c**). Stocks from the flash-frozen culture batch (approximately 150, 1mL vials) were stored at -80°C and used for all downstream experiments.

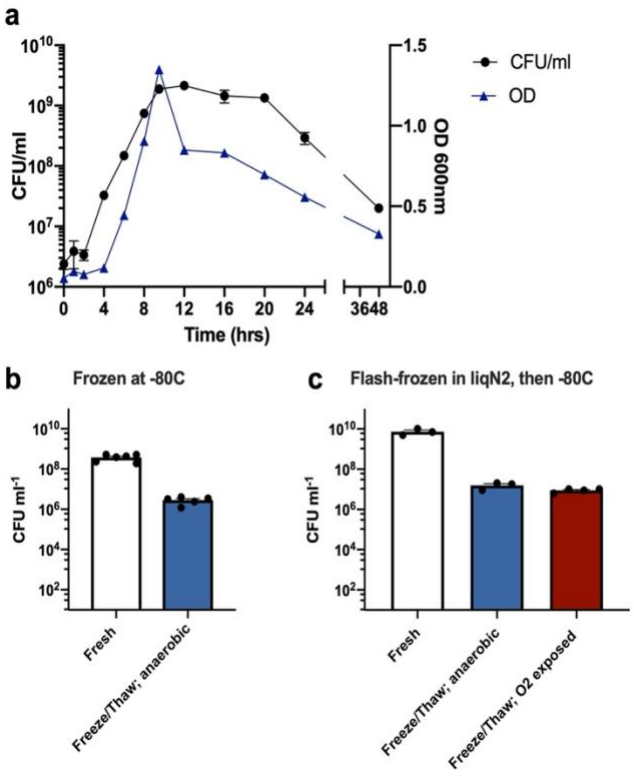

Figure 3.6: Growth and cellular enumeration of *A. caccae* LAHUC | a, Growth curves of *A. caccae* LAHUC grown in CMG for 48h represented by optical density (OD_{600}) and live cell counts (CFU/mL). **b**, Viable cell counts (CFU/mL) of cultures of *A. caccae* grown either directly after growth or following storage at -80°C in 25% glycerol. **c**, Viable cell counts (CFU/mL) of *A. caccae* directly after growth or following flash-freezing in liquid nitrogen before storage at -80°C in 25% glycerol. Samples were thawed for counting within an anaerobic chamber or thawed for 30 minutes while exposed to oxygen within a sterile field. Points represent biological replicates, bars represent mean ± s.e.m.

Antibiotic susceptibility of the strain was also characterized to determine which antibiotics could be used to eliminate the strain *in vitro* or *in vivo*. Whole-genome sequencing identified a tetracycline resistance gene in our isolate (**Fig. 3.7a**). To examine antibiotic susceptibility in culture, *A. caccae* LAHUC was spread on BHI agar plates which then were loaded with disks containing streptomycin, kanamycin, tetracycline, and ampicillin. Ampicillin inhibited the growth of *A. caccae* LAHUC, as demonstrated by a wide radius of inhibited growth around the antibiotic disk (**Fig. 3.7b, c**). Additionally, even though *A. caccae* LAHUC possesses a tetracycline resistance gene, this antibiotic inhibited growth although not to the extent of ampicillin (**Fig. 3.7b, c**).

a

Sample_ID	Contig_ID	AMR Gene	RefSeq_ID	%Identity	AMR gene length	Location of the	%Coverage	Antibiotic_Class
UChicago_66a	NODE_13	tet(32)	EF626943	98.125	1920	64554..66473	100.0	tetracycline

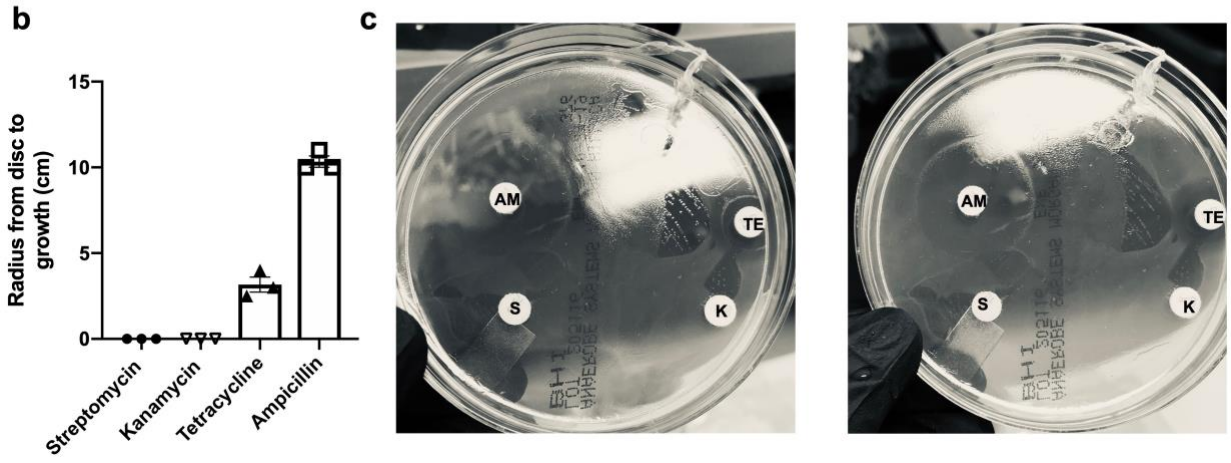

Figure 3.7: Antibiotic susceptibility of isolate *A. caccae* | a, Identification of antibiotic resistance genes from isolate *A. caccae* LAHUC (UChicago_66a) from whole genome shotgun sequencing from CosmosID ™. **b,** Radial distance from antibiotic disk to bacterial growth as a measure of antibiotic susceptibility. **c**, Representative images of *A. caccae* LAHUC growth on plates with antibiotic disks. Points represent biological replicates, bars represent mean ± s.e.m. AM: ampicillin, K: kanamycin, S: streptomycin, TE: tetracycline.

Various other characteristics of *A. caccae* were evaluated through *in vitro* cultures, which are summarized in (**Fig. 3.8**). As expected, *A. caccae* LAHUC produces substantial butyrate after culture in peptone yeast (PY) medium supplemented with glucose.

Interestingly, our isolate produces similar levels or significantly more butyrate in this medium than the two known type strains (**Fig. 3.8a**). We confirmed that this strain is spore-forming and Gram positive from cell staining, and oxygen tolerance tests confirm that it is a strict anaerobe (**Fig. 3.8b, c**). The Nagler laboratory has shown that indoles (metabolites derived from tryptophan) and flagella (bacterial proteins used for motility) have distinct roles in modulating the host immune system *in vivo* (*69*). *A. caccae* was cultured in PYG containing 0.175% agar to test its motility.

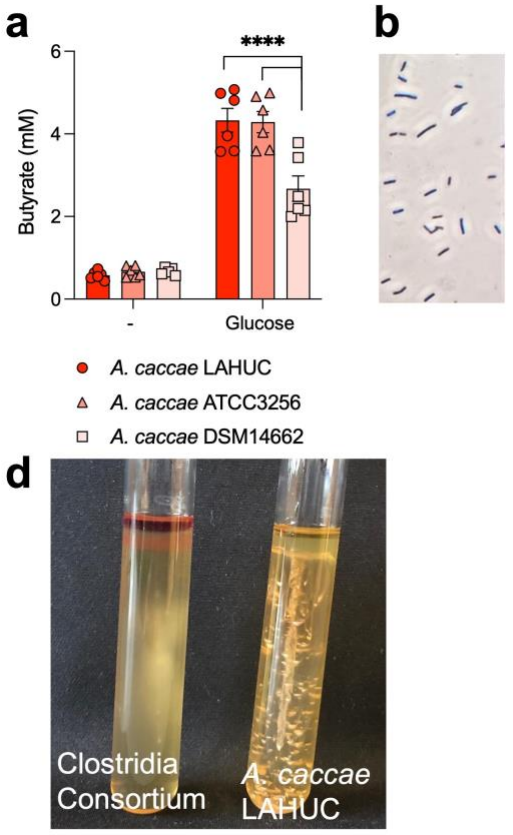

Characteristic	*A. caccae* LAHUC
Spore-forming	+
Strictly anaerobic	+
Gram status	+
Motile	-
Indole-producing	-
Butyrate-producing	+++
Propionate-producing	+
Human derived (known culture history and donor health status)	+
Shelf-stable in freeze-dried form	+

Figure 3.8: Summary of various cellular and metabolic characteristics of *A. caccae* LAHUC | a, Butyrate concentration from *A. caccae* strains cultured in minimal peptone yeast (PY) medium (-) or PY supplemented with glucose measured by HPLC UV-Vis. **b**, Representative Gram stain of *A. caccae* LAHUC. **c**, Table of characteristics of *A. caccae* LAHUC. **d**, Representative images of *in vitro* cultures demonstrate that *A. caccae* LAHUC is not motile and does not produce indole. Points represent biological replicates, bars represent mean ± s.e.m. Statistics were analyzed by two-way ANOVA with Sidak's multiple comparisons test. ****P<0.0001.

A primary culture of *A. caccae* LAHUC (or a consortium of murine-derived Clostridia) was stabbed into a culture tube of low-percentage agar medium. While members of the Clostridia consortium were able to spread throughout the medium, *A. caccae* was confined to the inoculation site, demonstrating that it is non-motile (**Fig. 3.8d**). *A. caccae* produces large amounts of gas during fermentation which form visible bubbles in the agar, but these do not affect the motility assay. Kovac's reagent was added on top of cultures of *A. caccae* or the Clostridia consortium to detect the presence of indole in the media. Kovac's reagent undergoes a color change from amber to red in the presence of indole, and the amber color atop the *A. caccae* culture demonstrates that this culture does not produce indole (**Fig. 3.8d**). However, we do not yet have evidence as to whether *A. caccae* LAHUC produces other indole-containing metabolites which may influence host physiology.

These results led us to hypothesize that butyrate production may be the most likely candidate for *A. caccae*'s immunoregulatory effect, as it does not produce other well-known host-modulating molecules like indole or flagella. We therefore focused on maximizing *A. caccae*'s ability to produce butyrate *in vitro* and *in vivo* to optimize its therapeutic efficacy as an LBP.

3.4 Analysis of butyrate production by *A. caccae* LAHUC in monoculture

As discussed above, *A. caccae* LAHUC produces comparable or greater butyrate concentrations *in vitro* than commercially available *A. caccae* type-strains. We also evaluated its butyrate production against other bacteria using *Ruminococcus bromii*, a non-butyrate producing Clostridia, as a control. Bacterial isolates (*A. caccae* and *R. bromii*) or a consortium of murine-derived Clostridia were cultured in PY or PYG media. As expected, both *A. caccae* LAHUC and *R. bromii* grew to a higher optical density in

PYG than PY, and more acetate accumulated in these cultures from the fermentation of glucose (**Fig. 3.9a, c**). However, *A. caccae* produced substantially more butyrate than both *R. bromii* and the Clostridia consortium in PYG (**Fig. 3.9b**). This may be due to the fact that the consortium contains many bacterial species competing for growth, some of which do not produce butyrate. However, we still confirm that *A. caccae* produces high levels of butyrate in comparison to other Clostridia.

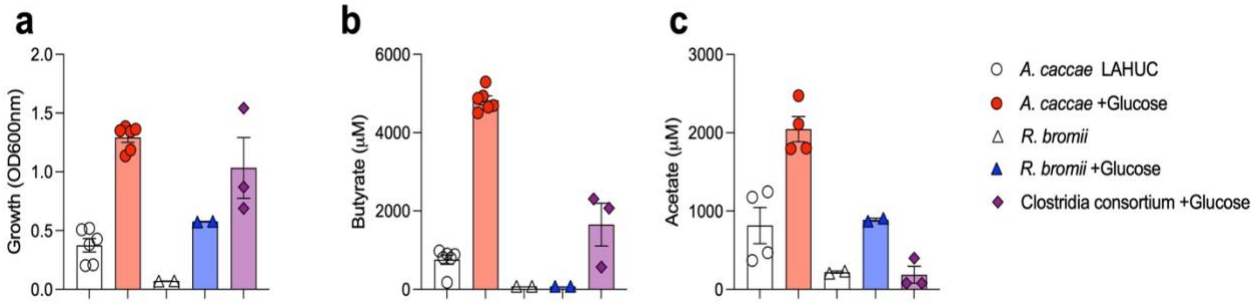

Figure 3.9: Growth and butyrate production *in vitro* from various Clostridia | **a**, Growth measured by optical density (OD600) of various bacteria after 48h in peptone yeast (PY) media alone or supplemented with 10mg/ml glucose. **b, c,** Butyrate (**b**) or acetate (**c**) accumulation in culture supernatants measured by HPLC UV-Vis. Points represent biological replicates, bars represent mean ± s.e.m.

To determine which carbon sources result in the greatest growth and butyrate production, *A. caccae* LAHUC was grown in PY media supplemented with various carbohydrates (glucose, sucrose, lactose, trehalose, cellobiose, or potato starch) (**Fig. 3.10a**). As previously shown, *A. caccae* LAHUC produced high concentrations of butyrate in media supplemented with glucose (**Fig. 3.10b**). Interestingly, *A. caccae* exhibits even higher growth and butyrate production from sucrose-supplemented media. Not all bacteria are similarly capable of consuming sucrose, and rarely is it comparably utilized to glucose. *A. caccae* was also able to consume lactose, but butyrate production was negligible. *A. caccae* was not able to grow or produce butyrate from trehalose, cellobiose, or potato starch. It was shown that the ability to consume trehalose may be a genetic signature of

pathogenic strains of *C. difficile* (*273*) and, as expected, *A. caccae* LAHUC does not seem to possess this trait.

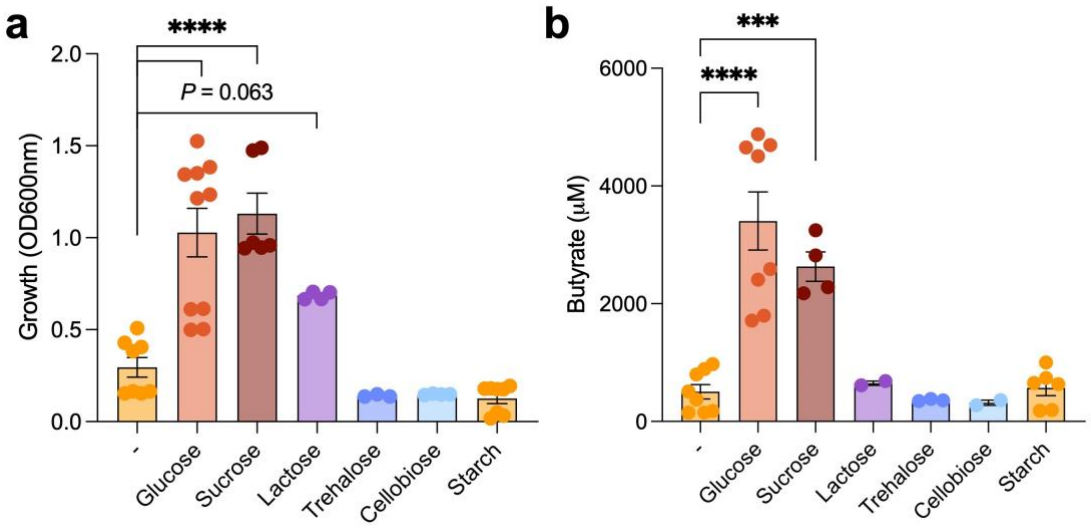

Figure 3.10: *A. caccae* grows and produces butyrate from simple sugars but not other carbon sources | a, Growth measured by optical density (OD600) of *A. caccae* after 48h culture in PY alone (-) or supplemented with 10mg/ml of various carbon sources. **b**, Butyrate accumulation in culture supernatants measured by HPLC UV-Vis. Bars represent mean ± s.e.m. of 2-6 biological replicates pooled from 2 independent experiments. Statistics analyzed by one-way ANOVA with Tukey's post-hoc test. ***P* < 0.01, ****P*<0.001, *****P* < 0.0001 versus PY (-) control.

3.5 *In vitro* mucus consumption

Most butyrate-producing Clostridia are not able to readily colonize GF animal hosts (*274*). This is thought to be due to their dependence on cross-feeding with other species to break down dietary fiber and create a metabolic niche for these secondary fermenters (*274*). However, our previous publication demonstrated that *A. caccae* readily colonized GF mice and mimicked the protective effect of the replete healthy microbiome to prevent an allergic response to a food antigen (*104*). This ability of *A. caccae* to colonize GF mice led us to question what it was utilizing as a carbon source in that environment.

Some bacterial taxa are capable of consuming host colonic mucus as a food source. The most notable of these taxa is *Akkermansia*, originally thought to be a pathobiont but more recently associated with health in a variety of disease contexts (*275–277*). Bacterial consumption of mucus can in some cases trigger mucus production, initiating a feed-forward loop and improving barrier integrity overall (*278*). It has been shown that the glycosylation of mucus can depend greatly on immune signaling, and that differential glycosylation can affect the ability of bacteria to consume the mucus (*264*). A report from Nagao-Kitamoto et al. treated mice with a neutralizing antibody against IL-22, a barrier-regulating cytokine, which altered mucus production and glycosylation patterns (*264*). In untreated mice, a mucus-consuming bacterium *Phascolarctobacterium faecium* was able to slow the progression of lethal *C. difficile* infection. However, anti-IL-22 treatment reduced *P. faecium*'s ability to colonize and prevented its protective effect (*264*).

To determine if *A. caccae* was able to consume murine mucus, and if differences in glycosylation could affect this, we collected colonic mucus from SPF mice for *in vitro* cultures as described in Chapter 2. We chose to collect mucus from *Cd11C*^{Cre}*Myd88*$^{fl/fl}$ mice since we have demonstrated that these mice have reduced ability to produce IL-22 compared to *Myd88*$^{fl/fl}$ littermates (**Fig. 3.11a**) (*69*). *Cd11C*^{Cre}*Myd88*$^{fl/fl}$ mice lack the ability to signal through pattern recognition receptors which rely on MyD88 in their CD11c^{+} cells, predominantly antigen presenting cells (APCs). This lack of activation in the APCs leads to reduced production of immune-activating cytokines such as IL-23, which signals to other local cell types such as ILC3s to produce IL-22. We predicted that this reduction in IL-22 might have an effect similar to the neutralizing antibody to IL-22 (*264*) in altering the mucus structure.

Colonic mucus from these mice was isolated and added to PY medium, which was used to grow a *P. faecium* type strain or *A. caccae* LAHUC. *P. faecium* requires succinate to grow, so succinate was also supplemented in all *P. faecium* cultures (PYS) (*279*). *P. faecium* exhibited significantly increased growth in media containing mucus from *Myd88*$^{fl/fl}$

mice but not *Cd11C*^{Cre}*Myd88*$^{fl/fl}$ littermate controls (**Fig. 3.11c**), mirroring previous studies (*264*). This increase in optical density was not due simply to the presence of mucus, as blank media containing each source of mucus had identical optical densities (**Fig. 3.11b**).

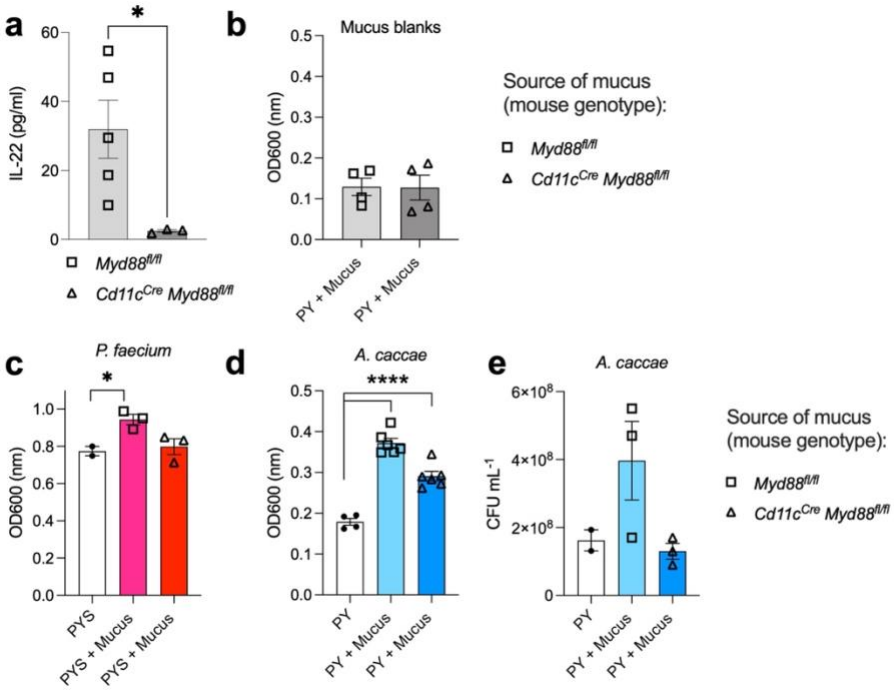

Figure 3.11: Commensal bacteria consume colonic mucus from IL-22-sufficient mice | a, IL-22 secreted from ileal *ex vivo* explants of *Myd88*$^{fl/fl}$ or *Cd11C*^{Cre} *Myd88*$^{fl/fl}$ mice measured by ELISA. **b**, Optical density of PY medium supplemented with colonic mucus in the absence of bacteria. Mucus was obtained from SPF *Myd88*$^{fl/fl}$ or *Cd11C*^{Cre} *Myd88*$^{fl/fl}$ mice. **c, d**, Bacterial growth measured by optical density (OD600) of *P. faecium* (**c**) or *A. caccae* (**d**) after 48h *in vitro* culture with or without colonic mucus. **e**, Viable cell count (CFU/mL) of *A. caccae* LAHUC from cultures in (**d**). Points represent biological replicates, bars represent mean ± s.e.m. Statistics are analyzed by student's t test (**a**) or one-way ANOVA with Tukey's post-hoc test (**c-e**). **P* < 0.05, *****P*< 0.0001.

Strikingly, *A. caccae* exhibited increased growth (OD600) in media containing mucus from both *Cd11C*^{Cre}*Myd88*$^{fl/fl}$ and *Myd88*$^{fl/fl}$ mice (**Fig. 3.11d**). This growth was greatest in media containing the mucus of *Myd88*$^{fl/fl}$ (IL-22 sufficient) mice. CFU counts also demonstrated a modest increase in *A. caccae* cell number with only the mucus of *Myd88*$^{fl/fl}$ mice (**Fig. 3.11e**). Additional experiments could examine growth of *P. faecium* or *A.*

caccae in media supplemented with commercially available mucins, as these colonic mucus preparations could contain other compounds. This preliminary data suggests that *A. caccae* may be able to consume murine mucus, a trait that would help to explain its ability to readily colonize GF mice. Further experiments in Chapter 4 will examine whether monocolonization with *A. caccae* affects host mucus production.

3.6 Cross-feeding between *A. caccae* LAHUC and *Ruminococcus bromii* results in terminal butyrate production from non-soluble starch

Butyrate is commonly described as the end-product of fiber fermentation; however, it should be clarified that the digestion of fiber is a multi-step process often carried out cooperatively by multiple different bacteria (*178*). These inter-species cross-feeding processes have been well described, and many bacterial taxa can be considered 'primary degraders', breaking down large polysaccharides via the production of carbohydrate active enzymes (CAZymes) (*189*, *280*). Other species are 'secondary fermenters', utilizing intermediate metabolites produced from the primary-stage digestion and converting them into smaller carbon byproducts (*248*). *A. caccae* is a classic example of a secondary fermenter – producing very few CAZymes itself, it relies on smaller sugars and metabolites, namely lactate and acetate, to grow and produce butyrate *in vivo* (*247*). Knowing this, we predicted that *A. caccae* may also be able to cross-feed with other members of the fecal microbiota, including acetate-producing primary degraders such as *R. bromii*.

As described above, *R. bromii* is an efficient consumer of potato starch and other starches in the human diet, while *A. caccae* is not able to metabolize these large carbohydrates (*187*– *189*). We predicted that *A. caccae* would, however, be able to utilize acetate derived from *R. bromii's* consumption of starch to produce butyrate. *A. caccae* and *R. bromii* were grown in PY alone or supplemented with nonsoluble potato starch or glucose. The two species were grown either in monocultures or co-cultures with

approximately equal cell densities. As predicted, all 3 bacterial groups (*A. caccae*, *R. bromii*, or the co-cultures) exhibited growth in PYG, which is used as a positive control, but only cultures that contained *A. caccae* (not *R. bromii* alone) also contained butyrate (**Fig. 3.12a, c**). *R. bromii* monocultures grew and produced acetate from both starch and glucose to similar extents, but there was little to no acetate detected in co-cultures, potentially due to consumption by *A. caccae* (**Fig. 3.12b**). Notably, high concentrations of butyrate were produced from *R. bromii* / *A. caccae* co-cultures supplemented with potato starch (**Fig. 3.12c**), showing that we can foster bacterial cross-feeding relationships *in vitro*.

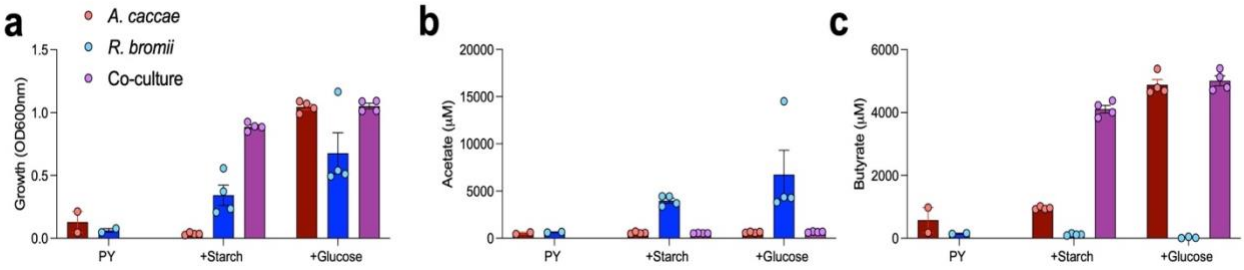

Figure 3.12: Co-cultures of *A. caccae* and *R. bromii* produce butyrate from potato starch | **a**, Growth measured by optical density (OD600) of *A. caccae*, *R. bromii*, or co-cultures after 48h culture in minimal PY media supplemented with 10mg/ml potato starch or glucose. **b**, **c** Acetate (**b**) and butyrate (**c**) accumulation in culture supernatants measured by HPLC UV-Vis. Points represent biological replicates, bars represent mean ± s.e.m.

Because *A. caccae* was able to produce butyrate in co-cultures with *R. bromii* in starch-supplemented media, we next sought to determine whether *A. caccae* could grow and produce butyrate from degraded starch products only, without *R. bromii* present. To test this, we set up a two-stage culture system. First, *R. bromii* was cultured in PY-Starch medium for 48h. These cultures were then spun down to pellet cells, and the supernatant was sterile filtered. *A. caccae* was then inoculated into PY media containing glucose, intact starch, a 1:1 mixture of fresh PY and the degraded starch media, or the spent medium alone. The controls replicated previous experiments and confirmed that *A. caccae* grew and produced butyrate from glucose but not PY alone or PY-Starch.

However, *A. caccae* was able to grow and produce butyrate from the degraded starch, either in the 0.5X or 1X concentrations (**Fig. 3.13a, b**). We predicted that the 1X degraded starch media would not support growth, as *R. bromii* would potentially have utilized other components of the media besides starch that would be necessary for growth. However even without the addition of fresh media, *A. caccae* grew and produced high levels of butyrate.

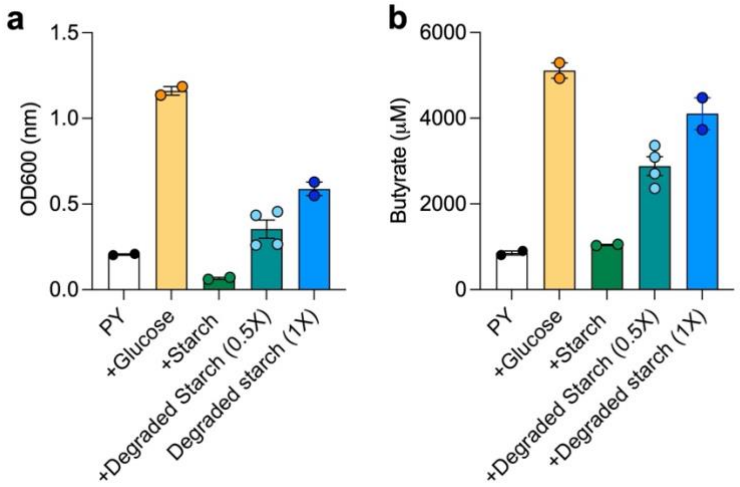

Figure 3.13: *A. caccae* grows and produces butyrate from degraded potato starch | a, Growth measured by optical density (OD600) after 48h culture of *A. caccae* in minimal PY media supplemented with 10mg/ml glucose, 10mg/ml potato starch, or degraded starch. *R. bromii* was previously cultured for 48h in PY plus potato starch to perform initial degradation, then culture supernatant was sterile filtered and mixed 1:1 with fresh PY media (degraded starch, 0.5X) or used directly as culture media for *A. caccae* (1X). **b**, Butyrate accumulation in culture supernatants measured by HPLC UV-Vis. Points represent biological replicates, bars represent mean ± s.e.m.

We then repeated this two-step sequential culture with a broader panel of complex carbohydrates including potato starch, amylopectin, inulin, and corn starch (**Fig. 3.14**). As previously, *R. bromii* was cultured in PY media containing 10mg/ml of the stated carbohydrate, then the culture supernatant was collected, sterile filtered, and used as growth media for *A. caccae*. Again, *A. caccae* grew and produced butyrate from the

degraded (‘d’) potato starch (**Fig. 3.14a, b**). *A. caccae* grew significantly utilizing the degraded amylopectin but did not produce substantial butyrate from amylopectin or inulin. These results may either indicate incomplete digestion of amylopectin and inulin by *R. bromii* or an inability of *A. caccae* to use intermediate products from these sources. *A. caccae* produced very high levels of butyrate from corn starch, however corn starch is not a true prebiotic for use *in vivo* because it is also broken down by human digestive enzymes.

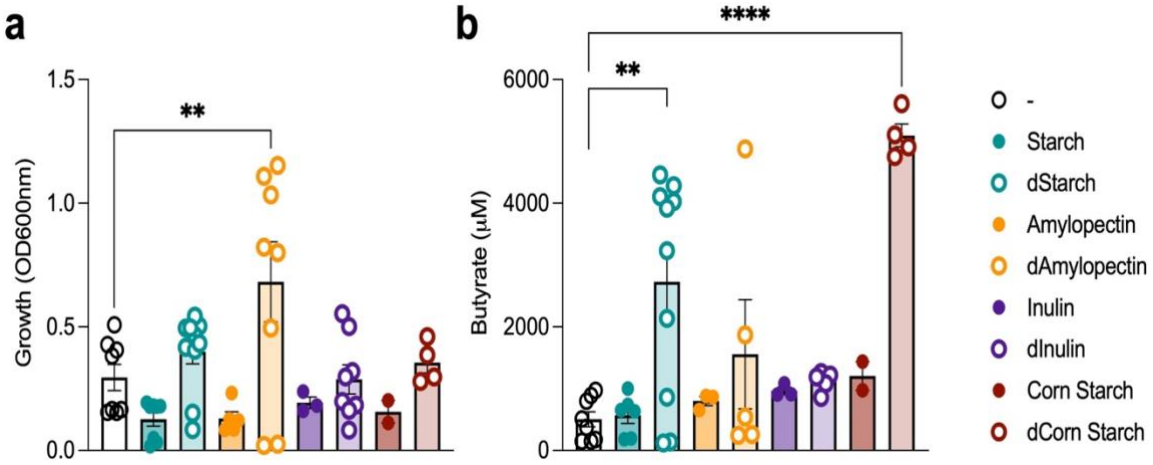

Figure 3.14: *A. caccae* grows and produces butyrate from various degraded starches and fibers | a, Growth measured by optical density (OD600) after 48h culture of *A. caccae* in PY medium (-) alone or supplemented with various carbohydrates, either neat or previously degraded. *R. bromii* was cultured for 48h in PY with various fibers, then culture supernatants containing degraded products (’d’) were sterile filtered and used directly as growth media for *A. caccae*. **b**, Butyrate accumulation measured by HPLC UV-Vis. Bars represent mean ± s.e.m., points represent biological replicates pooled from 3 independent experiments. Statistics analyzed by one-way ANOVA with Tukey’s post-hoc test. ***P*<0.01, *****P*<0.0001 versus (-) control.

Together this demonstrates that sequential cross-feeding relationships between *A. caccae* and *R. bromii* effectively allows terminal butyrate production from complex starch. By digesting large starches into acetate and smaller sugars, *R. bromii* produces carbohydrate products that can be fermented by *A. caccae* into butyrate. We next sought to determine whether these same relationships could be formed in a more complex, multi-species culture system.

3.7 Analysis of butyrate production by *A. caccae* LAHUC in co-cultures with fecal bacteria of an allergic infant

While we are interested in how *A. caccae* behaves in monoculture, we also wanted to understand how inter-species interactions could be manipulated to ensure that *A. caccae* would be able to grow and produce butyrate in the environment of a microbially replete host. Common prebiotics or dietary fibers are not directly accessible to *A. caccae* for consumption, but these products transit to the distal gut more readily than small metabolites. We therefore set up *in vitro* co-culture systems to examine butyrate production from various carbon sources in multi-species environments. These co-culture systems allowed analysis of cross-feeding between *A. caccae* and fecal bacteria utilizing various prebiotics which we predict would either transit successfully to the distal GI tract or provide the necessary metabolites for *A. caccae*'s production of butyrate.

Primary cultures of *A. caccae* LAHUC or a fecal slurry from a CMA infant were inoculated into PY supplemented with various carbon sources in mono-cultures or cocultures. Commonly used prebiotics including short chain fructoooligosaccharides (scFOS), cellobiose, and potato starch as well as a human milk oligosaccharide 2'fucossylactose (2'FL) and the sugar alcohol myo-inositol were examined for production of terminal butyrate in monocultures and co-cultures. *A. caccae* LAHUC produced high concentrations of butyrate from scFOS in monoculture, but none of the other prebiotics, as expected (**Fig. 3.15**). Interestingly, very little butyrate was produced from scFOS in the CMA culture, but very high levels were produced in the *A. caccae* / CMA co-cultures, suggesting that *A. caccae* is likely successfully competing for scFOS consumption within the CMA community. Overall, none of the tested prebiotics significantly increased butyrate in the CMA culture, potentially due to an overall lack of butyrate producing bacteria in this community. Neither 2'FL, myo-inositol, or cellobiose increased butyrate concentration in

the *A. caccae*/CMA co-cultures. The only “traditional” prebiotic that increased butyrate (although not significantly) was potato starch, which is explored in further experiments. This mirrors the previous experiments which showed that *A. caccae* cross-feeds with *R. bromii* to consume potato starch and may suggest that several species could act as primary degraders of potato starch.

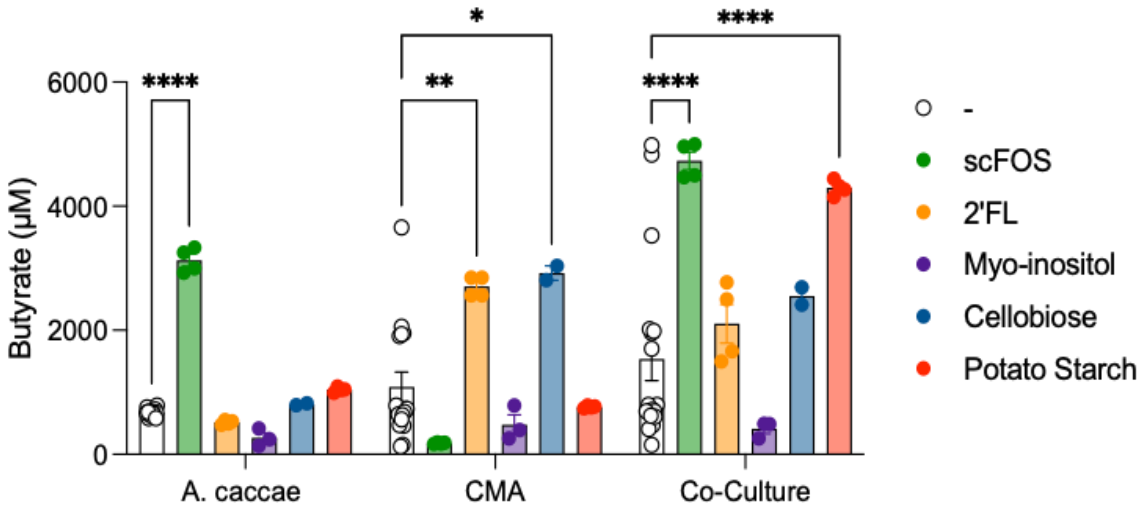

Figure 3.15: Butyrate production from various prebiotics in complex culture | *A. caccae* LAHUC and a fecal slurry from a cow’s milk allergic infant (CMA) were cultured alone or together (co-culture) in peptone yeast media (-) supplemented with 10mg/ml of various prebiotics. After 48h, butyrate was measured in culture supernatants by HPLC UV-Vis. Bars represent mean ± s.e.m., points represent biological replicates pooled from 2 independent experiments. Statistics are analyzed by two-way ANOVA with Kruskal Wallis post-hoc test comparing against the PY (-) group within each culture condition. *$P < 0.05$, **$P < 0.01$, ***$P < 0.001$, ****$P < 0.0001$.

Interestingly, while *A. caccae* does not produce butyrate from myo-inositol, this glucose-like sugar alcohol is available for its direct consumption and metabolism. While *A. caccae* produces high levels of butyrate from glucose (and most other tested metabolites), it instead produces very high concentrations of propionate from myo-inositol (**Fig. 3.16**). This has recently been reported in the literature as a unique trait of *Anaerostipes* species, including *A. caccae* (*281*), and is explored further in Chapter 4.

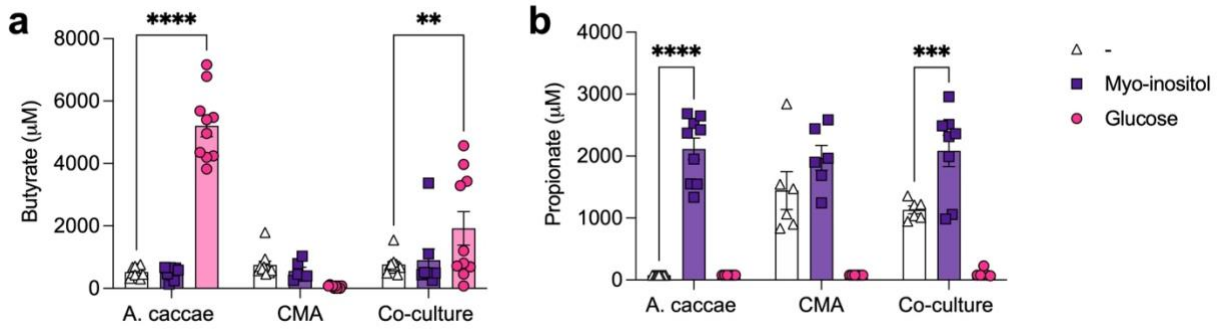

Figure 3.16: *A. caccae* produces propionate from myo-inositol *in vitro* | *A. caccae* LAHUC and a fecal slurry from a cow's milk allergic infant (CMA) were cultured alone or together (co-culture) in peptone yeast media (-) or supplemented with 10mg/ml of glucose or myo-inositol. Butyrate concentration (**a**) and propionate concentration (**b**) were measured in culture supernatants by HPLC UV-Vis after 48h culture. Bars represent mean ± s.e.m., points represent biological replicates pooled from 3 independent experiments. Statistics are analyzed by two-way ANOVA with Kruskal Wallis post-hoc test comparing against the PY (-) group within each culture condition. ***P* < 0.01, ****P* < 0.001, *****P* < 0.0001.

From these studies, we concluded that potato starch was the most promising prebiotic to increase butyrate *in vivo*. This will be further discussed in Chapter 4. However, in addition to these classical prebiotics, we explored prebiotics that could be more specific to *A. caccae* and its metabolic needs, specifically its ability to utilize lactate.

3.8 Lactate / acetate utilization

As described above, *Anaerostipes* species utilize lactate/acetate conversion to produce butyrate (*248*, *282*). Availability of lactate directly correlates with butyrate production by *A. caccae in vitro* (*63*). Lactate utilization is not particularly common among Clostridia (*247*), so we predicted that lactate may be an ideal prebiotic to increase the metabolic opportunity of *A. caccae*, uniquely. First to confirm *A. caccae*'s ability to produce butyrate from intermediate metabolites, we cultured *A. caccae* in lactate, acetate, or the combination as previously published (*282*). As expected, *A. caccae* exhibited significantly increased growth in media supplemented with lactate or acetate compared to the PY

control (**Fig. 3.17a**). However, butyrate only significantly increased in media supplemented with both lactate and acetate, demonstrating the necessity of both metabolites together for butyrate production (**Fig. 3.17b**). Clark et al. used a high-throughput *in vitro* culture system to characterize butyrate production by *A. caccae* and other species. This work showed that in the presence of simple sugars, *A. caccae* undergoes more rapid growth but produces relatively less butyrate, but with higher concentrations of acetate and lactate available, relatively more butyrate is produced per cell (*63*). A prebiotic that makes lactate available in the lower gut would be the ideal candidate for further study.

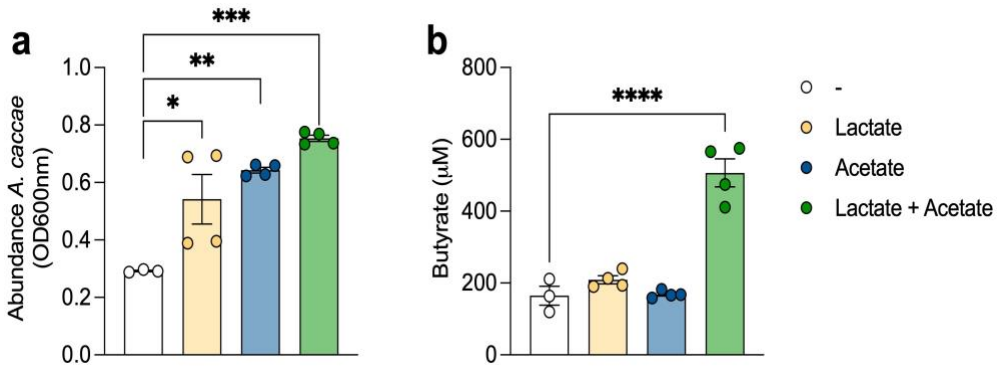

Figure 3.17: *A. caccae* produces butyrate from the combination of lactate and acetate | **a**, Growth measured by optical density (OD600) of *A. caccae* cultured for 48h in minimal peptone yeast media (-) supplemented with 40mM lactate, 33mM acetate, or the combination (*282*). **b**, Butyrate accumulation in culture supernatants measured by HPLC UV-Vis. Bars represent mean ± s.e.m., points represent biological replicates pooled from 2 independent experiments. Statistics are analyzed by one-way ANOVA with Tukey's post-hoc test. *$P < 0.05$, **$P < 0.01$, ***$P < 0.001$, ****$P < 0.0001$ versus PY (-) control.

3.9 Lactulose is a butyrate-potentiating prebiotic via lactate/acetate conversion and bacterial cross-feeding

To create opportunity for lactate-mediated cross-feeding, we utilized lactulose as a prebiotic. Lactulose is a synthetic disaccharide known to be broken down by lactic acid bacteria and Bifidobacteria, releasing large amounts of lactate and acetate in the colon

(*253*) (**Fig. 3.18a**). Lactulose is clinically used as a laxative, but at lower doses it has been studied as a prebiotic which shapes the composition of the fecal microbiota (*256*). Previous literature has demonstrated that in addition to increasing lactate, lactulose can increase butyrate and the relative abundance of *Anaerostipes* in an *in vitro* culture system of human fecal bacteria (*254*). Others have shown that lactulose administration *ad libitum* in water increases lactate and the relative abundance of *Bifidobacterium* in mice, along with a modest increase in butyrate and the relative abundance of *Clostridium* Cluster XIVa (*257*). We predicted that in combination with *A. caccae* LAHUC, lactulose would increase butyrate in our system by providing lactate and acetate.

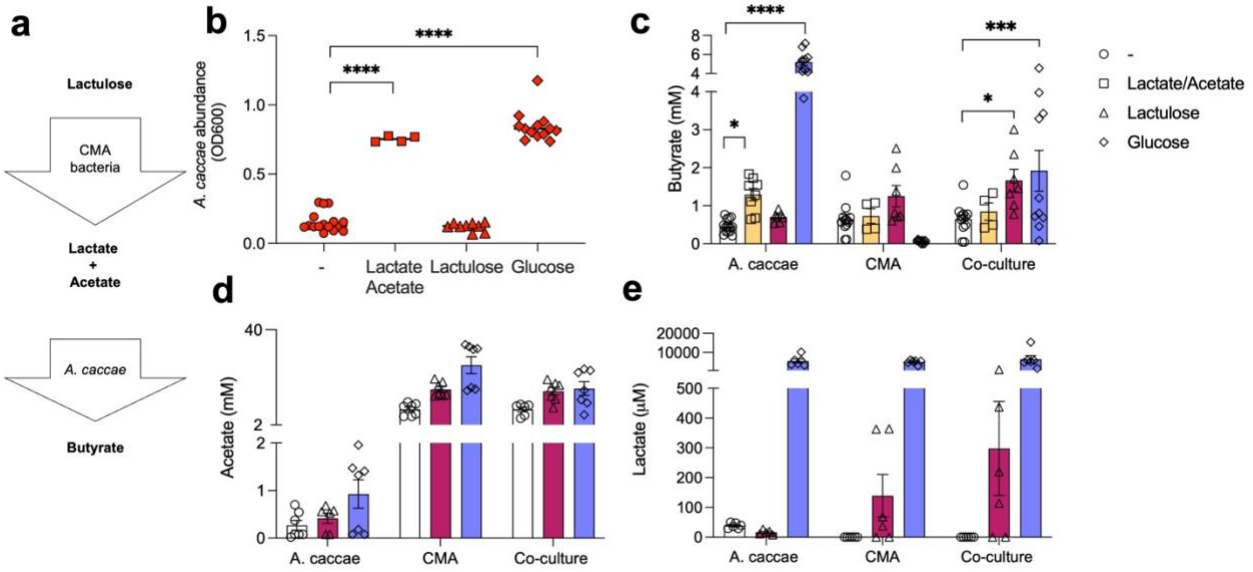

Figure 3.18: Lactulose increases butyrate and acetate concentration in cocultures of *A. caccae* and infant fecal bacteria | a, Diagram of bacterial cross-feeding for breakdown of lactulose into butyrate. **b**, Growth measured by optical density (OD600) of *A. caccae* monocultures grown for 48h in minimal peptone yeast media (-) supplemented with lactate and acetate, lactulose, or glucose. **c, d**, Butyrate (**c**) and acetate (**d**) accumulation in culture supernatants measured by HPLC UV-Vis. **e**, Lactate accumulation in culture supernatants measured by enzymatic Lactate Assay (Sigma). Points in **b** represent biological replicates pooled from 2 independent experiments. In **c-e**, points represent biological replicates, bars represent mean ± s.e.m. pooled from 3 independent experiments. Statistics are analyzed by one-way ANOVA Tukey's post-hoc test (**b**) or two-way ANOVA (**c-d**) with Sidak's post-hoc test. *$P < 0.05$, **$P < 0.01$, ***$P < 0.001$, ****$P < 0.0001$ versus PY (-) control.

Although lactulose is a small disaccharide, *A. caccae* does not produce the enzyme(s) necessary to break apart the two sugars and utilize them as a carbon source, resulting in no growth from lactulose in monoculture (**Fig. 3.18b**). We then utilized the *A. caccae* / CMA fecal slurry co-culture system previously described to examine potential cross-feeding. Neither *A. caccae* LAHUC nor the CMA fecal bacteria produce significant butyrate from lactulose in separate cultures (**Fig. 3.18c**). However, when cultured together there was a significant increase in butyrate, as well as a modest increase in lactate (**Fig. 3.18c, e**). Acetate was readily available in all cultures containing CMA bacteria (CMA and co-culture), so acetate is not predicted to be a limiting factor in this system (**Fig. 3.18d**). Lactulose will be explored further *in vivo* as a tool to increase butyrate in mice with dysbiotic microbiota.

3.10 Manufacturability and long-term stability

To determine whether *A. caccae* may be viable as a clinical product, we examined whether our isolate was amenable to storage as a lyophilized powder or to scale-up culture production. For initial lyophilization studies, *A. caccae* was grown in CMG medium for 48h, then cells were pelleted and resuspended in various preservation solutions (10% sucrose or R18 solution) (**Fig. 3.19a**). After fully freezing these solutions at -80°C in glass ampules, the cells were lyophilized to a powder form and stored at RT on the bench top for up to 1 year. Secondary cultures of these lyophilized stocks at various timepoints confirmed substantial growth in CMG medium and lack of contamination by PCR with *A. caccae*-specific primers (**Fig. 3.19b, c**).

We then partnered with Rise Therapeutics, a contract manufacturing organization (CMO), for large-scale culture of our *A. caccae* isolate. We provided frozen stocks of *A. caccae* LAHUC grown in animal product free (AF) tryptic soy broth (TSB), a medium which is suitable for clinical use. The team at Rise then used these stocks to inoculate two

sequential starter cultures in 50mL, then 150mL of AF-TSB, respectively before beginning 2L production in an anaerobic bioreactor (**Fig. 3.20a, b**).

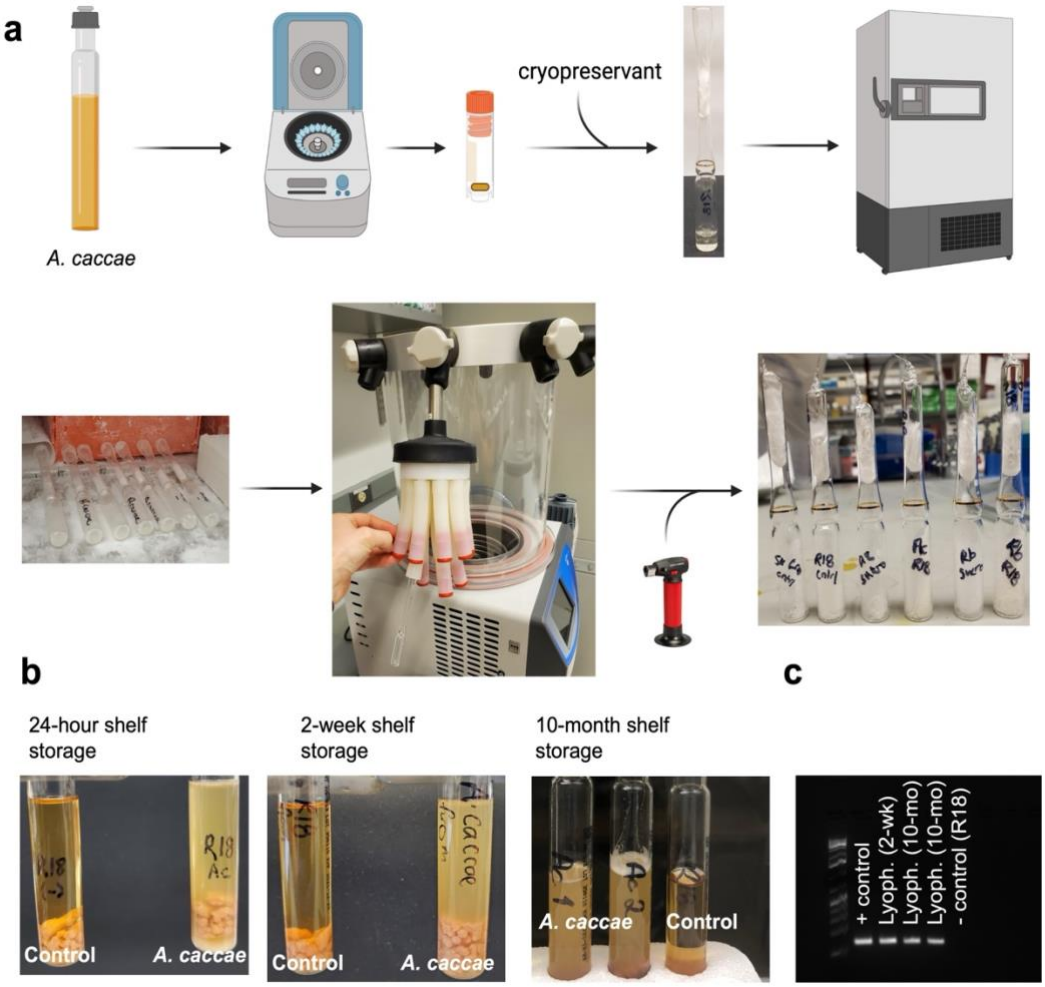

Figure 3.19: Process of lyophilizing *A. caccae* LAHUC and long-term stability | a, Lyophilization process. Cultures of *A. caccae* LAHUC in were reconstituted in cryopreservatives, aliquoted into glass ampules, flash frozen at -80°C, and vacuum dried using a lyophilizer. **b**, Growth of lyophilized *A. caccae* after various storage lengths at RT. Lyophilized stocks of *A. caccae*, or cryopreservative controls, were inoculated into CMG media and grown for 48h in an anaerobic chamber. Turbidity of cultures confirms growth. **c**, PCR of secondary cultures of lyophilized *A. caccae* (or cryopreservative, R18 control) using *A. caccae* specific primers.

In the 2L batch fermentation, the growth peaked at an optical density of approximately 6.0 after 6 hours of culture (**Fig. 3.20c**). The 2L culture was carried out for a total of 8h before the cells were removed and lyophilized. The lyophilization batch yielded a total of

43.84g of powder, which was aliquoted into glass vials with rubber stoppers and stored for further experiments. This project demonstrated that *A. caccae* LAHUC can be readily cultured in a clinically permissible medium at large volumes and yield a final product with high cell viability. We predict that *A. caccae* could feasibly be produced at scale as a clinical product, indicating more promise for further translation.

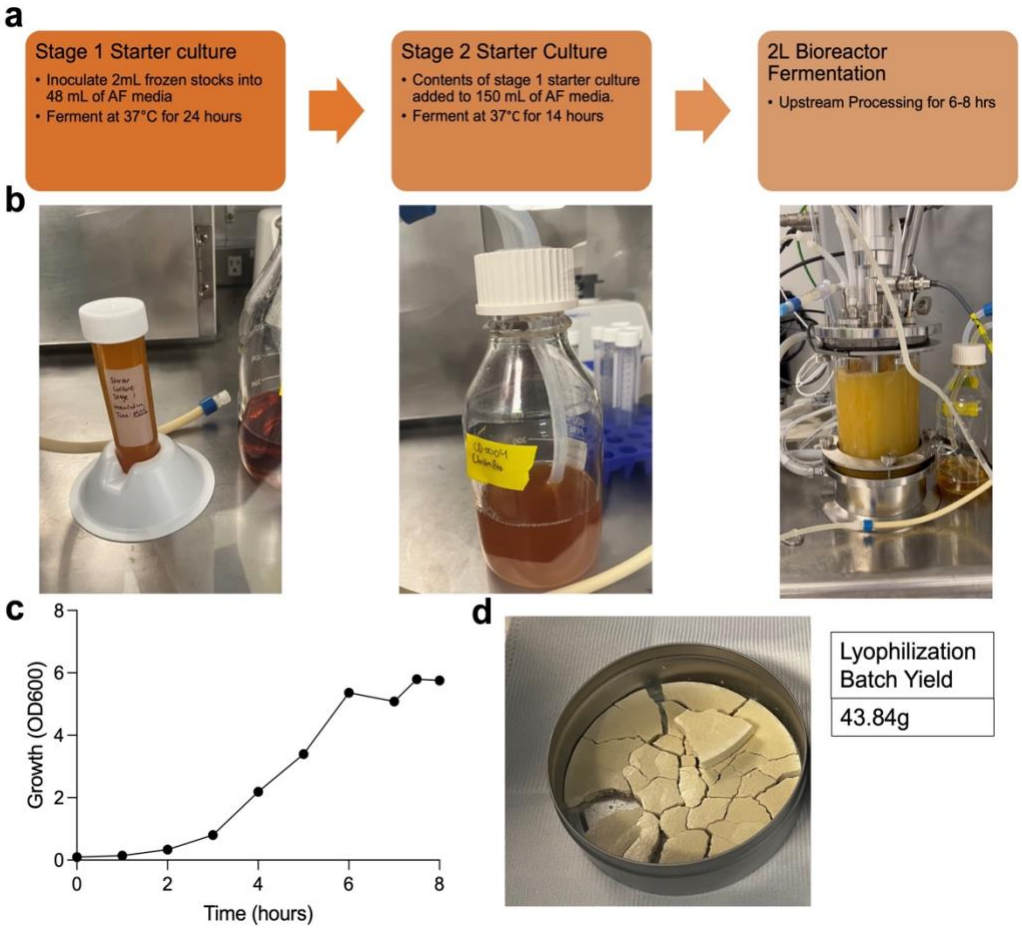

Figure 3.20: Scale-up production and manufacturing of *A. caccae* LAHUC | a, Workflow of culture scale-up to 2L batch fermentation performed by RISE Therapeutics. **b**, Representative images from various culture stages. **c**, Growth (measured by optical density, OD600) over hourly timepoints during 2L batch fermentation. **d**, Lyophilization batch yield. *A. caccae* cells obtained from 2L batch fermentation were lyophilized, resulting in 43.84g of cellular material.

3.11 Conclusion

Human fecal bacteria are complex, diverse and, their metabolic capabilities and interactions are only beginning to be understood. New techniques for *in vitro* anaerobic culturing opened doors to understanding basic characteristics of various bacteria. This chapter outlines our work in isolating a low abundance, relatively slow-growing species from the complex fecal community of a healthy infant. We characterized many aspects of our isolate, *A. caccae* LAHUC, from its genome and using basic microbiological techniques. Further studies examined and optimized its ability to produce butyrate, since we predict that butyrate production will be closely linked to this species' immunoregulatory function *in vivo*. We confirmed previous knowledge that *A. caccae* must be paired with other species to convert large polysaccharides into butyrate, utilizing either the single species *R. bromii* or a fecal slurry from a CMA infant. While we demonstrated that many prebiotics could be paired with *A. caccae in vivo*, we choose to focus on lactulose, since this prebiotic seemed most promising in its ability to make lactate available in the lower gut.

CHAPTER 4

BACTERIAL REGULATION OF EPITHELIAL BARRIER FUNCTION

4.1 Introduction

The intestinal lumen is a constant source of immune-stimulating antigens, both food-derived and microbe-derived. A single layer of intestinal epithelial cells (IECs) acts as the barrier between the luminal contents and the underlying intestinal lamina propria (LP). This epithelial layer is composed of diverse cell types which must be carefully controlled and constantly replenished, must retain integrity as a physical barrier via inter-cellular connections and other means, and sense and respond to stimuli from the lumen and the LP (*118*). Some of the ways in which commensal bacteria can impact intestinal barrier function will be explored in this chapter.

4.2 Monocolonization with *A. caccae* and oral administration of myo-inositol alters SCFA and mucus production in the colon

Previous work from our laboratory demonstrated that *A. caccae* (strain DSM 14622) can monocolonized GF mice and protected against allergic responses to food (*104*). Many obligate anaerobes are not able to persist in GF mice without prior introduction of another species to generate an anaerobic environment to provide a niche for these organisms (*274*). This is particularly true of secondary fermenters like *A. caccae*, which are not able to degrade complex dietary fibers; small, accessible sugars like glucose are largely consumed in the proximal gut and exist at low concentrations in the colon (*274*). In the previous chapter, we presented data which suggests that *A. caccae* may be able to consume colonic mucus to grow *in vitro* (**Fig. 3.11**), like other butyrate-producing

members of *Clostridium* cluster XIVa (*283*). This led to the hypothesis that *A. caccae* may also consume mucus in monocolonized mice in the absence of another carbon source. There are not many carbon sources that could be orally administered, transit to the colon, and be readily consumed by *A. caccae*. However, we showed that *A. caccae* can metabolize myo-inositol in monoculture, a glucose-like sugar alcohol (Chapter 3). Unlike glucose, myo-inositol is not metabolized by the host and readily transits to the distal colon. We thus examined whether *A. caccae* consumes mucus in monocolonized mice, with or without additional myo-inositol. *In vitro*, *A. caccae* produces large quantities of butyrate from glucose, but switches its metabolic profile in the presence of myo-inositol to produce propionate (**Fig. 3.16**). However, these dynamics have not yet been studied *in vivo*. We hypothesized that administration of myo-inositol would increase luminal levels of propionate, but not butyrate, *in vivo*.

GF mice were colonized at weaning with a single gavage of *A. caccae* LAHUC or sterile media as a control. Mice were housed in a positive-pressure housing gnotobiotic rack system for one week, during which time they received standard food and either standard water or water plus 10g/L myo-inositol. A single gavage of *A. caccae* was sufficient to colonize all mice, maintaining high abundance in the feces seven days later (**Fig. 4.1a**). GF mice have distended cecal morphology due to excess water accumulation in the absence of fiber digestion, and *A. caccae* monocolonization is not sufficient to reverse this morphology. SCFAs were quantified per weight of cecal contents, since all groups had similar weight and water content in the cecum. *A. caccae* produced minimal butyrate and no propionate in monocolonized mice, which was at or near the limit of detection (**Fig. 4.1b, c**). However, administration of myo-inositol in the water significantly increased cecal butyrate compared to both GF and *A. caccae*-monocolonized controls (**Fig. 4.1b**). Myo-inositol feeding additionally increased propionate in the cecum to measurable, albeit low, quantities (**Fig. 4.1c**). We had predicted that myo-inositol would increase luminal propionate but not butyrate; however, myo-inositol increased both

SCFAs. No differences were observed in luminal acetate (**Fig. 4.1d**), an SCFA which is produced by both colonocytes and bacteria.

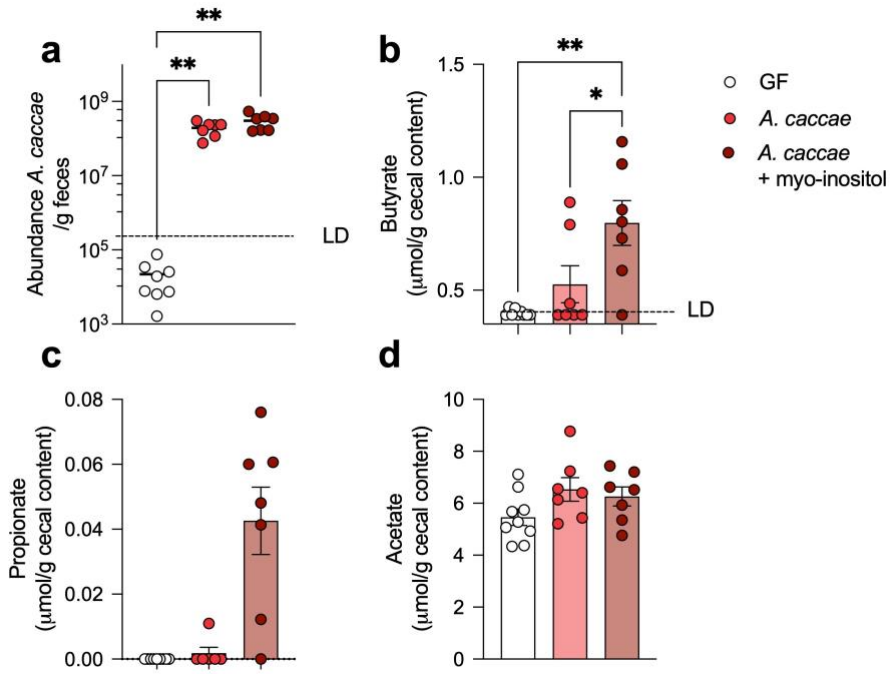

Figure 4.1: Treating *A. caccae*-monocolonized mice with myo-inositol increases short chain fatty acids in cecal contents | GF mice were colonized at weaning with *A. caccae* LAHUC by intragastric gavage, some received 10g/L myo-inositol in the drinking water for the duration of the experiment. **a**, Abundance of *A. caccae* in feces collected 7 days post-colonization measured by qPCR with *A. caccae*-specific primers. **b-d**, Concentration of butyrate (**b**), propionate (**c**), and acetate (**d**) in cecal contents measured by HPLC UV-Vis. Points represent individual mice, bars represent mean ± s.e.m. pooled from 3 independent experiments. Statistics are analyzed by one-way ANOVA with Tukey's post-hoc test. *$P < 0.05$, **$P < 0.01$.

Butyrate can stimulate colonic mucus production as a mechanism of mediating epithelial barrier function (*284*). Most of the work supporting this finding uses *in vitro* stimulation of cell lines or organoids (*284*, *285*). Mucus is the 'first line of defense' in the gut, and acts as a physical barrier to entrap or immobilize bacteria and other antigens to prevent them from accessing the epithelial surface (*278*). Mucus is produced by goblet cells (GCs), specialized epithelial cells which produce mucus glycoproteins via genes including *Muc2*. The differentiation and function of GCs are dysregulated in GF mice;

exemplifying the necessity of commensal bacteria to induce higher GC counts, mucus production, and mucosal homeostasis (*286*).

Cross-sections of the distal colon of GF mice or *A. caccae* monocolonized mice (either fed control water or myo-inositol water) were stained with periodic acid Schiff (PAS), which binds to glycans, brightly coloring the mucin-producing GCs which reside in colonic crypts (**Fig. 4.2a**). Feces were kept in the colonic histology sections to preserve integrity of the mucus layer which resides between the colonic epithelium and the feces (**Fig. 4.2a**). Monocolonization with *A. caccae* increased the mucus layer thickness and GC number in the distal colon compared to GF mice, but this effect was reversed by addition of myo-inositol (**Fig. 4.2b, c**). We hypothesized that the increased butyrate from the consumption of myo-inositol would increase colonic mucus, however mice which received both *A. caccae* and myo-inositol (and had the highest concentration of luminal butyrate) were similar to GF controls. This data was confirmed by RT-qPCR, which showed that mice treated with myo-inositol have decreased expression of *Muc2* in the colonic epithelial cell compartment (**Fig. 4.2d**). We predicted that colonization with *A. caccae* or increased SCFAs might also induce IL-22 production in the colonic LP, as both commensal Clostridia and SCFAs have been shown to induce IL-22 to modulate the epithelial barrier (*53*, *93*). However, there were no observable differences in *Il22* gene expression in the colonic LP of these mice (**Fig. 4.2e**).

Together these data suggest that the allergy-protective phenotype imparted by monocolonization with *A. caccae* is owed, in part, to a barrier-protective mechanism mediated by GC expansion and increased mucus production. It has been shown in the literature that bacterial consumption of mucus stimulates additional colonic mucus production, generating a feed-forward loop increasing GC numbers and mucus overall (*276*). We predict that in the absence of an alternative carbon source, *A. caccae* consumes colonic mucus, which overall results in low SCFA production but stimulates greater mucus production from the host.

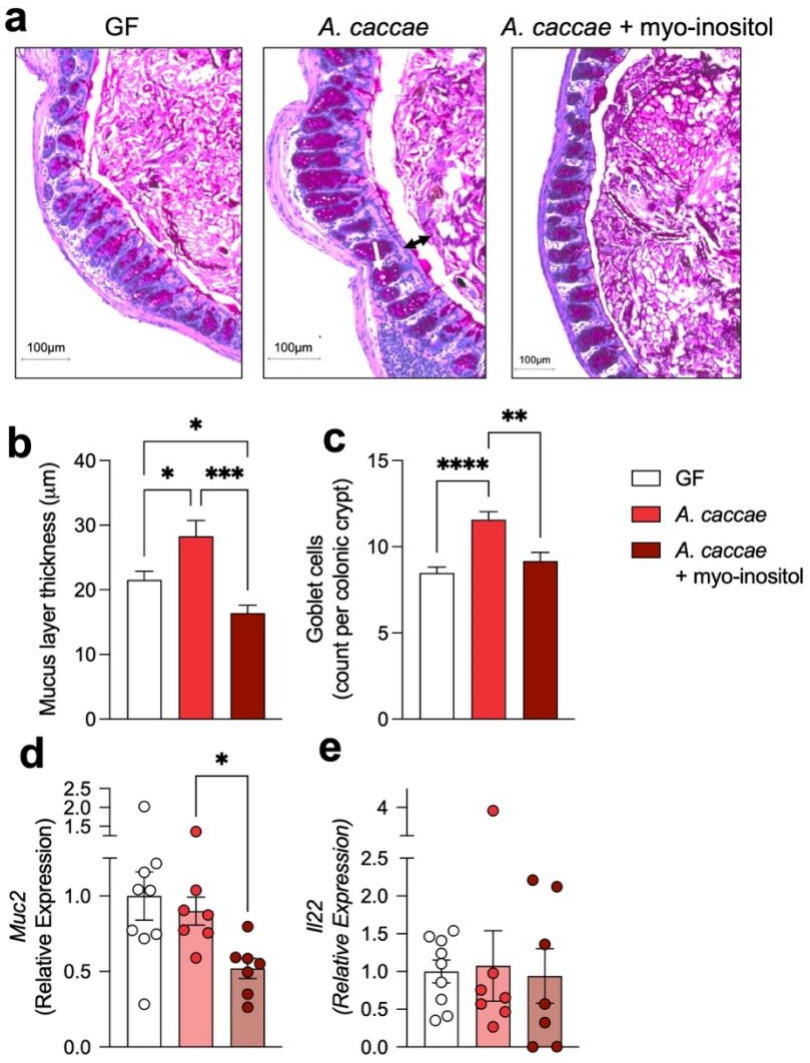

Figure 4.2: Monocolonization with *A. caccae* increases colonic mucus production, which is reversed by administration of myo-inositol | a, Representative images of colonic cross sections from each treatment group. White arrows show GCs (dark magenta), black arrow shows mucus thickness. The light magenta, fibrous matter at the top right of the images is fecal contents. **b, c**, Mucus layer thickness (**b**) and GC count per colonic crypt (**c**) from histological analysis. **d, e,** Relative gene expression of *Muc2* in colonic epithelial cells (**d**) and *Il22* in colonic lamina propria (**e**) measured by RT-qPCR. For b**-c**, at least 20 crypts and 20 measures of mucus thickness were recorded per mouse. Bars represent mean ± s.e.m. For **d-e**, points represent individual mice, bars represent mean ± s.e.m. Data is pooled from 3 independent experiments. Statistics are analyzed by one-way ANOVA with Tukey's post-hoc test. **P* < 0.05, ***P* < 0.01, ****P* < 0.001, ****P* < 0.0001.

Conversely, with a readily accessible carbon source e.g., myo-inositol, *A. caccae* produces high concentrations of SCFAs but does not elicit this direct GC/mucus effect.

We suggest that there may be two alternate pathways for barrier regulation in *A. caccae* monocolonized mice: one through direct interactions between *A. caccae* and colonic mucus/ GCs, and another indirectly through the production of SCFAs. Further experiments are necessary to determine whether, in the absence of myo-inositol, *A. caccae* resides within the mucus layer close to the epithelium. Further study could also uncover which glycoforms of mucus *A. caccae* is able to consume. We have shown that *A. caccae* is able to consume acetate, but this does not result in butyrate production. Colonic acetate may be another carbon source for *A. caccae* in monocolonized mice, which would allow this species to grow but not produce butyrate.

Overall, this controlled colonization system is useful for parsing direct interactions between a single bacterial species and the host, but it may not give much insight into the mechanisms at play in a microbially replete environment. For example, we do not expect *A. caccae* to consume large volumes of colonic mucus or colonic acetate in a replete microenvironment, due to competition for space along the epithelial wall and greater availability of nutrients in the presence of multiple cross-feeding partners. To understand *A. caccae*'s role in a broader context, we characterized the replete populations of fecal bacteria from human infants, and how these unique populations elicit disparate barrier programs in gnotobiotic mice.

4.3 Characterizing infant microbiotas in gnotobiotic mouse system

In earlier work we have extensively characterized differences in the fecal microbiota of healthy versus CMA infants in various cohorts (*103*, *104*). Colonizing GF mice with feces derived from four healthy or four CMA demographically matched infants affects the development of allergic responses to food in a model of cow's milk allergy (*104*). Specifically, healthy-colonized mice are protected from sensitization and allergic

responses to the milk allergen BLG, while CMA-colonized mice are susceptible (*104*). We now focus on one CMA (donor 6) and one healthy donor (donor 2) from the previous report to better understand the bacteria and mechanisms which were responsible for the allergy-protective phenotype.

We first sought to more fully characterize the bacterial composition of these healthy and CMA- infant-derived fecal communities in gnotobiotic mice. Fecal slurries from infant donors were i.g. gavaged to GF mice upon initial receipt approximately six years ago. Since then, these communities have been maintained in living, murine repositories. In all experiments, GF C3H/HeN mice were colonized at weaning with healthy or CMA microbiota by i.g. gavage with freshly collected feces from repository mice. Experimental mice were euthanized 7 days post-colonization and feces were collected for 16S rRNA sequencing to characterize the bacterial communities. Principal component analysis (PCA) of the 16S dataset showed that the two bacterial communities (healthy, CMA) were distinct, and the two groups form separate clusters (**Fig. 4.3a**).

We performed a linear discriminant analysis effect size (LEfSe) test to examine differences in relative abundance of bacterial taxa at the genus level between the two groups. The two bacterial communities were strikingly different, and there were many bacterial genera that were differentially abundant (**Fig. 4.3b**). The CMA microbiota was dominated by Gram negative bacteria including *Bacteroides* and *Parabacteroides*, while the healthy microbiota had significantly higher relative abundance of bacteria in the Erysipelotrichaceae family (*Longicatena*), and several other Clostridial genera. Healthy-colonized mice also had greater relative abundance of *Bifidobacterium*, a genus that is commonly in high abundance in the infant microbiota and has been associated with health in this age group (*35*). High abundance of *Bifidobacterium* in infant feces is generally associated with breastfeeding (*36*), but interestingly, the infant donors in this study were all breastfed for only 2-weeks before exclusive formula feeding (*104*). This persisting presence of *Bifidobacterium* in the healthy infant microbiome may also be correlated to

their health status. Overall, these results are similar to the initial characterization of the larger cohort (4 healthy and 4 CMA donors) described in 2019 (*104*).

We also re-analyzed 16S rRNA sequencing data from the previous report (*104*), now focusing only on healthy donor 2 and CMA donor 6. Comparing the differential abundance of bacteria in feces of healthy- or CMA-colonized mice in this data set revealed an enrichment of unclassified Lachnospiraceae, Erysipelotrichaceae, *Bifidobacterium*, and *Anaerostipes* in healthy-colonized mice (**Fig 4.3c**). Conversely, feces of CMA-colonized mice were enriched for *Parabacteroides* and *Bacteroides* (**Fig 4.3c**). These results are strikingly similar to the differentially enriched taxa observed in the more recent data (**Fig 4.3b**), demonstrating that these human-derived microbiotas have remained stable over several years. Maintaining fecal bacterial populations within living mouse repositories is a reproducible and reliable method for gnotobiotic research with human fecal communities.

In the previous report, *A. caccae* was identified to be more abundant in healthy-colonized mice (donors 1-4) versus CMA (donors 5-8), and its abundance correlated strongly with altered gene expression in the ileal epithelium of colonized mice (*104*). *Anaerostipes* was also enriched in mice colonized with feces from healthy donor 2 compared to CMA donor 6 (**Fig 4.3c**). Here we show that, several years later, *Anaerostipes* were still significantly more abundant in the feces of healthy-colonized mice than CMA (**Figs. 4.3b, 4.4a**).

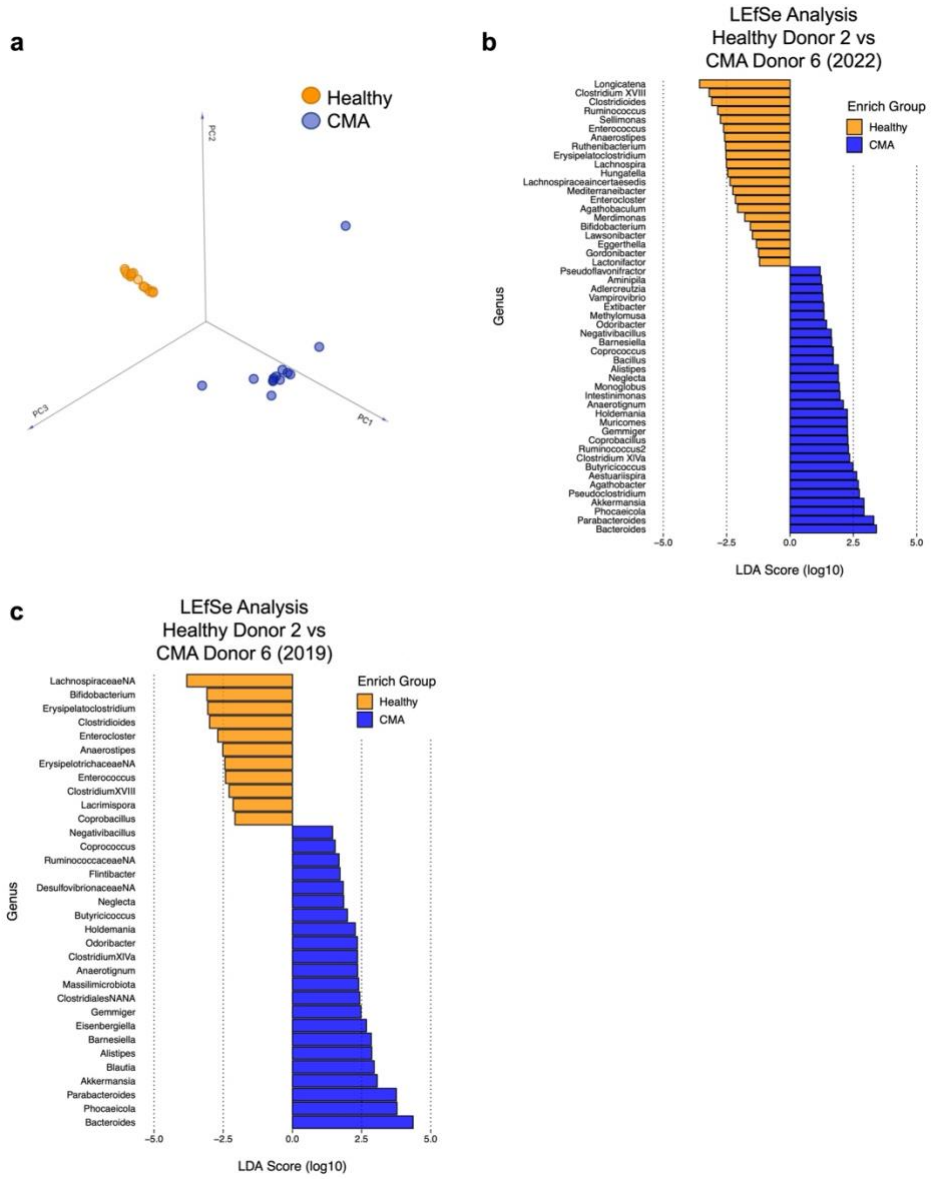

Figure 4.3: 16S rRNA sequencing analysis of bacterial taxa in fecal samples of mice colonized with feces from a healthy or cow's milk allergic infant | GF mice were colonized at weaning with feces from repository mice which harbor healthy infant (donor 2) or cow's milk allergic infant (CMA, donor 6) microbiota. Feces were collected 7d post-colonization for 16S rRNA sequencing. **a**, Principal component analysis (PCA) of 16S data. Each dot represents an individual mouse and is positioned along the top 3 axes of variance. **b**, Differentially abundant taxa analyzed by linear discriminant analysis effect size (LEfSe). Data was pooled from 3 independent experiments (*n* = 12 healthy, *n* = 11 CMA) . **c**, Reanalysis of 16s rRNA data from Ref. 104 comparing feces of mice colonized with feces derived from healthy donor 2 (*n* = 3) or CMA donor 6 (*n* = 4).

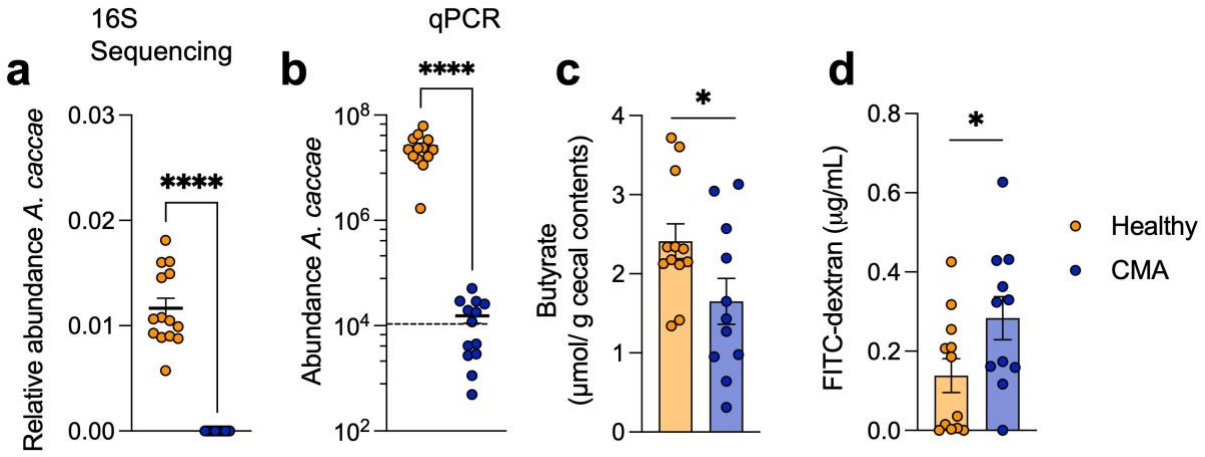

Figure 4.4: Healthy-colonized mice have increased abundance of *A. caccae*, increased butyrate, and improved barrier function compared to CMA mice | a, b, Relative abundance of *A. caccae* from 16S sequencing data (**a**) or total abundance measured by qPCR with species-specific primers (**b**). **c,** Butyrate concentration in cecal contents measured by HPLC UV-Vis. **d**, Concentration of FITC-dextran in serum following an i.g. gavage. Points represent individual mice, bars represent mean ± s.e.m. Data is from the same mice shown in **Fig. 4.3**. All data is pooled from 3 independent experiments. Statistics are analyzed by Student's t test. **P* < 0.05, ****P* < 0.0001.

As previously described, the relative abundance of *A. caccae* is only approximately 0.1% of the entire fecal population (**Fig. 4.4a**), but this low-abundance species seems to have an outsized effect on host phenotype. The relative and absolute abundance of *A. caccae* in CMA-colonized mice was at or near the limit of detection, confirming the near absence of this species in the CMA community (**Fig. 4.4a, b**). *A. caccae* is a characteristic species of the infant microbiota which peaks in abundance at 12 months of age (*37*) and is a potent butyrate producer (*246*). In fact, CMA-colonized mice (which are lacking *A. caccae*) had a significant reduction in luminal butyrate compared to healthy-colonized mice (**Fig. 4.4c**). Butyrate has many known barrier-modulating functions, and we predict that this lack of butyrate may have consequences on the intestinal barrier function of mice colonized with the CMA microbiota.

4.4 Healthy infant bacteria induce a barrier protective response in the small intestine

Previous work from our laboratory demonstrated that bacteria in the Clostridia class mediate a barrier protective response in mice which is critical to maintaining nonresponsiveness to food antigens (*53*). This barrier-protective phenotype effectively prevents food antigens from accessing systemic circulation and is dependent on the cytokine IL-22. These findings contributed to a Barrier Regulation Hypothesis of Allergen Sensitization, which posited that an intact epithelial barrier (initiated by the presence of commensal Clostridia) is required to prevent allergic sensitization along with a subsequent antigen-specific regulatory T cell response (*117*). Butyrate has been shown to regulate epithelial barrier function, a metabolite that we show is produced by *A. caccae* (**Fig. 3.8**) and is lacking in our CMA-colonized mice (**Fig. 4.4c**). We predict that the lack of a bacteria-induced barrier-protective response could be responsible for the heightened susceptibility to allergy observed in CMA-colonized mice. Similarly, the lack of butyrate in CMA-colonized mice could contribute to this effect.

To quantify intestinal barrier integrity, GF C3H/HeN mice were colonized at weaning with healthy or CMA microbiota. Feces from these experimental mice were collected 7 days later, and analyses of their fecal bacteria were shown in **Fig. 4.3** and **Fig. 4.4**. One week post-colonization, mice were i.g. gavaged with 4kDa FITC-dextran. After 2 hours, the presence of FITC-dextran in the serum was measured by fluorescence spectrometry; increased FITC-dextran in serum demonstrates greater permeability of the intestinal epithelial barrier. Within 2 hours of gavage, the FITC-dextran will transit fully through the small intestine but not yet reach the colon, allowing us to specifically analyze barrier integrity in the small intestine. In keeping with our hypothesis, we show that these two bacterial communities do not equally elicit barrier protective responses. The concentration

of FITC-dextran in the serum of CMA-colonized mice was significantly greater than that of healthy-colonized mice (**Fig. 4.4d**).

We previously described that the Clostridia-induced barrier protective response was dependent on IL-22 (*53*). Colonization with a consortium of murine Clostridia significantly increased IL-22 production in *ex vivo* intestinal explants (*69*). Additionally, treating mice with a neutralizing antibody against IL-22 abrogated the protective barrier effect and increased the concentration of PN antigen in serum following an i.g. gavage (*53*). To determine whether the CMA or healthy microbiota induce IL-22, GF C57BL/6 mice were colonized at weaning as described. Mice were euthanized one week later, and intestinal tissues were cultured *ex vivo* for 24h. Colonic and ileal (terminal 10cm of the small intestine) tissues were cultured without additional stimulation, and duodenal tissue (5cm just proximal to the ileum) was cultured in the presence of IL-23, an IL-22 stimulating cytokine, as positive controls. IL-22 was measured in culture supernatants by ELISA. Colonization with neither the CMA nor healthy microbiota induced significant IL-22 production in the ileum (**Fig. 4.5a**). However, colonic tissue from healthy-colonized mice produced significantly more IL22 than both CMA-colonized mice and GF controls (**Fig. 4.5b**). IL-23 stimulated controls demonstrated that CMA and healthy-colonized mice are similarly capable of producing high concentrations of IL-22 *ex vivo*, as are GF controls, although to a lesser extent (**Fig. 4.5c**).

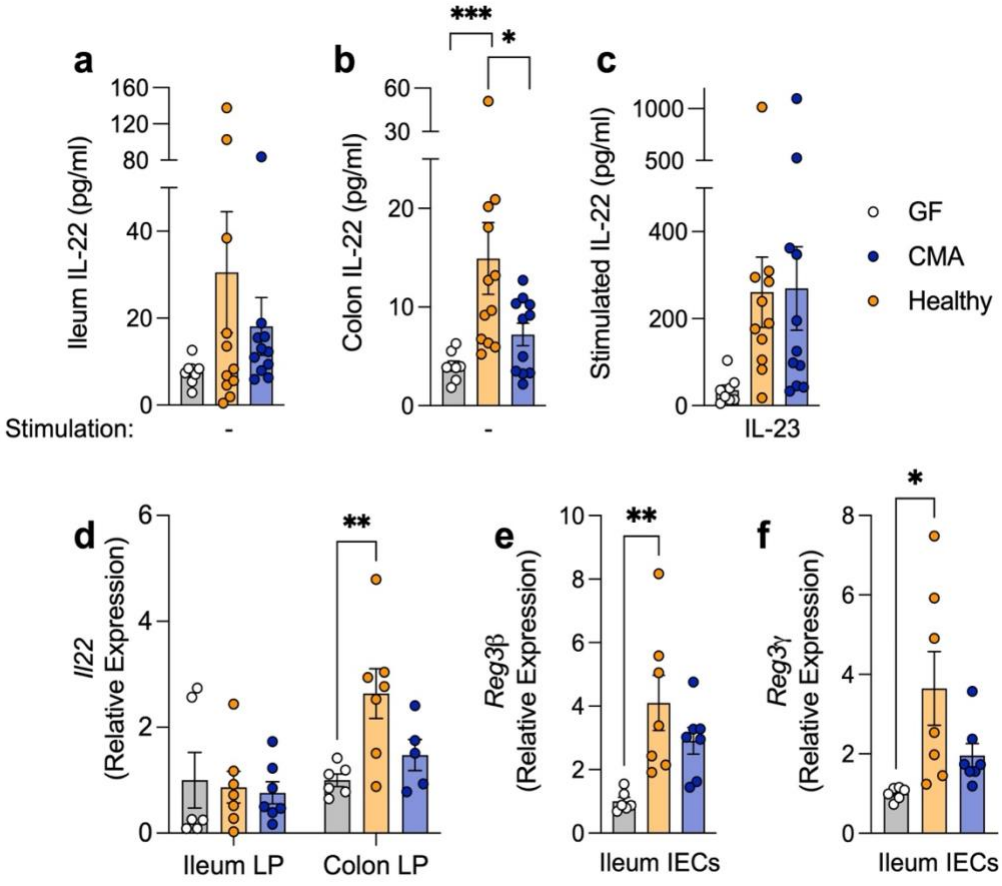

Figure 4.5: Colonization with healthy infant microbiota induces intestinal IL-22 production | GF C57BL/6 mice were colonized at weaning with feces from repository mice which harbor healthy infant or cow's milk allergic infant (CMA) microbiota. IL-22 secretion from ileal (**a**) and colonic tissues (**b**) cultured *ex vivo* for 24h measured by ELISA. **c**, IL22 secretion from duodenal tissue stimulated with IL-23 measured by ELISA. **d**, Relative expression of *Il22* in ileal or colonic lamina propria (LP) cells analyzed by RT-qPCR. **e, f,** Relative gene expression of *Reg3β* (**e**) and *Reg3*γ (**f**) in ileal intestinal epithelial cells. Gene expression was normalized to GF controls. Points represent individual mice, bars represent mean ± s.e.m. pooled from 3 independent experiments (**a-c**) or 2 independent experiments (**d-f**). Statistics are analyzed by one-way ANOVA with Tukey's post-hoc test. **P* < 0.05, ***P* < 0.01, ****P* < 0.001.

Production of IL-22 induces downstream expression of antimicrobial peptides (AMPs) from Paneth Cells within the small intestinal epithelial cell compartment, and these AMPs

are also demonstrative of a barrier-protective response (*53*). Colonization with the healthy infant microbiota (but not CMA microbiota) induced significantly greater expression of the AMPs *Reg3β* and *Reg3γ* in the ileal IEC compartment compared to GF controls (**Fig. 4.5e, f**). This suggests that healthy-colonized mice may also produce IL-22 in the ileum, although this was not observed in intestinal explants (**Fig. 4.5a**) or by RT-qPCR of the ileal LP at this timepoint (**Fig. 4.5d**). Colonization with the healthy microbiota significantly increased *Il22* gene expression in the colon LP (**Fig. 4.5d**), mirroring the IL-22 production observed in explant cultures.

Overall, we have demonstrated that the fecal bacteria of a healthy infant induce a barrier-protective phenotype characterized by decreased permeability to FITC-dextran in the small intestine and increased IL-22 production in the colon. This barrier-protective phenotype is less evident in CMA-colonized mice, which may contribute to their heightened response to allergic sensitization. The impaired barrier response in CMA-colonized mice may be due to their lack of butyrate (and butyrate producers like *A. caccae*). However, in this system with complex microbiota we cannot attribute these differences to butyrate alone. This necessitated further experiments to determine if butyrate is sufficient to induce a similar barrier protective response.

4.5 Butyrate administered via polymer micelles induces a barrier protective response in antibiotic treated mice

We hypothesized that the barrier deficiency observed in CMA-colonized mice may be due to their lack of butyrate-producing species like *A. caccae* and subsequent lower concentration of luminal butyrate. Butyrate is a critical molecule for homeostasis and immune regulation in the distal gut, and decreased abundance of butyrate or butyrate producing-bacteria has been strongly correlated with various disease indications in pre-clinical and clinical settings (*78*, *287*). However, there is conflicting evidence regarding

whether butyrate alone is sufficient to induce a barrier-protective effect. Butyrate is volatile, foul smelling, and rapidly absorbed in the upper GI tract. These factors limit research on the effects of sodium butyrate *in vivo*, often requiring intrarectal administration or long-term administration of sodium butyrate in drinking water at high concentrations (*86–88*, *98*, *242*).

Recent work from our group has shown that i.g. butyrate administered as a sodium salt (NaBut), which is the most commonly used method in the literature, is rapidly absorbed in the stomach and does not reach the lower gut (*92*). To address this limitation in delivery, we developed block copolymers to which butyrate was covalently conjugated and which self-assemble into micellar structures. One of these polymers is neutrally charged (NtL-ButM) and one is negatively charged (Neg-ButM); their surface charge affects their transit time through the lower GI tract and the pharmacokinetics of butyrate release. Co-administration of these two butyrate containing polymers (ButM) allows maximal delivery of butyrate along the length of the distal GI tract (*92*). ButM improved intestinal barrier function in the context of antibiotic-induced bacterial dysbiosis and chemically induced intestinal injury with the perturbant DSS (*92*). These experiments used SPF C57BL/6 mice, and serum FITC-dextran was the main readout of barrier function either 1.5h or 4h after i.g. gavage to analyze barrier integrity in the small intestine (1.5h) or both small and large intestine (4h).

Here, we replicated these experiments in C3H/HeN mice, which are used for all studies involving allergic phenotypes in the following chapter. SPF C3H/HeN mice were treated with a cocktail of antibiotics daily by i.g. gavage for one week prior to weaning (*53*). Neonatal administration of antibiotics is sufficient to induce bacterial dysbiosis and disrupt epithelial barrier function. Beginning at weaning, mice were i.g. gavaged twice daily with ButM or PBS for one week as described (*92*). Mice then received one i.g. gavage with 4kDA FITC-dextran, and fluorescence was measured in the serum 1.5h later. Treatment with ButM significantly reduced the concentration of FITC-dextran in the serum,

confirming that butyrate alone is sufficient to induce a barrier-protective response in C3H/HeN mice (**Fig. 4.6a**).

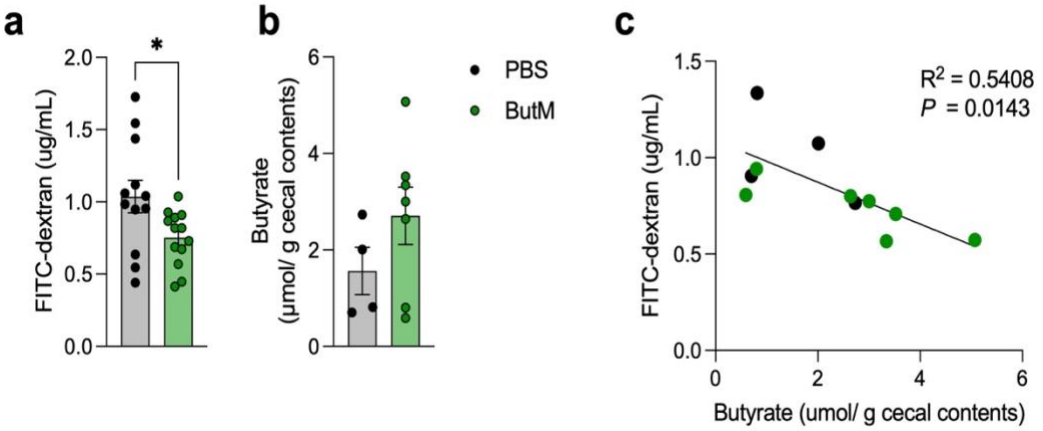

Figure 4.6: Butyrate micelle treatment improves intestinal barrier integrity in antibiotic-treated mice | SPF C3H/HeN mice were i.g. gavaged with a cocktail of antibiotics daily for one week pre-weaning. At weaning, mice were treated i.g. with PBS or butyrate-containing micelles (ButM) twice daily for one week before i.g. administration of 4kDa FITC-dextran. **a**, Concentration of FITC-dextran in serum. **b**, Butyrate concentration in cecal contents measured by HPLC UV-Vis. **c**, Linear correlation between serum FITC-dextran and cecal butyrate from **a** and **b**. Data in (**a**) is pooled from 2 independent experiments, data in **b, c** is from one representative experiment. Points represent individual mice, bars represent mean ± s.e.m. Data is analyzed by Student's t test (**a, b**) or simple linear regression (**c**). *$P < 0.05$.

ButM treatment modestly, but not significantly, increased the concentration of butyrate in the cecal contents (**Fig. 4.6b**). The release of butyrate from Neg-ButM in the cecum peaks approximately 8-12h after i.g. gavage (*92*). In this experiment cecal contents were collected only 6h after gavage, which was potentially too early to observe peak butyrate release. Although the difference in cecal butyrate was not significant, there was a strong negative correlation between serum FITC-dextran and cecal butyrate (**Fig. 4.6c**), contributing to our overall evidence that butyrate can directly modulate epithelial barrier function. ButM treatment induced a modest but significant increase in expression of *Reg3β* but not *Reg3γ* (**Fig. 4.7**) in ileal IECs. This suggests that ButM may weakly induce

IL-22 in the ileum, but more studies will be required to determine if the barrier protective effect of butyrate is mediated by IL-22.

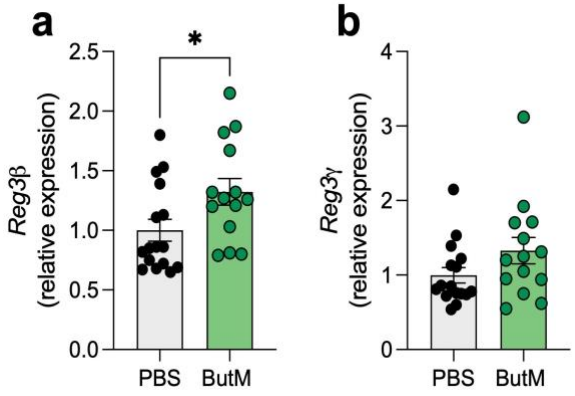

Figure 4.7: Butyrate treatment increases expression of antimicrobial peptides in ileal epithelial cells | Relative gene expression of *Reg3β* (**a**) and *Reg3*γ (**b**) in ileal intestinal epithelial cells measured by RT-qPCR. Data is from the same mice shown in **Fig. 4.6**. Data is pooled from 2 independent experiments. Points represent individual mice, bars represent mean ± s.e.m. Data is analyzed by Student's t test, **P* < 0.05.

4.6 Conclusion

We have previously demonstrated that various bacterial populations, including commensal Clostridia, healthy infant bacteria, and *A. caccae* can prevent allergic sensitization and a downstream allergic response in mice (*53*, *104*). A consortium of murine derived, spore forming Clostridia induce an IL-22-dependent barrier protective response, and this barrier response is necessary to prevent access of food antigens to systemic circulation (*53*). However, it was unknown whether human infant derived bacterial populations could elicit this same barrier protective effect, and if these populations or treatment with individual metabolites such as butyrate could mediate a similar response.

We predicted that the healthy microbiota, which is characterized by increased abundance of *A. caccae*, a butyrate-producing Clostridia, would induce a similar barrier-

protective phenotype as the murine-derived Clostridia consortium. In keeping with this hypothesis, colonization with healthy infant bacteria, but not that of a CMA infant, induced a barrier protective phenotype. This phenotype is characterized by increased production of *Reg3β* and *Reg3*γ by ileal IECs, IL-22 secretion in colonic explants, and reduced serum FITC-dextran.

Mucus has been described as a critical component of the epithelial barrier (*278*). It was not known whether *A. caccae* could utilize mucus as a carbon source when monocolonized in GF mice. Mucus-consuming bacteria, such as *Akkermansia municiphilia*, were at one time thought to be potential pathobionts due to their ability to gain greater access to the epithelium by feeding on epithelial mucus. However, more recent studies suggest that *Akkermansia* may have beneficial roles and is associated with homeostasis (*276*). In fact, *Akkermansia* strains are quickly entering clinical trials as LBPs and nutritional supplements (*277*). It is now suggested that mucus-consuming bacteria may actually elicit a barrier productive function; by consuming colonic mucus, they may signal to colonic GCs that more mucus is required, resulting in a feed forward loop of overall greater mucus production and epithelial barrier integrity (*288*).

We demonstrate that *A. caccae* may consume mucus in the absence of a viable carbon source *in vivo*, but that treatment with a prebiotic, non-host accessible carbohydrate (myo-inositol) may alter this organism's reliance on host mucus and allow it to produce SCFAs more efficiently. However, would the increased abundance of SCFAs also signal to GC to produce mucus? The data presented in **Fig. 4.1** and **Fig. 4.2** suggest that consumption of mucus by *A. caccae* in the absence of another carbon source may be more influential on GC number and function than the presence of prebiotic induced SCFAs. *A. caccae* only produces modest levels of butyrate in monocolonized mice, but these monocolonized mice have increased GC numbers and mucus thickness in the distal colon. However, in *A. caccae* monocolonized mice which also received myo-inositol in the water, both butyrate and propionate substantially increased, while GC numbers and mucus

consumption reduced to GF levels. *A. caccae* may have protected against allergic responses to BLG in monocolonized mice by increasing colonic mucus. However, we do not yet know if or how these mucus/GC dynamics are affected in microbially replete hosts.

In antibiotic-treated mice, butyrate alone is sufficient to induce a barrier protective phenotype when administered within polymer micelles (*92*). We predict that butyrate is critical to maintaining homeostasis and preventing allergic responses to food in microbially replete hosts. In the next chapter, we describe work to optimize bacterial formulations which increase luminal butyrate when administered to mice with the dysbiotic, CMA microbiota.

CHAPTER 5

A SYNBIOTIC BACTERIAL THERAPY INCREASES LUMINAL BUTYRATE AND TREATS FOOD ALLERGY IN MICE

5.1 Introduction

We have thus far demonstrated that we have isolated a butyrate-producing strain of *A. caccae*, which is capable of consuming various carbon sources *in vitro* in monoculture or via cross-feeding with other bacterial species. In this chapter we describe a pre-clinical model to examine the efficacy of this isolate as an LBP to prevent or reverse the development of allergy in mice. Previous work from our laboratory demonstrated that *A. caccae* (strain DSM 14662) prevented allergic responses to BLG in monocolonized mice (*104*). However, will *A. caccae* be sufficient to induce an allergy-protective phenotype in mice with a microbially replete, yet dysbiotic microbiome?

Others have shown that a consortium of Clostridiales is sufficient to prevent or treat food allergy in SPF, antibiotic treated mice (*111*). However, this report showed little to no long term engraftment of Clostridiales species. Lack of engraftment is one of the main limitations of current LBPs in pre-clinical and clinical settings. Engraftment often requires intensive treatment with antibiotics, further depleting the resident microbiota of already potentially dysbiotic hosts (*207*). We have instead opted for a synbiotic approach, in which *A. caccae* will be simultaneously administered with a prebiotic to aid in its engraftment and metabolic opportunity *in vivo* (**Fig. 5.1**). There is significant interest in development of clinical synbiotics, and some have shown that synbiotic administration improves engraftment and efficacy of *Bifidobacterium* probiotics in healthy adults (*174*). This report also demonstrated that synbiotic administration increased luminal butyrate in gnotobiotic

mice but did not examine any disease indications *in vivo*. We will address this gap by delivering an LBP which has already demonstrated health benefits.

Synbiotics are defined as intentional pairings of a prebiotic and LBP designed to confer a specific health benefit on the host. We are developing complementary synbiotics, since *A. caccae* may have some potential health benefits alone, and we are not using genetic tools or other strategies to achieve unique, selective consumption of the prebiotic by *A. caccae*. In fact, some of the prebiotics tested in the following chapter depend on cross-feeding relationships and initial degradation of the prebiotic by other host-resident microbes.

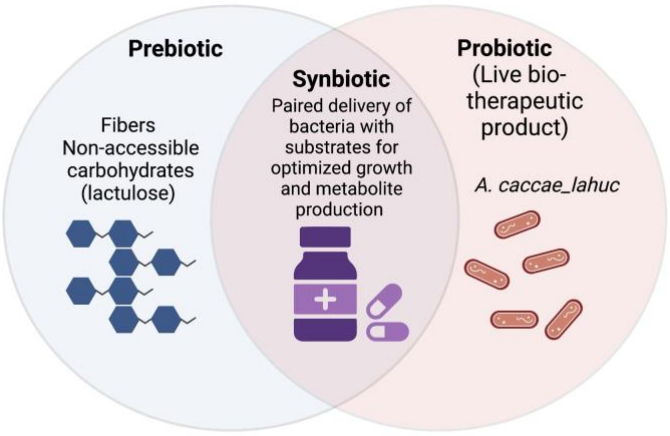

Figure 5.1: Synbiotic method | Experiments in this chapter will pursue co-administration of *A. caccae* LAHUC and prebiotic lactulose to mice with dysbiotic microbiota. We predict that this synbiotic strategy will improve therapeutic efficacy of *A. caccae* in a microbially replete environment.

While several prebiotics were tested *in vitro* and *in vivo*, lactulose was the only prebiotic administered which significantly increased luminal butyrate *in vivo*. Lactulose is digested by primary-degrader bacteria in the colon which produce high concentrations of lactate and acetate (*253*), small molecules that are utilized by *A. caccae* to produce butyrate (*247*). In the following chapter, we demonstrate that co-administration of *A. caccae* and lactulose, but neither alone, increases luminal butyrate and lactate in the

cecum of mice colonized with the fecal bacteria of a dysbiotic, CMA infant. Synbiotic treatment (*A. caccae* plus lactulose) shifts the composition of the fecal microbiota, increasing relative abundance of *Bifidobacterium* species which are the likely primary degraders of lactulose. This synbiotic regimen prevents the development of the allergic response to BLG, and mechanistic studies show that this effect may be mediated by decreased alarmin production upon initial sensitization and increased populations of Tfr cells and decreased IgE-secreting cells in the mLN. Finally, treatment with this synbiotic also demonstrated efficacy in treating allergic responses to PN in sensitized mice treated neonatally with antibiotics. This data demonstrates that our synbiotic has a therapeutic effect in different models, with different food antigens, different resident microbiota (CMA infant microbiota or SPF-antibiotic treated), and different timelines of treatment.

5.2 *A. caccae* readily engrafts in microbially replete hosts, but luminal butyrate does not correspondingly increase

As discussed above, engraftment of LBPs is consistently limited in clinical studies, even with extensive antibiotic pre-treatment. Although *A. caccae* readily colonizes GF mice, we did not know whether this would be the case in microbially replete mice. For this study, GF C3H/HeN mice were colonized at weaning with the CMA infant microbiota (**Fig. 5.2a**). As previously described, for all gnotobiotic experiments, mice with humanized microbiota are fed Nutramigen extensively-hydrolyzed casein formula (ECHF) diluted in in water. This is the same formula fed to the infant donor at the time of fecal collection and is required to maintain the integrity of human fecal bacteria in mice.

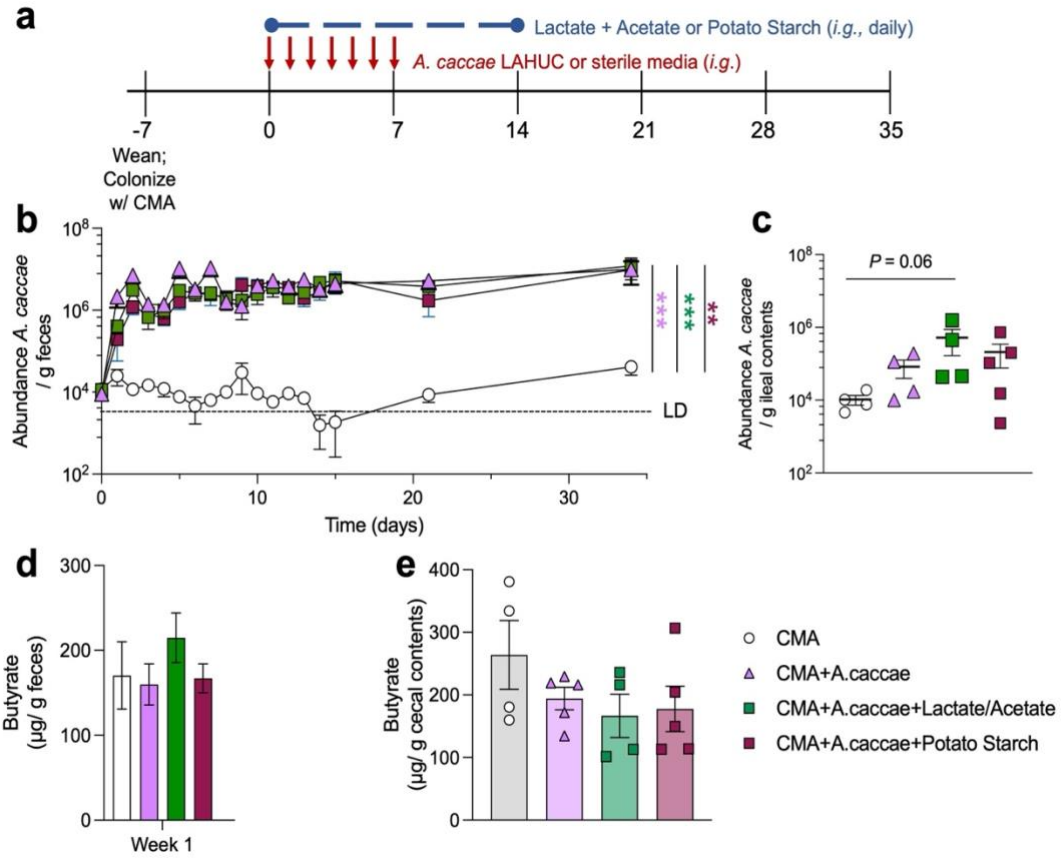

Figure 5.2: *A. caccae* readily engrafts in CMA-colonized mice, but does not increase luminal butyrate | a, Experimental timeline. GF C3H/HeN mice were colonized with CMA microbiota at weaning. Beginning one week later, mice received i.g. gavages with either *A. caccae* LAHUC or sterile media (control) daily for seven days. Mice also received daily i.g. gavages with 10mM lactate plus 10mM acetate, 10mM potato starch in PBS, or PBS. **b, c,** Abundance of *A. caccae* in feces (**b**) or ileal contents (**c**) measured by qPCR with species specific primers. **d, e,** Butyrate in feces (**d**) or cecal contents (**e**) measured by HPLC UV-Vis. For **b**, points represent the mean ± s.e.m. for each group. For **c** and **e**, points represent individual mice, bars represent the mean ± s.e.m. For **d**, 2 fecal pellets were collected from each mouse at various points throughout the first week of treatment, and bars represent mean ± s.e.m. Data is pooled from 2 independent experiments. Statistics are analyzed by area under the curve (**b**), or one-way ANOVA with Tukey's post hoc test (**c-e**). $^{**}P < 0.01$, $^{***}P < 0.0001$.

The CMA microbiota was allowed to grow and fill the environment for one week before beginning daily gavages with *A. caccae* LAHUC or sterile media as a control for one week (**Fig. 5.2a**). To determine whether prebiotics would aid in long-term engraftment of *A.*

caccae LAHUC and its ability to produce butyrate, mice were i.g. gavaged daily for 2 weeks with various prebiotics (either potato starch or the combination of lactate and acetate) which led to increased butyrate production *in vitro* (Chapter 3). Feces were collected throughout the experiment window to analyze abundance of *A. caccae*. During the week that mice were gavaged with *A. caccae*, feces were collected just prior to gavage (approximately 23 hours since last treatment), as it has been shown that non-colonizing bacteria will be undetectable in the feces as soon as 6 hours after i.g. gavage (*111*). Strikingly, even without any prebiotics, *A. caccae* readily engrafted in CMA mice, increasing in total abundance by approximately 2-logs, and this increased abundance was maintained for up to one month following the last i.g. treatment (**Fig. 5.2b**). At the conclusion of the experiment, the abundance of *A. caccae* was modestly increased in the ileum of treated mice, although not significantly (**Fig. 5.2c**). Mice treated with *A. caccae* and lactate plus acetate had the greatest abundance of *A. caccae* in the ileum, and additionally had slightly increased butyrate in the feces during the first week of treatment (**Fig. 5.2c, d**). This led us to pursue lactate plus acetate as prebiotics in further experiments.

Somewhat surprisingly, none of these treatments markedly increased the concentration of butyrate in the feces or cecal contents (**Fig. 5.2d, e**). We predicted that if *A. caccae* was present in the microenvironment, that it would produce butyrate. This does not seem to be the case, and presence of *A. caccae*, even with administration of additional prebiotics, did not increase the concentration of luminal butyrate in CMA-colonized mice. We suspected that *A. caccae* LAHUC might be deprived of some essential nutrients, which allowed this bacterium to survive but not produce substantial butyrate in the context of the CMA microbiota. This is similar to what we observed in the previous chapter using monocolonized mice; in the absence of a readily available carbon source, *A. caccae* did not produce high levels of butyrate *in vivo* (**Fig. 4.1**). Further

experiments sought to identify a more effective prebiotic to induce butyrate production in CMA-colonized mice.

5.3 Synbiotic treatment with *A. caccae* LAHUC and lactulose, but not other prebiotics, increases luminal butyrate and the relative abundance of *Bifidobacterium*

Because *A. caccae* so readily colonized CMA mice with 7 daily gavages, future colonization experiments reduced the treatments to 3 days of *A. caccae* LAHUC or sterile media gavages (**Fig. 5.3a**). In the previous experiment, butyrate was measured in the cecum several weeks after prebiotic gavages had stopped, so we may have missed a potential window during which administration of lactate and acetate increased cecal butyrate. For this experiment, mice were i.g. gavaged with *A. caccae* LAHUC or sterile media daily for 3 days. During that window, and for 2 weeks after, some mice also received i.g. gavages with prebiotics (lactate plus acetate or degraded potato starch products) every other day (**Fig. 5.3a**). In Chapter 3, we demonstrated that *A. caccae* produced butyrate very efficiently when grown in spent media from *R. bromii's* degradation of potato starch (**Fig. 3.13**). For this experiment, mice were gavaged with that same, spent media (dPotato Starch) to determine if previously degraded potato starch would be more efficacious than administration of potato starch itself. Additionally, one group received lactulose (at a sub-clinical, prebiotic dose) in the drinking formula according to the literature (*257*).

In keeping with previous findings, *A. caccae* efficiently engrafted in CMA mice, as demonstrated by substantially increased abundance in feces at euthanasia (**Fig. 5.3b**), yet *A. caccae*-treated mice did not have any increase in cecal butyrate compared to CMA controls (**Fig. 5.3c**). None of the prebiotics administered alone (lactate plus acetate or lactulose) increased cecal butyrate in mice also not treated with *A. caccae* (**Fig. 5.3c**).

Interestingly, administration of lactulose alone increased the abundance of resident *A. caccae* in the CMA microbiota, but this increased abundance didn't increase cecal butyrate (**Fig. 5.3b, c**). Lactulose has been reported to increase the relative abundance of *Anaerostipes in vitro* and *in vivo* (*254*, *257*), however this finding limited our ability to further study treatment with lactulose alone due to risk of contaminating our gnotobiotic

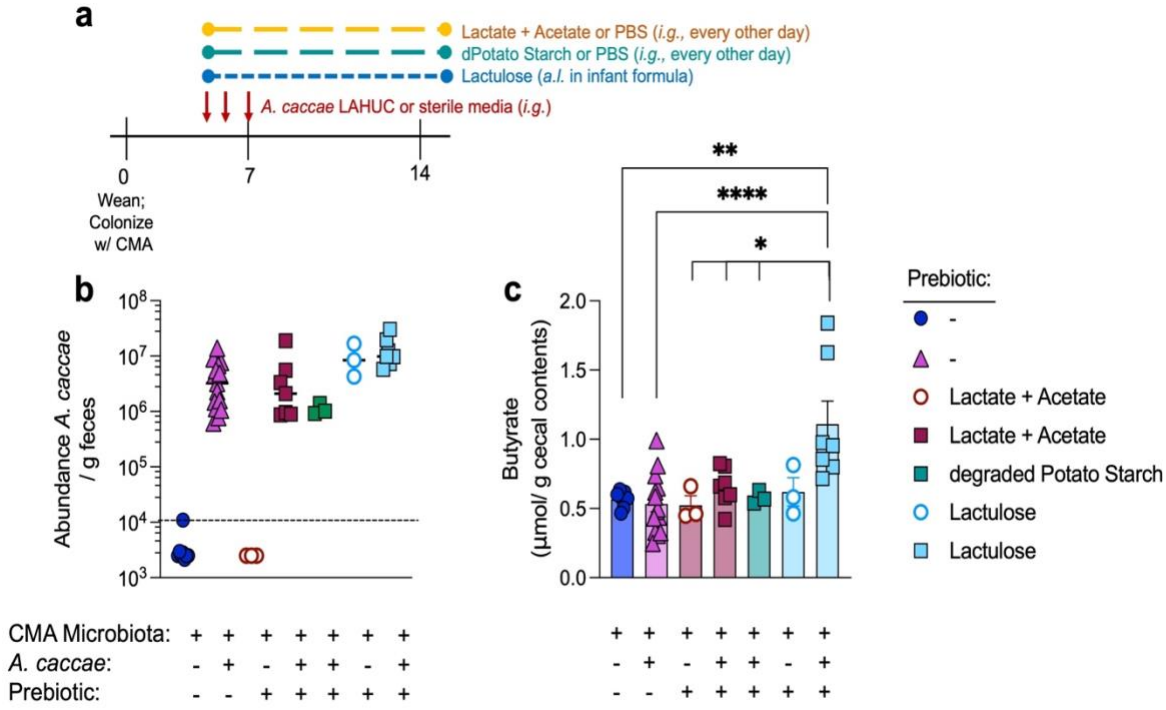

Figure 5.3: Synbiotic treatment with *A. caccae* and lactulose, but not other formulations, increases luminal butyrate in CMA-colonized mice | a, Experimental timeline. GF C3H/HeN mice are colonized with CMA microbiota at weaning, then receive i.g. gavages with either *A. caccae* LAHUC or sterile media (control) daily for three days. Mice also received prebiotics (or control solutions) by gavage or ad libitum. Some prebiotics (10mM lactate plus 10mM acetate or degraded potato starch products) or control PBS were gavaged on alternating days. Lactulose (5g/L) was added to the infant formula which is provided in water bottles. **b**, Abundance of *A. caccae* in feces collected throughout the experimental window measured by qPCR with species-specific primers. **c**, Butyrate in cecal contents measured by HPLC UV-Vis. Data is pooled from 6 independent experiments. Symbols represent individual mice, bars represent mean ± s.e.m. (circles = groups without *A. caccae* administered; triangles = *A. caccae* treatment alone; squares=synbiotic treatment). Data in **c** is analyzed by one-way ANOVA with Tukey's post hoc test. **P* < 0.05, ***P* < 0.01, *****P* < 0.0001.

isolators. Overall, only co-administration of *A. caccae* LAHUC and lactulose significantly increased cecal butyrate (**Fig. 5.3c**), and this effect was quite clear. We predict that breakdown of prebiotic lactulose into lactate and acetate in the distal GI tract will make these metabolites more readily available for consumption than in the CMA mice or with i.g. gavage of these metabolites, which likely don't transit well to the lower GI tract. Administration of lactate and acetate at a higher dose, or potentially in the formula, may exhibit a similar effect, but we continued to pursue lactulose for further synbiotic study.

It should be noted that conclusions from the experiments in **Fig. 5.3** are limited due to exposure to *A. caccae* from the gnotobiotic isolator prior to initial gavages. For these experiments, mice were weaned into separate gnotobiotic isolators which housed either CMA-colonized mice (blue and green groups, **Fig. 5.4**) or had previously housed CMA-colonized mice which had been treated with *A. caccae* (pink and red groups, **Fig. 5.4**). They were then colonized with the CMA fecal bacteria and gavaged with *A. caccae* four days later (**Fig. 5.4a**).

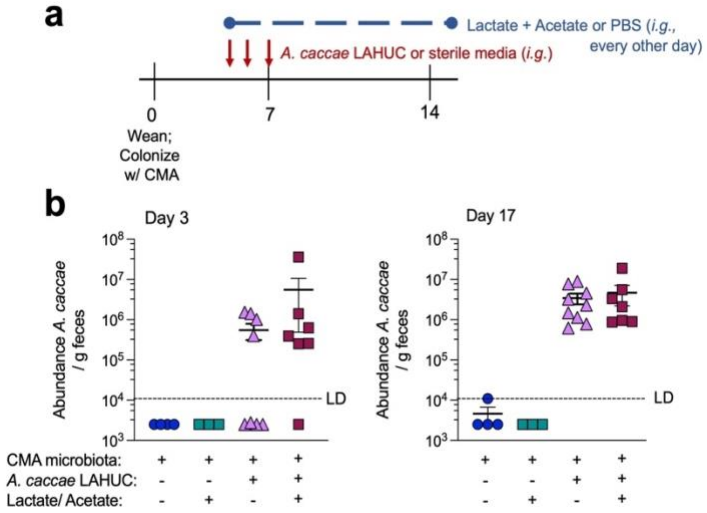

Figure 5.4: *A. caccae* persists within a gnotobiotic isolator and is capable of colonizing mice | a, Experimental design. This figure represents a subset of mice shown in **Fig. 5.3**. Mice were i.g. gavaged with *A. caccae* LAHUC or sterile media (controls), as well as 10mM lactate plus 10mM acetate or PBS (controls). **b**, Abundance of *A. caccae* in feces collected prior to *A. caccae* gavages (left) or at experiment termination (right) measured by qPCR with species-specific primers. Data is pooled from 2 independent experiments.

However, prior to gavages with *A. caccae*, several mice had measurable *A. caccae* in their feces on day 3 (**Fig. 5.4b**). These mice were simply exposed to *A. caccae* from the environment of the isolator. This was particularly striking because this isolator had not housed any mice for over 8 months due to the COVID-19 shut down, but *A. caccae* was clearly still present in the isolator at levels sufficient to colonize newly introduced mice. In the literature, *A. caccae* was described as a non-spore forming species. However, these results led us to conclude that *A. caccae* can persist as spores in the environment. For all future studies, all mice were weaned into the CMA isolator for colonization, and then transferred another isolator just prior to beginning *A. caccae* gavages to avoid this early environmental exposure.

In a long-term engraftment study, CMA-colonized mice were treated with *A. caccae* alone or the *A. caccae* / lactulose synbiotic with a similar regimen as above (**Fig. 5.5a**). Fecal samples were collected throughout the experiment window; at all timepoints during the 5-week administration of lactulose mice produced solid fecal pellets and mice treated with lactulose did not exhibit any laxative effects. As previously, synbiotic administration increased the concentration of butyrate in the cecum and additionally increased the concentration of lactate, although not significantly (**Fig. 5.5b, c**).

As observed in **Fig. 5.2**, *A. caccae* was present in the feces of mice treated with *A. caccae* LAHUC alone or with the synbiotic as soon as one day after the initial gavage and was maintained for one month further (**Fig. 5.5d**). There was no observable difference in abundance of *A. caccae* between mice treated with bacteria alone or the synbiotic, potentially signifying that the niche for this species is filled and cannot be further increased by addition of a prebiotic. This was confirmed by 16S rRNA sequencing, which showed that *Anaerostipes* were only measurable at the genus level in treated mice, but there was no difference in the relative abundance between mice treated with *A. caccae* alone or the synbiotic (**Fig. 5.5e**). This suggests that the addition of prebiotic lactulose increases the

butyrate output without impacting the overall abundance of *A. caccae*; likely lactulose is instead increasing the amount of butyrate per *A. caccae* cell rather than increasing *A. caccae* itself.

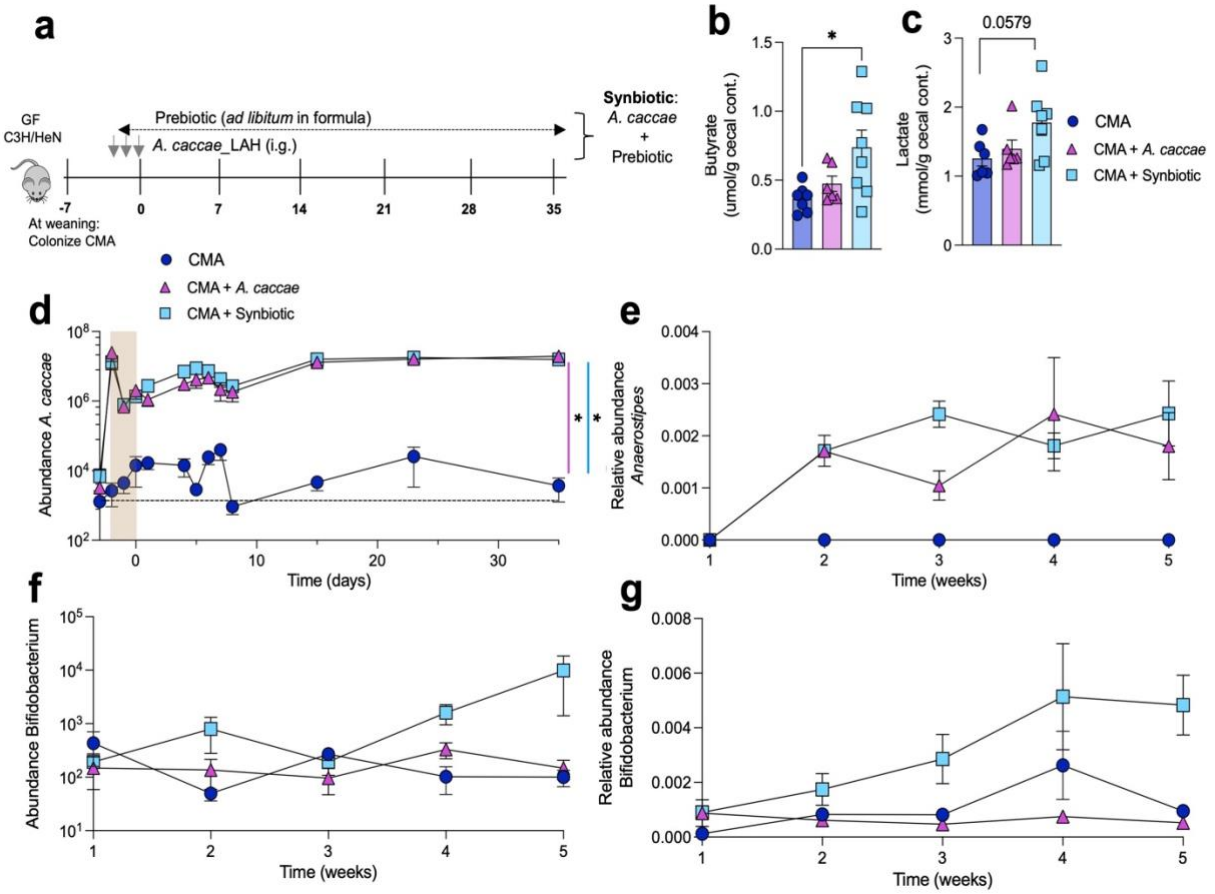

Figure 5.5: Synbiotic therapy with *A. caccae* and lactulose increases luminal acids and impacts the fecal microbiome | a, Experimental timeline. GF C3H/HeN mice were colonized with CMA microbiota at weaning, then received i.g. gavages with either *A. caccae* LAHUC or sterile media (control) daily for 3 days. Some mice additionally received lactulose-supplemented infant formula (EHCF) (5g/L) which is provided in water bottles. Control mice receive standard EHCF. **b, c**, Butyrate (**b**) and lactate (**c**) in cecal contents measured by HPLC UV-Vis or an enzymatic Lactate Assay (Sigma). **d, f,** Abundance of *A. caccae* (**d**) and *Bifidobacterium* (**f**) in feces measured by qPCR. **e, g**, Relative abundance of *Anaerostipes* (**e**) and *Bifidobacterium* (**g**) in feces measured by 16S rRNA sequencing. Data is pooled from 2 independent experiments. For **d-g**, points represent the mean ± s.e.m. for each group. For **b, c,** symbols represent individual mice, bars represent mean ± s.e.m. Statistics are analyzed by area under the curve (**d**), or one-way ANOVA with Tukey's post hoc test with log normalization (**b, c**). *$P < 0.05$.

We have previously described that *A. caccae* cannot break down lactulose alone, it depends on cross-feeding with other lactate-producing species (**Fig. 3.18**). *Bifidobacterium* is one of the taxa hypothesized to perform this initial breakdown of lactulose. Both CMA control mice and those treated with *A. caccae* LAHUC alone had low relative abundance of *Bifidobacterium*. Only those treated with the synbiotic exhibited increased relative abundance of *Bifidobacterium* over the 5-week treatment period, which was confirmed by qPCR (**Fig. 5.5f, g**).

5.4 *A. caccae* induces Foxp3$^+$ Rorγt$^+$ Treg populations in CMA-colonized mice

Previous literature has shown that commensal Clostridia or butyrate elicit expression of Foxp3$^+$Rorγt$^+$ Treg populations in the colonic lamina propria, and these cells specifically dampen Th2 responses in the gut (*146*). We examined Treg populations in the ileal- and cecal-colonic lymph nodes (iLN, cLN) of *A. caccae*-treated or control CMA mice by flow cytometry. *A. caccae* treatment increased the proportion of Foxp3$^+$Rorγt-expressing Tregs in both the iLN and cLN of CMA-colonized mice. Total Foxp3$^+$Rorγt$^+$ Treg cell numbers were increased by *A. caccae* treatment in the cLN only (**Fig. 5.6a**).

Across both groups, there were more Foxp3$^+$Rorγt$^+$ Tregs in the cLN than the iLN, which agrees with the literature suggest that these cells are more abundant in the colonic LP (*146*). *A. caccae* did not affect the percentages or numbers of total Foxp3$^+$ Tregs, as expected, but only increased the proportion of Foxp3$^+$Rorγt$^+$ Tregs (**Fig. 5.6b**). This suggests that commensal Clostridia may increase Foxp3$^+$Rorγt$^+$ Tregs by mechanisms other than butyrate production, since we showed that treatment with *A. caccae* alone did not increase the concentration of luminal butyrate (**Fig. 5.3b**). Now with two treatments in hand, one which induces luminal butyrate production (synbiotic therapy), and one which expands

Foxp3^{+}Rorγt^{+} Tregs (*A. caccae* LAHUC), we explored the potential for these two systems to impact the host in the context of allergic sensitization.

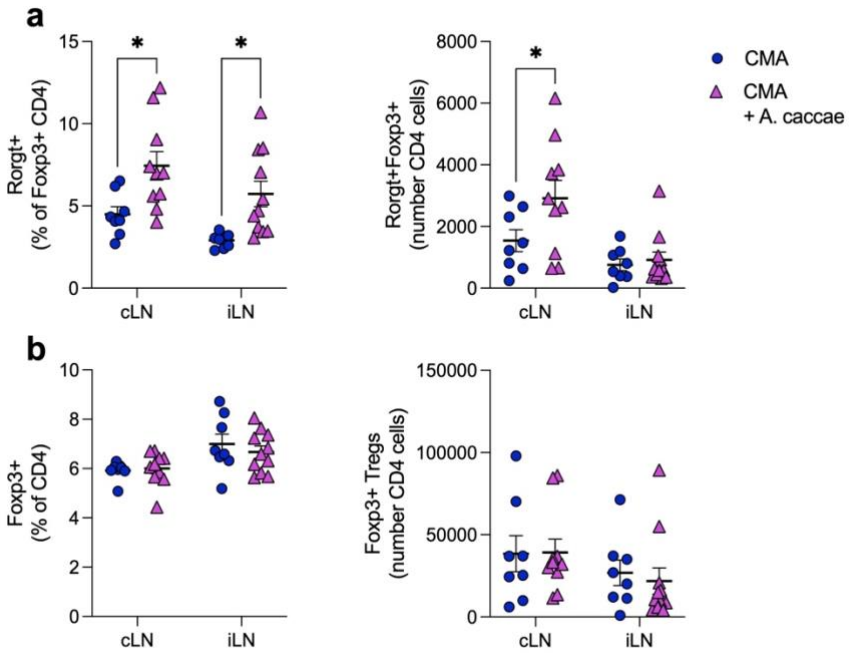

Figure 5.6: *A. caccae* colonization induces Foxp3^{+}Rorγt^{+} regulatory T cell expansion in the mesenteric lymph nodes of CMA-colonized mice | a, Abundance of Foxp3^{+}Rorγt^{+} CD4 T cells in the cecal-colonic- and ileal- lymph nodes (cLN, iLN) represented as proportion (left) and cell number (right). **b,** Total Foxp3^{+} CD4 Tregs in the iLN and cLN represented as proportion (left) and cell number (right). Data is pooled from 3 independent experiments and is from a subset of mice shown in **Fig. 5.3**. Symbols represent individual mice; error bars represent mean ± s.e.m. Statistics are analyzed two-way ANOVA with Sidak's post hoc test. *$P < 0.05$.

5.5 Synbiotic therapy with *A. caccae* and lactulose prevents the allergic response to BLG

We previously established that mice colonized with the feces of CMA infants develop strong allergic responses to BLG in a gnotobiotic allergy model, but those with the feces from healthy infants are protected from sensitization (*104*). Using this same model, we now demonstrate that mice with feces derived from one of these allergic (CMA donor 6) and one healthy (healthy donor 2) infants replicate our original findings. Additionally, some

mice were treated with either the synbiotic (*A. caccae* plus lactulose) or *A. caccae* alone by i.g. gavage beginning just prior to the first sensitization (**Fig. 5.7a**). The CMA-colonized mice exhibited more potent immediate allergic responses upon challenge, demonstrated by an anaphylactic drop in core body temperature and release of mucosal mast cell protease 1 (mMCPT-1) in the serum (**Fig. 5.7b, c, f, g**). In contrast, healthy colonized mice, and those treated with the synbiotic, had significantly less severe allergic responses (**Fig. 5.7b, c**).

Synbiotic treatment significantly reduced the concentration of BLG-specific IgE and IgG1 in the serum, demonstrating reduction in the antigen-specific immune response as well as the overall anaphylactic phenotype (**Fig. 5.7d, e**). This demonstrates that the synbiotic therapy completely prevents the development of allergy to BLG, blunting both sensitization (BLG-specific antibody production) and allergic response upon challenge (anaphylactic temperature drop, mMCPT-1).

As a control, we also tested whether *A. caccae* alone (without lactulose) would have a similar effect. We predicted that *A. caccae* alone would not be efficacious, as this monotherapy did not increase luminal butyrate (**Fig. 5.2, 5.3, 5.5**). However, *A. caccae* treated mice did have increased $Foxp3^{+}Ror\gamma t^{+}$ Treg populations, which could contribute to an allergy-protective phenotype (**Fig. 5.6**). CMA-colonized mice treated with *A. caccae* alone exhibited similar allergic responses to BLG as CMA controls across all measures (**Fig. 5.7f - i**). This provides more evidence that the synbiotic, and the corresponding increase in butyrate, are necessary for the protective effect of *A. caccae* in mice with dysbiotic microbiota.

Splenocytes were harvested 1 day post-challenge and cultured *ex vivo* for 72 hours either without stimulation or with BLG stimulation. Splenocytes from CMA-colonized mice were significantly stimulated to produce type-2 cytokines including IL-13, IL-5, and IL-9 in

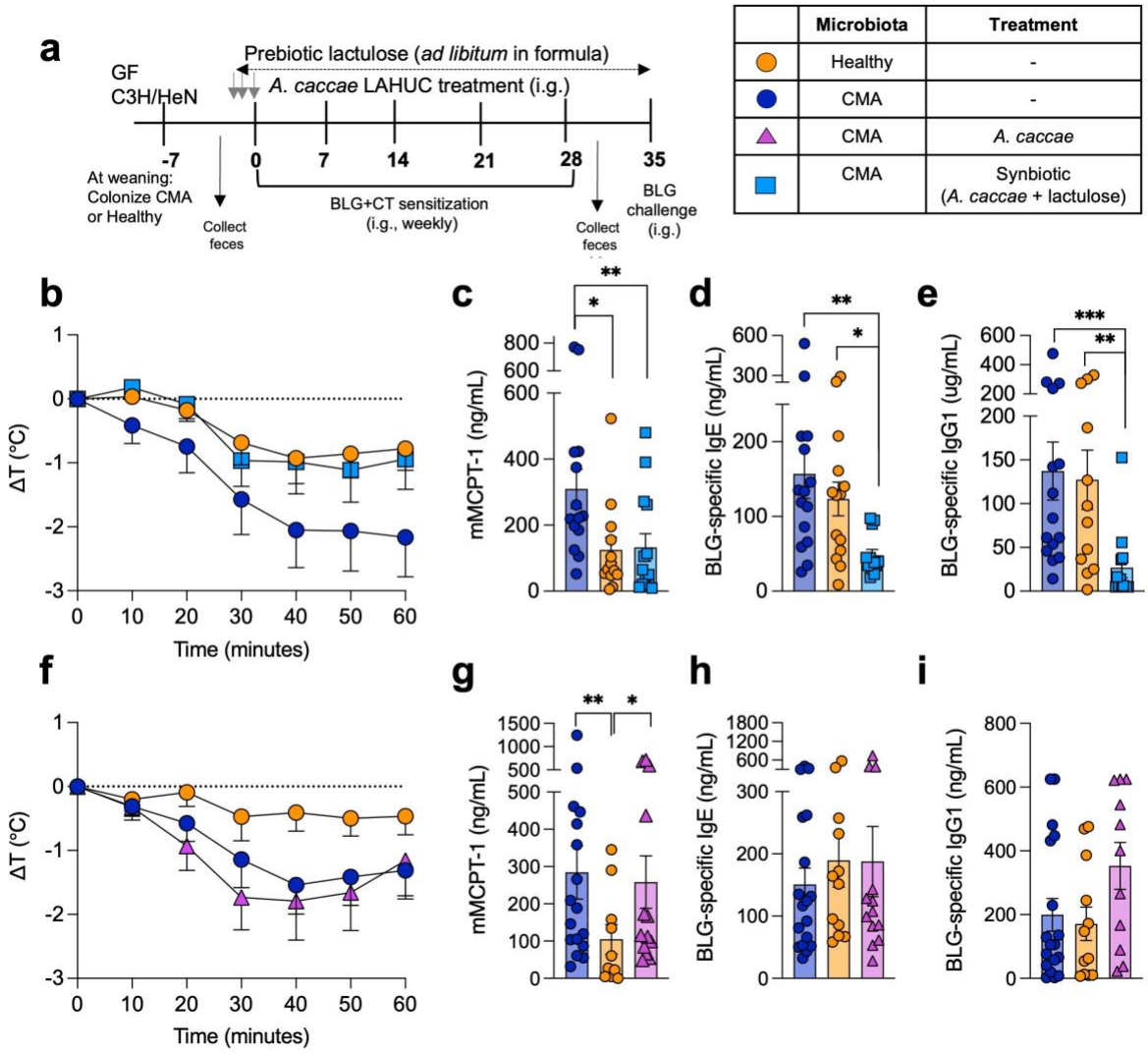

Figure 5.7: Synbiotic therapy, but not *A. caccae* alone, prevents allergic responses to BLG in CMA-colonized mice | a, Experimental timeline and groups. GF C3H/HeN mice were colonized with microbiota of a healthy or CMA infant at weaning, and some CMA-colonized mice were additionally treated with *A. caccae* LAHUC alone or *A. caccae* LAHUC plus lactulose (5g/L in water bottle). Control mice received gavages of sterile media in place of *A. caccae* LAHUC. Mice were sensitized and challenged with BLG as previously described (*104*). **b, f,** Change in core body temperature (ΔT) immediately following i.g. challenge with BLG measured using a rectal temperature probe. **c, g,** Mucosal mast cell protease 1 (mMCPT-1) measured by ELISA in serum collected 90min post-challenge. **d, e, h, i,** Concentration of BLG-specific antibodies IgE (**d, h**) and IgG1 (**e, i,**) in serum collected 24h post-challenge. Data is pooled from 3 independent experiments within each set of panels (**b-e, f-i**). For **b** and **f**, points represent the mean for each group, error bars represent s.e.m. For **c-e** and **g-i**, symbols represent individual mice, bars represent mean ± s.e.m. Statistics are analyzed by one-way ANOVA with Tukey's post hoc test with log normalization (**c-e, g-i**). **P* < 0.05, ***P* < 0.01, ****P* < 0.001.

response to BLG, and splenocytes from healthy-colonized mice were activated to a similar extent (**Fig. 5.8**). *A. caccae* treated mice also produced high IL-13 with BLG stimulation, which was significantly greater than that of synbiotic treated mice (**Fig. 5.8a**). Overall, synbiotic treated mice produced very low levels of all three of these cytokines in response to BLG, demonstrating that the synbiotic treatment reduced the Th2 cellular response to BLG systemically (**Fig. 5.8a - c**).

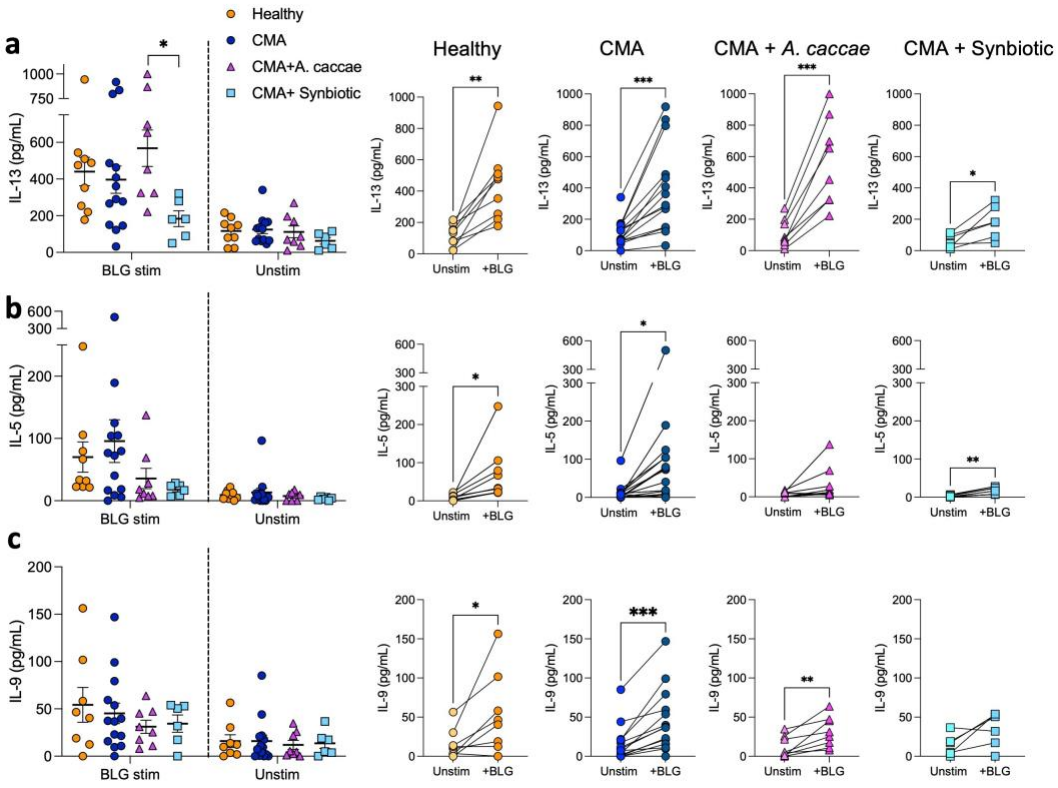

Figure 5.8: Type 2 cytokine production from splenocytes with *ex vivo* restimulation | Concentration of IL-13 (**a**), IL-5 (**b**), and IL-9 (**c**), in supernatants of splenocytes cultured without stimulation (unstim) or with BLG. Left panel shows all groups under stimulated and unstimulated culture conditions. Right panels show paired stimulation within each group, lines connect results from individual mice. Data is pooled from 2 independent experiments, which are representative of the experiments shown in **Fig. 5.7**. Symbols represent individual mice, error bars represent mean ± s.e.m. Statistics are analyzed by two-way ANOVA with Sidak's post hoc test (left) or paired Student's t test (right panels). **P* < 0.05, ***P* < 0.01, ****P* < 0.001.

Together these results demonstrate that this synbiotic therapy prevents an allergic response to BLG in CMA mice. This result is unique to the synbiotic co-administration, as *A. caccae* alone had no effect in this context. Further experiments were then performed to understand the cellular mechanisms behind this effect, and how a single species therapy could mediate the host response to BLG.

5.6 Synbiotic therapy with *A. caccae* and lactulose impacts the fecal microbiome in mice undergoing allergen sensitization

To understand how synbiotic therapy impacts the resident CMA microbiota, feces were collected pre-treatment (week 1) and post-treatment (week 5) from mice undergoing sensitization with BLG plus CT (**Fig. 5.7a**). 16S rRNA sequencing was performed to analyze the composition of the bacterial microbiome. PCA demonstrated that feces from the CMA- and healthy-colonized mice clustered separately along the primary axis of variation, (**Fig. 5.9a**) in keeping with previous data (**Fig. 4.3**). Both untreated and synbiotic-treated CMA-colonized mice clustered together at the pretreatment timepoint, but these two groups separated at week 5, demonstrating that synbiotic treatment modestly shifted the overall composition of the microbiota (**Fig. 5.9a**).

LEfSe analysis was performed comparing untreated and synbiotic-treated CMA-colonized mice at the 5 week timepoint, and as predicted, this analysis revealed that synbiotic treated mice had greater relative abundance of *Anaerostipes* and *Bifidobacterium* than untreated mice (**Fig. 5.9b**). The relative abundance of *Anaerostipes* and *Bifidobacterium* were confirmed by qPCR with primers specific for *A. caccae* (species level) or *Bifidobacterium* (genus level) (**Fig. 5.9c, d**).

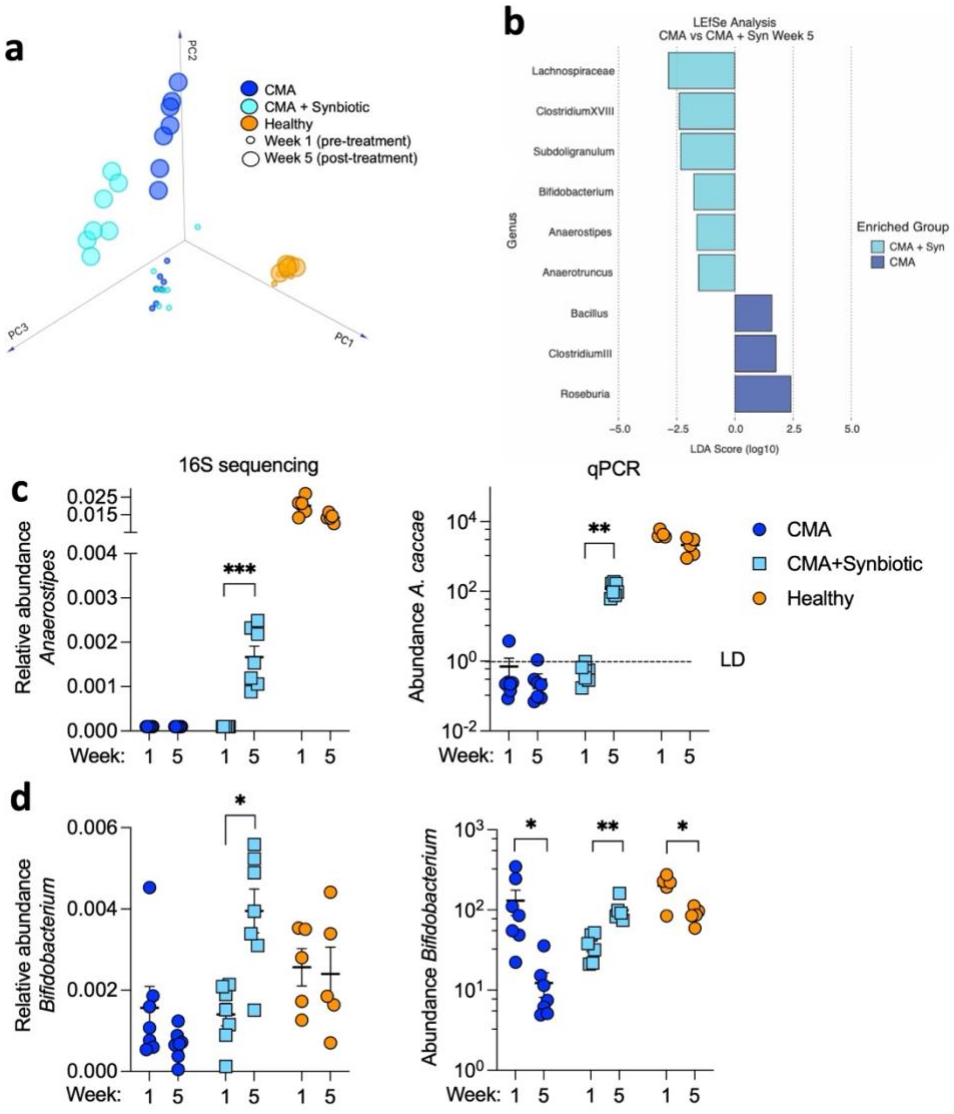

Figure 5.9: Synbiotic therapy shifts the fecal microbiome of CMA-colonized mice. | Experimental design is shown in **Fig. 5.7. a**, PCA analysis of 16S rRNA sequencing data showing the 3 top axes of variation. **b**, Differentially abundant taxa (genus level) between untreated and synbiotic-treated mice at the week-5 time point. **c, d**, Relative abundance measured by 16S sequencing (left), and total abundance measured by qPCR with specific primers (right) for *Anaerostipes* (**c**) and *Bifidobacterium* (**d**). qPCR primers were specific to *A. caccae* (species level) or *Bifidobacterium* (genus level). Symbols represent individual mice, error bars in **c-d** represent mean ± s.e.m. Statistics in **c-d** are analyzed by paired Student's t-test within each condition. **P* < 0.05, ***P* < 0.01, ****P* < 0.001.

While the synbiotic significantly increased both the relative and total abundance of *A. caccae* compared to CMA controls, it did not reach the same abundance as in mice

colonized with healthy infant microbiota (**Fig. 5.9c**). This is further evidence that *A. caccae* seems to be able to exert host-modulating properties, even at very low abundances. In addition to the changes described thus far, synbiotic treatment also significantly increased abundance of unclassified Lachnospiraceae, so we cannot rule out that the increased butyrate in this context is solely due to *A. caccae*. We have hypothesized that local increased concentrations of butyrate may open a metabolic niche for expansion of butyrate producing bacteria (*92*), which may be occurring here.

5.7 Short-term treatment with the synbiotic induces expression of *Il10* and *Il22* in the lamina propria but does not affect epithelial barrier function

We predicted that synbiotic treatment, and subsequent production of butyrate, may improve epithelial barrier function in CMA-colonized mice. As described in Chapter 4, CMA-colonized mice have disrupted epithelial barrier function, resulting in increased permeability to i.g. gavaged FITC-dextran at 7 days post-colonization. Epithelial permeability to FITC-dextran was examined in CMA-colonized mice treated with the synbiotic. These mice were colonized with the CMA microbiota at weaning, and treatment with the *A. caccae* plus lactulose synbiotic begun on day 4 following the same regimen as previously described (**Fig. 5.7c, Fig. 5.10a**). This short-term, 3-day treatment with the synbiotic was not sufficient to reduce the concentration of FITC-dextran detectable in the serum (**Fig. 5.10b**). We predict that treatment with the synbiotic for at least one week will be more efficacious. However, at this early timepoint the relative expression of *Il22* and *Il10* genes were increased in the colonic LP of synbiotic-treated mice (**Fig. 5.10c, d**). This provides some evidence that the synbiotic may regulate the barrier via IL-22, which may be observable (as changes in serum FITC-dextran) with a longer treatment time.

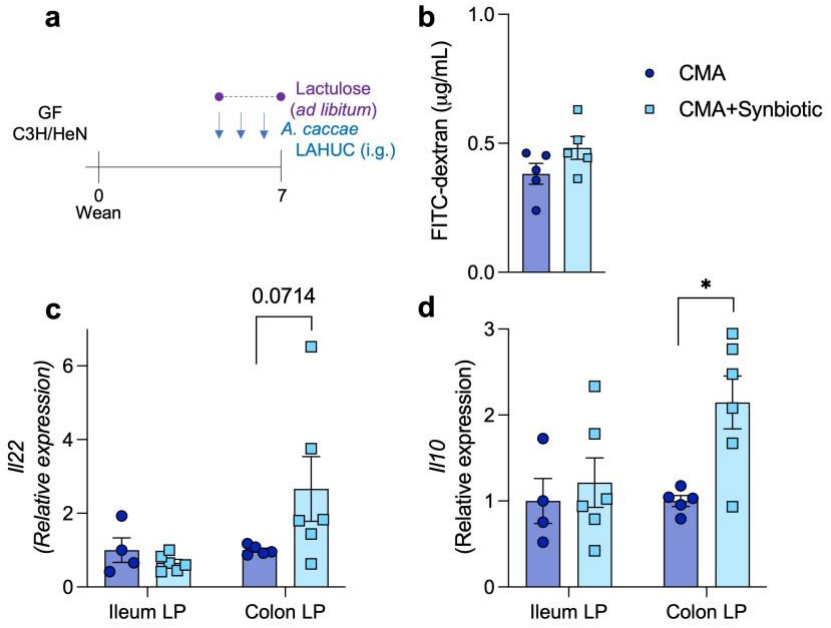

Figure 5.10: Short-term treatment with the synbiotic induces expression of *Il10* and *Il22* in the lamina propria but does not affect epithelial barrier function | **a**, Experimental design. GF C3H/HeN mice are colonized at weaning with CMA microbiota, then begin treatment with the synbiotic on day 4. **b**, Concentration of FITC-dextran measured in serum. **c, d**, Relative expression of *IL22* (**c**) and *IL10* (**d**) in ileal or colonic lamina propria (LP) cells measured by RT-qPCR. Data is pooled from 2 independent experiments. Symbols represent individual mice, bars represent mean ± s.e.m. Statistics in **c-d** are analyzed by two-way ANOVA with Sidak's post hoc test. **P* < 0.05.

5.8 Synbiotic therapy reduces the response to sensitization within the intestinal epithelium and increases T follicular regulatory cells in mesenteric lymph nodes

Our laboratory has proposed a dual mechanism of protection from food allergies: both a bacteria-induced intestinal barrier protective response and a food-antigen specific Treg response are required to prevent sensitization and allergic responses to food (*53*, *117*). Initial allergic sensitization is triggered by alarmins produced from epithelial cells, which are the first cells to sense and respond to luminal antigens (*117*). Classically, alarmin

expression is induced in IECs by physical damage, such as with helminth infection, but some bacteria (like SFB) or mucosal adjuvants may be able to induce this effect (*289*). In our system, colonization with the healthy- or CMA-infant microbiota did not induce expression of alarmin genes *Il25, Tslp*, or *Il33* in ileal IECs compared to GF controls (**Fig. 5.11a**). However, following two sensitizations with BLG plus CT, CMA-colonized mice expressed significantly higher transcripts of *Il25* and *Tslp* than mice colonized with the healthy infant microbiota (**Fig. 5.11b**). *Il33* was not induced by either colonization. Strikingly, mice treated with the synbiotic produced low relative transcripts of *Il25* and *Tslp*, behaving similarly to healthy-colonized controls (**Fig. 5.11b**). The epithelial alarmin profiles of these 3 groups mirrored their later response to allergen challenge; both healthy-colonized and synbiotic-treated mice exhibited minor allergic responses, while CMA-colonized mice responded strongly. This initial difference in alarmin expression is likely causally related to the development of allergic responses to food in these mice. However, the mechanism behind this differential response to sensitization is not yet known. We predict that enhanced mucus production may prevent access of the sensitizing agent from accessing the epithelium, but further experiments are necessary to test this hypothesis.

Epithelial alarmins induce ILC2 expansion in the small intestine LP, which contribute to overall type-2 immune responses mediated by Th2 cells. Beyond classical Th2 cells, T follicular helper (Tfh) and T follicular regulatory (Tfr) cells are of relevance to food allergy, as these cells directly provide help to maturing B cells in GCs and play critical roles in the induction of high affinity antibodies (*129*). There is some evidence that commensal bacteria, or bacterial products such as butyrate, can induce Tfr cells in the periphery (*97*), while IL-13^{+} Tfh cells are singly necessary for the induction of high-affinity IgE and IgG1 (*290*).

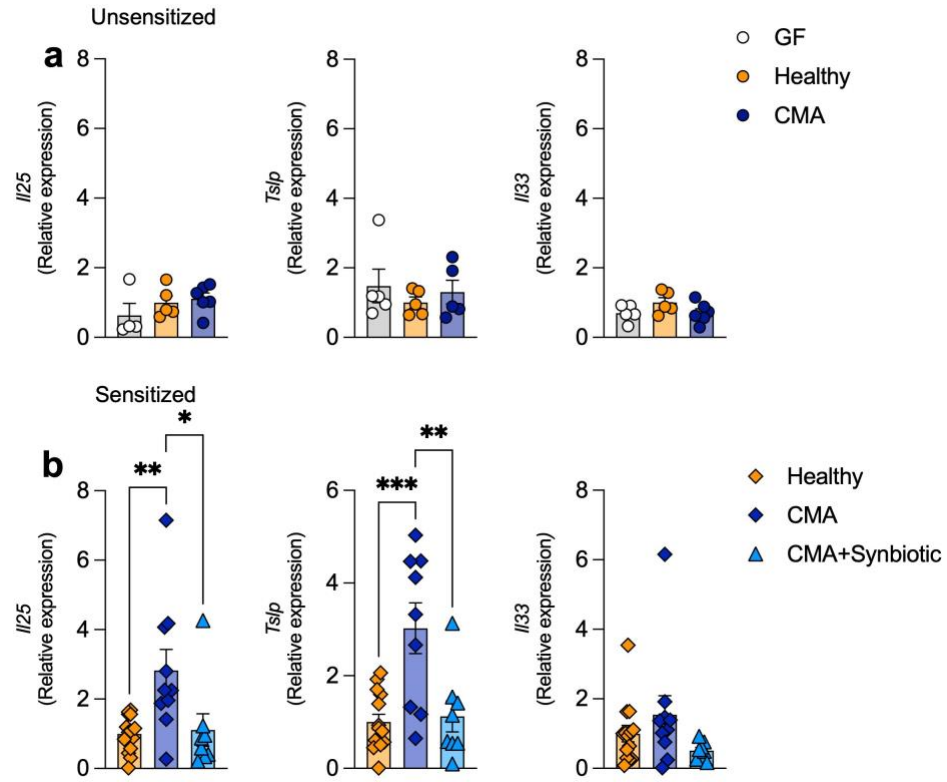

Figure 5.11: CMA-colonized mice express epithelial alarmin genes in response to sensitization, which is abrogated by synbiotic treatment | a, Relative expression of alarmin genes *Il25, Tslp*, and *Il33* in the ileal epithelial cell compartment of C3H/HeN mice 7 days post-colonization with infant microbiota. **b**, Relative expression of alarmin genes in the ileal epithelial cell compartment of gnotobiotic C3H/HeN mice sensitized twice with BLG plus CT. Gene expression is measured by RT-qPCR. Data is pooled from 2-3 independent experiments. Symbols represent individual mice, bars represent mean ± s.e.m. Statistics are analyzed by one-way ANOVA with Tukey's post hoc test. **P* < 0.05, ***P* < 0.01, ****P* < 0.001.

We analyzed Tfh and Tfr populations in the iLN and cLN by flow cytometry (**Fig. 5.12**). CMA mice had modestly, but significantly, increased Tfh cell proportions and numbers ($Foxp3^{-}Bcl6^{+}PD\text{-}1^{+}CD4^{+}$) in the iLN compared to healthy-colonized mice, which may additionally contribute to their heightened allergic responses to BLG (**Fig. 5.13a**). Conversely, treatment with the synbiotic increased Tfr cell populations ($Foxp3^{+}Bcl6^{+}PD\text{-}1^{+}CD4^{+}$) in the cLN compared to CMA- or healthy-colonized mice (**Fig. 5.13b, c**).

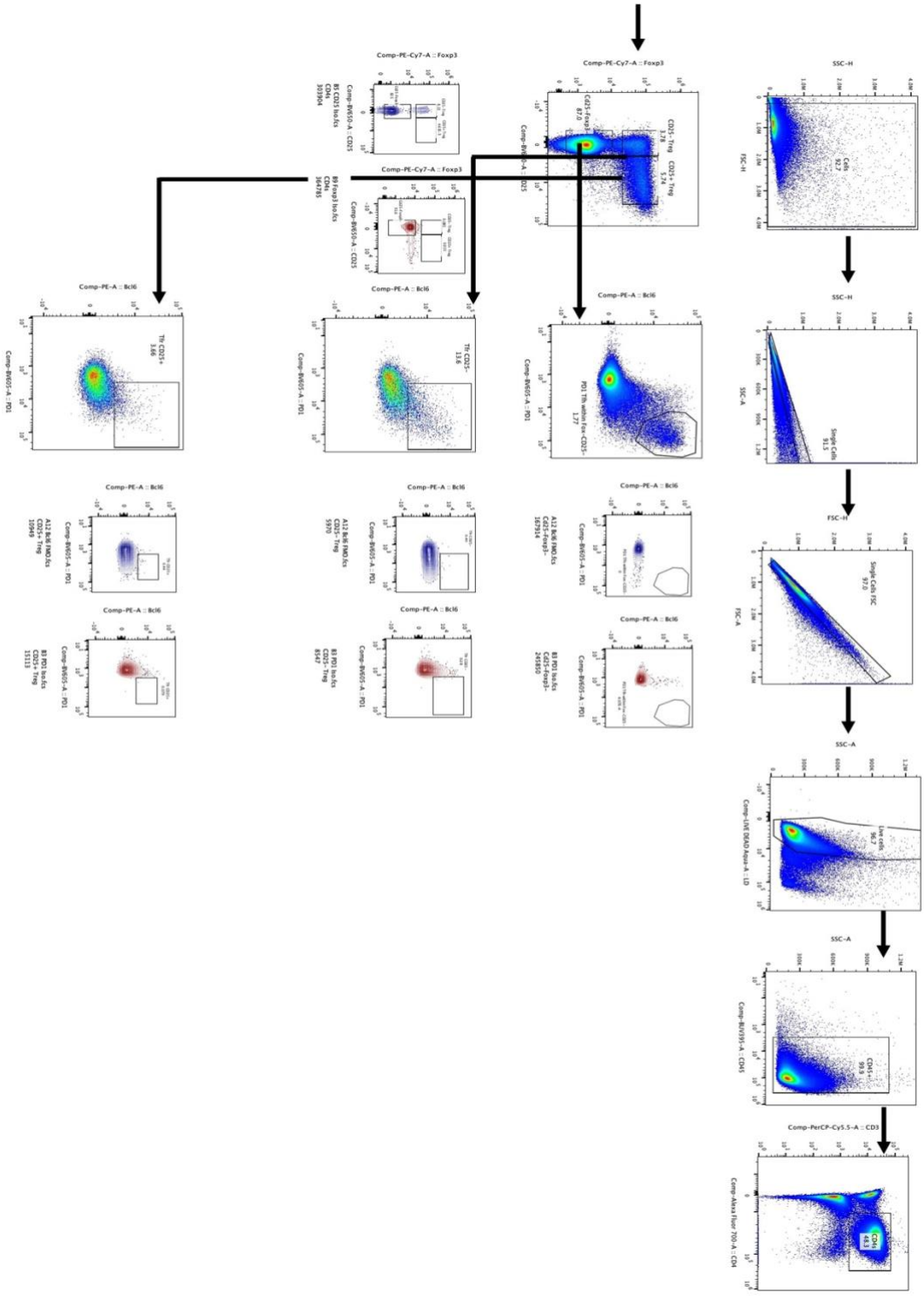

Figure 5.12: Gating strategy for identification of T follicular helper cells and T follicular regulatory cells in mesenteric lymph nodes.

While cells in the cLN may contribute less to allergic phenotypes than those in the iLN, they are more likely to get direct “input” from the cecum and colon, where more bacteria (and more butyrate) are present. Populations of Tfr cells are here stratified into $CD25^+$ and $CD25^-$ Tfr’s, as it has been shown that butyrate has a differential capacity to induce these two subsets (*97*). CD25 is the low affinity IL-2 receptor, and CD25 expression can be critical for Treg development (*291*). It has been suggested that $CD25^+$ and $CD25^-$ Tfr’s develop through different pathways, and that $CD25^-$ Tfr’s do not express IL-2 dependent Treg features but persist in GCs more effectively than $CD25^+$ Tfr’s (*292*, *293*).

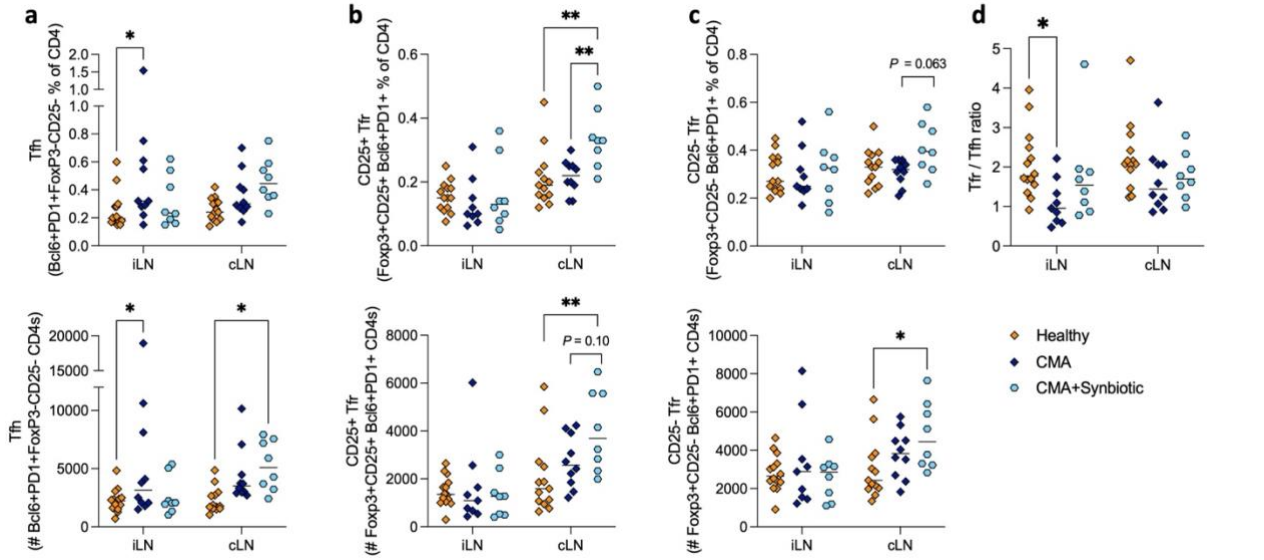

Figure 5.13: Commensal microbiota impact populations of T follicular helper (Tfh) cells and T follicular regulatory (Tfr) cells in mLN | GF C3H/HeN mice were colonized with the healthy or CMA microbiota at weaning and received two, weekly i.g. sensitizations with BLG + CT. Some mice were also treated with the synbiotic (*A. caccae* LAHUC plus lactulose). Populations of T follicular helper cells (Tfh, **a**), $CD25^+$ T follicular regulatory cells (Tfr, **b**), and $CD25^-$ Tfr cells (**c**) in the ileal- and cecal-colonic lymph nodes (iLN, cLN) from flow cytometric analysis. The top row shows the proportion of total CD4 cells, the bottom row shows absolute cell numbers. **d**, Ratio of total Tfr cells to Tfh cells using absolute numbers. Data is pooled from 2 independent experiments. Symbols represent individual mice, bars represent mean ± s.e.m. Statistics are analyzed by two-way ANOVA with Sidak’s post hoc test. **P* < 0.05, ***P* < 0.01.

Calculating the ratio of total Tfr to Tfh cell numbers within each lymph node revealed a clear dominance of Tfr cells in the iLN of healthy colonized mice compared to CMA, and this ratio was slightly increased in synbiotic treated mice, although not significantly (**Fig. 5.13d**). This regulation of follicular T cell populations may be a critical mechanism to prevent allergy and the induction of high affinity IgE antibodies. However, flow cytometry does not provide us with a true, functional readout of these cells' contributions to a larger phenotype. In future studies, it will be critical to understand whether the microbiota, specifically our synbiotic, is able to regulate GC reactions and the development of mature IgE responses in the GALT to prevent allergic disease.

5.9 Synbiotic therapy impacts local IgE production in the mesenteric lymph nodes

Allergic responses are canonically regulated by IgE antibodies. However, it is not yet clear where in the body IgE plasma cells (PC) mature or where they reside once activated. Recent work demonstrates that IgE^+ B cells specific to peanut antigens can be found in the GI tract of peanut-allergic individuals. Sequence similarity of the BCRs from these cells suggests that they may be undergoing CSR and SHM locally in the intestine (*137*, *138*). If IgE^+ B cells are developing in the GALT, then they may be influenced by the local microbiota. We therefore performed experiments to determine whether the microbiota, and synbiotic therapy, could affect populations of IgE- and IgG1-secreting cells in various lymphoid tissues.

GF C3H/HeN mice were colonized with the CMA microbiota at weaning. Synbiotic treatment (or control gavages) begun the following day, following a similar regimen as previously described (**Fig. 5.14a**). Mice were sensitized intragastrically with BLG plus CT 4 times, spaced 5 days apart, followed by a high-dose i.g. BLG challenge. In agreement with the data from the full allergic challenge model (**Fig. 5.7**), synbiotic treatment reduced

the concentration of BLG-specific IgE and IgG1 antibodies circulating in the serum, although not significantly (**Fig. 5.14b, c**). The synbiotic may also affect the concentrations of total and BLG-specific IgA measured in feces; further experiments will be necessary to determine this effect (**Fig. 5.14d, e**).

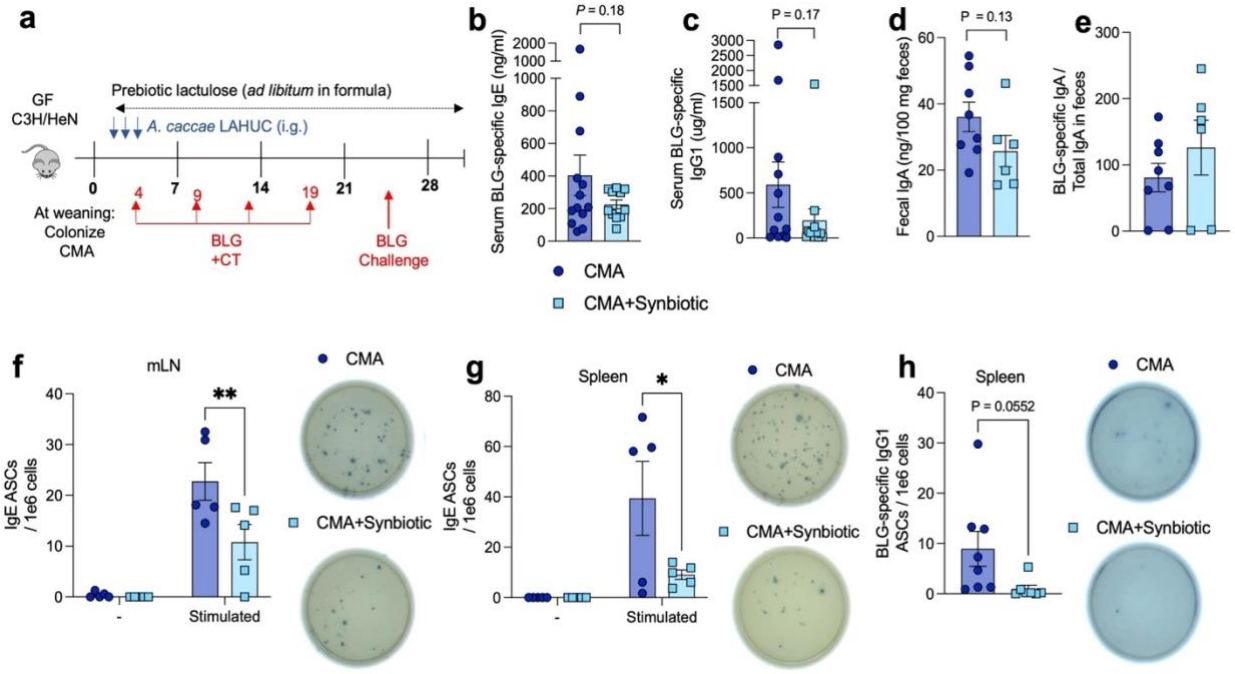

Figure 5.14: Synbiotic treatment affects systemic and mucosal antibody production | **a**, Experimental timeline. GF C3H/HeN mice were colonized at weaning with the CMA microbiota, treatment with *A. caccae* LAHUC (or sterile media controls) began the following day. Synbiotic-treated mice also received lactulose *ad libitum* in infant formula (EHCF). All mice were sensitized i.g. four times with BLG plus CT, then challenged i.g. with high-dose BLG. The experiment was terminated one week post-challenge. **b-c**, Concentration of BLG-specific IgE (**b**) and IgG1(**c**) in serum measured by ELISA. **d-e**, Total IgA (**d**) and BLG-specific IgA (**e**) in feces at euthanasia measured by ELISA. **f-g**, Number of IgE antibody secreting cells (ASCs) per million live cells originating from the mLN (**f**) or spleen (**g**) with representative photos measured by ELISpot. **h**, Number of BLG-specific IgG1 ASCs per million live cells from the spleen measured by ELISpot. Symbols represent individual mice, bars represent mean ± s.e.m. Data in **b-e** is pooled from 2 independent experiments, data in **f-h** are from one representative experiment. Statistics are analyzed by Student's t test (**b-e, h**) or two-way ANOVA with Sidak's post hoc test (**f, g**). *$P < 0.05$, **$P < 0.01$.

The role of food-specific IgA in regulating allergies is not yet clear (*125*), although this antibody class is more directly impacted by commensal microbiota (*131*). To observe IgE-secreting cells, single-cell suspensions from the mLNs and spleen were cultured for 5 days with stimuli for IgE secretion: anti-CD40, IL-4, and BLG. IgE antibody secreting cells (ASCs) do not actively produce and secrete IgE in high quantities at baseline, so this stimulation is required to observe IgE-ASCs by an enzyme-linked immunosorbent spot (ELISpot) assay.

Strikingly, synbiotic-treated mice harbored fewer IgE ASCs in the mLN than untreated CMA mice (**Fig. 5.14f**). This relationship was also observed in splenocytes, which were used as positive controls (**Fig. 5.14g**). Unfortunately, this assay did not allow us to observe antigen specificity of these IgE ASCs, although addition of BLG to the cultures should positively select for BLG-specific cells. For further studies, we will produce biotinylated IgE to use for detection of BLG-specific IgE ASCs. We will also examine IgE ASCs within Peyer's patches, as these cells will have the most contact with the microbiota and microbial metabolites. Low cell recovery from Peyer's patches has limited these studies thus far.

We were, however, able to quantify BLG-specific IgG1 ASCs from splenocytes. These cells were not cultured, and IgG1 ASCs were quantified directly after tissue harvest. Fewer BLG-specific IgG1 ASCs were detected in splenocytes of synbiotic treated mice compared to untreated CMA mice (**Fig. 5.14g**). Together these data build on previous findings that synbiotic treatment reduces circulating BLG-specific IgE and IgG1. We now show that this reduction in serum antibodies may be due to reduced populations of the cells that produce them. This is also novel evidence for the presence of IgE secreting cells residing in the GALT, which likely interact more directly with commensal microbiota and with food allergens than cells in distal immune organs. Bacterial regulation of IgE responses is still a relative mystery (*131*), and the mechanism of this observed effect of synbiotic treatment will be the subject of further study.

5.10 Synbiotic therapy with *A. caccae* and lactulose reduces the allergic response to peanut in previously sensitized mice

The data presented thus far support the hypothesis that our synbiotic (*A. caccae* LAHUC plus lactulose) effectively prevents the onset of allergy to BLG in gnotobiotic mice stably colonized with the feces from a dysbiotic, CMA infant. This protective effect may be mediated by regulating the epithelial alarmin response to sensitization, reducing Tfh cell populations and type 2 cytokine production, or eliminating IgE- and IgG1 secreting PCs. However, we also hypothesized that this synbiotic may be sufficient to treat mice which already have established allergic phenotypes and reduce their response to allergen re-exposure.

We have previously demonstrated that treatment with micelles with targeted release of butyrate (ButM) reduces the anaphylactic response to peanut in a therapeutic model of peanut allergy (*92*). To induce bacterial dysbiosis, mice were treated with vancomycin neonatally and throughout the sensitization period. Mice were sensitized with peanut (PN) plus CT i.g. for 4 weeks beginning at weaning, then antibiotics were removed, and they received twice daily gavages with ButM or PBS for 2 weeks. This short, 2-week treatment was sufficient to reduce the anaphylactic response to challenge, measured by drop in core body temperature, serum mMCPT-1 and histamine, as well as circulating PN-specific IgE (*92*). We predict that our synbiotic therapy may similarly protect against the allergic response to peanut in this model, as synbiotic treatment increases luminal butyrate.

The previously described experimental regimen was exactly replicated for the period of sensitization, and only the treatment window was altered for the synbiotic (**Fig. 5.15a**). Two days after vancomycin was removed from the drinking water, mice were i.g. gavaged with either *A. caccae* LAHUC (from a frozen glycerol stock) or sterile medium (CMG) as in previous experiments. These gavages took place during the first 3 days of each week

of the treatment window (6 gavages total). For synbiotic treatment, lactulose was added to drinking water throughout the remainder of the experiment. On day 7 of treatment (just prior to beginning the second set of *A. caccae* gavages), *A. caccae* was measurable in the feces of mice treated with *A. caccae* alone or the synbiotic (**Fig. 5.15b**). However, *A. caccae* may drop out over time (**Fig. 5.15c**). Prior to beginning treatment, a subset of mice was i.p. challenged with PN to confirm uniform sensitization (**Fig. 5.15d**). After two weeks of treatment, the remaining mice were i.p. challenged with PN and the anaphylactic response was measured.

Strikingly, the control-treated mice which received gavages of sterile CMG exhibited little to no allergic response upon challenge, as demonstrated by maintenance of core body temperature and low mMCPT-1 concentration in serum (**Fig. 5.15e-g**). To confirm that this wasn't an environmental effect, the pre-treatment controls were re-challenged. The mice which received no treatment maintained their allergic phenotype, as expected. We predict that the beneficial effect of CMG may be due to a 'prebiotic' effect of this rich culture medium. Feces collected throughout the treatment window of this experiment will be sequenced to determine bacterial composition and potential changes elicited by CMG treatment. Mice that were treated with *A. caccae* alone exhibited the highest mMCPT-1 in serum (**Fig. 5.15g**), which somewhat mirrors previous results that *A. caccae* alone is not protective in the context of a replete microenvironment. Overall, the results of this experiment were skewed due to limited long-term engraftment and a clear protective effect of CMG medium alone.

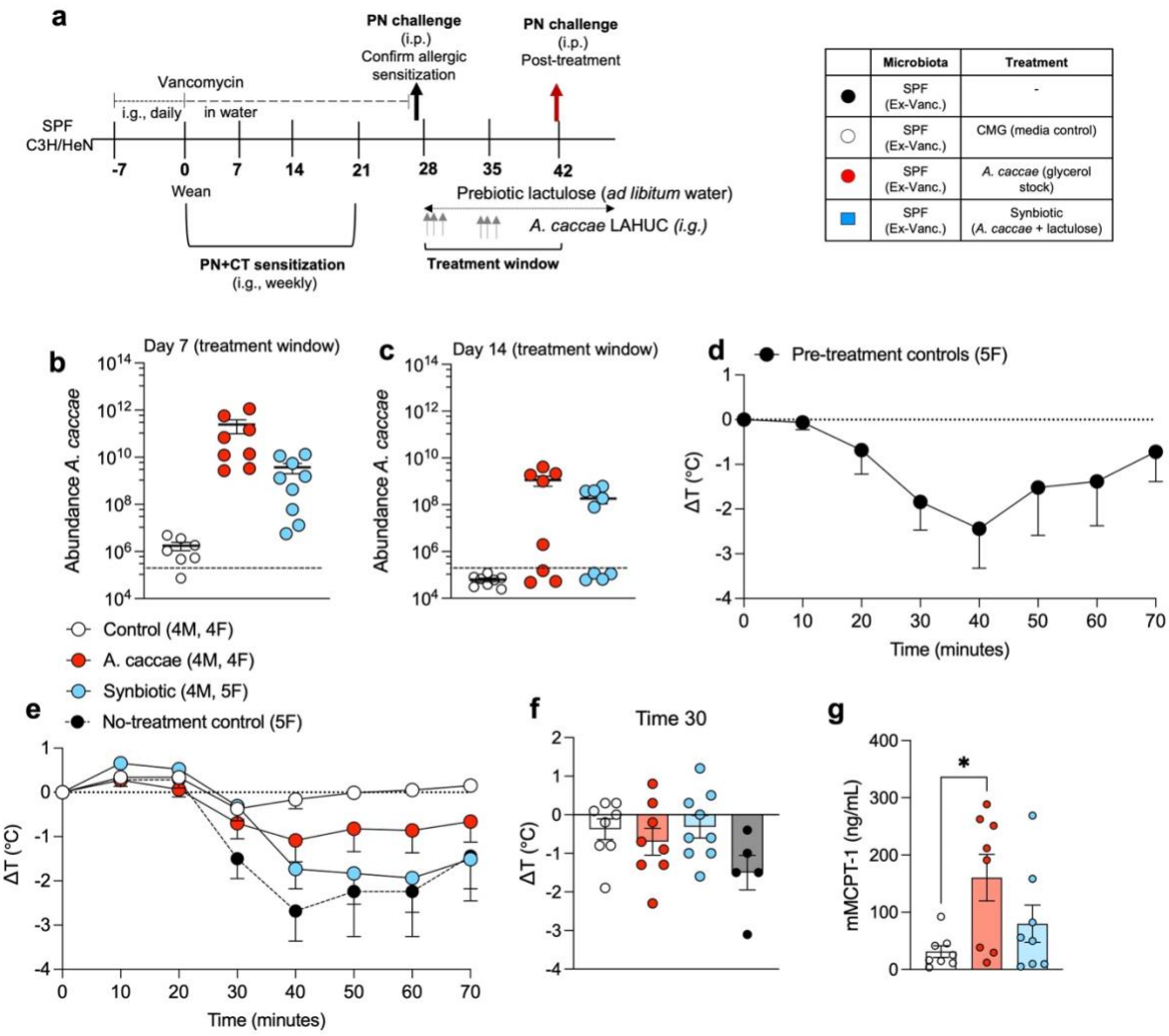

Figure 5.15: *A. caccae* modestly engrafts in antibiotic treated mice but does not significantly impact the allergic response to peanut alone or as a synbiotic | a, Experimental timeline adapted from (*92*). Vancomycin-treated SPF C3H/HeN mice were i.g. sensitized with peanut (PN) plus CT weekly for 4 weeks beginning at weaning. One week later, a subset of mice was i.p. challenged with PN to confirm uniform sensitization. Remaining mice were treated with sterile medium (CMG), *A. caccae* LAHUC, or the synbiotic for 2 weeks before i.p. challenge with PN. **b-c**, Abundance of *A. caccae* measured in feces measured by qPCR. **d-e**, Change in core body temperature (∆T) of pre-treatment controls (**d**) or experimental mice (**e**) immediately following PN challenge measured with a rectal probe. **f**, Change in core body temperature of mice at the 30-minute timepoint. **g,** Concentration of mMCPT-1 in serum 90min post-challenge measured by ELISA. For **d** and **e**, points represent the mean for each group, error bars represent s.e.m. For **b-c** and **f-g**, symbols represent individual mice, bars represent mean ± s.e.m. Statistics in **g** are analyzed by one-way ANOVA with Tukey's post hoc test. *P < 0.05.

Following the results of this initial experiment, another study was performed in which we slightly altered the *A. caccae* and synbiotic treatment regimen (**Fig. 5.16a**). In this experiment *A. caccae* LAHUC was administered in the form of a lyophilized powder which was reconstituted in PBS. Dosing mice with lyophilized bacteria is preferable to glycerol stocks because these powders are shelf stable, contain more viable cells, and avoid any unwanted effects of gavaging culture media. Treating mice with *A. caccae* LAHUC from a lyophilized powder resulted in more consistent and sustained colonization than in the initial study (**Fig. 5.16b**). Only treatment with the synbiotic, but not *A. caccae* alone, increased cecal butyrate, mirroring our previous results in an entirely different microbial context (**Fig. 5.16c**).

As previously, a subset of mice was i.p. challenged with PN before the treatment window began, which showed a modest but consistent temperature drop (**Fig. 5.16d**). After the 2-week treatment window, PBS-treated control mice exhibited a potent drop in core body temperature, and that of synbiotic treated mice was significantly less severe over the course of 70 minutes and at the 30 minute time point (**Fig. 5.16e, f**). Treatment with *A. caccae* alone had little to no therapeutic effect, again mirroring what was observed in the cow's milk allergy model. Synbiotic treatment also reduced the concentrations of mMCPT-1 and PN-specific IgG1 in serum, although not significantly (**Fig. 5.16g, h**). However, synbiotic treatment did not impact PN-specific IgE in serum (**Fig. 5.16i**).

Overall, these data demonstrate that lyophilized *A. caccae* LHUC successfully colonizes adult, antibiotic-treated SPF mice, and synbiotic administration with lactulose increases cecal butyrate. This synbiotic formulation effectively reduces the anaphylactic response to allergen challenge in previously sensitized mice and may be useful in therapeutic contexts as well as prophylactic contexts.

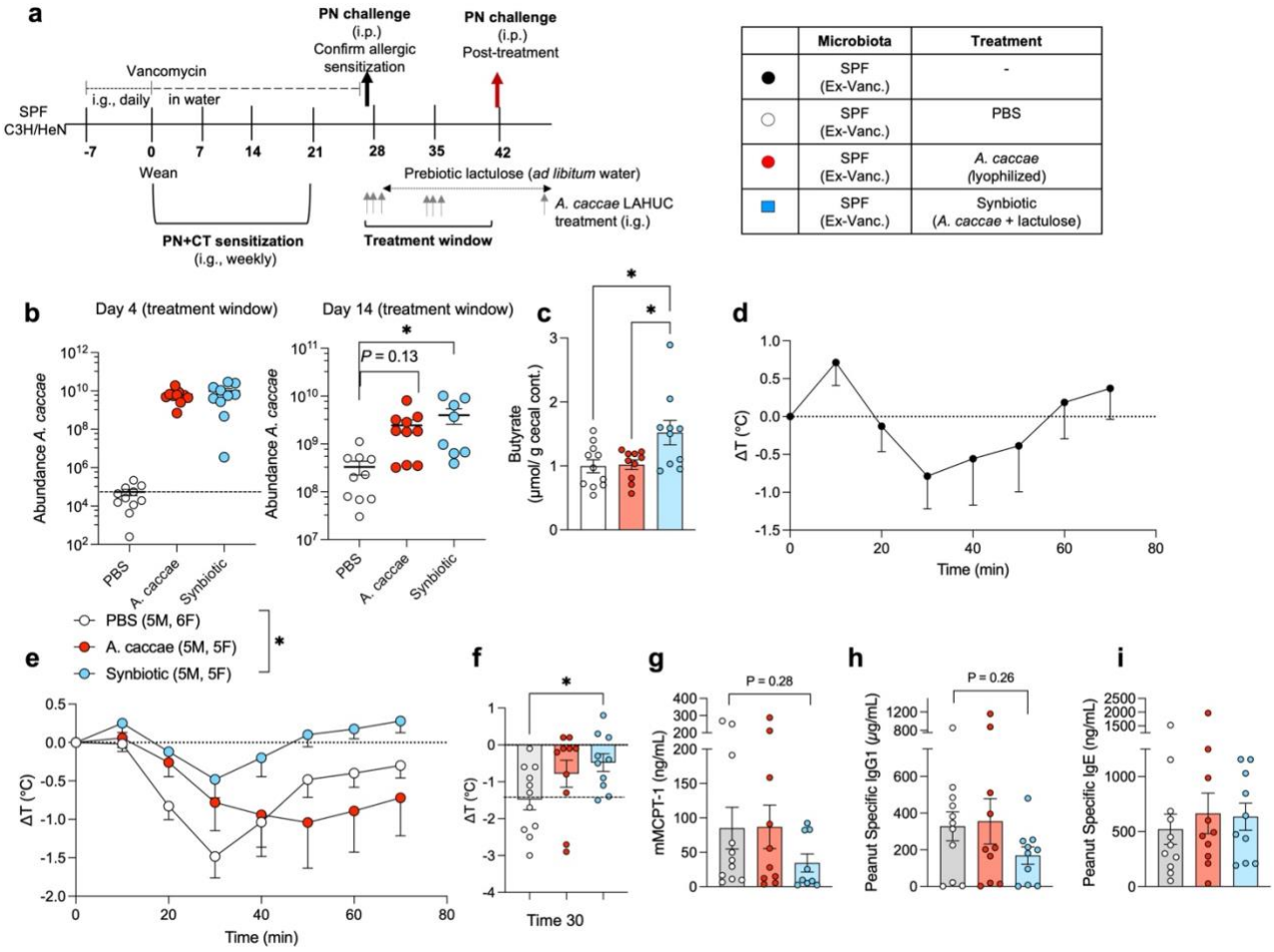

Figure 5.16: Synbiotic therapy increases luminal butyrate in vancomycin-treated mice and reduces the allergic response to peanut | **a**, Experimental timeline adapted from (*92*) and **Fig. 5.15**. Vancomycin-treated SPF C3H/HeN mice were i.g. sensitized with peanut (PN) plus CT weekly for 4 weeks beginning at weaning. One week later, a subset of mice was i.p. challenged with PN to confirm uniform sensitization. Remaining mice were treated with PBS, *A. caccae* LAHUC, or the synbiotic for 2 weeks before i.p. challenge with PN. **b**, Abundance of *A. caccae* measured in feces at stated timepoints during the treatment window measured by qPCR. **c**, Butyrate concentration in cecal contents measured by HPLC UV-Vis. **d-e**, Change in core body temperature (ΔT) of pre-treatment controls (**d**) or experimental mice (**e**) immediately following PN challenge measured with a rectal probe. **f**, Change in core body temperature of mice at the 30-minute time point. **g**, Concentration of mMCPT-1 in serum 90min post-challenge measured by ELISA. **h, i,** Concentration of PN-specific IgG1 (**h**) and IgE (**i**) in serum measured by ELISA. For **d** and **e**, points represent the mean for each group, error bars represent s.e.m. For **b-c** and **f-i**, symbols represent individual mice, bars represent mean ± s.e.m. Statistics are analyzed by area under the curve (**e**) or one-way ANOVA with Tukey's post hoc test (**c, f-i**). *$P < 0.05$.

5.11 Conclusion

Together we now have evidence that *A. caccae* LAHUC engrafts in mice with dysbiotic human microbiota and in antibiotic-treated SPF mice, additionally producing butyrate when co-administered with lactulose. Of the several prebiotics tested, none of them singly increased butyrate production *in vivo*, and neither did *A. caccae* alone. Interestingly, introduction of *A. caccae* alone did expand the population of $Foxp3^{+}Ror\gamma t^{+}$ Tregs in the cLN without sensitization. This suggests that *A. caccae*, or other bacteria may induce $Foxp3^{+}Ror\gamma t^{+}$ Treg populations through mechanisms other than SCFA production. Other mechanisms of host/synbiotic interaction were examined in the context of allergic sensitization. We demonstrated that synbiotic treatment reduced the epithelial alarmin response, induced populations of Tfr cells, and reduced populations of IgE-secreting and IgG1-secreting cells in various sites.

The synbiotic reduced the allergic response in models of both cow's milk allergy and peanut allergy, demonstrating that this strategy is truly antigen agnostic (and shows efficacy when challenge is administered by different routes, i.g. or i.p). Finally, this synbiotic can be introduced in early life near weaning or in adulthood, prior to allergen sensitization or afterwards. The broad applicability of this synbiotic suggests that it may contribute to mucosal homeostasis through a variety of mechanisms and in a variety of contexts.

CHAPTER 6

DISCUSSION, FUTURE DIRECTIONS, AND CONCLUSION

6.1 *In vitro* characterization of isolate *A. caccae* LAHUC

This project stemmed from previous work which demonstrated that *A. caccae* DSM 14662 had an allergy-protective effect in a gnotobiotic model of cow's milk allergy (*104*). This observation was highly impactful; the fact that a single species could mimic the protective effect of the replete healthy infant microbiota (*104*) suggested that *A. caccae* may be a promising candidate as a clinical LBP for food allergy. This first required isolation of a new strain from the feces of a healthy infant (donor 2, (*104*)).

The FDA requires that all LBPs be isolated from a human with known health history and have record of all cultures, with limited rounds of passaging (*177*). We isolated a novel strain of *A. caccae* from the feces of a healthy infant donor (*104*) in accordance with these guidelines. Novel isolate *A. caccae* LAHUC is closely related to other type strains of *A. caccae* (**Fig. 3.5**), but notably produces more butyrate than these strains *in vitro* (**Fig. 3.8**). We expect that butyrate production is likely critical to *A. caccae*'s therapeutic efficacy in a replete microenvironment, especially since this isolate does not exhibit other characteristics which have host-modulating effects such as flagella or indole production (**Fig. 3.8**) (*69*). We therefore focused our *in vitro* studies on understanding and maximizing *A. caccae*'s butyrate production. We predicted that we could co-deliver *A. caccae* with a specific prebiotic to maximize its butyrate production in a microbially replete host.

In monocultures *A. caccae* LAHUC only produces butyrate from small sugars (glucose, sucrose) or carbon metabolites (lactate and acetate) but cannot ferment more complex carbohydrates (**Figs. 3.10, 3.17**) (*247*, *282*). Interestingly, two prebiotic sugars, short-chain fructo-oligosaccharides (scFOS) and myo-inositol, were digested by *A. caccae* in

monoculture (**Figs. 3.15, 3.16**). *A. caccae* possesses a specific gene cluster which allows it to digest sucrose and scFOS, while this species is otherwise generally limited in its ability to digest polysaccharides (*294*). scFOS and myo-inositol stimulated the production of high concentrations of butyrate or propionate, respectively (**Figs. 3.15, 3.16**). This metabolic switch from production of butyrate to propionate in the presence of inositol has been previously described in *Anaerostipes* species (particularly *A. caccae* and A. *rhamnosivorans*), and this inositol conversion has been correlated to health status in large human cohorts (*281*). These findings guided us to examine the effects of myo-inositol in *A. caccae* monocolonized mice (discussed in Chapter 6.2). It will be interesting to understand the precise genetic and molecular cues which signal this propionate pathway, and how these dynamics change in monoculture versus complex microenvironments. In future studies, we plan to also study the effects of scFOS in *A. caccae* monocolonized mice and in the context of a replete microbiota.

Since we were interested in administering *A. caccae* LAHUC to microbially replete hosts, we also wanted to understand its behavior in co-cultures with other bacteria. *A. caccae* is a proficient cross-feeder, consuming byproducts of fiber digestion produced by other bacteria (namely lactate and acetate) and converting these products into butyrate (*248*). These relationships have previously been described between *A. caccae* and 'primary degrader' bacteria such as *Bifidobacterium*, *Lactobacillus*, and *Akkermansia* species (*249*, *251*, *282*). We built on these findings by culturing *A. caccae* LAHUC with *R. bromii*, a keystone species for degradation of potato starch (*185*). In media supplemented with nonsoluble, resistant potato starch, co-cultures of *A. caccae* and *R. bromii* (but neither alone) produced high concentrations of butyrate (**Fig. 3.12**). *R. bromii* produces acetate, but no butyrate in monoculture (**Fig. 3.12**). We suspect that *A. caccae* is consuming this acetate to produce butyrate, along with other small sugars released into the medium (**Fig. 3.12**). We further demonstrated that the production of butyrate from potato starch in this two-species system was sequential. We cultured *R. bromii* in media

supplemented with potato starch, or other complex carbohydrates, and then removed the *R. bromii* cells and cultured *A. caccae* in this 'spent media'. *A. caccae* readily grew and produced butyrate in 'spent media' utilizing products from *R. bromii*'s degradation of potato starch and corn starch (**Figs. 3.13, 3.14**).

A study from our group demonstrated that *R. bromii* is enriched in the feces of healthy twins compared their food-allergic siblings (*112*). This increased abundance of *R. bromii* correlated strongly with differences in the fecal metabolome of this cohort (*112*). Others have shown that dietary supplementation with potato starch increases the relative abundance of *R. bromii* in feces, resulting in a corresponding increase in fecal butyrate (*187–189*). Together these findings, along with our results from these *in vitro* cross-feeding experiments, led us to hypothesize that dietary supplementation with potato starch may have beneficial effects in children with food allergies. In an ongoing interventional study, our collaborator is administering potato starch to peanut-allergic children undergoing OIT (NCT05138757). We predict that potato starch, and downstream production of butyrate, may have beneficial effects in modulating the gut immune system, potentially reducing the symptoms and increasing efficacy of OIT. The results of this study will contribute to the literature supporting microbiome-modulating effects of potato starch and expand upon these by demonstrating whether these effects additionally exert a health benefit in allergic children.

In addition to this two-species culture system, we also cultured *A. caccae* together with a fecal slurry from a CMA infant (donor 6, (*104*)) to better screen prebiotics which may be co-delivered with *A. caccae* LAHUC in our gnotobiotic mouse model. In this system, potato starch again increased butyrate production only when *A. caccae* was co-cultured with the other bacteria (**Fig. 3.15**). However, we later showed that potato starch administered by i.g. gavage did not increase butyrate production *in vivo* (**Fig. 5.2**). An alternative administration regimen, consisting of more frequent and higher dosing, may more effectively increase the butyrate concentration in mice. Here, we instead focused on

finding a prebiotic to specifically support the known metabolic needs of *A. caccae*, namely lactate. A high throughput *in vitro* culture system demonstrated that *A. caccae*'s butyrate production in monoculture or 2-species systems depends specifically on the availability of lactate (*63*). This work suggested that in the presence of simple sugars, *A. caccae* undergoes rapid proliferation but produces relatively less butyrate. Conversely, in the presence of lactate and acetate, *A. caccae* produces butyrate most efficiently (*63*).

To increase the availability of lactate and acetate in the distal colon, we utilized lactulose, a prebiotic known to be digested into these metabolites by colonic bacteria (*253*). *A. caccae* was not able to ferment lactulose in monoculture, and neither *A. caccae* alone nor feces from a CMA infant donor produced butyrate from lactulose *in vitro* (**Fig. 3.18**). However, co-culturing *A. caccae* and the CMA feces in the presence of lactulose significantly increased the concentration of butyrate and modestly increased lactate (**Fig. 3.18**). We suggest that the CMA microbiota contains many species capable of performing the initial breakdown of lactulose but relatively few butyrate producing taxa. *A. caccae* can fill this niche, utilizing those intermediate products to produce butyrate. We extended these results *in vivo* using gnotobiotic, CMA-colonized mice and showed that co-administration of *A. caccae* LAHUC and lactulose, but neither alone, increased luminal butyrate and lactate (discussed further in Chapter 6.3). We predict that lactulose is likely not the only prebiotic that could be co-delivered with *A. caccae* to induce this butyrate production. Future studies will explore other substances, including HMOs, scFOS and potato starch, to determine if these more commonly used prebiotics could induce a similar butyrate-potentiating effect *in vitro* and *in vivo*. While the microbiome-modulating effects of lactulose are becoming more widely accepted (*256, 300*), its medicinal properties as a laxative at high doses (*253*) may limit its potential for large-scale adaptation as a clinical prebiotic.

Finally, we have pursued stability studies and scale-up manufacturing to demonstrate

A. caccae LAHUC's potential as a clinical product. *A. caccae* LAHUC can be lyophilized into a powder form and stored at room temperature for several months, maintaining cell viability and avoiding contamination (**Fig. 3.19**). Additionally, we have partnered with Rise Therapeutics, a contract manufacturing organization skilled in anaerobic bacteriology, to begin scale-up culture and production. Clinical LBPs must be cultured in media without any animal products (*177*), so we transitioned our isolate into animal-free tryptic soy broth (AF-TSB) for this work. Initial scale-up with Rise demonstrated that *A. caccae* LAHUC successfully grew in AF-TSB in a 2L batch fermentation reactor, reaching a high optical density of approximately 6.0 (**Fig. 3.20**). Cells from this culture were lyophilized, and ongoing studies are testing the stability of this lyophilized powder (namely cell viability) after long term storage at various temperatures (4°C, 25°C, 40°C).

Overall, we have isolated a novel strain of *A. caccae* which is suitable for production as a clinical LBP. We characterized its growth and metabolic products through *in vitro* culture techniques and through analysis of its genome. Ongoing work in collaboration with the Mimee laboratory (UChicago) is further characterizing the genome of *A. caccae* LAHUC and developing gene editing tools to modify this species as well as other commensal Clostridia. These studies will contribute to our knowledge about this strain and create opportunities to manipulate its genome to improve its therapeutic capacity. We have thus far attempted to improve *A. caccae*'s butyrate output by pairing it with other bacterial species and various carbohydrates. However, genetic editing could further improve its butyrate output, or allow this species to selectively utilize a specific carbon source for its metabolism.

6.2 Bacterial regulation of epithelial barrier function

The intestinal epithelium functions as a barrier between the lumen and the rest of the body, preventing hyper immune activation to the abundant luminal food-derived and

microbial antigens (*117*, *118*). We have shown that in the absence of commensal Clostridia, mice have dysregulated epithelial barrier function, which allows translocation of food antigens into systemic circulation and downstream allergic sensitization (*53*). Clostridia are essential in regulating this barrier function, which is characterized by production of IL-22 from ILC3s, expression of AMPs from Paneth cells as well as increased populations of mucus-secreting GCs (*53*). In more recent work we also showed that butyrate delivered to the distal GI tract via conjugation to polymer micelles (ButM) increases epithelial barrier integrity, preventing translocation of FITC-dextran into the serum of mice treated with DSS or antibiotics (*92*). We now expand upon these studies to understand how human-derived microbiota, either feces from healthy or CMA infants, or *A. caccae* LAHUC impact intestinal barrier integrity. These studies have furthered our understanding of microbial regulation of the host epithelium and help to understand the disparate phenotypes of mice colonized with the healthy or CMA feces in our model of cow's milk allergy (*104*). Colonization with healthy infant-derived feces or *A. caccae* is sufficient to prevent allergic responses to the milk allergen BLG. Conversely, CMA-colonized mice are not protected (*104*). In this thesis, we demonstrate that the healthy infant microbiota induces a barrier-protective phenotype in colonized mice, which is lacking in CMA-colonized mice. This may, in part, explain their different outcomes in this model of cow's milk allergy.

We previously showed that *A. caccae* monocolonized mice are protected from developing allergic responses to BLG (*104*). We thus designed experiments to determine if *A. caccae*, like other Clostridia, regulates epithelial barrier function. In addition to studying the effects of *A. caccae* monocolonization, we also treated some mice with myo-inositol, a glucose-like sugar alcohol which *A. caccae* ferments into propionate *in vitro* (**Fig. 3.16**) to determine if addition of this prebiotic would alter *A. caccae*'s SCFA production *in vivo*. Administration of myo-inositol did in fact increase the concentration of propionate as well as butyrate in the cecum of *A. caccae* monocolonized mice (**Fig. 4.1**).

Mice monocolonized with *A. caccae* had little butyrate measurable in the cecum, and these low levels may not be sufficient to induce immunoregulatory responses in mice. However, only *A. caccae* monocolonized mice that were not treated with myo-inositol had increased GC numbers in colonic crypts and increased mucus layer thickness (**Fig. 4.2**). This led us to predict that *A. caccae* may elicit a barrier protective phenotype in monocolonized mice by inducing mucus production, either by consuming host mucus or otherwise interacting with the colonic epithelium. Conversely, in the presence of an accessible carbon source (in this case, myo-inositol), *A. caccae* did not directly depend on host-derived carbohydrates, and thus did not induce this GC/ mucus response. Further work in this area will determine if *A. caccae* (with or without myo-inositol) induces IL-22, or if administration of myo-inositol alters the allergic response to BLG in *A. caccae* monocolonized mice. We suspect that although mice treated with myo-inositol do not have increased GC numbers or function, the SCFAs produced by *A. caccae* in this context may still result in protection from an allergic response. Additionally, we could explore the effects of myo-inositol in the context of a replete microbiota, e.g., in CMA-colonized mice. We do not yet know if *A. caccae* (or other bacterial taxa) would be able to ferment myo-inositol into SCFAs in this complex environment, although we predict that they would.

In addition to these monocolonization experiments, we performed most of our studies using gnotobiotic mice colonized with feces derived from healthy or CMA infant donors (*104*). Fecal slurries obtained from these donors were first gavaged to GF mice almost 6 years ago, and feces from these initial recipient (repository) mice have been used to colonize all subsequent mice. These bacterial communities have remained remarkably stable over time as maintained in these living repositories. In our previous publication, we demonstrated that mice colonized with feces derived from four healthy infant donors had increased relative abundance of Lachnospiraceae, Erysipelotrichaceae and other taxa compared to mice colonized with feces from four CMA donors. Conversely, CMA-colonized mice had increased relative abundance of Parabacteroides and unclassified

Clostridiales (*104*). Nearly 6 years later, we show that mice colonized with feces from healthy- and CMA- repositories from two donors (healthy donor 2, CMA donor 6 (*104*)) have distinct microbiome compositions, and that these two communities are distinct from each other (**Fig. 4.3**). Further, the healthy microbiota is consistently characterized by increased relative abundance of Lachnospiraceae and Eryipelotrichaceae genera, while the CMA microbiota is dominated by *Bacteroides* and *Parabacteroides* (**Fig. 4.3**). Healthy-colonized mice also have increased cecal butyrate compared to CMA-colonized mice, demonstrating functional differences in these two communities (**Fig. 4.4**). Metagenomic analysis of feces from mice colonized with microbiota derived from a different CMA donor (donor 5, (*104*)) demonstrated that this microbiome contains more LPS synthesis genes than that of a healthy donor, which may have inflammatory consequences (*159*). Further metagenomic and metabolomic analyses of the microbiota used in this study (derived from healthy donor 2 and CMA donor 6, (*104*)) could provide greater insight into specific functional differences between these communities.

Beyond these differences in the microbiome composition of healthy- and CMA-colonized mice, we also demonstrate that these mice have differing epithelial barrier function. Colonization with the healthy microbiota (from feces of repository mice) induces IL-22 production, expression of downstream AMP genes *Reg3β* and *Reg3*γ, and reduces intestinal permeability to FITC-dextran (**Figs. 4.4, 4.5**). The CMA microbiota does not elicit this same effect, strengthening our previous conclusions that the healthy infant microbiota contains specific taxa which can regulate host health and immunity (*104*). The epithelial barrier function observed in healthy-colonized mice likely contributes to their protection from developing allergic responses to food. Future studies could ablate this barrier function during sensitization (i.e., with a neutralizing antibody to IL-22) to determine if the allergy-protective effect of the healthy microbiota is mediated by IL-22 -dependent barrier function. Additionally, various factors (i.e., butyrate, *A. caccae*) could be introduced to the

CMA microbiota in attempts to improve their epithelial barrier function and downstream allergic phenotype.

6.3 A synbiotic formulation of *A. caccae* LAHUC and lactulose exerts a variety of microbiome- and host-modulating effects to prevent and treat allergic responses to food in mice

Based on our previous findings, we predicted that administration of *A. caccae* LAHUC to CMA-colonized mice would reduce their susceptibility to developing allergic responses to food. CMA-colonized mice have lower representation of Lachnospiraceae taxa and low levels of luminal butyrate compared to healthy-colonized mice (*104*). Additionally, colonization with this microbiota did not elicit an IL-22 -dependent barrier protective phenotype (**Figs. 4.4, 4.5**), and after sensitization with the allergen BLG, CMA-colonized mice developed allergic responses to this antigen upon i.g. challenge (*104*). For these reasons we refer to the CMA microbiota as a dysbiotic community. We postulated that introduction of *A. caccae*, a butyrate-producing species in the family Lachnospiraceae, into this community would rescue this dysbiosis and attenuate the allergic phenotype of CMA-colonized mice.

A. caccae readily colonizes GF mice (*104*), however it was not known if the same would be true for mice with a replete, yet dysbiotic, microbiota. To improve engraftment and metabolic opportunity for *A. caccae* LAHUC, we administered this species as a synbiotic with various prebiotics. Strikingly, *A. caccae* readily engrafted in both CMA-colonized mice and vancomycin-treated SPF mice even in the absence of additional prebiotic supplementation (**Figs. 5.2, 5.5, 5.16**). However, neither *A. caccae* LAHUC nor any of the prebiotics we tested increased luminal butyrate in CMA-colonized mice when administered alone (**Fig. 5.3**). Only synbiotic administration of *A. caccae* LAHUC and lactulose increased luminal butyrate concentration *in vivo* (**Figs. 5.3, 5.5, 5.16**).

Many groups have administered prebiotic fibers in clinical studies with the goal of increasing fecal butyrate production (*178*, *179*). However, results of these studies are often highly variable and dependent on the specific prebiotic as well as the baseline, resident microbiota of the individual participants (*178*, *187–190*). The modern, Western diet is largely deficient in fiber, and after generations of consuming this diet the fiber-consuming bacteria in the human gut may be so depleted that re-introduction of fiber may not be sufficient to recover these taxa, as has been shown in mice (*17*). We predict that the prebiotics administered in these previous studies may have been partially broken down by the resident microbiota, but in the absence of an efficient butyrate-producer, the prebiotic would not be fully fermented into this final product. Administration of a butyrate-producing LBP may address this gap, and delivery as a synbiotic will help to ensure the LBP's growth and opportunity.

In our studies, we demonstrated that our synbiotic therapy (*A. caccae* LAHUC plus lactulose) prevented the development of allergic responses to BLG in CMA-colonized mice, but *A. caccae* alone did not protect (**Fig. 5.7**). This fits with our hypothesis that butyrate is critical to *A. caccae*'s therapeutic efficacy since we demonstrated that administration of *A. caccae* alone did not increase luminal butyrate (**Fig. 5.3**). The same is true in PN-sensitized, vancomycin-treated mice: only treatment with the synbiotic (but not *A. caccae* alone) increased cecal butyrate and reduced the anaphylactic response to PN challenge (**Fig. 5.16**).

The *A. caccae* synbiotic may prevent allergic responses to food through various mechanisms, regulating both innate and adaptive immunity. Following two sensitizations with BLG plus CT, CMA-colonized mice expressed significantly greater transcripts of alarmin genes *Il25* and *Tslp* in the ileal epithelial cell compartment than healthy-colonized mice (**Fig. 5.11**). Treatment with the synbiotic completely prevented this alarmin response, reducing the expression to levels similar to those detected in healthy-colonized mice (**Fig. 5.11**). The synbiotic therapy may reduce all downstream Th2 activation by

preventing this initial, innate response to sensitization. The mechanism of how commensal bacteria could regulate epithelial alarmin expression is not yet known. We predicted that the synbiotic may increase mucus production in the small intestine, which could trap BLG and CT and prevent them from being sensed by the epithelium. Future studies will be required to determine if mucus production is involved in this phenotype.

We also examined the effect of synbiotic treatment on T cell populations in the mLNs in BLG-sensitized mice. Th2 cells are the canonical regulators of allergy, but Tfh cells also play a major role in that these cells directly interact with B cells in the GC and affect their maturation into high-affinity, antibody-secreting PCs (*295*). Tfh cells that produce IL-13, specifically, are involved in the maturation of IgG1 and IgE-producing PCs (*125*, *290*). Conversely, Tfr cells oppose the actions of Tfh cells and produce tolerogenic cytokines (IL-10) and inhibitory receptors (CTLA-4) to reduce B cell activation in the GC (*295*). We demonstrate that CMA-colonized mice had greater proportions and cell numbers of Tfh in the iLN than healthy-colonized mice, which may additionally contribute to their development of allergic responses (**Fig. 5.13**). Conversely, synbiotic treatment expanded populations of Tfr cells (both $CD25^+$ and $CD25^-$ subsets) in the cLN of BLG-sensitized, CMA-colonized mice (**Fig. 5.13**). Butyrate (in the form of butyrylated starch) has been shown to increase these Tfr populations (particularly $CD25^-$ cells) in a murine model of rheumatoid arthritis (*97*). However, the role of Tfr cells in regulating food allergy is not yet clear, and it seems that Tfr cells may either prevent or promote IgE maturation depending on the specific model and genetic background of mice (*296–298*). In our model, we predict that this expansion of Tfr cells may have a beneficial role in preventing the development of high affinity IgE antibody-secreting cells (ASCs), since synbiotic treated mice express fewer IgE-ASCs in the mLN than untreated, CMA-colonized mice (**Fig. 5.14**). Future work will expand on this observation by characterizing BLG-specific IgE cells, although these low abundance cells may be difficult to identify with current methods. This direct T/ B cell regulation by a single commensal species has not yet been described and could

contribute to our understanding of bacterial regulation of allergic responses to food overall.

The mechanisms described so far all explain how prophylactic treatment with the synbiotic may prevent the development of allergic responses to BLG. However, this synbiotic also showed efficacy in a therapeutic model of peanut allergy, in which mice were sensitized to PN and subsequently treated with the synbiotic (or *A. caccae* LAHUC alone) after they had become fully allergic. We have previously shown that short-term treatment with butyrate-conjugated micelles (ButM) reduced the allergic response to PN in this model (*92*), and here we demonstrated that the synbiotic is similarly effective (**Fig. 5.16**). We predict that in the therapeutic model, both the synbiotic and ButM may be impacting the accumulation or function of downstream effector cells such as mast cells. Mucosal mast cells accumulate in the intestine in response to allergic sensitization and express FcεR1 which binds allergen specific IgE (*299*). Upon allergen re-exposure, the antigen will cross-link surface-bound IgE, initiating an intracellular signaling cascade which results in cellular degranulation and release of proteases, particularly mMCPT-1 (*299*). *In vitro*, butyrate has been shown to decrease FCεR1 expression and activation markers on mast cells via HDAC inhibition (*99*). We predict that our therapeutics (ButM and the *A. caccae* synbiotic), which both increase butyrate concentrations in the lower GI tract, may reduce accumulation or activation of mucosal mast cells. Further experiments will be required to determine the exact mechanisms imparted by these treatments in this therapeutic peanut allergy model.

6.4 Conclusion

The interactions between the human host and commensal microbiota are complex, dynamic, and diverse. The three-way system between host biology, the environment, and the microbiome must maintain careful balance to preserve health and homeostasis. Any

perturbations in this system can heighten susceptibility to disease or dysfunction. We are just beginning to understand the mechanisms of these interactions, identifying key bacterial species and their products which modulate host immunity, as well as host-factors which regulate the composition of the microbiota. The rise of genetic sequencing and 'omics technologies (metagenomics, metabolomics, etc.) is rapidly expanding our access to data which can help to understand the complex ecological dynamics within the human gut microbiome (*9*, *164*, *165*). However, it is difficult to determine causality from these 'omics studies. Identifying, isolating, and characterizing specific bacterial species which causally impact the host is imperative in translating this new understanding into meaningful therapeutics (*167*, *168*).

Our laboratory has previously examined the fecal microbiome (*103*, *104*, *112*) and metabolome (*112*) of individuals with food allergies. These studies have shown, across different cohorts and demographics, a reproducible lack of butyrate-producing Clostridia in infants with cow's milk allergy or children and adult twins with various food allergies (*103*, *104*, *112*). We also established causality, by demonstrating that members of the healthy infant fecal microbiota, particularly *A. caccae*, protect against the development of allergic responses to BLG in a gnotobiotic murine model (*104*). This finding was later replicated with another cohort of healthy and food allergic infants in a different model of murine food allergy (*111*), demonstrating the generalizability of our findings.

This thesis expands upon previous work by attempting to harness the immunoregulatory effect observed in *A. caccae* monocolonized mice and utilize this species as an LBP for food allergy. We hypothesized that this species, a butyrate-producing Clostridia with established host-beneficial properties, could prevent or treat allergic responses to food in mice with dysbiotic microbiota. We first isolated a strain of this species, *A. caccae* LAHUC, from the feces of a healthy infant donor (*104*) and extensively characterized the growth and phenotype of this isolate *in vitro*. We then demonstrated that, surprisingly, this isolate readily engrafts in mice with an existing

microbiota (either CMA-colonized mice or vancomycin-treated SPF mice). However, this engraftment does not increase the concentration of butyrate in the cecal contents – only co-administration of *A. caccae* LAHUC with prebiotic lactulose increases luminal butyrate. We hypothesized that butyrate is critical to *A. caccae*'s allergy-protective effect, and with these two formulations (*A. caccae* LAHUC administered alone or as a synbiotic), we had an internal control to study the effects of a therapeutic LBP, with or without corresponding butyrate. Prebiotic lactulose may alone have some therapeutic effects (*255*, *300*); however, these have not yet been consistently shown in mice or humans (*256*, *257*). We instead focused on the potential beneficial role of *A. caccae* in the context of lactulose or alone.

We applied our synbiotic therapy to established models of cow's milk allergy in a gnotobiotic system (*104*) or peanut allergy in SPF mice treated neonatally with antibiotics (*53*, *92*). Strikingly, in both models, the synbiotic treatment reduced the anaphylactic response to allergen challenge, but treatment with *A. caccae* LAHUC alone had minimal effect. This contributes to our understanding that butyrate derived from *A. caccae* is critical to its immunoregulatory effect, as only the synbiotic increases luminal butyrate. The synbiotic likely impacts the development of allergies through various mechanisms. We demonstrated that some of these mechanisms may involve modulation of the fecal microbiome, blunting the epithelial alarmin response to sensitization, expanding populations of Tfr cells in mLN, and reducing populations of IgE-secreting cells in the mLN.

Overall, this work demonstrates that paired delivery of a butyrate-producing bacterium with a rationally chosen prebiotic can lead to its persistence and modulation of the resident microbiota, as well as regulation of the host immune system in the context of food allergies. There is significant clinical interest in developing pre- pro- and syn-biotics (*179*, *219*). However, the results of earlier studies have been highly variable and overall, there is not much evidence to date for efficacy of these strategies in prevention or treatment of

food allergy (*101*, *230*, *235*, *237*). Many of these strategies have relied upon administration of probiotics which are readily culturable (e.g., *Lactobacillus* and *Bifidobacterium* sp.), but often do not engraft in the host and do not have demonstrable mechanisms of host interaction in this context (*103*, *230*). Our synbiotic overcomes this limitation, by increasing resident populations of bacteria (*Bifidobacterium*), and additionally by achieving engraftment of a Clostridial species which can readily utilize the fermentation products produced by these “classical probiotics” to produce butyrate. The immunoregulatory properties of butyrate are well described (*92*, *178*, *287*), and a lack of butyrate or butyrate-producing species is correlated with atopy (*45*, *105*). The synbiotic which we developed here contains a bacterium which readily engrafts, produces butyrate, and further expands resident populations of beneficial bacteria to result in an overall allergy-protective effect in dysbiotic hosts. Our data suggests that our infant-derived isolate of *A. caccae*, administered as a synbiotic, may be an effective LBP in future clinical studies.

BIBLIOGRAPHY

1. Tipton, L., Darcy, J. L., and Hynson, N. A. (2019). A Developing Symbiosis: Enabling Cross-Talk Between Ecologists and Microbiome Scientists. *Front. Microbiol. 10.*
2. Ley, R. E., Hamady, M., Lozupone, C., Turnbaugh, P. J., Ramey, R. R., Bircher, J. S., Schlegel, M. L., Tucker, T. A., Schrenzel, M. D., Knight, R., and Gordon, J. I. (2008). Evolution of mammals and their gut microbes. *Science 320*, 1647–51.
3. Byndloss, M. X., Pernitzsch, S. R., and Bäumler, A. J. (2018). Healthy hosts rule within: ecological forces shaping the gut microbiota. *Mucosal Immunol. 11,* 1299-1305.
4. Litvak, Y., and Bäumler, A. J. (2019). Microbiota-Nourishing Immunity: A Guide to Understanding Our Microbial Self. *Immunity 51*, 214–224.
5. Goodman, A. L., Kallstrom, G., Faith, J. J., Reyes, A., Moore, A., Dantas, G., and Gordon, J. I. (2011). Extensive personal human gut microbiota culture collections characterized and manipulated in gnotobiotic mice. *Proc. Natl Acad Sci. USA 108*, 6252–7.
6. The Human Microbiome Project Consortium (2012). Structure, function and diversity of the healthy human microbiome. *Nature 486*, 207–214.
7. Browne, H. P., Forster, S. C., Anonye, B. O., Kumar, N., Neville, B. A., Stares, M. D., Goulding, D., and Lawley, T. D. (2016). Culturing of 'unculturable' human microbiota reveals novel taxa and extensive sporulation. *Nature 533*, 543–546.
8. Sender, R., Fuchs, S., and Milo, R. (2016). Are We Really Vastly Outnumbered? Revisiting the Ratio of Bacterial to Host Cells in Humans. *Cell 164*, 337–40.
9. Sorbara, M. T., Littmann, E. R., Fontana, E., Moody, T. U., Kohout, C. E., Gjonbalaj, M., Eaton, V., Seok, R., Leiner, I. M., and Pamer, E. G. (2020). Functional and

Genomic Variation between Human-Derived Isolates of Lachnospiraceae Reveals Inter- and Intra-Species Diversity. *Cell Host & Microbe 28*, 134–146.

10. Levy, M., Kolodziejczyk, A. A., Thaiss, C. A., and Elinav, E. (2017). Dysbiosis and the immune system. *Nat. Rev. Immunol. 17*, 219–232.

11. Fischbach, M. A. (2018). Microbiome: Focus on Causation and Mechanism. *Cell 174*, 785–790.

12. Buffie, C. G., and Pamer, E. G. (2013). Microbiota-mediated colonization resistance against intestinal pathogens. *Nat. Rev. Immunol. 13*, 790–801.

13. Yatsunenko, T. et al. (2012). Human gut microbiome viewed across age and geography. *Nature 486*, 222–7.

14. Schnorr, S. L. et al. (2014). Gut microbiome of the Hadza hunter-gatherers. *Nat. Commun. 5*, 3654.

15. Sonnenburg, J. L., and Sonnenburg, E. D. (2019). Vulnerability of the industrialized microbiota. *Science, 366,* 6464

16. Vangay, P. et al. (2018). US Immigration Westernizes the Human Gut Microbiome. *Cell 175*, 962–972.

17. Sonnenburg, E. D., Smits, S. A., Tikhonov, M., Higginbottom, S. K., Wingreen, N. S., and Sonnenburg, J. L. (2016). Diet-induced extinctions in the gut microbiota compound over generations. *Nature 529*, 212–215.

18. Bisanz, J. E., Upadhyay, V., Turnbaugh, J. A., Ly, K., and Turnbaugh, P. J. (2019). Meta-Analysis Reveals Reproducible Gut Microbiome Alterations in Response to a High-Fat Diet. *Cell Host & Microbe 26*, 265–272.

19. Becattini, S., Taur, Y., and Pamer, E. G. (2016). Antibiotic-Induced Changes in the Intestinal Microbiota and Disease. *Trends Mol. Med 22*, 458–478.

20. Dethlefsen, L., and Relman, D. A. (2011). Incomplete recovery and individualized responses of the human distal gut microbiota to repeated antibiotic perturbation. *Proc. Natl Acad Sci. USA 108 Suppl 1*, 4554–61.

21. Strachan, D. P. (1989). Hay fever, hygiene, and household size. *BMJ (Clinical research ed.) 299*, 1259–60.

22. Wills-Karp, M., Santeliz, J., and Karp, C. L. (2001). The germless theory of allergic disease: revisiting the hygiene hypothesis. *Nat Rev Immunol 1*, 69–75.

23. Schaub, B., Lauener, R., and von Mutius, E. (2006). The many faces of the hygiene hypothesis. *J Allergy Clin Immunol 117*, 969–977.

24. Iweala, O. I., and Nagler, C. R. (2019). The Microbiome and Food Allergy. *Annu Rev Immunol 37*, 377–403.

25. Torow, N., Hand, T. W., and Hornef, M. W. (2023). Programmed and environmental determinants driving neonatal mucosal immune development. *Immunity 56*, 485–499.

26. Bokulich, N. A., Chung, J., Battaglia, T., Henderson, N., Jay, M., Li, H., D Lieber, A., Wu, F., Perez-Perez, G. I., Chen, Y., Schweizer, W., Zheng, X., Contreras, M., Dominguez-Bello, M. G., and Blaser, M. J. (2016). Antibiotics, birth mode, and diet shape microbiome maturation during early life. *Sci Transl Med 8*, 343ra82.

27. Bäckhed, F. et al. (2015). Dynamics and Stabilization of the Human Gut Microbiome during the First Year of Life. *Cell Host & Microbe 17*, 690–703.

28. Aagaard, K., Ma, J., Antony, K. M., Ganu, R., Petrosino, J., and Versalovic, J. (2014). The Placenta Harbors a Unique Microbiome. *Sci Transl Med 6*, 237.

29. Kennedy, K. M. et al. (2023). Questioning the fetal microbiome illustrates pitfalls of low-biomass microbial studies. *Nature 613*, 639–649.

30. Sordillo, J. E. et al. (2017). Factors influencing the infant gut microbiome at age 3-6 months: Findings from the ethnically diverse Vitamin D Antenatal Asthma Reduction Trial (VDAART). *J Allergy Clin Immunol 139*, 482– 491.

31. Wampach, L. et al. (2018). Birth mode is associated with earliest strain-conferred gut microbiome functions and immunostimulatory potential. *Nat Commun 9*, 5091.

32. Hourigan, S. K., and Dominguez-Bello, M. G. (2023). Microbial seeding in early life. *Cell Host & Microbe 31*, 331–333.

33. Bager, P., Wohlfahrt, J., and Westergaard, T. (2008). Caesarean delivery and risk of atopy and allergic disease: meta-analyses. *Clin Exp Allergy 38*, 634–42.

34. Shao, Y., Forster, S. C., Tsaliki, E., Vervier, K., Strang, A., Simpson, N., Kumar, N., Stares, M. D., Rodger, A., Brocklehurst, P., Field, N., and Lawley, T. D. (2019). Stunted microbiota and opportunistic pathogen colonization in caesarean-section birth. *Nature 574*, 117–121.

35. Chu, D. M., Ma, J., Prince, A. L., Antony, K. M., Seferovic, M. D., and Aagaard, K. M. (2017). Maturation of the infant microbiome community structure and function across multiple body sites and in relation to mode of delivery. *Nat Med 23*, 314–326.

36. Bogaert, D., van Beveren, G. J., de Koff, E. M., Lusarreta Parga, P., Balcazar Lopez, E., Koppensteiner, L., Clerc, M., Hasrat, R., Arp, K., Chu, M. L. J., de Groot,P. C., Sanders, E. A., van Houten, M. A., and de Steenhuijsen Piters, W. A. (2023). Mother-to-infant microbiota transmission and infant microbiota development across multiple body sites. *Cell Host & Microbe 31*, 447–460.

37. Stewart, C. J. et al. (2018). Temporal development of the gut microbiome in early childhood from the TEDDY study. *Nature 562*, 583–588.

38. Kim, Y.-G. et al. (2017). Neonatal acquisition of Clostridia species protects against colonization by bacterial pathogens. *Science 356*, 315–319.

39. Al Nabhani, Z., Dulauroy, S., Marques, R., Cousu, C., Al Bounny, S., Déjardin, F., Sparwasser, T., Bérard, M., Cerf-Bensussan, N., and Eberl, G. (2019). A Weaning Reaction to Microbiota Is Required for Resistance to Immunopathologies in the Adult. *Immunity 50*, 1276–1288.

40. Torow, N., and Hornef, M. W. (2017). The Neonatal Window of Opportunity: Setting the Stage for Life-Long Host-Microbial Interaction and Immune Homeostasis. *J Immuno*l *198,* 2

41. Tamburini, S., Shen, N., Wu, H. C., and Clemente, J. C. (2016). The microbiome in early life: implications for health outcomes. *Nat Med 22*, 713–22.

42. Gasparrini, A. J., Wang, B., Sun, X., Kennedy, E. A., Hernandez-Leyva, A., Ndao, I. M., Tarr, P. I., Warner, B. B., and Dantas, G. (2019). Persistent metagenomic signatures of early-life hospitalization and antibiotic treatment in the infant gut microbiota and resistome. *Nat Micro 4*, 2285–2297.

43. Murk, W., Risnes, K. R., and Bracken, M. B. (2011). Prenatal or early-life exposure to antibiotics and risk of childhood asthma: a systematic review. *Pediatrics 127*, 1125–38.

44. Fouhy, F., Guinane, C. M., Hussey, S., Wall, R., Ryan, C. A., Dempsey, E. M., Murphy, B., Ross, R. P., Fitzgerald, G. F., Stanton, C., and Cotter, P. D. (2012). High-throughput sequencing reveals the incomplete, short-term recovery of infant gut microbiota following parenteral antibiotic treatment with ampicillin and gentamicin. *Antimicrob Agents Chemother 56*, 5811–20.

45. Cait, A. et al. (2019). Reduced genetic potential for butyrate fermentation in the gut microbiome of infants who develop allergic sensitization. *J Allergy Clin Immunol 144*, 1638–1647.

46. Lundgren, S. N., Madan, J. C., Emond, J. A., Morrison, H. G., Christensen, B. C., Karagas, M. R., and Hoen, A. G. (2018). Maternal diet during pregnancy is related with the infant stool microbiome in a delivery mode-dependent manner. *Microbiome 6*, 109.

47. Stampfli, M., Frei, R., Divaret-Chauveau, A., Schmausser-Hechfellner, E., Karvonen, A. M., Pekkanen, J., Riedler, J., Schaub, B., von Mutius, E., Lauener, R., Roduit, C., and Protection against Allergy–Study in Rural Environments Study Group (2022). Inverse associations between food diversity in the second year of life and allergic diseases. *Ann Allergy Asthma Immunol 128*, 39–45.

48. Bantz, S. K., Zhu, Z., and Zheng, T. (2014). The Atopic March: Progression from Atopic Dermatitis to Allergic Rhinitis and Asthma. *J Clin Cell Immunol 05*, 2.

49. Fujimura, K. E. et al. (2016). Neonatal gut microbiota associates with childhood multisensitized atopy and T cell differentiation. *Nat Med 22*, 1187–1191.

50. Huttenhower, C. et al. (2012). Structure, function and diversity of the healthy human microbiome. *Nature 486*, 207-14.

51. Ivanov, I. I. et al. (2009). Induction of Intestinal Th17 Cells by Segmented Filamentous Bacteria. *Cell 139*, 485–498.

52. Ivanov, I. I., Tuganbaev, T., Skelly, A. N., and Honda, K. (2022). T Cell Responses to the Microbiota. *Annu Rev Immunol 40*, 559–587.

53. Stefka, A. T., Feehley, T., Tripathi, P., Qiu, J., McCoy, K., Mazmanian, S. K., Tjota, M. Y., Seo, G.-Y., Cao, S., Theriault, B. R., Antonopoulos, D. A., Zhou, L., Chang, E. B., Fu, Y.-X., and Nagler, C. R. (2014). Commensal bacteria protect against food allergen sensitization. *Proc. Natl Acad Sci. USA 111*, 13145– 13150.

54. Atarashi, K. et al. (2013). Treg induction by a rationally selected mixture of Clostridia strains from the human microbiota. *Nature 500*, 232–6.

55. Narushima, S., Sugiura, Y., Oshima, K., Atarashi, K., Hattori, M., Suematsu, M., and Honda, K. (2014). Characterization of the 17 strains of regulatory T cell-inducing human-derived Clostridia. *Gut microbes 5*, 3 333-339

56. Surana, N. K., and Kasper, D. L. (2017). Moving beyond microbiome-wide associations to causal microbe identification. *Nature 552*, 244–247.

57. Caballero, S., Kim, S., Carter, R. A., Leiner, I. M., Sušac, B., Miller, L., Kim, G. J., Ling, L., and Pamer, E. G. (2017). Cooperating Commensals Restore Colonization Resistance to Vancomycin-Resistant Enterococcus faecium. *Cell Host & Microbe 21*, 592–602.

58. Kim, S. G. et al. (2019). Microbiota-derived lantibiotic restores resistance against vancomycin-resistant Enterococcus. *Nature 572*, 665–669.

59. Tanoue, T. et al. (2019). A defined commensal consortium elicits CD8 T cells and anti-cancer immunity. *Nature 565*, 600–605.

60. Wong, S. H., and Yu, J. (2019). Gut microbiota in colorectal cancer: mechanisms of action and clinical applications. *Nat Rev Gastroenterol Hepatol 16*, 690–704.

61. Faith, J. J., Ahern, P. P., Ridaura, V. K., Cheng, J., and Gordon, J. I. (2014). Identifying Gut Microbe–Host Phenotype Relationships Using Combinatorial Communities in Gnotobiotic Mice. *Sci Transl Med 6*, 220

62. Venturelli, O. S., Carr, A. C., Fisher, G., Hsu, R. H., Lau, R., Bowen, B. P., Hromada, S., Northen, T., and Arkin, A. P. (2018). Deciphering microbial interactions in synthetic human gut microbiome communities. *Mol Sys Bio 14*, e8157.

63. Clark, R. L., Connors, B. M., Stevenson, D. M., Hromada, S. E., Hamilton, J. J., Amador-Noguez, D., and Venturelli, O. S. (2021). Design of synthetic human gut microbiome assembly and butyrate production. *Nat Commun 12*, 3254.

64. Stephen-Victor, E., Crestani, E., and Chatila, T. A. (2020). Dietary and Microbial Determinants in Food Allergy. *Immunity 53*, 277–289.

65. Vatanen, T. et al. (2016). Variation in Microbiome LPS Immunogenicity Contributes to Autoimmunity in Humans. *Cell 165*, 842–53.

66. Clasen, S. J., Bell, M. E. W., Borbón, A., Lee, D.-H., Henseler, Z. M., de la CuestaZuluaga, J., Parys, K., Zou, J., Wang, Y., Altmannova, V., Youngblut, N. D., Weir, J. R., Gewirtz, A. T., Belkhadir, Y., and Ley, R. E. (2023). Silent recognition of flagellins from human gut commensal bacteria by Toll-like receptor 5. *Sci Immunol 8*, 79.

67. Zelante, T., Iannitti, R. G., Cunha, C., De Luca, A., Giovannini, G., Pieraccini, G., Zecchi, R., D'Angelo, C., Massi-Benedetti, C., Fallarino, F., Carvalho, A., Puccetti, P., and Romani, L. (2013). Tryptophan catabolites from microbiota engage arylhydrocarbon receptor and balance mucosal reactivity via interleukin-22. *Immunity 39*, 372–85.

68. Lamas, B. et al. (2016). CARD9 impacts colitis by altering gut microbiota metabolism of tryptophan into aryl hydrocarbon receptor ligands. *Nat Med 22*, 598–605.

69. Kemter, A., Patry, R., Arnold, J., Campbell, E., Hesser, L., Ionescu, E., and Nagler, C. (2022). Flagella and indole produced by commensal bacteria protect the intestinal barrier to prevent food allergy. *J Immunol* 208 (1_Supplement), 115-116.

70. Scott, S. A., Fu, J., and Chang, P. V. (2020). Microbial tryptophan metabolites regulate gut barrier function via the aryl hydrocarbon receptor. *Proc. Natl Acad Sci. USA 117*, 19376–19387.

71. Grizotte-Lake, M., Zhong, G., Duncan, K., Kirkwood, J., Iyer, N., Smolenski, I., Isoherranen, N., and Vaishnava, S. (2018). Commensals Suppress Intestinal Epithelial Cell Retinoic Acid Synthesis to Regulate Interleukin-22 Activity and Prevent Microbial Dysbiosis. *Immunity 49*, 1103–1115.

72. Campbell, C., McKenney, P. T., Konstantinovsky, D., Isaeva, O. I., Schizas, M., Verter, J., Mai, C., Jin, W.-B., Guo, C.-J., Violante, S., Ramos, R. J., Cross, J. R., Kadaveru, K., Hambor, J., and Rudensky, A. Y. (2020). Bacterial metabolism of bile acids promotes generation of peripheral regulatory T cells. *Nature 581*, 475–479.

73. Song, X., Sun, X., Oh, S. F., Wu, M., Zhang, Y., Zheng, W., Geva-Zatorsky, N., Jupp, R., Mathis, D., Benoist, C., and Kasper, D. L. (2020). Microbial bile acid metabolites modulate gut RORγ+ regulatory T cell homeostasis. *Nature 577*, 410–415.

74. Li, W. et al. (2021). A bacterial bile acid metabolite modulates Treg activity through the nuclear hormone receptor NR4A1. *Cell Host & Microbe 29*, 1366–1377.

75. Wu, R., Yuan, X., Li, X., Ma, N., Jiang, H., Tang, H., Xu, G., Liu, Z., and Zhang, Z. (2022). The bile acid-activated retinoic acid response in dendritic cells is involved in food allergen sensitization. *Allergy 77*, 483–498.

76. Wu, W., Sun, M., Chen, F., Cao, A. T., Liu, H., Zhao, Y., Huang, X., Xiao, Y., Yao, S., Zhao, Q., Liu, Z., and Cong, Y. (2017). Microbiota metabolite short-chain fatty acid acetate promotes intestinal IgA response to microbiota which is mediated by GPR43. *Mucosal Immunol 10*, 946–956.

77. Lee, Y.-S. et al. (2018). Microbiota-Derived Lactate Accelerates Intestinal Stem-CellMediated Epithelial Development. *Cell Host & Microbe 24*, 833–846.

78. Ríos-Covián, D., Ruas-Madiedo, P., Margolles, A., Gueimonde, M., de los ReyesGavilán, C. G., and Salazar, N. (2016). Intestinal Short Chain Fatty Acids and their Link with Diet and Human Health. *Front Microbiol 7.*

79. Tan, J., McKenzie, C., Potamitis, M., Thorburn, A. N., Mackay, C. R., and Macia. (2014) The role of short-chain fatty acids in health and disease. *Adv Immunol121*, 91-119.

80. Sorbara, M. T., and Pamer, E. G. (2022). Microbiome-based therapeutics. *Nat Rev Microbiol 20*, 365–380.

81. Donohoe, D. R., Garge, N., Zhang, X., Sun, W., O'Connell, T. M., Bunger, M. K., and Bultman, S. J. (2011). The microbiome and butyrate regulate energy metabolism and autophagy in the mammalian colon. *Cell Metab*, *13,* 5 517-526.

82. Kelly, C. J. et al. (2015). Crosstalk between Microbiota-Derived Short-Chain Fatty Acids and Intestinal Epithelial HIF Augments Tissue Barrier Function. *Cell Host & Microbe 17*, 662–71.

83. Byndloss, M. X. et al. (2017). Microbiota-activated PPAR-*γ* signaling inhibits dysbiotic Enterobacteriaceae expansion. *Science 357*, 6351

84. Tan, J. K., McKenzie, C., Mariño, E., Macia, L., and Mackay, C. R. (2017). Metabolite Sensing G Protein–Coupled Receptors—Facilitators of Diet-Related Immune Regulation. *Ann Rev Immunol 35*, 371–402.

85. Zhao, Y., Chen, F., Wu, W., Sun, M., Bilotta, A. J., Yao, S., Xiao, Y., Huang, X., Eaves-Pyles, T. D., Golovko, G., Fofanov, Y., D'Souza, W., Zhao, Q., Liu, Z., and Cong, Y. (2018). GPR43 mediates microbiota metabolite SCFA regulation of antimicrobial peptide expression in intestinal epithelial cells via activation of mTOR and STAT3. *Mucosal Immunol 11*, 752–762.

86. Arpaia, N., Campbell, C., Fan, X., Dikiy, S., van der Veeken, J., deRoos, P., Liu, H., Cross, J. R., Pfeffer, K., Coffer, P. J., and Rudensky, A. Y. (2013). Metabolites produced by commensal bacteria promote peripheral regulatory T-cell generation. *Nature 504*, 451–5.

87. Furusawa, Y. et al. (2013). Commensal microbe-derived butyrate induces the differentiation of colonic regulatory T cells. *Nature 504*, 446–450.

88. Smith, P. M., Howitt, M. R., Panikov, N., Michaud, M., Gallini, C. A., Bohlooly-Y, M., Glickman, J. N., and Garrett, W. S. (2013). The microbial metabolites, short chain fatty acids, regulate colonic T reg cell homeostasis. *Science 341*, 6145.

89. Kaye, D. M. et al. (2020). Deficiency of Prebiotic Fiber and Insufficient Signaling Through Gut Metabolite-Sensing Receptors Leads to Cardiovascular Disease. *Circulation 141*, 1393–1403.

90. Singh, N., Gurav, A., Sivaprakasam, S., Brady, E., Padia, R., Shi, H., Thangaraju,M., Prasad, P. D., Manicassamy, S., Munn, D. H., Lee, J. R., Offermanns, S., and Ganapathy, V. (2014). Activation of Gpr109a, receptor for niacin and the commensal metabolite butyrate, suppresses colonic inflammation and carcinogenesis. *Immunity 40*, 128–39.

91. Schulthess, J., Pandey, S., Capitani, M., Rue-Albrecht, K. C., Arnold, I., Franchini, F., Chomka, A., Ilott, N. E., Johnston, D. G., Pires, E., McCullagh, J., Sansom, S. N., Arancibia-Cárcamo, C. V., Uhlig, H. H., and Powrie, F. (2019). The Short Chain Fatty Acid Butyrate Imprints an Antimicrobial Program in Macrophages. *Immunity 50*, 432–445.

92. Wang, R. et al. (2023). Treatment of peanut allergy and colitis in mice via the intestinal release of butyrate from polymeric micelles. *Nat Biomed Eng 7*, 38–55.

93. Chun, E., Lavoie, S., Fonseca-Pereira, D., Bae, S., Michaud, M., Hoveyda, H. R., Fraser, G. L., Gallini Comeau, C. A., Glickman, J. N., Fuller, M. H., Layden, B. T., and Garrett, W. S. (2019). Metabolite-Sensing Receptor Ffar2 Regulates Colonic Group 3 Innate Lymphoid Cells and Gut Immunity. *Immunity 51*, 871–884.

94. Yang, W. et al. (2020). Intestinal microbiota-derived short-chain fatty acids regulation of immune cell IL-22 production and gut immunity. *Nat Commun 11*, 4457.

95. Rosser, E. C. et al. (2020). Microbiota-Derived Metabolites Suppress Arthritis by Amplifying Aryl-Hydrocarbon Receptor Activation in Regulatory B Cells. *Cell Metab 31*, 837–851.

96. Zou, F., Qiu, Y., Huang, Y., Zou, H., Cheng, X., Niu, Q., Luo, A., and Sun, J. (2021). Effects of short-chain fatty acids in inhibiting HDAC and activating p38 MAPK are critical for promoting B10 cell generation and function. *Cell Death Dis 12*, 582.

97. Takahashi, D. et al. (2020). Microbiota-derived butyrate limits the autoimmune response by promoting the differentiation of follicular regulatory T cells. *EBioMedicine 58*, 102913.

98. Tan, J., McKenzie, C., Vuillermin, P. J., Goverse, G., Vinuesa, C. G., Mebius, R. E., Macia, L., and Mackay, C. R. (2016). Dietary Fiber and Bacterial SCFA Enhance Oral Tolerance and Protect against Food Allergy through Diverse Cellular Pathways. *Cell Rep 15*, 2809–2824.

99. Folkerts, J., Redegeld, F., Folkerts, G., Blokhuis, B., van den Berg, M. P. M., de Bruijn, M. J. W., van IJcken, W. F. J., Junt, T., Tam, S.-Y., Galli, S. J., Hendriks, R. W., Stadhouders, R., and Maurer, M. (2020). Butyrate inhibits human mast cell activation via epigenetic regulation of FcεRI-mediated signaling. *Allergy 75*, 1966–1978.

100. Macia, L., and Mackay, C. R. (2019). Dysfunctional microbiota with reduced capacity to produce butyrate as a basis for allergic diseases. *J Allergy Clin Immunol 144*, 1513–1515.

101. Wopereis, H., Sim, K., Shaw, A., Warner, J. O., Knol, J., and Kroll, J. S. (2018). Intestinal microbiota in infants at high risk for allergy: Effects of prebiotics and role in eczema development. *J Allergy Clin Immunol 141*, 1334–1342.

102. Bunyavanich, S., Shen, N., Grishin, A., Wood, R., Burks, W., Dawson, P., Jones, S. M., Leung, D. Y. M., Sampson, H., Sicherer, S., and Clemente, J. C. (2016).

Early-life gut microbiome composition and milk allergy resolution. *J Allergy Clin Immunol 138*, 1122–1130.

103. Berni Canani, R., Sangwan, N., Stefka, A. T., Nocerino, R., Paparo, L., Aitoro, R., Calignano, A., Khan, A. A., Gilbert, J. A., and Nagler, C. R. (2016). Lactobacillus rhamnosus GG-supplemented formula expands butyrate-producing bacterial strains in food allergic infants. *ISME J 10*, 742–750.

104. Feehley, T., Plunkett, C. H., Bao, R., Choi Hong, S. M., Culleen, E., Belda-Ferre, P., Campbell, E., Aitoro, R., Nocerino, R., Paparo, L., Andrade, J., Antonopoulos, A., Berni Canani, R., and Nagler, C. R. (2019). Healthy infants harbor intestinal bacteria that protect against food allergy. *Nat Med 25*, 448–453.

105. De Filippis, F., Paparo, L., Nocerino, R., Della Gatta, G., Carucci, L., Russo, R., Pasolli, E., Ercolini, D., and Berni Canani, R. (2021). Specific gut microbiome signatures and the associated pro-inflammatory functions are linked to pediatric allergy and acquisition of immune tolerance. *Nat Commun 12*, 5958.

106. Gupta, R. S., Warren, C. M., Smith, B. M., Jiang, J., Blumenstock, J. A., Davis, M. M., Schleimer, R. P., and Nadeau, K. C. (2019). Prevalence and Severity of Food Allergies Among US Adults. *JAMA Netw Open 2*, e185630.

107. Sampath, V. et al. (2021). Food allergy across the globe. *J Allergy Clin Immunol 148*, 1347–1364.

108. Gupta, R. S., Warren, C. M., Smith, B. M., Blumenstock, J. A., Jiang, J., Davis, M. M., and Nadeau, K. C. (2018). The public health impact of parent-reported childhood food allergies in the United States. *Pediatrics 142*, 6

109. Valenta, R., Hochwallner, H., Linhart, B., and Pahr, S. (2015). Food allergies: the basics. *Gastroenterology 148*, 1120–31.

110. Caubet, J. C., Lin, J., Ahrens, B., Gimenez, G., Bardina, L., Niggemann, B., Sampson, H. A., and Beyer, K. (2017). Natural tolerance development in cow's milk allergic children: IgE and IgG4 epitope binding. *Allergy 72*, 1677–1685.

111. Abdel-Gadir, A. et al. (2019). Microbiota therapy acts via a regulatory T cell MyD88/RORγt pathway to suppress food allergy. *Nat Med 25*, 1164-1174

112. Bao, R., Hesser, L., He, Z., Zhou, X., Nadeau, K., and Nagler, C. R. (2021). Fecal microbiome and metabolome differ in healthy and food allergic twins. *J Clin Invest 131*, e141935.

113. Harris, N. L., and Loke, P. (2017). Recent Advances in Type-2-Cell-Mediated Immunity: Insights from Helminth Infection. *Immunity 47*, 1024–1036.

114. Leyva-Castillo, J.-M. et al. (2019). Mechanical Skin Injury Promotes Food Anaphylaxis by Driving Intestinal Mast Cell Expansion. *Immunity 50*, 1262–1275.

115. Brough, H. A., Nadeau, K. C., Sindher, S. B., Alkotob, S. S., Chan, S., Bahnson, H. T., Leung, D. Y. M., and Lack, G. (2020). Epicutaneous sensitization in the development of food allergy: What is the evidence and how can this be prevented? *Allergy 75*, 2185–2205.

116. Chinthrajah, S., Cao, S., Liu, C., Lyu, S.-C., Sindher, S. B., Long, A., Sampath, V., Petroni, D., Londei, M., and Nadeau, K. C. (2019). Phase 2a randomized, placebocontrolled study of anti–IL-33 in peanut allergy. *JCI Insight 4*, 22.

117. Wesemann, D. R., and Nagler, C. R. (2016). The Microbiome, Timing, and Barrier Function in the Context of Allergic Disease. *Immunity 44*, 728–738.

118. Peterson, L. W., and Artis, D. (2014). Intestinal epithelial cells: regulators of barrier function and immune homeostasis. *Nat Rev Immunol 14*, 141–53.

119. Niess, J. H., Brand, S., Gu, X., Landsman, L., Jung, S., McCormick, B. A., Vyas, J. M., Boes, M., Ploegh, H. L., Fox, J. G., Littman, D. R., and Reinecker, H.-C. (2005).

CX3CR1-Mediated Dendritic Cell Access to the Intestinal Lumen and Bacterial Clearance. *Science 307*, 254–258.

120. Tong, P., and Wesemann, D. R. (2015). Molecular Mechanisms of IgE Class Switch Recombination. *Curr Top Microbiol Immunol 388*, 21–37.

121. Khodoun, M. V., Strait, R., Armstrong, L., Yanase, N., and Finkelman, F. D. (2011). Identification of markers that distinguish IgE- from IgG-mediated anaphylaxis. *Proc Natl Acad Sci USA 108*, 12413–8.

122. Finkelman, F. D., Khodoun, M. V., and Strait, R. (2016). Human IgE-independent systemic anaphylaxis. *J Allergy Clin Immunol 137*, 1674– 1680.

123. Reber, L. L., Hernandez, J. D., and Galli, S. J. (2017). The pathophysiology of anaphylaxis. *J Allergy Clin Immunol 140*, 335–348.

124. Kanagaratham, C., El Ansari, Y. S., Lewis, O. L., and Oettgen, H. C. (2020). IgE and IgG Antibodies as Regulators of Mast Cell and Basophil Functions in Food Allergy. *Front Immunol 11.*

125. Zhang, B., Liu, E., Gertie, J. A., Joseph, J., Xu, L., Pinker, E. Y., Waizman, D. A., Catanzaro, J., Hamza, K. H., Lahl, K., Gowthaman, U., and Eisenbarth, S. C. (2020). Divergent T follicular helper cell requirement for IgA and IgE production to peanut during allergic sensitization. *Sci Immunol 5*, 47.

126. Erazo, A., Kutchukhidze, N., Leung, M., Christ, A. P. G., Urban, J. F., Curotto de Lafaille, M. A., and Lafaille, J. J. (2007). Unique maturation program of the IgE response in vivo. *Immunity 26*, 191–203.

127. He, J.-S. et al. (2013). The distinctive germinal center phase of IgE+ B lymphocytes limits their contribution to the classical memory response. *J Exp Med 210*, 2755–71.

128. Xiong, H., Dolpady, J., Wabl, M., Curotto de Lafaille, M. A., and Lafaille, J. J. (2012). Sequential class switching is required for the generation of high affinity IgE antibodies. *J Exp Med 209*, 353–64.

129. Chen, Q., Liu, H., Luling, N., Reinke, J., and Dent, A. L. (2023). Evidence that HighAffinity IgE Can Develop in the Germinal Center in the Absence of an IgG1-Switched Intermediate. *J Immunol 210,* 7 905-915.

130. Hara, S., Sasaki, T., Satoh-Takayama, N., Kanaya, T., Kato, T., Takikawa, Y., Takahashi, M., Tachibana, N., Kim, K. S., Surh, C. D., and Ohno, H. (2019). Dietary Antigens Induce Germinal Center Responses in Peyer's Patches and Antigen-Specific IgA Production. *Front Immunol 10*, 2432.

131. Campbell, E., Hesser, L. A., and Nagler, C. R. (2021). B cells and the microbiota: a missing connection in food allergy. *Mucosal Immunol 14*, 4–13.

132. Pier, J., Liu, E. G., Eisenbarth, S., and Järvinen, K. M. (2021). The role of immunoglobulin A in oral tolerance and food allergy. *Ann Allergy Asthma Immunol 126*, 467–468.

133. Reboldi, A., and Cyster, J. G. (2016). Peyer's patches: organizing B-cell responses at the intestinal frontier. *Immunol Rev 271*, 230–245.

134. Cahenzli, J., Köller, Y., Wyss, M., Geuking, M. B., and McCoy, K. D. (2013). Intestinal Microbial Diversity during Early-Life Colonization Shapes Long-Term IgE Levels. *Cell Host & Microbe 14*, 559–570.

135. Levin, M., Levander, F., Palmason, R., Greiff, L., and Ohlin, M. (2017). Antibody encoding repertoires of bone marrow and peripheral blood-a focus on IgE. *J Allergy Clin Immunol 139*, 1026–1030.

136. Heeringa, J. J., Rijvers, L., Arends, N. J., Driessen, G. J., Pasmans, S. G., van Dongen, J. J. M., de Jongste, J. C., and van Zelm, M. C. (2018). IgE-expressing

memory B cells and plasmablasts are increased in blood of children with asthma, food allergy, and atopic dermatitis. *Allergy 73*, 1331–1336.

137. Hoh, R. A. et al. (2020). Origins and clonal convergence of gastrointestinal IgE+ B cells in human peanut allergy. *Sci Immunol 5*, 45.

138. Wesemann, D. R., and Nagler, C. R. (2020). Origins of peanut allergy-causing antibodies. *Science 367*, 1072–1073.

139. He, J.-S., Subramaniam, S., Narang, V., Srinivasan, K., Saunders, S. P., Carbajo, D., Wen-Shan, T., Hidayah Hamadee, N., Lum, J., Lee, A., Chen, J., Poidinger, M., Zolezzi, F., Lafaille, J. J., and Curotto de Lafaille, M. A. (2017). IgG1 memory B cells keep the memory of IgE responses. *Nat Commun 8*, 641.

140. Looney, T. J., Lee, J.-Y., Roskin, K. M., Hoh, R. A., King, J., Glanville, J., Liu, Y., Pham, T. D., Dekker, C. L., Davis, M. M., and Boyd, S. D. (2016). Human B-cell isotype switching origins of IgE. *J Allergy Clin Immunol 137*, 579–586.

141. Weiner, H. L., da Cunha, A. P., Quintana, F., and Wu, H. (2011). Oral tolerance. *Immunol Rev 241*, 241–59.

142. Coombes, J. L., Siddiqui, K. R., Arancibia-Cárcamo, C. V., Hall, J., Sun, C.-M., Belkaid, Y., and Powrie, F. (2007). A functionally specialized population of mucosal CD103+ DCs induces Foxp3+ regulatory T cells via a TGF-*β*– and retinoic acid–dependent mechanism. *J Exp Med 204*, 1757–1764.

143. Esterházy, D., Loschko, J., London, M., Jove, V., Oliveira, T. Y., and Mucida, D. (2016). Classical dendritic cells are required for dietary antigen-mediated induction of peripheral T(reg) cells and tolerance. *Nat Immunol 17*, 545–55.

144. Kim, M., Galan, C., Hill, A. A., Wu, W.-J., Fehlner-Peach, H., Song, H. W., Schady, D., Bettini, M. L., Simpson, K. W., Longman, R. S., Littman, D. R., and Diehl, G. E. (2018). Critical Role for the Microbiota in CX3CR1+ Intestinal Mononuclear Phagocyte Regulation of Intestinal T Cell Responses. *Immunity 49*, 151–163.

145. Esterházy, D., Canesso, M. C. C., Mesin, L., Muller, P. A., de Castro, T. B. R., Lockhart, A., ElJalby, M., Faria, A. M. C., and Mucida, D. (2019). Compartmentalized gut lymph node drainage dictates adaptive immune responses. *Nature 569*, 126–130.

146. Ohnmacht, C. et al. (2015). The microbiota regulates type 2 immunity through RORγt T cells. *Science 349*, 989–93.

147. Sefik, E. et al. (2015). Individual intestinal symbionts induce a distinct population of RORγt+ regulatory T cells. *Science 349*, 993–997.

148. Akagbosu, B. et al. (2022). Novel antigen-presenting cell imparts Treg-dependent tolerance to gut microbiota. *Nature 610*, 752–760.

149. Kedmi, R. et al. (2022). A RORγt+ cell instructs gut microbiota-specific Treg cell differentiation. *Nature 610*, 737–743.

150. Lyu, M. et al. (2022). ILC3s select microbiota-specific regulatory T cells to establish tolerance in the gut. *Nature 610*, 744–751.

151. Wohlfert, E. A. et al. (2011). GATA3 controls Foxp3+ regulatory T cell fate during inflammation in mice. *J Clin Invest 121*, 4503–4515.

152. Panduro, M., Benoist, C., and Mathis, D. (2016). Tissue Tregs. *Ann Rev Immunol 34*, 609–633.

153. Hong, S.-W., Krueger, P. D., Osum, K. C., Dileepan, T., Herman, A., Mueller, D. L., and Jenkins, M. K. (2022). Immune tolerance of food is mediated by layers of CD4+ T cell dysfunction. *Nature 607*, 762–768.

154. Bashir, M. E. H., Louie, S., Shi, H. N., and Nagler-Anderson, C. (2004). Toll-like receptor 4 signaling by intestinal microbes influences susceptibility to food allergy. *J Immunol 172*, 6978–87.

155. Hong, S.-W., O, E., Lee, J. Y., Lee, M., Han, D., Ko, H.-J., Sprent, J., Surh, C. D., and Kim, K. S. (2019). Food antigens drive spontaneous IgE elevation in the absence of commensal microbiota. *Sci Adv 5*, eaaw1507.

156. Wyss, M., Brown, K., Thomson, C. A., Koegler, M., Terra, F., Fan, V., Ronchi, F.,Bihan, D., Lewis, I., Geuking, M. B., and McCoy, K. D. (2019). Using Precisely Defined in vivo Microbiotas to Understand Microbial Regulation of IgE. *Front Immunol 10*, 3107.

157. Noval Rivas, M. et al. (2013). A microbiota signature associated with experimental food allergy promotes allergic sensitization and anaphylaxis. *J Allergy Clin Immunol 131*, 201–12.

158. Solis, A. G., Klapholz, M., Zhao, J., and Levy, M. (2020). The bidirectional nature of microbiome-epithelial cell interactions. *Curr Op Microbiol 56*, 45–51.

159. Campbell, E., Maccio-Maretto, L., Hesser, L. A., Kemter, A., Berni Canani, R., Nocerino, R., Paparo, L., Patry, R., and Nagler, C. (2022). TLR4 regulates proinflammatory intestinal immune responses mediated by an atopic gut microbiota. *BioRxiv.*

160. Sano, T., Huang, W., Hall, J. A., Yang, Y., Chen, A., Gavzy, S. J., Lee, J.-Y., Ziel, J. W., Miraldi, E. R., Domingos, A. I., Bonneau, R., and Littman, D. R. (2015). An IL-23R/IL-22 Circuit Regulates Epithelial Serum Amyloid A to Promote Local Effector Th17 Responses. *Cell 163*, 381–393.

161. Lee, J.-Y. et al. (2020). Serum Amyloid A Proteins Induce Pathogenic Th17 Cells and Promote Inflammatory Disease. *Cell 180*, 79–91.

162. Zimmermann, P., Messina, N., Mohn, W. W., Finlay, B. B., and Curtis, N. (2019). Association between the intestinal microbiota and allergic sensitization, eczema, and asthma: A systematic review. *J Allergy Clin Immunol 143*, 467–485.

163. NASPGHAN Nutrition Report Committee (2006). Clinical Efficacy of Probiotics. *J Pediatr Gastr Nutr 43*, 550–557.

164. Zhernakova, A. et al. (2016). Population-based metagenomics analysis reveals markers for gut microbiome composition and diversity. *Science 352*, 565–9.

165. Zierer, J., Jackson, M. A., Kastenmüller, G., Mangino, M., Long, T., Telenti, A., Mohney, R. P., Small, K. S., Bell, J. T., Steves, C. J., Valdes, A. M., Spector, T. D., and Menni, C. (2018). The fecal metabolome as a functional readout of the gut microbiome. *Nat Genet 50*, 790–795.

166. Mimee, M., Citorik, R. J., and Lu, T. K. (2016). Microbiome therapeutics - Advances and challenges. *Adv Drug Deliv Rev 105*, 44–54.

167. Skelly, A. N., Sato, Y., Kearney, S., and Honda, K. (2019). Mining the microbiota for microbial and metabolite-based immunotherapies. *Nat Rev Immunol 19*, 305–323.

168. Surana, N. K. (2019). Moving Microbiome Science from the Bench to the Bedside: a Physician-Scientist Perspective. *mSystems 4*, 3.

169. Nagler, C. R. (2020). Drugging the microbiome. *J Exp Med 217*, 4 e20191642.

170. Paquet, J.-C., Claus, S. P., Cordaillat-Simmons, M., Mazier, W., Rawadi, G., Rinaldi, L., Elustondo, F., and Rouanet, A. (2021). Entering First-in-Human Clinical Study With a Single-Strain Live Biotherapeutic Product: Input and Feedback Gained From the EMA and the FDA. *Front Med 8,* 716266*.*

171. Vieira, A. T., Fukumori, C., and Ferreira, C. M. (2016). New insights into therapeutic strategies for gut microbiota modulation in inflammatory diseases. *Clin Transl Immunol 5*, e87.

172. Sonnenburg, E. D., and Sonnenburg, J. L. (2014). Starving our Microbial Self: The Deleterious Consequences of a Diet Deficient in Microbiota-Accessible Carbohydrates. *Cell Metab 20*, 779–786.

173. Kukkonen, K., Savilahti, E., Haahtela, T., Juntunen-Backman, K., Korpela, R., Poussa, T., Tuure, T., and Kuitunen, M. (2007). Probiotics and prebiotic galactooligosaccharides in the prevention of allergic diseases: A randomized, double-blind, placebo-controlled trial. *J Allergy Clin Immunol 119*, 192–198.

174. Button, J. E., Autran, C. A., Reens, A. L., Cosetta, C. M., Smriga, S., Ericson, M., Pierce, J. V., Cook, D. N., Lee, M. L., Sun, A. K., Alousi, A. M., Koh, A. Y., Rechtman, D. J., Jenq, R. R., and McKenzie, G. J. (2022). Dosing a synbiotic of human milk oligosaccharides and B. infantis leads to reversible engraftment in healthy adult microbiomes without antibiotics. *Cell Host & Microbe 30*, 712–725.

175. Suez, J., Zmora, N., Segal, E., and Elinav, E. (2019). The pros, cons, and many unknowns of probiotics. *Nat Med 25*, 716–729.

176. Hill, C., Guarner, F., Reid, G., Gibson, G. R., Merenstein, D. J., Pot, B., Morelli, L., Canani, R. B., Flint, H. J., Salminen, S., Calder, P. C., and Sanders, M. E. (2014). Expert consensus document. The International Scientific Association for Probiotics and Prebiotics consensus statement on the scope and appropriate use of the term probiotic. *Nat Rev Gastroenterol Hepatol 11*, 506–14.

177. O'Toole, P. W., Marchesi, J. R., and Hill, C. (2017). Next-generation probiotics: the spectrum from probiotics to live biotherapeutics. *Nat Microbiol 2*, 17057.

178. Makki, K., Deehan, E. C., Walter, J., and Bäckhed, F. (2018). The Impact of Dietary Fiber on Gut Microbiota in Host Health and Disease. *Cell Host & Microbe 23*, 705–715.

179. Sanders, M. E., Merenstein, D. J., Reid, G., Gibson, G. R., and Rastall, R. A. (2019). Probiotics and prebiotics in intestinal health and disease: from biology to the clinic *Nat Rev Gastroenterol Hepatol 16*, 605–616.

180. Buyken, A. E., Goletzke, J., Joslowski, G., Felbick, A., Cheng, G., Herder, C., and Brand-Miller, J. C. (2014). Association between carbohydrate quality and inflammatory markers: systematic review of observational and interventional studies, *Am J Clin Nutr 99*, 813–833.

181. O'Keefe, S. J. D. et al. (2015). Fat, fibre and cancer risk in African Americans and rural Africans. *Nat Commun 6*, 6342.

182. Zhao, L. et al. (2018). Gut bacteria selectively promoted by dietary fibers alleviate type 2 diabetes. *Science 359*, 1151–1156.

183. Grabitske, H. A., and Slavin, J. L. (2009). Gastrointestinal Effects of Low-Digestible Carbohydrates. *Crit Rev Food Sci Nutr 49*, 327–360.

184. Mego, M., Accarino, A., Tzortzis, G., Vulevic, J., Gibson, G., Guarner, F., and Azpiroz, F. (2017). Colonic gas homeostasis: Mechanisms of adaptation following HOST-G904 galactooligosaccharide use in humans. *Neurogastroenterol Motil 29*, e13080.

185. Ze, X., Duncan, S. H., Louis, P., and Flint, H. J. (2012). Ruminococcus bromii is a keystone species for the degradation of resistant starch in the human colon. *ISME J 6*, 1535–1543.

186. Mukhopadhya, I. et al. (2018). Sporulation capability and amylosome conservation among diverse human colonic and rumen isolates of the keystone starch-degrader Ruminococcus bromii. *Env Microbiol 20*, 324–336.

187. Walker, A. W. et al. (2011). Dominant and diet-responsive groups of bacteria within the human colonic microbiota. *ISME J 5*, 220–230.

188. Salonen, A., Lahti, L., Salojärvi, J., Holtrop, G., Korpela, K., Duncan, S. H., Date, P., Farquharson, F., Johnstone, A. M., Lobley, G. E., Louis, P., Flint, H. J., and de Vos, W. M. (2014). Impact of diet and individual variation on intestinal microbiota composition and fermentation products in obese men. *ISME J 8*, 2218– 2230.

189. Baxter, N. T., Schmidt, A. W., Venkataraman, A., Kim, K. S., Waldron, C., and Schmidt, T. M. (2019). Dynamics of Human Gut Microbiota and Short-Chain Fatty Acids in Response to Dietary Interventions with Three Fermentable Fibers. *mBio 10*, 02566–18.

190. Wastyk, H. C., Fragiadakis, G. K., Perelman, D., Dahan, D., Merrill, B. D., Yu, F. B., Topf, M., Gonzalez, C. G., Van Treuren, W., Han, S., Robinson, J. L., Elias, J. E., Sonnenburg, E. D., Gardner, C. D., and Sonnenburg, J. L. (2021). Gut-microbiota targeted diets modulate human immune status. *Cell 184*, 4137–4153.

191. Spencer, S. P., Fragiadakis, G. K., and Sonnenburg, J. L. (2019). Pursuing Human Relevant Gut Microbiota-Immune Interactions. *Immunity 51*, 225–239.

192. Bode, L. (2012). Human milk oligosaccharides: Every baby needs a sugar mama. *Glycobiology 22*, 1147–1162.

193. Plaza-Díaz, J., Fontana, L., and Gil, A. (2018). Human Milk Oligosaccharides and Immune System Development. *Nutrients 10*, 1038.

194. Vandenplas, Y., Berger, B., Carnielli, V., Ksiazyk, J., Lagström, H., Sanchez Luna, M., Migacheva, N., Mosselmans, J.-M., Picaud, J.-C., Possner, M., Singhal, A., and Wabitsch, M. (2018). Human Milk Oligosaccharides: 2’-Fucosyllactose (2’-FL) and Lacto-N-Neotetraose (LNnT) in Infant Formula. *Nutrients 10*, 1161.

195. Eiseman, B., Silen, W., Bascom, G. S., and Kauvar, A. J. (1958). Fecal enema as an adjunct in the treatment of pseudomembranous enterocolitis. *Surgery 44*, 854–9.

196. Pamer, E. G. (2014). Fecal microbiota transplantation: effectiveness, complexities, and lingering concerns. *Mucosal immunol 7*, 210–4.

197. DeFilipp, Z., Bloom, P. P., Torres Soto, M., Mansour, M. K., Sater, M. R., Huntley, M. H., Turbett, S., Chung, R. T., Chen, Y.-B., and Hohmann, E. L. (2019). Drug-Resistant E. coli Bacteremia Transmitted by Fecal Microbiota Transplant. *N Engl J Med 381*, 2043–2050.

198. Yelin, I., Flett, K. B., Merakou, C., Mehrotra, P., Stam, J., Snesrud, E., Hinkle, M., Lesho, E., McGann, P., McAdam, A. J., Sandora, T. J., Kishony, R., and Priebe, G. P. (2019). Genomic and epidemiological evidence of bacterial transmission from probiotic capsule to blood in ICU patients. *Nat Med 25*, 1728–1732.

199. Kassam, Z., Lee, C. H., Yuan, Y., and Hunt, R. H. (2013). Fecal microbiota transplantation for Clostridium difficile infection: systematic review and meta-analysis. *Am J Gastroenterol 108*, 500–8.

200. Rossen, N. G., Fuentes, S., van der Spek, M. J., Tijssen, J. G., Hartman, J. H., Duflou, A., Löwenberg, M., van den Brink, G. R., Mathus-Vliegen, E. M., de Vos, W. M., Zoetendal, E. G., D'Haens, G. R., and Ponsioen, C. Y. (2015). Findings From a Randomized Controlled Trial of Fecal Transplantation for Patients With Ulcerative Colitis. *Gastroenterology 149*, 110–118.

201. Aggarwala, V., Mogno, I., Li, Z., Yang, C., Britton, G. J., Chen-Liaw, A., Mitcham, J., Bongers, G., Gevers, D., Clemente, J. C., Colombel, J.-F., Grinspan, A., and Faith, J. (2021). Precise quantification of bacterial strains after fecal microbiota transplantation delineates long-term engraftment and explains outcomes. *Nat Microbiol 6*, 1309–1318.

202. Wei, S., Bahl, M. I., Baunwall, S. M. D., Dahlerup, J. F., Hvas, C. L., and Licht, T. R. (2022). Gut microbiota differs between treatment outcomes early after fecal

microbiota transplantation against recurrent *Clostridioides difficile* infection. *Gut Microbes 14*, 1 2084306.

203. Kwak, S., Choi, J., Hink, T., Reske, K. A., Blount, K., Jones, C., Bost, M. H., Sun, X., Burnham, C.-A. D., Dubberke, E. R., and Dantas, G. (2020). Impact of investigational microbiota therapeutic RBX2660 on the gut microbiome and resistome revealed by a placebo-controlled clinical trial. *Microbiome 8*, 125.

204. REBYOTA (2022). Prescribing Information. *Parsippany, NJ: Ferring Pharmaceuticals Inc*.

205. Walter, J., and Shanahan, F. (2023). Fecal microbiota-based treatment for recurrent Clostridioides difficile infection. *Cell 186*, 1087.

206. Garber, K. (2020). First microbiome-based drug clears phase III, in clinical trial turnaround. *Nat Rev Drug Discov 19*, 655–656.

207. Dsouza, M. et al. (2022). Colonization of the live biotherapeutic product VE303 and modulation of the microbiota and metabolites in healthy volunteers. *Cell Host & Microbe 30*, 583–598.

208. Feuerstadt, P. et al. (2022). SER-109, an Oral Microbiome Therapy for Recurrent Clostridioides difficile Infection. *N Engl J Med386*, 220–229.

209. van der Lelie, D., Oka, A., Taghavi, S., Umeno, J., Fan, T.-J., Merrell, K. E., Watson, S. D., Ouellette, L., Liu, B., Awoniyi, M., Lai, Y., Chi, L., Lu, K., Henry, C. S., and Sartor, R. B. (2021). Rationally designed bacterial consortia to treat chronic immune-mediated colitis and restore intestinal homeostasis. *Nat Commun 12*, 3105.

210. Aggarwal, N., Breedon, A. M. E., Davis, C. M., Hwang, I. Y., and Chang, M. W. (2020). Engineering probiotics for therapeutic applications: recent examples and translational outlook. *Curr Opin Biotechnol 65*, 171–179.

211. Mimee, M., Tucker, A. C., Voigt, C. A., and Lu, T. K. (2015). Programming a Human Commensal Bacterium, Bacteroides thetaiotaomicron, to Sense and Respond to Stimuli in the Murine Gut Microbiota. *Cell Syst 1*, 62–71.

212. Guo, C.-J., Allen, B. M., Hiam, K. J., Dodd, D., Van Treuren, W., Higginbottom, S., Nagashima, K., Fischer, C. R., Sonnenburg, J. L., Spitzer, M. H., and Fischbach, M. A. (2019). Depletion of microbiome-derived molecules in the host using Clostridium genetics. *Science 366*, 6471.

213. Shepherd, E. S., DeLoache, W. C., Pruss, K. M., Whitaker, W. R., and Sonnenburg, J. L. (2018). An exclusive metabolic niche enables strain engraftment in the gut microbiota. *Nature 557*, 434–438.

214. Isabella, V. M. et al. (2018). Development of a synthetic live bacterial therapeutic for the human metabolic disease phenylketonuria. *Nat Biotechnol 36*, 857–864.

215. Steidler, L., Hans, W., Schotte, L., Neirynck, S., Obermeier, F., Falk, W., Fiers, W., and Remaut, E. (2000). Treatment of murine colitis by Lactococcus lactis secreting interleukin-10. *Science 289*, 1352–5.

216. Frossard, C. P., Steidler, L., and Eigenmann, P. A. (2007). Oral administration of an IL-10-secreting Lactococcus lactis strain prevents food-induced IgE sensitization. *J Allergy Clin Immunol 119*, 952–9.

217. Hendrikx, T., Duan, Y., Wang, Y., Oh, J.-H., Alexander, L. M., Huang, W., Stärkel, P., Ho, S. B., Gao, B., Fiehn, O., Emond, P., Sokol, H., van Pijkeren, J.-P., and Schnabl, B. (2019). Bacteria engineered to produce IL-22 in intestine induce expression of REG3G to reduce ethanol-induced liver disease in mice. *Gut 68*, 1504–1515.

218. Swanson, K. S., Gibson, G. R., Hutkins, R., Reimer, R. A., Reid, G., Verbeke, K., Scott, K. P., Holscher, H. D., Azad, M. B., Delzenne, N. M., and Sanders, M. E. (2020). The International Scientific Association for Probiotics and Prebiotics

(ISAPP) consensus statement on the definition and scope of synbiotics. *Nat Rev Gastroenterol Hepatol 17*, 687–701.

219. Pandey, K. R., Naik, S. R., and Vakil, B. V. (2015). Probiotics, prebiotics and synbiotics- a review. *J Food Sci Technol 52*, 7577–87.

220. Salminen, S., Collado, M. C., Endo, A., Hill, C., Lebeer, S., Quigley, E. M. M., Sanders, M. E., Shamir, R., Swann, J. R., Szajewska, H., and Vinderola, G. (2021). The International Scientific Association of Probiotics and Prebiotics (ISAPP) consensus statement on the definition and scope of postbiotics. *Nat Rev Gastroenterol Hepatol 18*, 649–667.

221. Żółkiewicz, J., Marzec, A., Ruszczyński, M., and Feleszko, W. (2020). Postbiotics-A Step Beyond Pre- and Probiotics. *Nutrients 12*, 8 2189.

222. Braido, F., Melioli, G., Cazzola, M., Fabbri, L., Blasi, F., Moretta, L., Canonica, G. W., and AIACE Study Group (2015). Sub-lingual administration of a polyvalent mechanical bacterial lysate (PMBL) in patients with moderate, severe, or very severe chronic obstructive pulmonary disease (COPD) according to the GOLD spirometric classification: A multicentre, double-blind, randomised, controlled, phase IV study (AIACE study: Advanced Immunological Approach in COPD Exacerbation). *Pulm Pharmacol Ther 33*, 75–80.

223. Cardinale, F., Lombardi, E., Rossi, O., Bagnasco, D., Bellocchi, A., and Menzella, F. (2020). Epithelial dysfunction, respiratory infections and asthma: the importance of immunomodulation. A focus on OM-85. *Expert Rev Respir Med 14*, 1019–1026.

224. Investigators, T. P. G. o. C. (2018). AR101 Oral Immunotherapy for Peanut Allergy. *N Eng J Med 379*, 1991–2001.

225. Patrawala, S., Ramsey, A., Capucilli, P., Tuong, L.-A., Vadamalai, K., and Mustafa, S. S. (2022). Real-world adoption of FDA-approved peanut oral immunotherapy with palforzia. *J Allergy Clin Immunol Pract 10*, 1120– 1122.

226. Chu, D. K., Wood, R. A., French, S., Fiocchi, A., Jordana, M., Waserman, S., Brożek, J. L., and Schünemann, H. J. (2019). Oral immunotherapy for peanut allergy (PACE): a systematic review and meta-analysis of efficacy and safety. *The Lancet 393*, 2222-2232.

227. Hofmann, A. M., Scurlock, A. M., Jones, S. M., Palmer, K. P., Lokhnygina, Y., Steele, P. H., Kamilaris, J., and Burks, A. W. (2009). Safety of a peanut oral immunotherapy protocol in children with peanut allergy. *J Allergy Clin Immunol 124*, 286–291.

228. Ho, H. e., and Bunyavanich, S. (2019). Microbial Adjuncts for Food Allergen Immunotherapy. *Curr Allergy Asthma Rep 19,* 5.

229. Boyle, R. J. et al. (2016). Prebiotic-supplemented partially hydrolysed cow's milk formula for the prevention of eczema in high-risk infants: a randomized controlled trial. *Allergy 71*, 701–710.

230. Fox, A., Bird, J. A., Fiocchi, A., Knol, J., Meyer, R., Salminen, S., Sitang, G., Szajewska, H., and Papadopoulos, N. (2019). The potential for pre-, pro- and synbiotics in the management of infants at risk of cow's milk allergy or with cow's milk allergy: An exploration of the rationale, available evidence and remaining questions. *World Allergy Organ J 12*, 100034.

231. Shi, Y., Xu, L.-Z., Peng, K., Wu, W., Wu, R., Liu, Z.-Q., Yang, G., Geng, X.-R., Liu, J., Liu, Z.-G., Liu, Z., and Yang, P.-C. (2015). Specific immunotherapy in combination with Clostridium butyricum inhibits allergic inflammation in the mouse intestine. *Sci Rep 5*, 17651.

232. Zhang, J., Su, H., Li, Q., Wu, H., Liu, M., Huang, J., Zeng, M., Zheng, Y., and Sun, X. (2017). Oral administration of Clostridium butyricum CGMCC0313-1 inhibits *β*lactoglobulin-induced intestinal anaphylaxis in a mouse model of food allergy. *Gut Path 9*, 11.

233. Thang, C. L., Baurhoo, B., Boye, J. I., Simpson, B. K., and Zhao, X. (2011). Effects of Lactobacillus rhamnosus GG supplementation on cow's milk allergy in a mouse model. *Allergy Asthma Clin Immunol 7*, 20.

234. Neau, E., Delannoy, J., Marion, C., Cottart, C.-H., Labellie, C., Holowacz, S., Butel, M.-J., Kapel, N., and Waligora-Dupriet, A.-J. (2016). Three Novel Candidate Probiotic Strains with Prophylactic Properties in a Murine Model of Cow's Milk Allergy. *Appl Environ Microbiol 82*, 1722–1733.

235. Nocerino, R., Di Costanzo, M., Bedogni, G., Cosenza, L., Maddalena, Y., Di Scala, C., Della Gatta, G., Carucci, L., Voto, L., Coppola, S., Iannicelli, A. M., and Berni Canani, R. (2019). Dietary Treatment with Extensively Hydrolyzed Casein Formula Containing the Probiotic Lactobacillus rhamnosus GG Prevents the Occurrence of Functional Gastrointestinal Disorders in Children with Cow's Milk Allergy. *J Pediatr 213*, 137–142.

236. Tang, M. L., Ponsonby, A. L., Orsini, F., Tey, D., Robinson, M., Su, E. L., Licciardi, P., Burks, W., and Donath, S. (2015). Administration of a probiotic with peanut oral immunotherapy: A randomized trial. *J Allergy Clin Immunol 135,* 3.

237. Sorensen, K., Cawood, A. L., Gibson, G. R., Cooke, L. H., and Stratton, R. J. (2021). Amino Acid Formula Containing Synbiotics in Infants with Cow's Milk Protein Allergy: A Systematic Review and Meta-Analysis. *Nutrients 13*, 3.

238. Burks, A. W., Harthoorn, L. F., Van Ampting, M. T. J., Oude Nijhuis, M. M., Langford, J. E., Wopereis, H., Goldberg, S. B., Ong, P. Y., Essink, B. J., Scott, R. B., and Harvey, B. M. (2015). Synbiotics-supplemented amino acid-based formula supports

adequate growth in cow's milk allergic infants. *Pediatr Alllergy Immunol 26*, 316–22.

239. Candy, D. C. A., Van Ampting, M. T. J., Oude Nijhuis, M. M., Wopereis, H., Butt, A. M., Peroni, D. G., Vandenplas, Y., Fox, A. T., Shah, N., West, C. E., Garssen, J., Harthoorn, L. F., Knol, J., and Michaelis, L. J. (2018). A synbiotic-containing amino acidic-based formula improves gut microbiota in non-IgE-mediated allergic infants. *Pediatr Res 83*, 677–686.

240. Mariño, E. et al. (2017). Gut microbial metabolites limit the frequency of autoimmune T cells and protect against type 1 diabetes. *Nat Immunol 18*, 552–562.

241. Clarke, J. M., Topping, D. L., Bird, A. R., Young, G. P., and Cobiac, L. (2008). Effects of high-amylose maize starch and butyrylated high-amylose maize starch on azoxymethane-induced intestinal cancer in rats. *Carcinogenesis 29*, 2190–2194.

242. Scheppach, W., Sommer, H., Kirchner, T., Paganelli, G.-M., Bartram, P., Christl, S., Richter, F., Dusel, G., and Kasper, H. (1992). Effect of butyrate enemas on the colonic mucosa in distal ulcerative colitis. *Gastroenterology 103*, 51–56.

243. Butzner, J. D., Parmar, R., Bell, C. J., and Dalal, V. (1996). Butyrate enema therapy stimulates mucosal repair in experimental colitis in the rat. *Gut 38*, 568–573.

244. Luceri, C., Femia, A. P., Fazi, M., Di Martino, C., Zolfanelli, F., Dolara, P., and Tonelli, F. (2016). Effect of butyrate enemas on gene expression profiles and endoscopic/histopathological scores of diverted colorectal mucosa: A randomized trial. *Dig Liver Dis 48*, 27–33.

245. Clarke, J. M., Young, G. P., Topping, D. L., Bird, A. R., Cobiac, L., Scherer, B. L., Winkler, J. G., and Lockett, T. J. (2012). Butyrate delivered by butyrylated starch increases distal colonic epithelial apoptosis in carcinogen-treated rats. *Carcinogenesis 33*, 197–202.

246. Schwiertz, A., Hold, G. L., Duncan, S. H., Gruhl, B., Collins, M. D., Lawson, P. A., Flint, H. J., and Blaut, M. (2002). Anaerostipes caccae gen. nov., sp. nov., a new saccharolytic, acetate-utilising, butyrate-producing bacterium from human faeces. *Syst Appl Microbiol 25*, 46-51.

247. Duncan, S. H., Louis, P., and Flint, H. J. (2004). Lactate-Utilizing Bacteria, Isolated from Human Feces, That Produce Butyrate as a Major Fermentation Product. *Appl Env Microbiol 70*, 5810–5817.

248. Rivière, A., Selak, M., Lantin, D., Leroy, F., and De Vuyst, L. (2016). Bifidobacteria and Butyrate-Producing Colon Bacteria: Importance and Strategies for Their Stimulation in the Human Gut. *Front Microbiol 7*, 979

249. Chia, L. W., Hornung, B. V. H., Aalvink, S., Schaap, P. J., de Vos, W. M., Knol, J., and Belzer, C. (2018). Deciphering the trophic interaction between Akkermansia muciniphila and the butyrogenic gut commensal Anaerostipes caccae using a metatranscriptomic approach. *Antonie van Leeuwenhoek 111*, 859–873.

250. Bui, T. P. N., Schols, H. A., Jonathan, M., Stams, A. J. M., de Vos, W. M., and Plugge, C. M. (2019). Mutual Metabolic Interactions in Co-cultures of the Intestinal Anaerostipes rhamnosivorans With an Acetogen, Methanogen, or Pectin-Degrader Affecting Butyrate Production. *Front Microbiol 10*, 2449.

251. Chia, L. W., Mank, M., Blijenberg, B., Bongers, R. S., van Limpt, K., Wopereis, H., Tims, S., Stahl, B., Belzer, C., and Knol, J. (2021). Cross-feeding between Bifidobacterium infantis and Anaerostipes caccae on lactose and human milk oligosaccharides. *Benef Microbes 12*, 69–83.

252. Sato, T., Matsumoto, K., Okumura, T., Yokoi, W., Naito, E., Yoshida, Y., Nomoto, K., Ito, M., and Sawada, H. (2008). Isolation of lactate-utilizing butyrate-producing bacteria from human feces and in vivo administration of Anaerostipes caccae strain L2 and galacto-oligosaccharides in a rat model. *FEMS Microbiol Ecol 66*, 528– 36.

253. Schumann, C. (2002). Medical, nutritional and technological properties of lactulose. An update. *E J Nutr 41*, 1–1.

254. Bothe, M. K., Maathuis, A. J. H., Bellmann, S., van der Vossen, J. M. B. M., Berressem, D., Koehler, A., Schwejda-Guettes, S., Gaigg, B., Kuchinka-Koch, A., and Stover, J. F. (2017). Dose-Dependent Prebiotic Effect of Lactulose in a Computer-Controlled In Vitro Model of the Human Large Intestine. *Nutrients 9*, 767.

255. Calatayud, M., Duysburgh, C., Van den Abbeele, P., Franckenstein, D., KuchinaKoch, A., and Marzorati, M. (2022). Long-Term Lactulose Administration Improves Dysbiosis Induced by Antibiotic and C. difficile in the PathoGutTM SHIME Model. *Antibiotics 11*, 1464.

256. Karakan, T., Tuohy, K. M., and Janssen-van Solingen, G. (2021). Low-Dose Lactulose as a Prebiotic for Improved Gut Health and Enhanced Mineral Absorption. *Front Nutr 8*, 672925.

257. Zhai, S., Zhu, L., Qin, S., and Li, L. (2018). Effect of lactulose intervention on gut microbiota and short chain fatty acid composition of C57BL/6J mice. *Microbiologyopen 7*, e00612.

258. Rettedal, E. A., Gumpert, H., and Sommer, M. O. A. (2014). Cultivation-based multiplex phenotyping of human gut microbiota allows targeted recovery of previously uncultured bacteria. *Nat Commun 5*, 4714.

259. Kurakawa, T., Ogata, K., Matsuda, K., Tsuji, H., Kubota, H., Takada, T., Kado, Y., Asahara, T., Takahashi, T., and Nomoto, K. (2015). Diversity of Intestinal Clostridium coccoides Group in the Japanese Population, as Demonstrated by Reverse Transcription-Quantitative PCR. *PLOS ONE 10*, e0126226.

260. Matsuki, T., Watanabe, K., Fujimoto, J., Takada, T., and Tanaka, R. (2004). Use of 16S rRNA gene-targeted group-specific primers for real-time PCR analysis of predominant bacteria in human feces. *Appl Env Microbiol 70*, 7220–8.

261. Turner, S., Pryer, K. M., Miao, V. P., and Palmer, J. D. (1999). Investigating deep phylogenetic relationships among cyanobacteria and plastids by small subunit rRNA sequence analysis. *J Eukaryot Microbiol 46*, 327–38.

262. Amann, R. I., Ludwig, W., and Schleifer, K. H. (1995). Phylogenetic identification and in situ detection of individual microbial cells without cultivation. *Microbiol Rev 59*, 143–69.

263. Tyagi, A. M., Yu, M., Darby, T. M., Vaccaro, C., Li, J. Y., Owens, J. A., Hsu, E., Adams, J., Weitzmann, M. N., Jones, R. M., and Pacifici, R. (2018). The Microbial Metabolite Butyrate Stimulates Bone Formation via T Regulatory Cell-Mediated Regulation of WNT10B Expression. *Immunity 49*, 1116-1131.

264. Nagao-Kitamoto, H. et al. (2020). Interleukin-22-mediated host glycosylation prevents Clostridioides difficile infection by modulating the metabolic activity of the gut microbiota. *Nat Med 26*, 608–617.

265. Upadhyay, V., Poroyko, V., Kim, T.-j., Devkota, S., Fu, S., Liu, D., Tumanov, A. V., Koroleva, E. P., Deng, L., Nagler, C., Chang, E. B., Tang, H., and Fu, Y.-X. (2012). Lymphotoxin regulates commensal responses to enable diet-induced obesity. *Nat Immunol 13*, 947–953.

266. Kreymborg, K., Etzensperger, R., Dumoutier, L., Haak, S., Rebollo, A., Buch, T., Heppner, F. L., Renauld, J.-C., and Becher, B. (2007). IL-22 is expressed by Th17 cells in an IL-23-dependent fashion, but not required for the development of autoimmune encephalomyelitis. *J Immunol 179*, 8098– 104.

267. Gorski, S. A., Hahn, Y. S., and Braciale, T. J. (2013). Group 2 Innate Lymphoid Cell Production of IL-5 Is Regulated by NKT Cells during Influenza Virus Infection. *PLoS Path 9*, e1003615.

268. Sittipo, P., Kim, H. K., Han, J., Lee, M. R., and Lee, Y. K. (2021). Vitamin D3 suppresses intestinal epithelial stemness via ER stress induction in intestinal organoids. *Stem Cell Res Ther 12*, 285.

269. Tashiro, N., Segawa, R., Tobita, R., Asakawa, S., Mizuno, N., Hiratsuka, M., and Hirasawa, N. (2019). Hypoxia inhibits TNF-*α*-induced TSLP expression in keratinocytes. *PLOS ONE 14*, e0224705.

270. Segata, N., Izard, J., Waldron, L., Gevers, D., Miropolsky, L., Garrett, W. S., and Huttenhower, C. (2011). Metagenomic biomarker discovery and explanation. *Genome Biol 12*, R60.

271. Cao, Y., Dong, Q., Wang, D., Zhang, P., Liu, Y., and Niu, C. (2022). microbiomeMarker: an R/Bioconductor package for microbiome marker identification and visualization. *Bioinformatics 38*, 4027–4029.

272. Safronova, V., and Novikova, N. (1996). Comparison of two methods for root nodule bacteria preservation: Lyophilization and liquid nitrogen freezing. *J Microbiol Meth 24*, 231–237.

273. Collins, J., Robinson, C., Danhof, H., Knetsch, C. W., van Leeuwen, H. C., Lawley, T. D., Auchtung, J. M., and Britton, R. A. (2018). Dietary trehalose enhances virulence of epidemic Clostridium difficile. *Nature 553*, 291–294.

274. Maslowski, K. M. (2019). Metabolism at the centre of the host–microbe relationship. *Clin Exp Immunol 197*, 193–204.

275. Everard, A., Belzer, C., Geurts, L., Ouwerkerk, J. P., Druart, C., Bindels, L. B., Guiot, Y., Derrien, M., Muccioli, G. G., Delzenne, N. M., de Vos, W. M., and Cani, P. D. (2013). Cross-talk between Akkermansia muciniphila and intestinal epithelium controls diet-induced obesity. *Proc Natl Acad Sci USA 110*, 9066–9071.

276. Derrien, M., Belzer, C., and de Vos, W. M. (2017). Akkermansia muciniphila and its role in regulating host functions. *Microb Pathog 106*, 171–181.

277. Depommier, C. et al. (2019). Supplementation with Akkermansia muciniphila in overweight and obese human volunteers: a proof-of-concept exploratory study. *Nat Med 25*, 1096–1103.

278. Paone, P., and Cani, P. D. (2020). Mucus barrier, mucins and gut microbiota: the expected slimy partners? *Gut 69*, 2232–2243.

279. Ogata, Y., Suda, W., Ikeyama, N., Hattori, M., Ohkuma, M., and Sakamoto, M. (2019). Complete Genome Sequence of Phascolarctobacterium faecium JCM 30894, a Succinate-Utilizing Bacterium Isolated from Human Feces. *Microbiol Resour Announc 8*, e01487-18.

280. Louis, P., and Flint, H. J. (2017). Formation of propionate and butyrate by the human colonic microbiota. *Env Microbiol 19*, 29–41.

281. Bui, T. P. N., Mannerås-Holm, L., Puschmann, R., Wu, H., Troise, A. D., Nijsse, B., Boeren, S., Bäckhed, F., Fiedler, D., and deVos, W. M. (2021). Conversion of dietary inositol into propionate and acetate by commensal Anaerostipes associates with host health. *Nat Commun 12*, 4798.

282. Moens, F., Verce, M., and De Vuyst, L. (2017). Lactate- and acetate-based crossfeeding interactions between selected strains of lactobacilli, bifidobacteria and colon bacteria in the presence of inulin-type fructans. *Int J Food Microbiol 241*, 225–236.

283. Van den Abbeele, P., Belzer, C., Goossens, M., Kleerebezem, M., De Vos, W. M., Thas, O., De Weirdt, R., Kerckhof, F.-M., and Van de Wiele, T. (2013). Butyrateproducing Clostridium cluster XIVa species specifically colonize mucins in an in vitro gut model. *ISME J 7*, 949–61.

284. Hatayama, H., Iwashita, J., Kuwajima, A., and Abe, T. (2007). The short chain fatty acid, butyrate, stimulates MUC2 mucin production in the human colon cancer cell line, LS174T. *Biochem Biophys Res Commun 356*, 599–603.

285. Willemsen, L. E. M. (2003). Short chain fatty acids stimulate epithelial mucin 2 expression through differential effects on prostaglandin E1 and E2 production by intestinal myofibroblasts. *Gut 52*, 1442–1447.

286. Johansson, M. E., Jakobsson, H. E., Holmén-Larsson, J., Schütte, A., Ermund, A., Rodríguez-Piñeiro, A. M., Arike, L., Wising, C., Svensson, F., Bäckhed, F., and Hansson, G. C. (2015). Normalization of Host Intestinal Mucus Layers Requires Long-Term Microbial Colonization. *Cell Host & Microbe 18*, 582–592.

287. van der Hee, B., and Wells, J. M. (2021). Microbial Regulation of Host Physiology by Short-chain Fatty Acids. *Trends Microbiol 29*, 700–712.

288. Belzer, C., and de Vos, W. M. (2012). Microbes inside—from diversity to function: the case of Akkermansia. *ISME J 6*, 1449–1458.

289. Malik, A., Sharma, D., Zhu, Q., Karki, R., Guy, C. S., Vogel, P., and Kanneganti, T.-D. (2016). IL-33 regulates the IgA-microbiota axis to restrain IL-1*α*–dependent colitis and tumorigenesis. *J Clin Invest 126*, 4469–4481.

290. Gowthaman, U. et al. (2019). Identification of a T follicular helper cell subset that drives anaphylactic IgE. *Science 365*, eaaw6433.

291. Fontenot, J. D., Gavin, M. A., and Rudensky, A. Y. (2003). Foxp3 programs the development and function of CD4+CD25+ regulatory T cells. *Nat Immunol 4*, 330–6.

292. Ritvo, P.-G. G., Churlaud, G., Quiniou, V., Florez, L., Brimaud, F., Fourcade, G., Mariotti-Ferrandiz, E., and Klatzmann, D. (2017). Tfr cells lack IL-2R*α* but express decoy IL-1R2 and IL-1Ra and suppress the IL-1–dependent activation of Tfh cells. *Sci Immunol 2*, eaan0368.

293. Wing, J. B., Kitagawa, Y., Locci, M., Hume, H., Tay, C., Morita, T., Kidani, Y., Matsuda, K., Inoue, T., Kurosaki, T., Crotty, S., Coban, C., Ohkura, N., and Sakaguchi, S. (2017). A distinct subpopulation of CD25- T-follicular regulatory cells localizes in the germinal centers. *Proc Natl Acad Sci USA 114*, E6400-E6409.

294. Tanno, H., Fujii, T., Ose, R., Hirano, K., Tochio, T., and Endo, A. (2019). Characterization of fructooligosaccharide-degrading enzymes in human commensal Bifidobacterium longum and Anaerostipes caccae. *Biochem Biophys Res Commun 518*, 294–298.

295. Chen, Q., and Dent, A. L. (2022). Regulation of the IgE response by T follicular regulatory cells. *J Allergy Clin Immunol 150*, 1048–1049.

296. Clement, R. L., Daccache, J., Mohammed, M. T., Diallo, A., Blazar, B. R., Kuchroo, V. K., Lovitch, S. B., Sharpe, A. H., and Sage, P. T. (2019). Follicular regulatory T cells control humoral and allergic immunity by restraining early B cell responses. *Nat Immunol 20*, 1360–1371.

297. Xie, M. M., Chen, Q., Liu, H., Yang, K., Koh, B., Wu, H., Maleki, S. J., Hurlburt, B. K., Cook-Mills, J., Kaplan, M. H., and Dent, A. L. (2020). T follicular regulatory cells and IL-10 promote food antigen-specific IgE. *J Clin Invest 130*, 3820–3832.

298. Gonzalez-Figueroa, P., Roco, J. A., Papa, I., Núñez Villacís, L., Stanley, M., Linterman, M. A., Dent, A., Canete, P. F., and Vinuesa, C. G. (2021). Follicular regulatory T cells produce neuritin to regulate B cells. *Cell 184*, 1775–1789.

299. Reber, L. L., Sibilano, R., Mukai, K., and Galli, S. J. (2015). Potential effector and immunoregulatory functions of mast cells in mucosal immunity. *Mucosal Immuno 8*, 444–463.

300. Odenwald, M. et al. (2023). Prebiotic activity of lactulose optimizes gut metabolites and prevents systemic infection in liver disease patients. *MedRxIV*.